The Dissertation Committee for William Andrew Barr Certifies that this is the approved version of the following dissertation:

The Paleoenvironments of Early Hominins in the Omo Shungura Formation (Plio-Pleistocene, Ethiopia): Synthesizing Multiple Lines of Evidence Using Phylogenetic Ecomorphology

Committee:

Denné Reed, Supervisor

John Kappelman

Liza Shapiro

René Bobe

Kaye Reed

The Paleoenvironments of Early Hominins in the Omo Shungura Formation (Plio-Pleistocene, Ethiopia): Synthesizing Multiple Lines of Evidence Using Phylogenetic Ecomorphology

by

William Andrew Barr, B.S; M.A.

Dissertation

Presented to the Faculty of the Graduate School of

The University of Texas at Austin

in Partial Fulfillment

of the Requirements

for the Degree of

Doctor of Philosophy

The University of Texas at Austin

May 2014

Dedication

For Christina, who was with me every step of this long journey: I couldn't have done it without you, babe! And for my family, who have always cheered me on in all my endeavors.

Acknowledgements

Like any dissertation, this project could not have been completed without the assistance of many individuals and institutions.

First, thanks are owed to my advisor, Denné Reed. I am grateful to Denné for serving as a sounding board, a never-ending source of new ideas, and for treating me like a colleague. Thanks also for always inviting me to participate in a wide variety of field and lab research projects. I owe you a lot! Liza Shapiro was a never-ending source of advice and moral support: she was always ready with a critical editorial eye. She also throws the best parties, which manage to bring together people from all walks of life (even academics!). I will really miss eating lunch in the loco-lab. John Kappelman's own research on bovid ecomorphology was an important inspiration for this project. He also provided invaluable assistance that helped me more fully understand the functional morphology of the bovid hock. Thanks for the many pieces of advice over the years! My external committee members Kaye Reed and René Bobe offered important insights on paleoenvironmental reconstruction that improved this dissertation significantly. Thanks also to Rob Scott, who was an honorary external member of my dissertation committee. His insights on ecomorphology were very important in the development of this project.

My dissertation was funded by a National Science Foundation Graduate Research Fellowship and a Wenner-Gren Dissertation Fieldwork Grant. Thanks to both of these organizations their support.

Permission to study fossils was granted by the Ethiopian Authority for Research and Conservation of Cultural Heritage (ARCCH). Thanks to Zeray Alemseged for advice and assistance working in Ethiopia. Thanks are also owed to Mogus Mekonnen for

helping to make daily life in Addis a little more entertaining. Thanks to Bill Kimbel for allowing me to stay at the IHO house.

Access to extant specimens was facilitated by Eileen Westwig at the American Museum of Natural History in New York, New York and by Darrin Lunde at the National Museum of Natural History in Washington, DC. Special thanks to Will Harcourt-Smith and Eric Delson for loaning equipment and facilitating my visit to the AMNH.

Thanks are owed to Liam Revell for advice on how to properly perform the character simulations in Chapter 2 using his fantastic R package *phytools*. I received significant training in phylogenetic statistical methods at the AnthroTree Workshop, which is supported by the NSF (BCS-0923791) and the National Evolutionary Synthesis Center (NSF grant EF-0905606). Many thanks to Manuel Hernandez Fernandez, for graciously providing a Newick file of his ruminant phylogeny.

Fellow graduate students throughout my time at UT-Austin were a constant source of encouragement. Thanks to Stacey Tecot, Laura Alport, Magdalena Muchlinski, Carrie Veilleux, Matt Kilberger, Angel Zeininger, Amy Hallberg, Laurel Carnes, Carl Toborowsky, Gabrielle Russo, Amber Heard-Booth, Brett Nachman, Jaime Mata-Miguez, Kelsey Ellis, Kat Bannar-Martin, Matt Chimera, Kim Valenta, Krista Church, Rick Smith, Lina Maria Valencia-Rodriguez, Addison Kemp, Sierra Castedo, Laura Abondano. Special thanks to Brett….I might not have made it through without the constant commiseration and the many, many, many beers. Adam Gordon and Dave Raichlen were no longer at UT by the time I arrived, but they treated me like an academic little brother at the AAPA meetings, and I really appreciated the camaraderie and advice.

The Paleoenvironments of Early Hominins in the Omo Shungura Formation (Plio-Pleistocene, Ethiopia): Synthesizing Multiple Lines of Evidence Using Phylogenetic Ecomorphology

William Andrew Barr, PhD

The University of Texas at Austin, 2014

Supervisor: Denné N. Reed

Ever since Darwin claimed that expanding savannas were the driving force behind humanity's divergence from other apes, our understanding of human evolution has been inextricably linked to the environmental context in which our ancestors evolved. This dissertation explores various aspects of the use of one method of paleoenvironmental reconstruction -- bovid ecomorphology -- and provides new data on paleoenvironmental conditions in the Omo Shungura Formation (Plio-Pleistocene, Ethiopia).

Chapter 2 uses phylogenetic simulations to explore the performance of Discriminant Function Analysis (DFA) on simulated ecomorphological data containing phylogenetic signal. DFA is shown to "over-perform" in situations in which predicted and predictor variables both contain phylogenetic signal. Phylogenetic Generalized Least Squares (PGLS) is shown to be a very useful technique for explicitly testing functional hypotheses in ecomorphology while controlling for phylogenetic signal and body size.

Chapter 3 presents a functional analysis of the bovid astragalus, which is one of the most commonly preserved bones in the fossil record. Several functional hypotheses linking habitat-specific locomotor performance with the morphology of the astragalus are tested using PGLS. Strong support is found for three of these hypotheses. Thus, the

astragalus is shown to be a useful ecomorphological predictor element, a point that is confirmed by the DFA analyses in Chapter 4.

Chapter 5 provides new paleoenvironmental data on the Omo Shungura Formation based on habitat reconstructions from astragalar ecomorphology in addition to dietary reconstructions based on dental mesowear. Astragalar data point to a major environmental shift beginning ~2.58 Ma, which is later in time compared with some prior habitat reconstructions using different methods. Furthermore, astragalar data show environmental fluctuations of similar magnitude later in the sequence. Mesowear data on the Shungura Tragelaphini do not offer evidence for any significant grazing adaptation, in spite of relatively high carbon isotope signatures reported based on studies of tooth enamel. These data raise questions regarding the diet of fossil Tragalephini.

Table of Contents

List of Tables

List of Figures

Chapter 1: Introduction

Ever since Charles Darwin claimed that expanding savannas were the driving force behind humanity's divergence from other apes, our understanding of human evolution has been inextricably linked to the environmental context in which our ancestors evolved. In this dissertation project, I explore various aspects of the use of one method of paleoenvironmental reconstruction: bovid ecomorphology. I then use ecomorphology to provide environmental reconstructions for the Omo Shungura Formation (Plio-Pleistocene, Ethiopia).

ENVIRONMENTAL HYPOTHESES OF HUMAN EVOLUTION

Paleoenvironmental reconstruction provides the environmental context that is needed to answer "why" questions about human evolution. One major unresolved question is: why did the human lineage bifurcate into two distinct genera (*Homo* and *Paranthropus*) near the Plio-Pleistocene boundary sometime around 2.58 Ma? This time period coincides broadly with global climate cooling and aridification trends caused by the onset of Northern Hemisphere Glaciation (Shackleton et al., 1984; deMenocal, 2004), and with the probable first appearance dates for the robust australopith genus *Paranthropus* and our own genus *Homo* (Schrenk et al., 1993; Kimbel, 1995; Kimbel et al., 1996).

The broad contemporaneity of these events comprises the evidence for the influential Turnover Pulse Hypothesis (TPH), which maintains that phylogenetic turnover in Plio-Pleistocene hominins – as well as antelope (Vrba, 1995) and rodents (Wesselman, 1995) – is causally related to the global climatic transition towards cooler, more arid environments (Vrba, 1985, 1988; Vrba et al., 1989). The TPH is one corollary of Vrba's Habitat Theory (1992), which views turnover events (speciation and extinction) as

exceedingly rare in the absence of climatic forcing. Lineages that exhibit habitat specificity find their preferred habitats increasingly fragmented during episodes of climate change. Isolated populations in highly fragmented habitat patches are at higher risk of extinction and speciation (Vrba, 1992). Thus, a broad array of distantly related lineages are expected to respond to climate change with coordinated bursts of extinction and speciation, which are visible as pulses of faunal turnover in the fossil record. Though Vrba has forcefully argued for the presence of turnover pulses in the African fossil record (1985; 1988, 1995), other authors have failed to detect pulses (White, 1995; Behrensmeyer et al., 1997), or have detected multiple smaller pulse events instead (Bobe and Behrensmeyer, 2004).

Specific predictions follow from Vrba's theory as applied to human evolution. If the TPH correctly explains the cause of Plio-Pleistocene hominin speciation, then the hominins preceding the climatic event must have been ***ecologically specialized*** on heavily wooded habitats. If Pliocene hominins (such as *A. afarensis*) were instead habitat generalists, then large patches of suitable habitat would have persisted during episodes of climate change. Thus, the effective habitat of *A. afarensis* would not have undergone substantial vicariance, and habitat theory would not predict phylogenetic turnover (Vrba, 1987, 1992).

The notion that pre-Pleistocene hominins were closed-habitat specialists receives some support from the closed-woodland reconstructions of the 4.4 million year Aramis site, which has yielded spectacular fossils of the species *Ardipithicus ramidus* (Louchart et al., 2009; White et al., 2009). However, the reconstruction of the habitats surrounding Aramis as closed woodland has been controversial. Cerling and colleagues (2010) reevaluated the published paleosol carbonate data and concluded that the habitat occupied by *Ardipithecus* at Aramis likely included less than 25% woody cover. An independent

analysis of additional soil carbonate samples (Gani and Gani, 2011) confirmed the importance of more open habitats at Aramis, which might reflect a relatively closed river-margin habitat imbedded in a more open floodplain. In addition, the well-known species *A. afarensis*, the best-known direct ancestor of later hominins (Johanson and White, 1979; Strait et al., 1997), has been characterized as eurytopic generalist capable of living in several types of habitat (Reed, 2008). Thus, there does not appear to be compelling evidence for a high degree of habitat specialization among early hominins, which may weaken the hypothesis that phylogenetic turnover in the hominin lineage is causally related to a climate regime shift, as suggested by the TPH.

More recently, Potts (1996, 1998 a) has suggested that the increase in variability in global climate during the Pleistocene arguably played a more central role in shaping hominin evolution than the directional changes in global climate highlighted in Vrba's earlier work on the TPH. This focus on climatic variability led Potts to posit a type of "Variability Selection", in which natural selection favors characteristics that enable organisms to cope with variability, rather than characteristics that are adaptive to a particular kind of environment. Under this view, hallmark characteristics of genus *Homo* such as increased encephalization, technological sophistication, and behavioral flexibility would be seen as adaptations to increased global climate variability.

Despite debates surrounding preferred habitats of various hominin species, and hominin responses to climate change, there is no doubt that a major episode of global climate change occurred 2.8 - 2.5 Ma, and that this event brought on increasingly cool, arid, and variable global conditions (Shackleton et al., 1984; deMenocal, 2004). Evaluating the impact of this and other global-scale climate phenomena on continental terrestrial evolution has become a major focus of research (Behrensmeyer et al., 1997; Potts, 1998 a; Bobe et al., 2002; Kingston, 2007; Reed, 2008). Because the Omo

Shungura Formation is one of the richest records of mammalian evolution from 3.6 to 1.39 Ma, a precise understanding of ecological change recorded in these deposits is imperative for understanding the relationship between global climate change and human evolution. The Shungura Formation possesses a time depth and dense record of deposition that make possible intra-site comparisons of environmental conditions before and after the period of global climatic change. Reconstructing these environments involves weaving multiple lines of evidence into synthetic views of dynamic ecosystems (Potts, 1998 b; Kingston, 2007).

ECOMORPHOLOGY

One important method for environmental reconstruction is ecomorphology. This method is designed to glean ecological data from fossils based on relationships between form and function that are independent of taxonomic identifications (Kappelman, 1991; Behrensmeyer et al., 1992). Antelopes (family Bovidae), are particularly useful for ecomorphology because they are often the numerically dominant group in fossil assemblages and because many bovid species are habitat specialists (Vrba, 1980).

This dissertation focuses on the ecomorphology of bovid astragali and molar teeth. These two anatomical elements provide complementary information about locomotion and diet, respectively. Comparing dietary reconstructions (molars) with locomotor reconstructions (astragali) facilitates a more integrated view of past environments than would be possible using evidence from a single anatomical region. Furthermore, these skeletal elements are extremely abundant in the fossil record. Indeed, isolated molars and astragali are often the most abundant cranial and postcranial elements in a given fossil assemblage (Hussain et al., 1983). Thus, astragali and molar teeth provide a robust statistical sample from which to infer the past relative abundance of

bovids with different locomotor and dietary adaptations. Patterns in relative abundance of bovid dietary and locomotor adaptations can serve as clues as to the ecological characteristics of the habitats from which the fossils were sampled.

Some controversy exists, however, regarding the relationship between bovid astragalar morphology and habitat preference. Several studies have used Discriminant Function Analysis (DFA) to produce statistically significant classifications for bovid astragali that predict habitat preference at rates that far exceed chance. However, recent work (Klein et al., 2010) has challenged prior studies of astragalar morphology by suggesting that the observed differences between bovids from different habitats merely reflect differences in body size. These authors also hinted that phylogenetic relationships between species might be responsible for anatomical similarities between bovids occupying similar habitats. If true, this critique calls into question the ability of ecomorphology to deduce functional links between morphology and habitat.

The critique of Klein and colleagues highlights the fact that previous studies of bovid astragalar morphology have not tested specific functional hypotheses regarding astragalar function in relation to habitat, and have not controlled for body size differences and for phylogenetic signal. This dissertation presents the first study that tests form-function hypotheses regarding astragalar function in a phylogenetic statistical framework using strict controls for body size.

Dental mesowear is likely less influenced by phylogenetic signal than astragalar morphology because mesowear variables develop in response to the particular ways in which a tooth is used during the lifetime of an individual (See Chapter 5 for more detailed discussion). Mesowear occupies an intermediate position between unworn tooth morphology, which is heavily influenced by long-term adaptation (and thus phylogenetic signal), and microwear, which can change rapidly depending on the properties of foods

recently eaten (Fortelius and Solounias, 2000). Mesowear reflects the medium-term response of cusp height and shape to differing types of wear (tooth-tooth versus tooth-food, see Chapter 5). Thus, mesowear provides a useful method for predicting the physical properties of foods habitually eaten by bovids.

STRUCTURE OF THE DISSERTATION

The dissertation is divided in to six chapters. This introductory chapter provides a brief introduction to the topics covered in the subsequent chapters.

Chapter 2 addresses the general question of why phylogenetic comparative methods are needed in ecomorphology. This chapter presents a simulation study focused on the issues surrounding phylogenetic signal in ecomorphology. These phylogenetic simulations demonstrate that methods used in previous studies, particularly DFA, have significant limitations with regard to differentiating between phylogenetic signal and functional signal. The simulations further demonstrate that phylogenetic comparative methods, particularly PGLS, are well suited for testing functional hypotheses relating anatomical form and ecological function. Thus, Chapter 2 effectively demonstrates how using phylogenetic comparative methods makes it possible to tease apart functional signal from the influences of body size and phylogeny, despite warnings to the contrary (Klein et al., 2010).

Chapter 3 introduces a framework for interpreting the morphology of the bovid astragalus and its relationship to habitat. Specific predictions emanating from this functional framework are tested using an analysis of a large extant comparative sample of bovid astragali. The results demonstrate that, when controlling for body size and phylogenetic signal using phylogenetic comparative statistical methods, there are

significant differences in astragalar morphology between bovids from different habitats, which conform to functional predictions.

Chapter 4 takes up the question of how to predict habitat preferences using fossil astragali. Using the results from Chapter 3, a set of functionally relevant variables is used to evaluate the predictive ability of astragalar metrics for predicting habitats using DFA. DFA results indicate that habitat predictions are most reliable for the extreme ends of the habitat spectrum (Open and Closed), with less reliability for intermediate habitats (Light Cover and Heavy Cover). While the predictive ability of the astragalus is lower than that of some other anatomical elements, this reduction in rate of successful predictions is offset, to some degree, by the large sample sizes of astragali available. This situation contrasts with that of other skeletal elements, which sometimes have a higher habitat classification accuracy rate for each specimen as compared to astragali, but are typically preserved in much smaller sample sizes.

Chapter 5 presents an analysis of habitat change through time in the Shungura Formation of Southeastern Ethiopia using evidence from mesowear analysis of isolated teeth, and from ecomorphological analysis of astragali. Results confirm earlier findings indicating major environmental changes during the period from 2.8 – 2.5 Ma, but also point to environmental perturbations later in the sequence. This chapter offers additional evidence for cyclical change in Shungura habitats at shorter temporal scales, at the level of geological submember. While it is difficult to pinpoint a cause of these submember-level environmental fluctuations, the timing is broadly consistent with global climate cycles of solar insolation driven by orbital dynamics. Finally, the dietary reconstructions provided in this chapter offer new insights into the diets of Shungura Bovidae through time. Particularly interesting are the dietary reconstructions of the Shungura Tragelaphini, which have recently been shown to have very high carbon isotope ratios, in the

neighborhood of modern grazers (Bibi et al., 2013). The mesowear from Chapter 5 offer complementary data on the types of foods consumed by these bovids. No evidence of a grazing signal for the Shungura Tragelaphini is revealed by the mesowear analysis in this chapter, which raises questions regarding how the mesowear and stable-isotope data might be reconciled.

Finally, in Chapter 6, I provide a closing summary and discuss future directions and unresolved questions.

Chapter 2: Phylogenetic comparative methods in ecomorphology

In this chapter, I examine the use of phylogenetic comparative methods in ecomorphology. Specifically, I use phylogenetic simulation techniques to create datasets with varying levels of phylogenetic signal in the continuous (predictor) variables and the categorical (predicted) variables. These datasets are used to explore the performance of standard ecomorphological statistical methods as well as phylogenetic comparative methods. These simulations serve to illustrate a methodological framework that forms the basis for analyses in subsequent chapters. A version of this chapter has been published in the American Journal of Physical Anthropology (Barr and Scott, 2014)[1].

BACKGROUND

Discriminant Function Analysis (DFA) is a multivariate technique designed to discover an additive combination of weighted values for a set of measured continuous variables that best classifies individuals into a category (Sokal and Rohlf, 2001; Manly, 2004). DFA is fundamentally a descriptive technique for accessing the ability of measured variables to classify a training dataset for which the predicted category is known *a priori* (Manly, 2004). However, the purpose of most DFAs in physical anthropology is to use the resulting discriminant functions outside the training set in order to classify cases for which the categorical variable is unknown. In this chapter, I use phylogenetic simulations to evaluate the performance of DFA in situations where the

[1] Author contributions: Robert Scott contributed to the analytical plan and helped revise the manuscript. W. Andrew Barr planned and performed simulations, analyzed the data, wrote and revised the manuscript.

predicted category and the predictor variables exhibit varying levels of phylogenetic signal.

At least three major types of studies have relied on DFA in physical anthropology. 1) DFA is routinely employed intraspecifically. For example, the method is often used to predict sex or ancestry in samples of modern humans in forensic anthropology (Safont et al., 2000; Walker, 2005; Ousley et al., 2009). In such studies, the goal is to create discriminant functions that can be used to predict the sex or ancestry of unknown cases from medico-legal or archaeological contexts. 2) DFA has been used taxonomically in several ways. Rak and colleagues (2002) performed DFA on samples of modern human and Neanderthal mandibles to illustrate the distinctiveness of Neanderthal mandibular morphology. Gebo and Schwartz (2006) used a DFA of modern hominoid tali in order to evaluate the taxonomic affinities of fossil hominin tali. Dagosto and colleagues (2010) employed DFA to classify primate tali as either strepsirrhine or haplorhine, with the goal of establishing the affinity of fossil primate tali from Southeast-Asia. 3) DFA is commonly used in ecomorphological[2] studies that aim to classify unknown cases into dietary or locomotor categories. For instance, DFA has been used to predict primate diets from dental morphology (Schwartz, 2000; Boyer, 2008; Bunn et al., 2011). DFA is ubiquitous in studies of bovid locomotor ecomorphology that have sought to reconstruct past habitats at hominoid and hominin-bearing fossil sites (Kappelman, 1988, 1991; Plummer and Bishop, 1994; Kappelman et al., 1997; Scott et al., 1999; DeGusta and

[2] Ecomorphology refers to the study of morphology with regard to the ecological context in which the morphology occurs. The term "functional morphology" is restricted to explicit study of links between morphology and a particular biomechanical function (Bock & Wahlert, 1965, Bock, 1994). "Ecomorphology" is broader than "functional morphology" because ecomorphology is concerned with how functions are put to use in different ecological contexts (equivalent to the "biological roles" of Bock & Wahlert, 1965).

Vrba, 2003, 2005; Kovarovic and Andrews, 2007; Plummer et al., 2008; Bishop et al., 2011).

The uses of DFA in physical anthropology are diverse, but nearly all of them involve categorical prediction beyond the training sample used to formulate the DFA. DFA can only be reliable in predicting cases outside the training set if predictions are grounded in well-understood relationships between the measured variables and the predicted categorical variable. In other words, classifying a training set is of little use unless the underlying cause of differences between categories in the training set can be expected to operate in cases outside the training set. In ecomorphology, the underlying relationship is assumed to be functional. Indeed, ecomorphology has been described as "taxon-free" because taxonomic identifications for each specimen are not required; the goal of ecomorphology is to make ecological predictions based on biomechanical links between form and function rather than on taxonomic assumptions about the ecology of an organism (Kappelman, 1991).

Recent work has called into question the degree to which ecomorphology is, in fact, taxon-free. Klein and coauthors (2010) argued that the choice of taxa included in a training set, as well as the available sample size for each taxon, could alter the predictive performance of DFA. Therefore these authors maintain that DFA is not properly considered "taxon-free", but rather "taxon-dependent" (Klein et al., 2010). Additional issues arise when considering how to deal with multiple non-independent data points for each taxon, which can lead to inflated significance and erroneous results (Mundry and Sommer, 2007). Furthermore, issues involved in the composition of training samples run deeper than the selection of which taxa to include.

Even if all living species are included in a training set, DFA is not free of taxonomic issues, because the taxa in the training set are related to one another in a

hierarchical phylogeny. Closely related species comprise higher-level taxonomic groups that share recent common ancestors and, therefore, often share both morphological and ecological characteristics inherited from this common ancestor. Datasets with this structure, in which closely related species are more similar to one another than randomly selected species, are said to exhibit phylogenetic signal (Münkemüller et al., 2012).

Antelopes (bovids) exhibit phylogenetic signal both in habitat preferences and in many morphometric variables that have been used for ecomorphology (Scott and Barr, In Press). It has long been recognized that many bovid lineages are highly conservative in their habitat preference (Vrba, 1980; Greenacre and Vrba, 1984; Kappelman, 1984; Shipman and Harris, 1988). Thus, in a DFA training set many of the taxa representative of a particular habitat will be closely related to one another. For instance, in the dataset of bovid habitat preferences used in the present study, 63% of the forest-adapted species are from a single taxonomic tribe[3], Cephalophini and an additional 27% are from a second tribe, Tragelaphini. This strong relationship between habitat preference and phylogeny raises an issue of phylogenetic pseudo-replication. Standard statistical methods treat each taxon as an independent data point, but this treatment is inappropriate when data sets exhibit phylogenetic signal (Smith, 1994; Nunn, 1995). A large literature on phylogenetic comparative methods has demonstrated that issues of phylogenetic non-independence can lead to incorrect interpretations of data that possesses a high degree of phylogenetic signal (Felsenstein, 1985; Harvey and Pagel, 1991; Martins and Garland, 1991; Garland et al., 1993; Garland and Carter, 1994; Nunn and Barton, 2001; Rohlf, 2006; Revell, 2009). Phylogenetic Generalized Least Squares (PGLS) has emerged as the most flexible

[3] The tribal terminology used here reflects common usage rather than explicit hypotheses about monophyly.

and appropriate method for testing hypotheses of trait correlation when datasets exhibit phylogenetic signal (Freckleton et al., 2002).

In the case of bovid habitat prediction, correlations between a measurement (*x*) and habitat preference could be driven by the fact that both variables have strong phylogenetic signal. If this were the case, then predicting habitats for fossil bovids based on variable x would be nearly the same as making taxonomic assumptions about habitat preference (*i.e.*, assuming that the habitat preferences of the fossil are the same as modern members of the same taxonomic group). The expectation, even if variable *x* were functionally unrelated to habitat preference (the null hypothesis), is that groups of bovids sharing similar habitats would have similar average values for *x* simply because many of them are closely related. When phylogenetic signal is not explicitly taken into account, then the chance of committing a Type I error (Rohlf, 2006), or incorrectly rejecting a true null hypothesis, is increased. Ecomorphology thus requires a tool that can explicitly take phylogenetic signal into account.

Consideration of phylogenetic signal in bovid ecomorphology is not a new idea. In a study employing ecomorphology to predict bovid habitat preference from femoral morphology, Kappelman highlighted the fact that bovids retain habitat preferences and femoral morphological complexes at the level of taxonomic tribe (Kappelman, 1991). Despite this phylogenetic signal in morphology and habitat preference, Kappelman argued that the demonstrated differences in femoral morphology between habitat groups were functionally significant, citing convergence between distantly related bovids occupying the same habitat type as evidence (Kappelman, 1991). I regard this point concerning adaptive convergence as critical for ecomorphology. Indeed, morphological convergence in distantly related taxa in similar ecological contexts provides the strongest possible evidence that a particular character is functionally related to that ecological

context. By explicitly considering the phylogenetic structure of a dataset, PGLS constitutes a formal statistical method for testing for this type of convergence.

It should be noted that in extreme cases where predictor variables and predicted categories both track the phylogeny very closely, it may be difficult to distinguish the results of functional adaptation from those of phylogenetic signal because the predictions of the competing hypotheses are similar. In these extreme cases, instances of convergent evolution are especially critical for demonstrating functional adaptation. However, the evolutionary history of a clade may result in few or no instances of convergence, thus leaving behind a sub-optimal phylogenetic structure for testing hypotheses (e.g., Garland et al., 1993). In such a case, strong phylogenetic autocorrelation in morphology has little bearing on whether functional adaptation has been at work. However, when functional adaptation is the alternative hypothesis for which evidence is being sought (as in ecomorphology) then lack of convergence may make it difficult to demonstrate that functional adaptation explains the data better than phylogenetic signal alone.

The main goal of this chapter is to assess the utility of DFA as a tool for making these distinctions, and to demonstrate how PGLS can be used to quantitatively test for significant functional convergence. While this chapter focuses on the case of bovid habitat prediction, the results should be relevant for any case in which variables contain phylogenetic signal.

METHODS

I simulated continuous variables that were either random with respect to the phylogeny, or were evolving according to a Brownian motion[4] model of trait evolution along the bovid phylogeny. To investigate the influence of body mass, I simulated characters that differed in their range of correlations with species-average body mass. For comparison, I also simulated characters with no phylogenetic signal and no correlation with body size. Thus, four pools of continuous characters were simulated with different levels of correlation to body size and with different levels of phylogenetic signal. Each pool of characters consisted of 10,000 characters. In subsequent analyses, subsets of each of these four character pools were drawn and analyzed with DFA and PGLS. Each character pool was analyzed using the actual habitat assignments (with and without size-correction) and with randomly chosen habitat assignments (with and without size-correction). This procedure yielded the 16 analyses listed in Table 2.1.

[4] Brownian motion is a process in which instantaneous character changes are random and independent from previous and subsequent changes (Felsenstein, 1985). The process is governed by a single instantaneous rate parameter σ^2, which represents instantaneous variance, *i.e.* how large any character change can be at a given point on the tree. Brownian motion is the simplest possible model of character evolution. Under Brownian motion simulations, taxa share similar character values in inverse proportion to their phylogenetic distance, measured as the sum of the branch lengths connecting their respective tips.

Character Pool	**Analytical Method**
$r = 0$ (no phylogenetic signal)	Size-corrected
$r = 0$ (no phylogenetic signal)	Raw data
$r = 0$ (phylogenetic signal)	Size-corrected
$r = 0$ (phylogenetic signal)	Raw data
high r (phylogenetic signal)	Size-corrected
high r (phylogenetic signal)	Raw data
low r (phylogenetic signal)	Size-corrected
low r (phylogenetic signal)	Raw data
$r = 0$ (no phylogenetic signal, random habitats)	Size-corrected
$r = 0$ (no phylogenetic signal, random habitats)	Raw data
$r = 0$ (phylogenetic signal, random habitats)	Size-corrected
$r = 0$ (phylogenetic signal, random habitats)	Raw data
high r (phylogenetic signal, random habitats)	Size-corrected
high r (phylogenetic signal, random habitats)	Raw data
low r (phylogenetic signal, random habitats)	Size-corrected
low r (phylogenetic signal, random habitats)	Raw data

Table 2.1: Sixteen analyses conducted in this chapter. One character pool has no phylogenetic signal and no correlation with body size. The three remaining character pools all have phylogenetic signal and vary only in the allowed range of r values. All four character pools were analyzed with body size-corrections, and without size-corrections, as well as with actual habitat assignments and random habitat assignments.

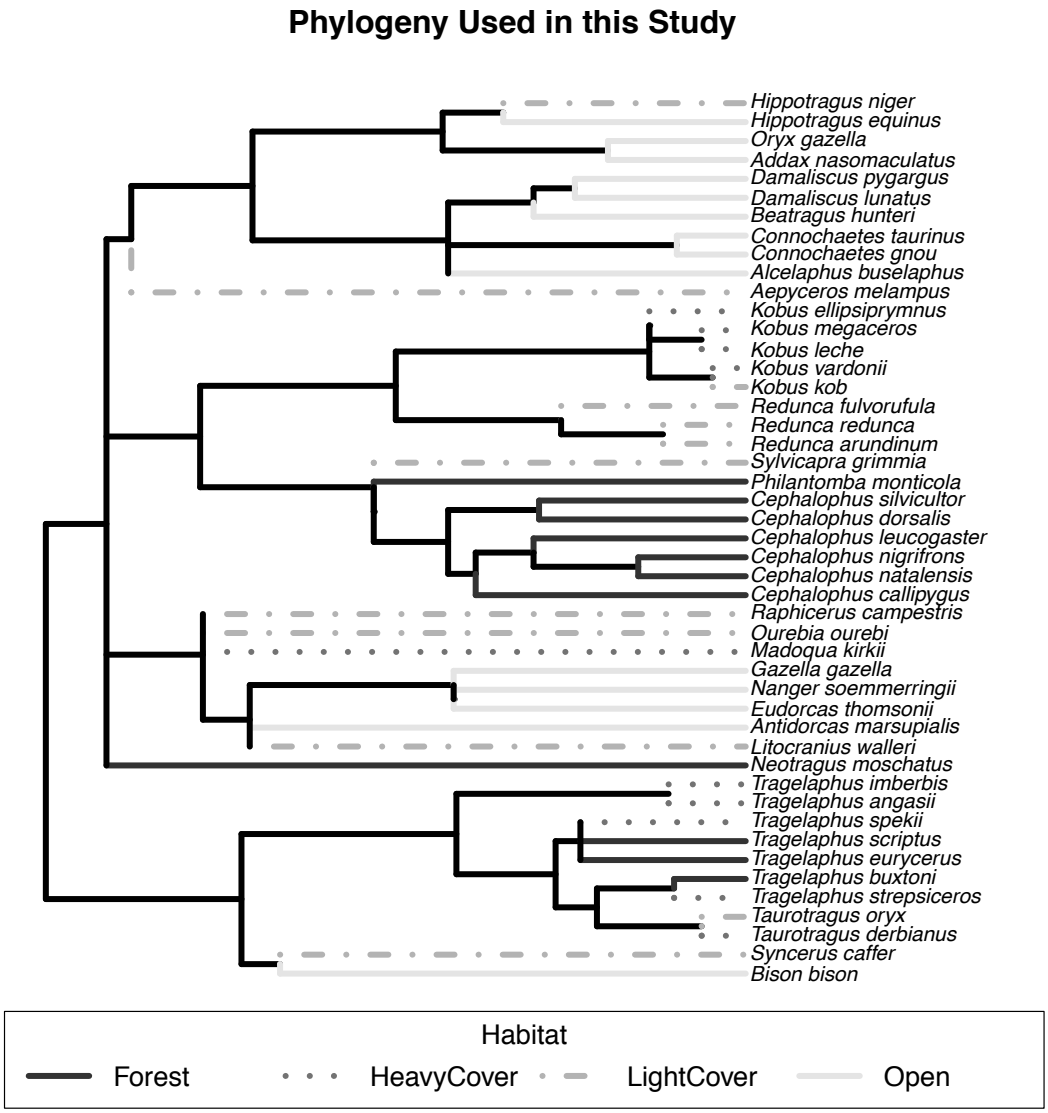

Figure 2.1: Bovid phylogeny used in this study. Taxonomy and the tree topology follow Hernandez-Fernandez & Vrba (2005). As detailed in the legend, each taxon is represented by a shaded dotted or solid line that indicates the habitat classification used in this study. Only the tips of the phylogeny are coded according to habitat. The solid lines deeper in the phylogeny (i.e. all edges besides the tip edges) do not reflect any hypothesis about ancestral states for habitat preference.

Mean Body Mass (kg)	Habitat	Taxon
94.7	Open	*Addax nasomaculatus*
52.3	Light Cover	*Aepyceros melampus*
164	Open	*Alcelaphus buselaphus*
33.2	Open	*Antidorcas marsupialis*
78.6	Open	*Beatragus hunteri*
620	Open	*Bison bison*
18.8	Forest	*Cephalophus callipygus*
20	Forest	*Cephalophus dorsalis*
13	Forest	*Cephalophus leucogaster*
12	Forest	*Cephalophus natalensis*
14.2	Forest	*Cephalophus nigrifrons*
61.3	Forest	*Cephalophus silvicultor*
154	Open	*Connochaetes gnou*
196	Open	*Connochaetes taurinus*
131	Open	*Damaliscus lunatus*
76.7	Open	*Damaliscus pygargus*
22.6	Open	*Eudorcas thomsonii*
21.2	Open	*Gazella gazella*
260	Open	*Hippotragus equinus*
234	Light Cover	*Hippotragus niger*
202	Heavy Cover	*Kobus ellipsiprymnus*
79.5	Light Cover	*Kobus kob*
87.4	Heavy Cover	*Kobus leche*
85.2	Heavy Cover	*Kobus megaceros*
71	Heavy Cover	*Kobus vardonii*
38.5	Light Cover	*Litocranius walleri*
4.77	Heavy Cover	*Madoqua kirkii*
41	Open	*Nanger soemmerringii*
5.6	Forest	*Neotragus moschatus*
186	Open	*Oryx gazella*
17.1	Light Cover	*Ourebia ourebi*
4.86	Forest	*Philantomba monticola*
11.6	Light Cover	*Raphicerus campestris*
57.7	Light Cover	*Redunca arundinum*
28.9	Light Cover	*Redunca fulvorufula*
42.7	Light Cover	*Redunca redunca*
15.5	Light Cover	*Sylvicapra grimmia*

Table 2.2: Taxa examined. Species mean body mass data (kg) comes from PanTHERIA database (Jones et al., 2009). Habitat classifications drawn from the sources in the text. Taxonomy follows Hernández-Fernández and Vrba (2005).

Table 2.2 continued

593	Light Cover	*Syncerus caffer*
643	Heavy Cover	*Taurotragus derbianus*
561	Light Cover	*Taurotragus oryx*
87	Heavy Cover	*Tragelaphus angasii*
215	Forest	*Tragelaphus buxtoni*
268	Forest	*Tragelaphus eurycerus*
93.3	Heavy Cover	*Tragelaphus imberbis*
43.3	Forest	*Tragelaphus scriptus*
75	Heavy Cover	*Tragelaphus spekii*
205	Heavy Cover	*Tragelaphus strepsiceros*

The phylogeny used for the simulations comes from the Hernández Fernández and Vrba (2005) ruminant supertree. I trimmed this tree to include 47 bovid species for which habitat characterizations in the literature were unambiguous (listed in Table 2.2). The trimmed phylogeny appears in Figure 2.1. Habitat preferences were compiled from several sources (Kingdon, 1974; Estes, 1992; Kappelman et al., 1997; Nowak, 1999; Scott, 2004; Skinner and Chimimba, 2006; Kovarovic and Andrews, 2007). The habitat classification scheme follows prior studies (Kappelman et al., 1997; Scott et al., 1999) in recognizing four ordered categories defined in terms of degree of canopy cover: forest, heavy cover, light cover, and open habitats. Species-mean body mass data comes from the PanTHERIA database (Jones et al., 2009). All simulations and analyses were performed using the R Statistical Programming Language version 2.15.1 (R Development Core Team, 2011). All figures except the phylogenetic tree were created using ggplot2 package for R, version 0.9.3.1 (Wickham, 2009).

I simulated morphometric variables with phylogenetic signal as follows. In these simple simulations, there are only two factors influencing trait values: a body size component (**M**) plus a Brownian motion component (**B**).

Eq 1: $y = r \times \mathrm{M} + \sqrt{(1 - r^2)} \times \mathrm{B}$

Equation 1 shows the derivation of measurement y for taxon x. In Equation 1, r is the correlation coefficient between body size and the simulated variable y. M is the body mass, measured as the natural log of species mean body mass (kg) for taxon x. Analogous to a regression model, r^2 is the proportion of the variance in y that can be attributed to body size. The remainder ($1 - r^2$) is independent from body size, and therefore in these simulations is attributable to Brownian motion. The B component was computed using the fastBM() function in the *phytools* package version 0.2-0 (Revell, 2012).

To sample random deviates from a population with this variance structure, I multiplied the body size values by $\sqrt{r^2} = r$ and the Brownian components for each taxon by $\sqrt{(1 - r^2)}$. The R code for simulating a single character is given in Appendix A. All of the R code for doing the simulations, analyses, and figures is available online (https://github.com/wabarr/DFA-phylosim).

Simulation parameters

The first character pool **r=0 (no phylogenetic signal)** is a special case, because it lacks phylogenetic signal. The character pool was produced by drawing characters from a normal distribution with mean = 100 and standard deviation = 5. Experimenting with different values confirmed that the choice of values for the mean and the standard deviation did not affect the DFA classification success of subsequent analyses.

The three remaining character pools were modeled with phylogenetic signal using Equation 1. These character pools differed in their values for the parameter r, (the correlation coefficient between a trait and species-average body mass). The special case **r=0 (no phylogenetic signal)** character pool was simulated with no correlation to body

mass, and no Brownian motion component. The **r=0 (phylogenetic signal)** pool was simulated with *r* set to 0 for all variables. Substituting 0 for *r* in Equation 1 eliminates any influence of body mass, and the resulting variable consists purely of Brownian motion. The **low r** character pool included variables exhibiting low correlation with body size. Often, ratios of two measurements (e.g. length / width) are used in ecomorphological studies. These ratios typically have a low but non-zero correlation with body size. Because different traits may have different correlation coefficients with respect to body size, I assigned values of *r* that were sampled from a uniform distribution with a minimum of 0 and a maximum of 0.45. This range approximates the range of correlation coefficients observed in ecomorphological studies that use ratios with low body size correlation (e.g. Kappelman, 1988; Plummer and Bishop, 1994; Kappelman et al., 1997). The **high r** character pool was formulated to simulate the use of raw characters that exhibit very high correlations with body mass (e.g. Degusta & Vrba, 2003). I assigned values of *r* sampled from a uniform distribution with a minimum of 0.8 and a maximum of 1.0, which reflects a biologically reasonable range of correlation coefficients for raw morphometric variables.

I used the natural log of species-mean body mass (kg) as an estimate of the body size component, M. The Brownian motion component, B, was calculated using the fastBM() function from the *phytools* package version 0.2-0 (Revell, 2012). This function requires an estimate of the Brownian motion instantaneous rate parameter σ^2. Previous studies have shown that the mean squared value of the Phylogenetic Independent Contrasts (PICs) for a variable over a given phylogeny provides an unbiased estimator of σ^2 (Garland, 1992; Revell, 2008; Mahler et al., 2010). PICs for logged body mass were computed using the function pic() from the *ape* package version 3.0-1 and used to calculate the estimate for σ^2.

Statistical Analysis

For each of the 16 distinct analyses in Table 2.1, I performed the following steps.

1. A subset of 7-12 variables was drawn from the appropriate pool of characters. Each subset of 7-12 characters represents the measured continuous variables in an ecomorphological analysis.
2. A single DFA on the discriminability of habitats was conducted on this subset of 7-12 variables. The statistical significance of the DFA was accessed and recorded, as well as the percentage of correct habitat assignments.
3. PGLS was conducted on each character individually against the habitat category.
4. Steps 1-3 were repeated 2000 times.
5. The average performance of DFA and PGLS over the 2000 iterations was assessed.

The number of characters drawn per subset (7-12) spans the range of characters used in most published ecomorphological studies (Kappelman, 1991; Plummer and Bishop, 1994; Kappelman et al., 1997; Scott et al., 1999; DeGusta and Vrba, 2003, 2005; Kovarovic and Andrews, 2007; Plummer et al., 2008). Characters were sampled for each subset without replacement, so each character could only appear once in each subset. Characters were replaced between rounds of sampling so that any character was free to appear in multiple subsets.

In analyses where body size corrections were applied, each variable was divided by the geometric mean of all variables in the subset (Jungers et al., 1995). I computed the natural logarithm of the resulting variables to improve normality.

Linear DFA was performed on each subset of 7-12 characters using the lda() function from the *MASS* package version 7.3-16. Wilks' lambda was computed to assess the statistical significance of the DFA. The classification performance was evaluated using two validation techniques: resubstitution and cross-validation (Manly, 2004). Resubstitution simply classifies the entire training set using the single DFA created from the same training set and computes the percentage of successful classifications. Using cross-validation, the classification for each specimen is achieved by withholding the specimen, calculating a new DFA using the remaining individuals, and using the resulting DFA to classify this specimen.

PGLS was conducted on each of the variables individually with respect to the habitat variable using the pgls() function in the *caper* package version 0.5 (Orme et al., 2011). Because the habitat variable is categorical, this procedure can be thought of as analogous to a phylogenetic ANOVA. However, the underlying mechanics rely on dummy coding the categorical variable into several binary variables, and this use of the pgls() function is completely distinct from the Monte Carlo-based phylogenetic ANOVA of Garland *et al*. (1993). The significance of the PGLS was assessed by the overall p-value of the model. Note that 7-12 PGLS analyses were conducted for each subset (i.e., one PGLS for each character), as compared to a single DFA for each subset. Thus, the odds of finding a significant result are significantly increased due to these multiple hypothesis tests. Thus, I also applied the False Discovery Rate (FDR) technique as a correction for multiple hypothesis tests (Benjamini and Hochberg, 1995). FDR is a widely implemented technique for dealing with multiple hypothesis tests. FDR is significantly less conservative than the Bonferroni correction, which is well known to be overly conservative (Rice, 1989). PGLS was judged to be statistically significant if the FDR corrected overall p-value was less than 0.05.

Dataset	Analytical Method	% DFA significant	mean % success (resubstitution, cross-validation)	PGLS Type I error Rate	PGLS Type I error rate with FDR
r = 0 (no phylogenetic signal, actual habitats)	Size-corrected	4.78%	55.43% , 25.4%	6.67%	1.16%
r = 0 (no phylogenetic signal, actual habitats)	Raw Data	4.47%	55.2% , 25.47%	6.65%	1.29%
r = 0 (phylogenetic signal, actual habitats)	Size-corrected	38.82%	61.24% , 34.44%	12.77%	4.15%
r = 0 (phylogenetic signal, actual habitats)	Raw Data	40.30%	61.33% , 34.5%	12.79%	4.28%
high r (phylogenetic signal, actual habitats)	Size-corrected	33.27%	60.71% , 33.39%	12.42%	3.78%
high r (phylogenetic signal, actual habitats)	Raw Data	36.82%	60.66% , 33.81%	0.14%	0.02%
low r (phylogenetic signal, actual habitats)	Size-corrected	39.55%	61.45% , 34.42%	12.82%	4.08%
low r (phylogenetic signal, actual habitats)	Raw Data	45.07%	61.93% , 35.49%	13.19%	4.64%
r = 0 (no phylogenetic signal, random habitats)	Size-corrected	5.62%	25.21% , 25.05%	7.40%	1.56%
r = 0 (no phylogenetic signal, random habitats)	Raw Data	5.42%	24.98% , 24.89%	7.13%	1.46%
r = 0 (phylogenetic signal, random habitats)	Size-corrected	5.53%	24.59% , 25.07%	8.01%	1.92%
r = 0 (phylogenetic signal, random habitats)	Raw Data	4.85%	25.03% , 24.84%	8.07%	1.92%
high r (phylogenetic signal, random habitats)	Size-corrected	3.78%	25.07% , 24.75%	8.26%	2.06%
high r (phylogenetic signal, random habitats)	Raw Data	5.25%	25.17% , 24.85%	7.75%	3.85%
low r (phylogenetic signal, random habitats)	Size-corrected	5.08%	24.79% , 25.12%	7.74%	1.64%
low r (phylogenetic signal, random habitats)	Raw Data	5.03%	24.7% , 24.88%	8.19%	1.86%

Table 2.3: Results of all analyses. For each dataset and analytical method, I report the percentage of DFAs that were statistically significant according to Wilkes' lambda, the mean DFA correct classification rates (using resubstitution and cross-validation), the PGLS Type I error rate (*i.e.* the percentage of PGLS analyses significant at $p <= 0.05$), and the PGLS Type I error rate after applying the False Discovery Rate (FDR) method of accessing significance with multiple hypothesis tests.

RESULTS

I present the results of all 16 analyses in Table 2.3. I report the percentage of DFAs that were statistically significant according to Wilks' lambda, the DFA correct classification rates, the PGLS Type I error rate (i.e. the percentage of PGLS analyses that were statistically significant at $p<0.05$), and the PGLS Type I error rate after applying the FDR correction.

DFA Results

The analyses showed dramatic differences in the percentage of the DFAs that were statistically significant according to Wilks' lambda. Using actual habitats, fewer than 5% of the DFAs were statistically significant with the $r = 0$ (no phylogenetic signal) character pool, regardless of body size correction. Analyses using the three remaining character pools containing phylogenetic signal showed elevated proportions of statistically significant DFAs when using actual habitats. For the high r character pool, 33.3% and 36.8% of the DFAs were significant for the size-corrected and raw data analyses, respectively. Slightly higher rates of statistical significance were obtained from the low r character pool, with 39.6% and 45.1% of DFAs showing significance for the size-corrected and raw data analyses, respectively. For analyses using the $r = 0$ (phylogenetic signal) character pool, 38.8% and 40.3% of the DFAs showed statistical significance for the size-corrected and raw data analyses, respectively.

In general, DFAs using actual habitats were statistically significant most often when phylogenetic signal was maximized (i.e. $r = 0$ or r was low and therefore variables reflected mostly phylogenetic signal). DFAs using raw data were statistically significant slightly more often than DFAs using size-corrected data.

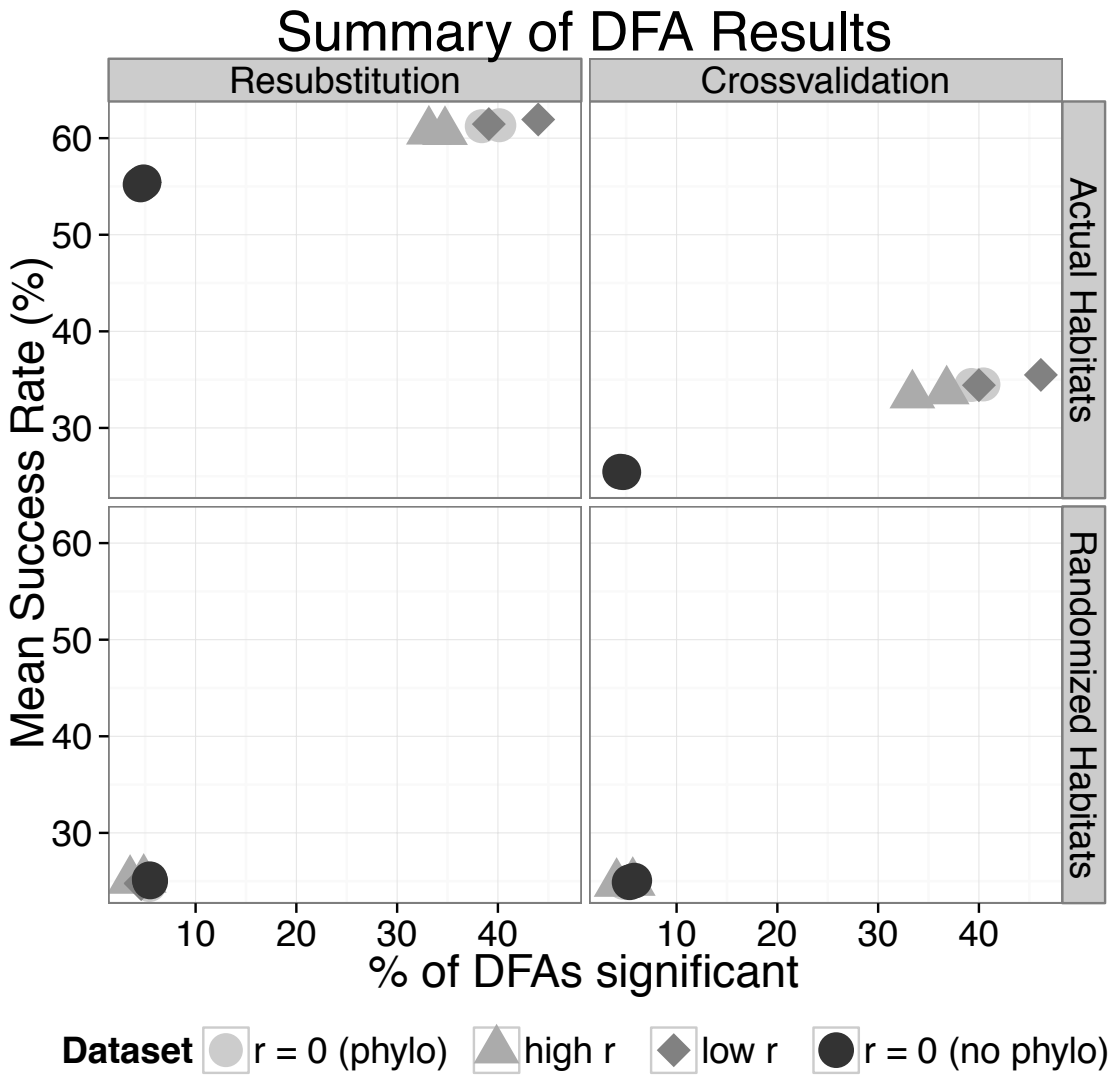

Figure 2.2: Summary plots showing mean DFA success rates on the vertical axis and the percentage of DFAs that were statistically significant on the horizontal axis. The four subplots separate results by the validation method used (resubstitution or cross-validation) and by the method of habitat assignment (actual habitats or randomized habitats). The legend identifies the level of phylogenetic signal in the dataset. For clarity, raw-data and size-corrected analyses are not differentiated in the legend. Thus, each quadrant contains two points for every symbol in the legend, but some symbols plot on top of one another.

The DFA classification results are presented graphically in Figure 2.2. Mean rates of correct habitat assignment are given on the vertical axis, and the percentage of significant DFAs is given on the horizontal axis. This figure illustrates several important points regarding DFA success rates. First, when habitats are randomized, DFAs are rarely significant (< 5.6% of cases). Furthermore, with randomized habitats, classification accuracies are extremely consistent at approximately 25%, which represents the logical expectation for random chance assignments when there are four habitat categories. In other words, in all analyses with randomized habitats, DFA has neither inflated rates of significance, nor inflated classification accuracies.

These results contrast to analyses using the actual habitats, in which only the r = 0 (no phylogenetic signal) character pool shows levels of statistical significance below 5%. All other analyses showed high rates of statistical significance, as well as classification accuracies that are consistently above the random expectation of 25%. Figure 2.2 also demonstrates very pronounced differences in the performance of the two techniques of validation: cross-validation and resubstitution. Whenever actual habitats are used, resubstitution produces dramatically higher classification success rates (60.66% - 61.93%) than does cross-validation, although cross-validation still results in classification success rates (33.39% - 35.49%) that are consistently higher than the random expectation of 25%.

I present a subset of the DFA classification results (size-corrected, actual habitats) in Figure 2.3. When actual habitats are used, the only case in which classification success rates approximate the random expectation (25%, indicated by a dotted horizontal line in Figure 2.3) is when crossvalidation is used on the r = 0 (no phylogenetic signal) character pool. Figure 2.3 clearly illustrates the effect of increasing the number of characters used in the DFA on the classification accuracy. Increasing the number of

characters in the DFA results in increased correct classification rates, especially when resubstitution is the validation method. This positive correlation has been noted previously in other ecomorphological studies (Scott, 2004; Kovarovic and Andrews, 2007; Kovarovic et al., 2011).

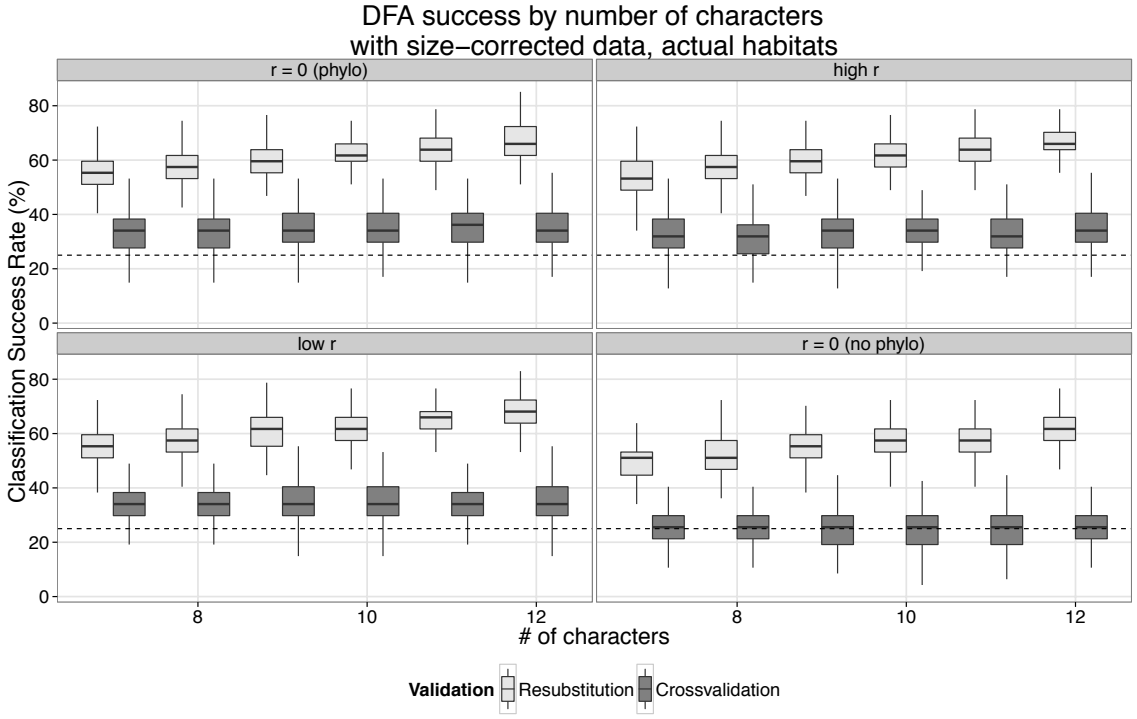

Figure 2.3: Plots showing DFA success rates as a function of the number of characters used. The vertical axis shows success rates of size-corrected DFAs using actual habitat assignments. The horizontal axis shows the number of characters used in the DFA. Dashed line indicates the 25% success rate expected for random habitat assignment. The legend identifies the validation method used: resubstitution or cross-validation.

PGLS Results

The results of the PGLS analyses are presented in Table 2.3. In analyses using actual habitats, raw PGLS Type I errors are in the range of 6.65% - 13.19%, with the exception of the high r raw-data analysis, which has a much lower error rate of 0.14%. When False Discovery Rate (FDR) corrections are applied, to control for multiple hypothesis tests, the Type I error rates drop to the range of 1.16% - 4.64%, with the high r raw-data analysis again being an outlier at 0.02%. Using randomized habitats, the Type I error rate was very stable, in the range of 7.13% - 8.26%, with an FDR corrected range of 1.46% - 3.85%.

DISCUSSION

In this chapter, I present results of analysis of simulated continuous characters evolving at random, as well as continuous characters evolving along a bovid phylogeny by Brownian motion. In all cases, the simulated characters lacked a biomechanical relationship to the habitat categories, though these categories were strongly related to phylogeny.

Results demonstrate that, when using actual habitat assignments and predictor variables with phylogenetic signal, DFAs were statistically significant in 33% - 45% of cases. DFA was rarely significant when there was no phylogenetic signal in the predictor variables and/or when the habitat assignments were randomized. In terms of correct classification rates, DFA using resubstitution always dramatically outperformed random category assignment, even when predictor variables were simply random noise. With randomized habitats, the correct classification rates using either cross-validation or resubstitution approximated random expectations (25%). When using cross-validation and actual habitats, DFA performance approximated random category assignment for random variables with no phylogenetic signal. The correct classification rate of DFAs

with actual habitats dramatically increased in cases in which phylogenetic signal was present in the predictor variables, whether cross-validation or resubstitution was used. These DFAs had a mean rate of classification success of approximately 61% using resubstitution and 34.3% using cross-validation. These rates represent 2.44 and 1.37 times the correct classification rate expected from random chance habitat assignments (25%). Thus, resubstitution clearly overestimates the discriminability between groups. Body size-corrections have only a subtle impact on the classification success rates of DFA. PGLS had acceptable levels of Type I error in all analyses when FDR corrections were applied to control for multiple hypothesis tests.

These results suggest that DFA has some significant limitations when used to test for functional relationships because the method returns highly significant classification results in 33% - 45% of simulated cases where predictor variables and the habitat category both possessed phylogenetic signal. PGLS with FDR corrections on these same data are only rarely significant (<5%). In practice, a lack of significance in the PGLS results would alert a researcher that the relationship between the variables might be explainable by phylogenetic signal alone, while the DFA results could offer no such warning.

DFA produces relatively high classification success rates on these simulated data because the purpose of DFA is to detect differences between groups without regard to the source of those differences. The DFAs in this simulation study identified differences between species in different habitat categories; however, the source of those differences was largely phylogenetic signal. The critical points for ecomorphology are 1) that DFA is not capable of detecting the source of differences between groups and 2) that non-independence among data points can lead to overestimates of discriminability of groups

(Mundry & Sommer, 2007). PGLS with FDR corrections can alert the researcher that differences between habitat groups might be explainable by phylogenetic signal.

In ecomorphology, we are interested in testing hypotheses regarding functional adaptation in specific ecological contexts. As suggested by previous authors (Kappelman, 1991), adaptive convergence between distantly related species in the same ecological context provides the strongest evidence for functional adaptation. In this chapter, I tested for such convergence in the simulated data using PGLS. In contrast to the DFA results, the PGLS analyses with FDR corrections in this study were quite successful at correctly accepting the null hypothesis of no biomechanical relationship between the simulated variables and the predicted categories. This is not surprising, as PGLS is specifically designed to take into account phylogenetic distances between taxa, and to test for the presence of convergence in excess of what would be expected based on phylogenetic signal alone.

Some of the simulations in this chapter used a randomized habitat variable to model cases in which an ecological categorical variable does not possess phylogenetic signal. An important result from these simulations is that the problem of DFA over-performance disappeared. This finding suggests that phylogenetic signal must be present in the continuous predictor variables ***and*** the categorical predicted variables in order to incur the risk of DFA over-performance that is highlighted in this chapter. One consequence of this finding is that, if the possibility of phylogenetic signal in the categorical variable can be eliminated, then the need to control for phylogenetic signal in the predictor variables is diminished dramatically, at least insofar as DFA over-performance is concerned. Thus, testing for phylogenetic signal in categorical ecological variables may be desirable, especially when evaluating existing DFAs in the literature that were performed before phylogenetic comparative methods were available.

Methods of testing for phylogenetic signal in discrete characters are less straightforward than methods for continuous characters. I present one example of how this might be done in Appendix B. This method was suggested by Pagel (1994) and the necessary tools are available in the R package *geiger* (Harmon et al., 2008). The method is based on a likelihood ratio test comparing continuous-time Markov models of discrete character evolution for categorical variables under a given phylogeny against the same model with an equal-branch lengths star phylogeny (eliminating phylogenetic signal). In the case of the bovid phylogeny used here, this method suggests that phylogenetic signal is indeed present for the actual habitat categories and that it disappears when habitat categories are randomized (see Appendix B). This method could be adapted to test for phylogenetic signal in categorical variables in previously published studies.

Based on these simulation results, I would argue that PGLS with FDR corrections has some advantages as compared to using DFA in isolation. In particular, the ability of PGLS to explicitly evaluate the phylogenetic structure of the dataset, and to search for convergence in excess of phylogenetic expectations is lacking in DFA. Thus, PGLS is a very useful tool for demonstrating a functional relationship between variables in advance of including the variables in DFA or any other method of categorical prediction. This process of vetting variables before inclusion in a DFA is critical because DFA in isolation is not well suited for testing functional hypotheses in an evolutionary framework, as illustrated by these simulations.

These results do not imply, nor am I suggesting, that any previously published ecomorphological DFA results are driven solely or predominantly by phylogenetic signal. In fact, I strongly suspect that many ecomorphological predictions are rooted in functionally well-characterized character complexes that have robust functional links to their ecological context. Indeed, the classification success rates of most published

ecomorphological DFAs exceed the success rates observed in my simulations. I would caution, however, against using these results as a baseline of comparison for evaluating the success of other DFAs, because the rates of correct classification achieved will vary depending on which taxa are included and on which phylogenetic tree is used. These simulations demonstrate that a variety of factors besides functional signal can affect DFA success rates, including phylogenetic signal and the number of characters used. I advocate that characters should be functionally validated in advance using PGLS with FDR corrections and that DFA only be used as a classifying algorithm after validation.

While the goal of this study is to demonstrate the importance of selecting a method capable of sorting out functional and phylogenetic influences, I am not suggesting that morphological patterns reflecting shared phylogenetic history are not meaningful. Indeed morphological patterns that track phylogeny are absolutely critical for taxonomic and phylogenetic purposes. However, ecomorphology aims to deduce ecological categories based on biomechanical links to function, not based on phylogeny. Thus, it is important to use a tool that can effectively control for patterns expected based on phylogenetic history while testing for the presence of patterns reflecting functional adaptation.

Finally, the use of statistical methods controlling phylogenetic signal does not rule out the possibility that closely related species may evince similar morphology because natural selection has acted to conserve ecological function among closely related forms occupying the same habitat. However, if closely related taxa have experienced strong selection to conserve particular functions in particular ecological contexts, then closely related taxa in similar contexts should be *even more similar* than would be predicted based on phylogenetic distance alone. This phenomenon is discussed in the ecological literature as phylogenetic niche conservatism, and its prevalence has been debated (Losos

et al., 2003; Wiens and Graham, 2005). Regardless of how common or rare phylogenetic niche conservatism is, it constitutes a hypothesis to be tested and distinguished from the null hypothesis of phylogenetic signal in direct proportion to evolutionary relatedness (Losos, 2008).

In summary, even when the null hypothesis is true and there is no biomechanical relationship between the ecological category and the measured variables, DFA commonly gives significant results that could be easily interpreted as reflecting a biomechanical signal that is, in fact, absent. The use of DFA in ecomorphology with no control for phylogenetic signal implies accepting *a priori* the assumption that phylogenetic niche conservatism is strong. However, this assumption of strong ecological conservatism in lineages is exactly the assumption that ecomorphology aims to avoid through the use of functional morphology to predict ecological traits, rather than making predictions based on taxonomic assumptions.

Phylogenetic comparative methods are designed to test for relationships between variables while controlling for phylogenetic signal in proportion to phylogenetic distance. This chapter demonstrates that PGLS with FDR corrections is highly effective at correctly accepting the null hypothesis when there is, in fact, no biomechanical relationship between a set of variables and the predicted category. Thus, these results suggest that PGLS with FDR corrections should be used to validate variables before inclusion in DFA or any other method of categorical prediction.

CONCLUSIONS

1. The presence of phylogenetic signal in both the predictor variables and the predicted category dramatically increases the likelihood of obtaining a statistically significant DFA.
2. In cases where predictor variables and predicted categories both possess phylogenetic signal, PGLS with FDR corrections is much more conservative than DFA. This leads to acceptable levels of PGLS Type I error and elevated levels of DFA Type I error in simulations in which predictor variables and predicted categories both possess phylogenetic signal.
3. Using resubstitution overestimates the discriminability of groups. Cross-validation should be preferred over resubstitution as a method for evaluating the success of DFA (Kovarovic et al., 2011).
4. PGLS with FDR corrections is well suited for evaluating functional signals in predictor variables. I suggest using PGLS to validate characters before inclusion in DFA or any other method of prediction. Or, to put the findings of this chapter most simply: First PGLS, then DFA.

Chapter 3: Functional morphology of the bovid astragalus in relation to habitat

In this chapter, I use the methodological framework outlined in Chapter 2 to analyze the functional morphology of the bovid astragalus in relationship to habitat. This chapter introduces a functional framework for interpreting bovid astragalar morphology, and tests several hypotheses about astragalar function. The related question of how to predict habitat preferences from astragalar morphology is taken up in Chapter 4.

INTRODUCTION

Bovid astragali are dense tarsal bones that are rarely destroyed by carnivore consumption (Brain, 1980) and are more resistant to hydraulic transport as compared to lighter, less dense elements (Behrensmeyer, 1975). These characteristics are favorable for preservation in the fossil record and, as a result, astragali are often the most abundant mammalian postcranial skeletal element in fossil collections (Hussain et al., 1983). Figure 3.1 illustrates the abundance of bovid astragali in the Omo Shungura fossil collection versus several other postcranial elements commonly used to infer habitat preference. As shown in the figure, bovid astragali offer a robust statistical sample for inferring past habitats, provided that the morphology of the astragalus is functionally linked to habitat preference. Habitat predictions based on fossil bovid astragali have been used to reconstruct paleoenvironments at sites relating to early hominin evolution. For example, interpretations of astragalar morphology played an important role in the *Ardipithecus* habitat reconstruction at the 4.4Ma site of Aramis in Ethiopia (White et al., 2009).

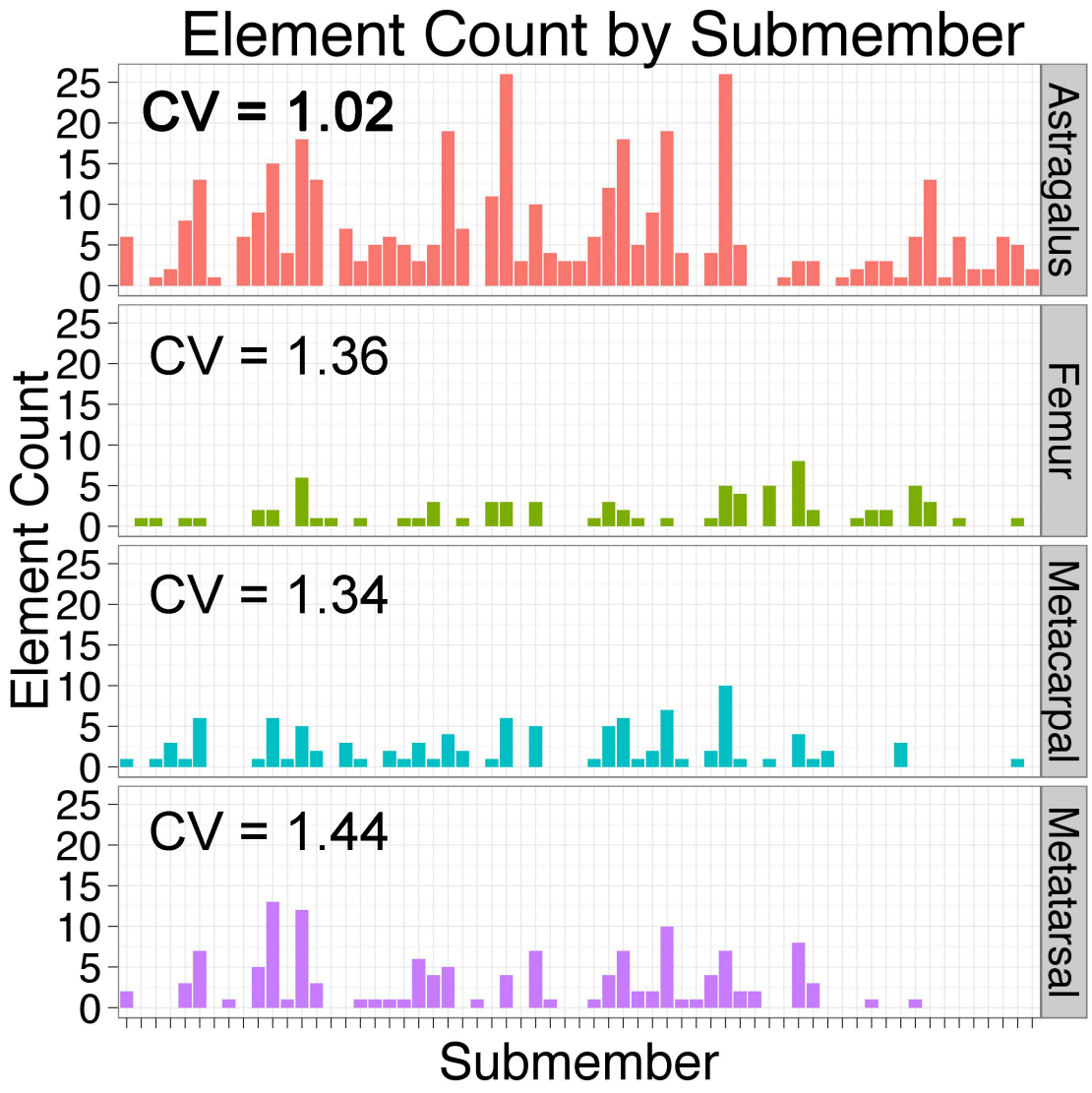

Figure 3.1: Plot of the abundance of postcranial elements by submember in the American collection of the Omo Shungura Formation. The plot illustrates how abundant astragali are relative to several other elements. Further, the plot illustrates that there is less variation in astragalar preservation through time, as shown by the lower coefficient of variation (CV).

To date, research on the ecomorphology of the bovid astragalus has been based upon raw measurements that were not corrected for body size and which were accompanied by little functional justification. Indeed, a recent study (Klein et al., 2010)

suggested that prior work on astragalar ecomorphology merely captured body size differences between habitat groups and that the morphology of the astragalus does not reflect meaningful functional signals related to habitat. Thus, the link between bovid astragalar morphology and habitat is poorly understood and disputed. In order to make reliable habitat predictions for fossils based upon astragalar morphology, these issues must be directly addressed. This chapter outlines a functional framework for interpreting the morphology of the bovid astragalus and for testing hypotheses relating astragalar morphology to habitat preference.

Bovid Ecomorphology and Habitat

Studies of bovid locomotor ecomorphology aim to link bony anatomy with habitat-specific locomotor regimes reflecting distinct predator avoidance strategies. Bovids occupying structurally open environments (e.g., grasslands) must flee from predators over open ground (Jarman, 1974). Thus, open-country cursors tend to have adaptations favoring rapid locomotion such as restricted rotational mobility in limb joints (Kappelman, 1988). Bovids occupying structurally closed environments (e.g., forests) face numerous physical obstacles to flight and must instead rely on crypsis to avoid predators (Jarman, 1974). As a result, closed-country bovids show fewer cursorial adaptations, and have a tendency towards increased rotational limb mobility, which is useful for negotiating complex locomotor substrates and winding forest paths (Kappelman, 1988).

Because bovids are abundant as fossils and many taxa are habitat specialists, researchers have used a variety of skeletal elements to infer bovid habitat preferences based on limb morphology hypothesized to relate to cursoriality in open-country cursors and joint mobility in species occupying closed-country habitats (Kappelman, 1988, 1991;

Plummer and Bishop, 1994; Kappelman et al., 1997; Scott et al., 1999; Kovarovic and Andrews, 2007).

It is important to note that, as a taxonomic family all bovids posses skeletal features linked to cursoriality in their common ancestor (Schaeffer, 1947). Nonetheless, extant bovids exhibit considerable variation in the degree to which they rely on cursoriality as a predator avoidance strategy. These differences in predator avoidance should be reflected in the anatomy of the ankle joint because highly cursorial bovids are subjected to strong natural selection pressure from cursorial carnivore predators (Jarman, 1974). Accordingly, even within the generally cursorial bovid bauplan, open-country bovids are expected to possess more extreme adaptations for decreased rotational mobility and rapid fore-aft limb velocities compared to closed-country bovids (Gentry, 1970; Kappelman, 1988; Hildebrand and Goslow, 2001; Plummer et al., 2008).

Three main studies examining bovid astragalar ecomorphology have been published (DeGusta and Vrba, 2003; Weinand, 2007; Plummer et al., 2008). These studies have focused on creating Discriminant Function Analyses (DFAs) for predicting habitat preference, but none has explicitly tested functional hypotheses regarding links between bovid astragalar morphology and habitat preference.

Degusta and Vrba (2003) collected eight caliper measurements and used raw (not size-corrected) measurements to produce a Discriminant Function Analysis (DFA) that correctly classified 67% of their extant sample into known habitat categories. These authors avoided any discussion of how their measurements might be related to differences in locomotor function (Degusta and Vrba, 2003:1018) and the functional relevance of this measurement scheme is thus unclear.

The study by Weinand (2007) reexamined a subset of measurements used by Degusta and Vrba, and extended the comparative dataset to include Southeast Asian

bovids. This study focused on comparing classification accuracies of parametric versus non-parametric methods to predict habitat preferences using the measurement scheme established by Degusta and Vrba (2003). Weinand concluded that both parametric and non-parametric methods produced similar classification accuracies, and that a combination of parametric and non-parametric methods produced the highest accuracy.

Plummer and colleagues (2008) published an ecomorphological study comprising many measurements similar to those of Degusta and Vrba (2003). However, Plummer et al. used a larger set of 24 measurements and subsequently selected seven ratios and four raw (not size-corrected) measurements selected specifically because they maximized the success rate of the DFA. This augmented set of measurements resulted in a much higher DFA classification success (87%) than was achieved by Degusta and Vrba (67%). However, DFA success rates are related to other factors besides functional signal including: phylogenetic signal, body size signal, and the number of measurements used to create the DFA (Kovarovic et al., 2011; Barr and Scott, 2014, and see Chapter 2). Thus, it is not clear how well this measurement scheme captures functionally relevant variation in the bovid astragalus.

Most recently, Klein and colleagues (2010) addressed astragalar ecomorphology in a paper concerned primarily with the use of bovid metapodial morphometrics for taxonomic identification. These authors conducted Principal Components Analysis (PCA) on metapododials and noted that, in PCA plots, individuals tended to cluster by genus rather than by habitat preference. The paper also included a brief comment regarding Klein and colleagues' reanalysis of Degusta and Vrba's (2003) astragalar dataset. The PCA results of Klein and colleagues demonstrated that the first principal component (PC1) of the astragalar dataset explained 98.6% of sample variance and correlated nearly perfectly with a body size proxy (geometric mean of all linear

measurements). PC2 was interpreted to reflect size-free shape variation, which explained a mere 0.53% of the variance. Furthermore, Klein et al. argued that the shape component did not discriminate well between bovids from different habitat groups. Klein and colleagues argued that the measurement schemes of Degusta & Vrba (2003) and, by extension, the similar scheme from Plummer et al. (2008) captured virtually no size-independent shape differences in bovid astragali from different habitats. They suggested that ecomorphology based on these measurement schemes would predict habitat preferences only insofar as bovids from different habitats differ in body size (Klein et al., 2010).

Thus, there are currently questions surrounding the use of the astragalus as an ecomorphological predictor element. Previous work could be interpreted to suggest that the morphology of the astragalus is developmentally canalized, implying that there is too little functionally meaningful variation in the astragalus to successfully sort taxa by habitat. However, while body size clearly plays a major role, the literature lacks a systematic analysis of bovid astragalar morphology that controls for body size differences. Therefore, the functional link between astragalar morphology and habitat remains unclear.

Furthermore, no prior study of bovid astragalar morphology has statistically controlled for the potential impact of phylogenetic signal on the relationship between morphology and habitat preference. Bovid habitat preferences are intimately intertwined with their phylogeny, as habitat preference in bovids is highly conserved at the level of taxonomic tribe (Vrba, 1980; Greenacre and Vrba, 1984; Kappelman, 1984; Shipman and Harris, 1988). Additionally, many morphological measurements used as ecomorphological predictors possess phylogenetic signal (Scott and Barr, In Press), which means that individuals with close phylogenetic relationships tend to possess trait

values that are more similar to one another than to randomly chosen individuals (Münkemüller et al., 2012). This situation creates analytical issues; indeed, a large body of literature has demonstrated that treating species as independent data points without controlling for phylogenetic signal can lead to erroneous interpretations regarding character correlations (Felsenstein, 1985; Harvey and Pagel, 1991; Martins and Garland, 1991; Garland et al., 1993; Garland and Carter, 1994; Nunn and Barton, 2001; Rohlf, 2006; Revell, 2009). The issue of greatest concern raised in the comparative methods literature is the increased rate of Type I error (*i.e.,* more frequent false positive results) when phylogenetic signal is not controlled statistically (Rohlf, 2006).

The multivariate technique used in previous studies, DFA, is an extremely useful technique for classifying specimens into categories defined *a priori*. However, the technique is not well suited for identifying the source of differences between predicted categories (Chapter 2; Barr and Scott, 2014). Therefore, even while previous authors have published DFAs that predict habitat categories, these results remain open to question by researchers suggesting that a majority of the morphological variation between bovids from different habitats is related only to body size differences or phylogenetic signal (Klein et al, 2010). In order to address these issues, the current study employs phylogenetic comparative methods to control for both body size and phylogenetic signal while testing explicit functional hypotheses relating the morphology of the bovid astragalus to habitat.

FUNCTIONAL MORPHOLOGY OF THE BOVID HOCK (ANKLE)

The astragalus of most mammals has a single proximal trochlea for articulation with the tibia and a rounded distal head for the navicular. This primitive condition is common in a wide variety of modern and fossil mammals. Figure 3.2 contrasts the

Paleocene condylarth *Arctocyon*, which evinces the primitive configuration, with *Ovis*, a modern sheep displaying the derived condition found in artiodactlys. Artiodactyls possess the typical proximal tibial trochlea, but additionally possess a trochleated distal head that articulates with both the navicular and cuboid, which are fused in bovids. Thus, the artiodactyl astragalus serves as a double hinge joint between the metatarsus and the tibia. Compared with other mammals, artiodactyl astragali have a more deeply excavated tibial trochlea fitting tongue-in-groove with the deeply excavated distal tibia (Schaeffer, 1947). Artiodactyls also possess a sagittally reoriented astragalocalcaneal facet. This reorientation dramatically reduces inversion and eversion and largely restricts ankle motion to the antero-posterior (parasagittal) direction (Schaeffer, 1947). This reorientation stabilizes the joint and has been interpreted as an adaptation for cursoriality in the earliest fossil artiodactyls (Schaeffer, 1948).

Plantarflexion and dorsiflexion of the foot with respect to the distal tibia is achieved by a combination of motion across two main joints: the upper ankle joint between the tibia and the astragalus and the transverse tarsal joint between the astragalus and the cubonavicular (see Figure 3.3). Motion is also possible at the lower ankle joint between the astragalus and the calcaneus; the action of this joint will be discussed further in the next section. The axes of rotation about the upper ankle and transverse tarsal joints are essentially parallel, such that the composite motion of the artiodactyl hock is restricted to an antero-posterior hinge motion (Schaeffer, 1947).

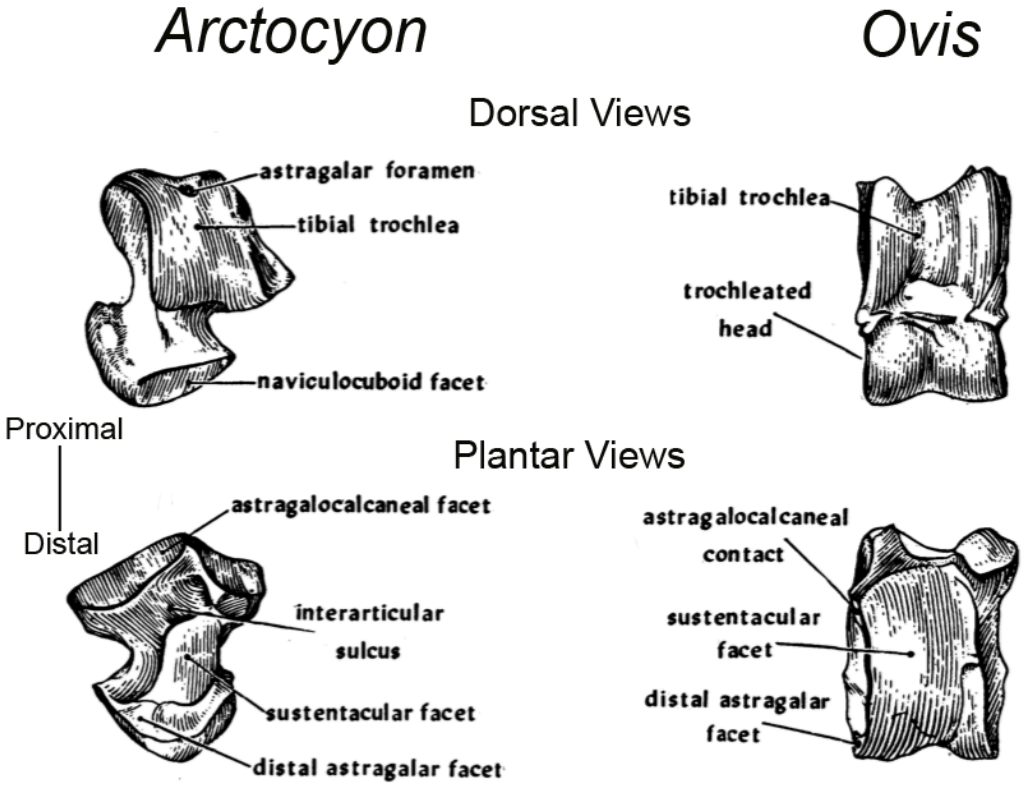

Figure 3.2: Comparison of the astragalus of *Arctocyon*, an arctocyonid condylarth from the Paleocene, and *Ovis*, a modern sheep. *Arctocyon* evinces a single tibial trochlea, rounded head, and an astragolocalcaneal facet that is essentially coplanar with the sustentacular facet. *Ovis* exemplifies the derived artiodactyl condition with a trochleated head and an astragalocalcaneal facet that is nearly orthogonal to the sustentacular facet. Modified from Schaeffer (1948) his Figure 3. Note: Schaeffer referred to *Arctocyon* by a synonym, *Claenodon*.

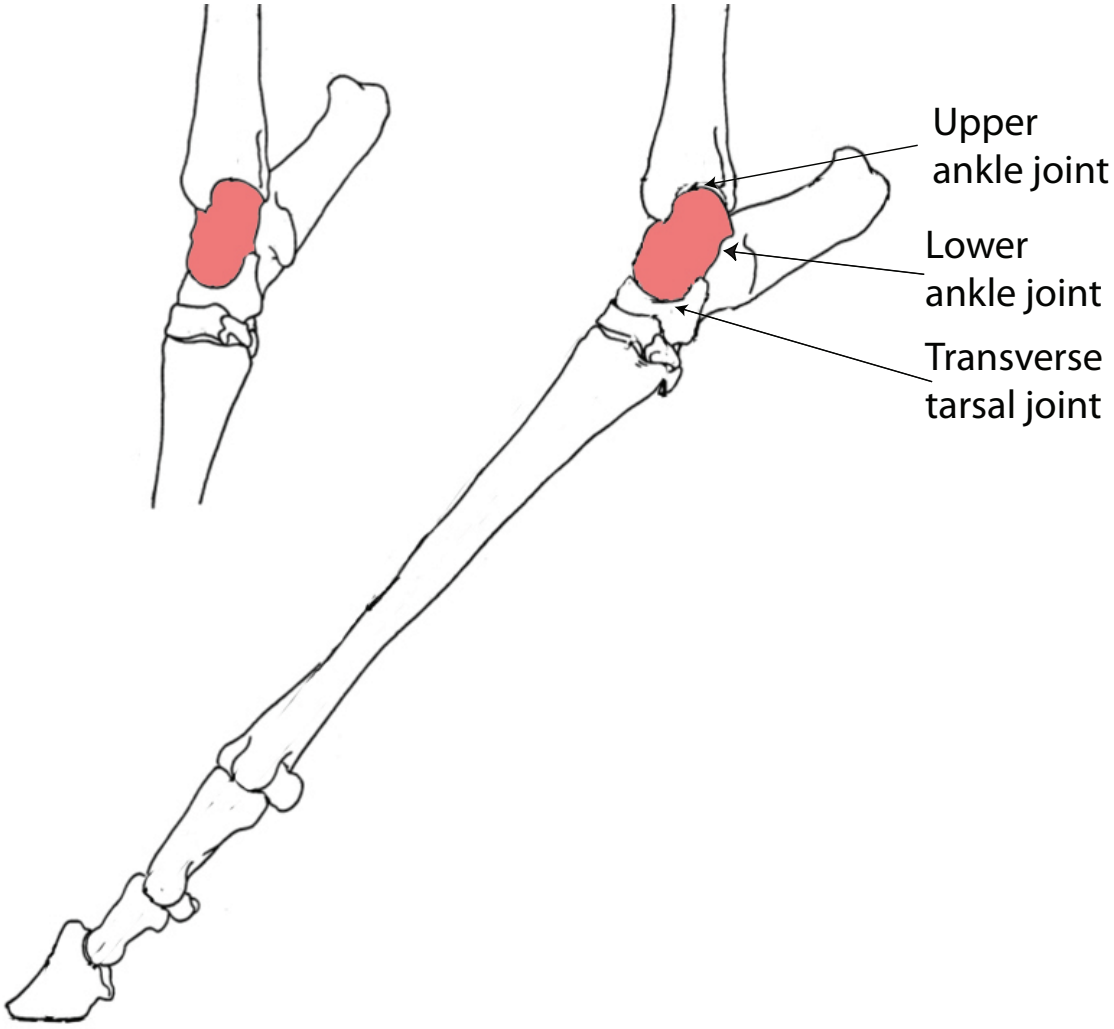

Figure 3.3: Position of the astragalus in the bovid hindlimb in two states of flexion. Modified from Schaeffer (1947: his Figure 9). The astragalus is filled in gray. Three joints are labeled: the upper ankle joint between the tibia and the astragalus, the lower ankle joint between the astragalus and the calcaneus, and the transverse tarsal joint between the astragalus and the cubonavicular.

Ignoring for a moment the distinct axes of rotation at the upper ankle and transverse tarsal joint, the composite action of the hock joint in the sagittal plane may be viewed as a simple first class lever system, with the calcaneus comprising the lever (force) arm for the hock plantarflexors, the length of the remaining tarsals, metatarsal,

and phalanges constituting the load (resistance) arm, and the astragalus serving as the fulcrum or center of rotation (see Figure 3.4).

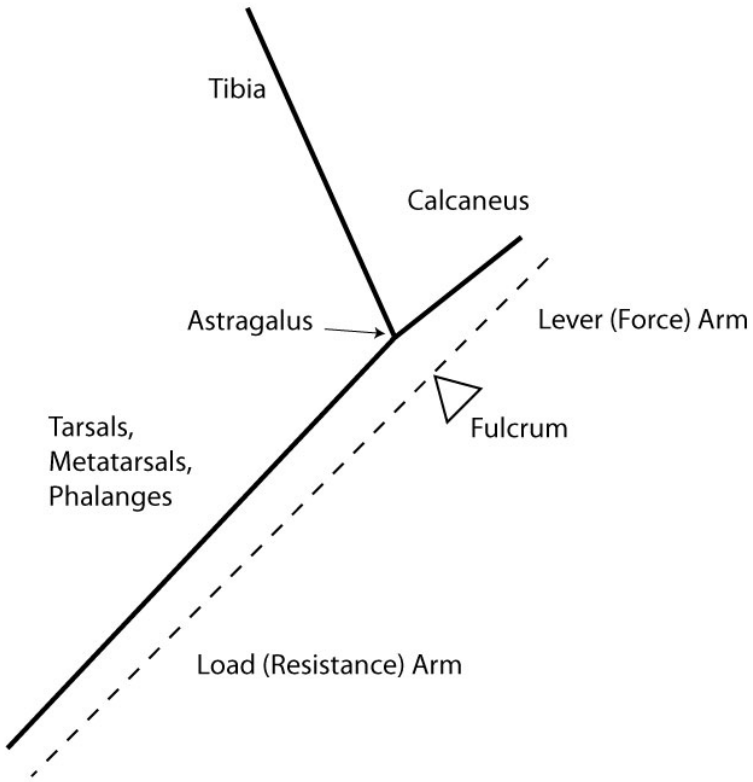

Figure 3.4: Schematic diagram of the bovid hock joint as a simple first class lever system during plantarflexion. Note: this diagram is simplified, and does not consider the multiple centers of rotation that are present in the bovid astragalus.

Based on the principles of mechanical lever systems, the relative proportions of the lever and load arms will affect the relative speed and power of this first class lever system. Specifically, increasing the relative length of the calcaneus (or, equivalently, reducing the relative length of the distal limb elements) will result in a more powerful but

slower lever system. Conversely, a relative shortening of the calcaneus (or relative elongation of the distal limb elements) will result in a lever system capable of producing more rapid movements, but with less power. Scott (1979, 1985) demonstrated that highly cursorial open-country bovids have elongate metapodials, suggesting that the hock joint in cursors is adapted for speed in plantarflexion. No comparable data have been published for bovid calcanei. However, unpublished data from a pilot study suggest that highly cursorial open-country pronghorn (*Antilocapra americana*) have relatively short calcanei as compared to more saltatorial white-tailed deer (*Odocoileus virginianus*), a species that favors forests and woodlands with a preference for ecotones and disturbed areas (Curran, 2009). These data suggest that devoted cursors combine their elongate metapodials with relatively short calcanei to favor speed in plantarflexion, but further study of the relative lengths of bovid calcanei with respect to habitat is needed to clarify this point.

The function of the astragalus is, in fact, more complicated than the depiction of the simple first lever system shown in Figure 3.4. Schaeffer (1947) provided an early look at the function of the artiodactyl hock, describing the astragalus as a cam-like structure, which rotates in a cavity formed by the calcaneus, distal tibia, and cubonavicular (Schaeffer, 1947). Schaeffer's primary concern was in identifying the functional advantage, if any, of the double-trochleated astragalus over more primitive single-trochlea systems common in other mammals. Schaeffer suggested that the additional joint rotation made possible by the artiodactyl distal trochlea is advantageous because it brings the calcaneus into a more favorable position for the action of the hock plantarflexors in extreme stages of dorsiflexion, which "undoubtedly assists in the development of great initial propulsive power by the time the foot is in contact with the ground" (Schaeffer, 1947: 21).

Photographs of an osteological specimen of *Ammotragus lervia* are shown in Figure 3.5 in various stages of the stride cycle to demonstrate the order in which the joints of the hock are active. At the beginning of the stride cycle when the joint is maximally dorsiflexed (Figure 3.5A) the distal limb elements begin to rotate about the axis of the transverse tarsal joint. This rotation continues until the stage of Figure 3.5D, at which point the astragalus, calcaneus, and cubonavicular reach a close-packed position and no further rotation at the transverse tarsal joint is possible. Thus, nearly all rotation about the transverse tarsal joint is completed before the onset of rotation about the upper ankle joint (Schaeffer, 1947, see radiographs in his Figure 4 and text discussion). Beginning at approximately the position shown in Figure 3.5E, the fulcrum of rotation at the hock shifts to the upper ankle joint, and plantarflexion continues until the calcaneus comes to rest in a sulcus on the posterior margin of the distal tibia when the hock is maximally plantarflexed (Figure 3.5G).

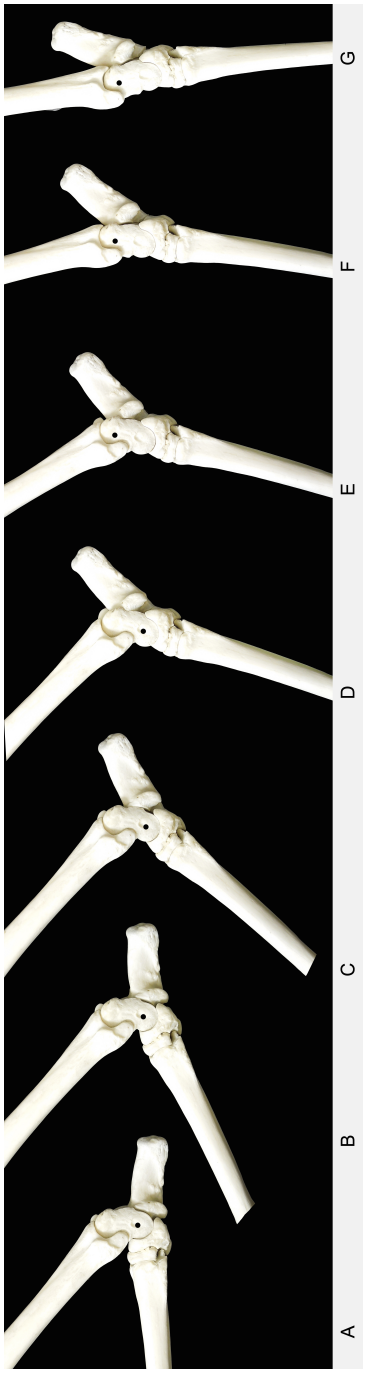

Figure 3.5: Photographs of *Ammotragus lervia* hock joints in medial view in various stages of the stride cycle from extreme dorsiflexion (A) to extreme plantarflexion (G). The operative center of rotation of the joint is indicated by a black dot on the astragalus

Dynamic Mechanical Advantage of Hock Plantarflexors

During hock rotation about the transverse tarsal joint during plantarflexion (Figure 3.5A-D), the calcaneus moves with respect to the astragalus and cubonavicular. This motion is related to the action of the astragalus as a cam. In the context of simple machines, a cam is a rotating part that, due to its non-circular (*e.g.,* elliptical) shape, causes movement in another part, which is termed the "follower" (Jacobs, 1921). Figure 3.6 shows a schematic illustration of the astragalus in lateral outline. The heavy red portion of the lateral outline approximates the cam surface, beginning at the distal trochlea and continuing proximally to include the calcaneal (sustentacular) facet. The calcaneus is represented as a simple rectangle. Figure 3.6 demonstrates how the elongate ellipse of the astragalar cam causes posterior displacement of the calcaneus as the astragalus rotates during plantarflexion.

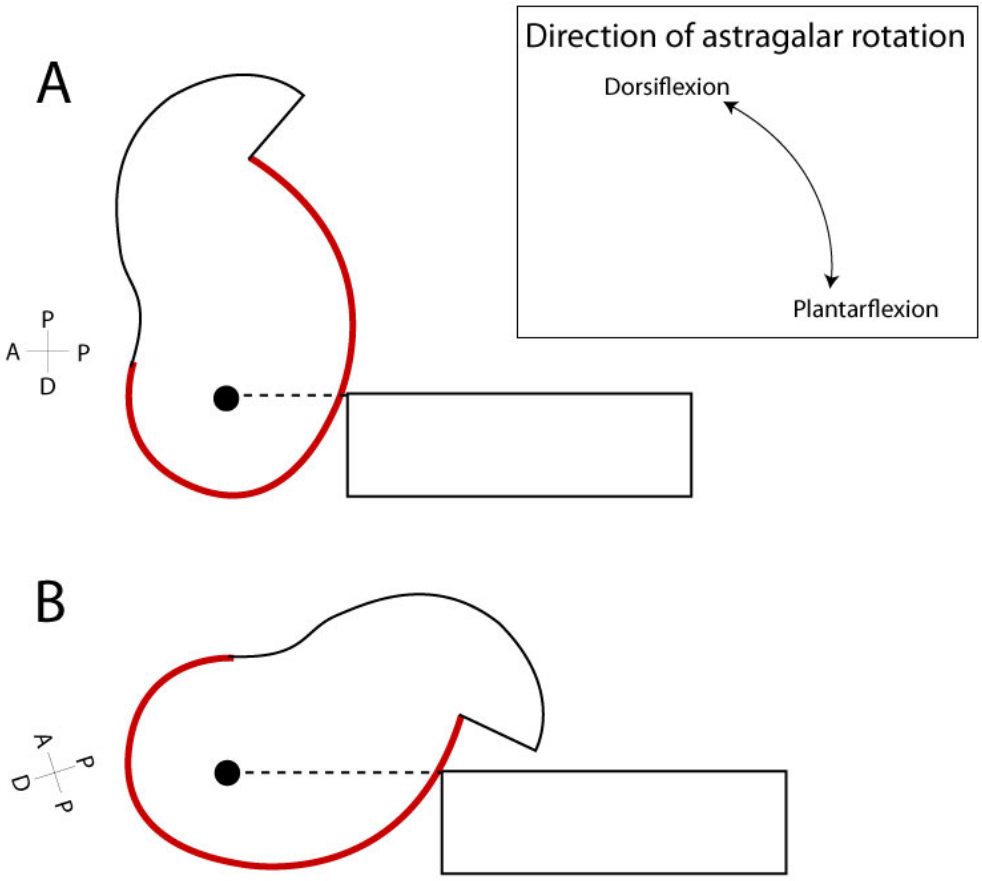

Figure 3.6: Schematic diagram of the lateral outline of an astragalus rotating as a cam. The heavy red portion of the astragalar outline shows the surface of the cam, comprising the lateral outline of the distal trochlea and the calcaneal (sustentacular) facet. The circle indicates the center of rotation at the transverse tarsal joint. Dotted lines indicate the distance between the axis of rotation and the calcaneus, which is represented by a simple rectangle. The system is shown in extreme dorsiflexion (A) and then in extreme plantarflexion (B) with resulting posterior displacement of calcaneus.

The displacement of the calcaneus can be observed in photographs of osteological specimens in which the position of the transverse tarsal joint axis is held constant. In Figure 3.7 the joint is shown in two stages of flexion, with a vertical line representing the approximate position of the center of rotation at the transverse tarsal joint. In stages of extreme dorsiflexion, the cavity between the cubonavicular and the calcaneus is filled by

the distal trochlea of the astragalus. However, as the astragalus rotates during plantarflexion, the cavity between the calcaneus and cubonavicular must accommodate the rotating astragalus, which is ellipsoid and elongate in the antero-posterior dimension. Thus, astragalar rotation causes the cavity to expand by displacing the calcaneus posteriorly as the calcaneus slides across the astragalocalcaneal facet and the obliquely oriented calcaneocuboid facet. Observations of the joint surfaces clearly indicate that this motion occurs, and the displacement of the calcaneus is also observable in radiographs of an intact cadaveric sheep hindlimb (Schaeffer, 1947, his Figure 4). Through this movement, a major portion of the functional length of the astragalus is added to the effective length of the calcaneus.

This displacement of the calcaneus only occurs during the initial stages of plantarflexion (Figure 3.5 A-D), and is complete when the calcaneus, astragalus and cubonavicular reach a close-packed position and joint rotation commences at the upper ankle joint. Thus, during the first stages of plantarflexion, the posterior displacement of the calcaneus progressively increases the mechanical advantage of the hock plantarflexors. The estimated measurements of the functional length of the *Ammotragus lervia* calcaneus in Figure 3.7 show that this lengthening effect is pronounced, with the lever arm lengthening by > 10% during this process. Schaeffer suggests that the transverse tarsal joint is still the operative axis of rotation at the hock at the point of limb touchdown, but that rotation at the upper ankle joint begins shortly thereafter (Schaeffer 1947: 21). If this interpretation of the timing of limb touchdown is correct, then the dynamic lever system achieves maximum mechanical advantage at approximately the time of the beginning of the propulsive phase.

The dimensions of the astragalus thus determine the magnitude of this dynamic lengthening effect, with relatively proximo-distally elongate astragali displacing the

calcaneus further posteriorly as compared with proximo-distally shorter astragali. Holding calcaneal length constant, greater displacement of the calcaneus by an elongate astragalus would result in a larger increase in mechanical advantage, and therefore increase power in dorsiflexion in hocks with elongate astragali. Proximo-distally shorter astragali would only cause a modest posterior displacement of the calcaneus during astragalar rotation. Highly cursorial open-country bovids are thus predicted to have relatively short astragali to maintain a short lever arm for the hock plantarflexors and maintain the speed of limb rotation during cursorial locomotion. Calculation of the precise mechanical advantage of hock plantarflexors through the stride cycle will require more data on calcaneal lengths and is a subject for future research.

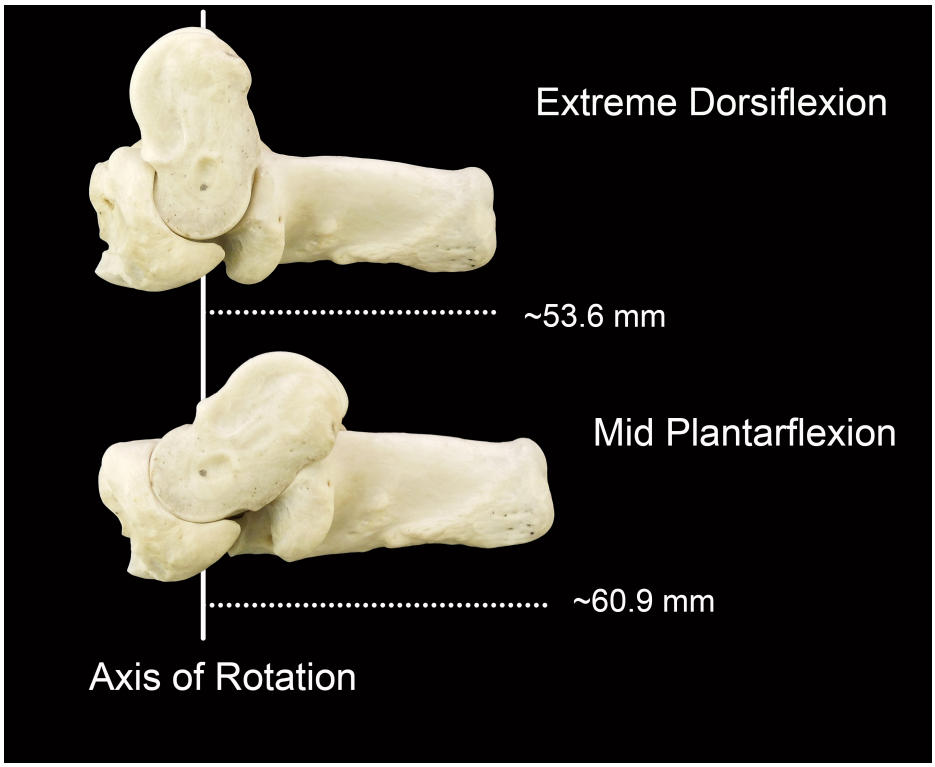

Figure 3.7: Medial views of astragalus, calcaneus and cubonavicular of *Ammotragus lervia* in positions attained during extreme dorsiflexion and during mid plantarflexion (approximately the level in Figure 3.5D). The vertical white line represents the approximate position of the axis of rotation at the transverse tarsal joint. The approximate functional length of the calcaneus (as estimated with calipers) is indicated.

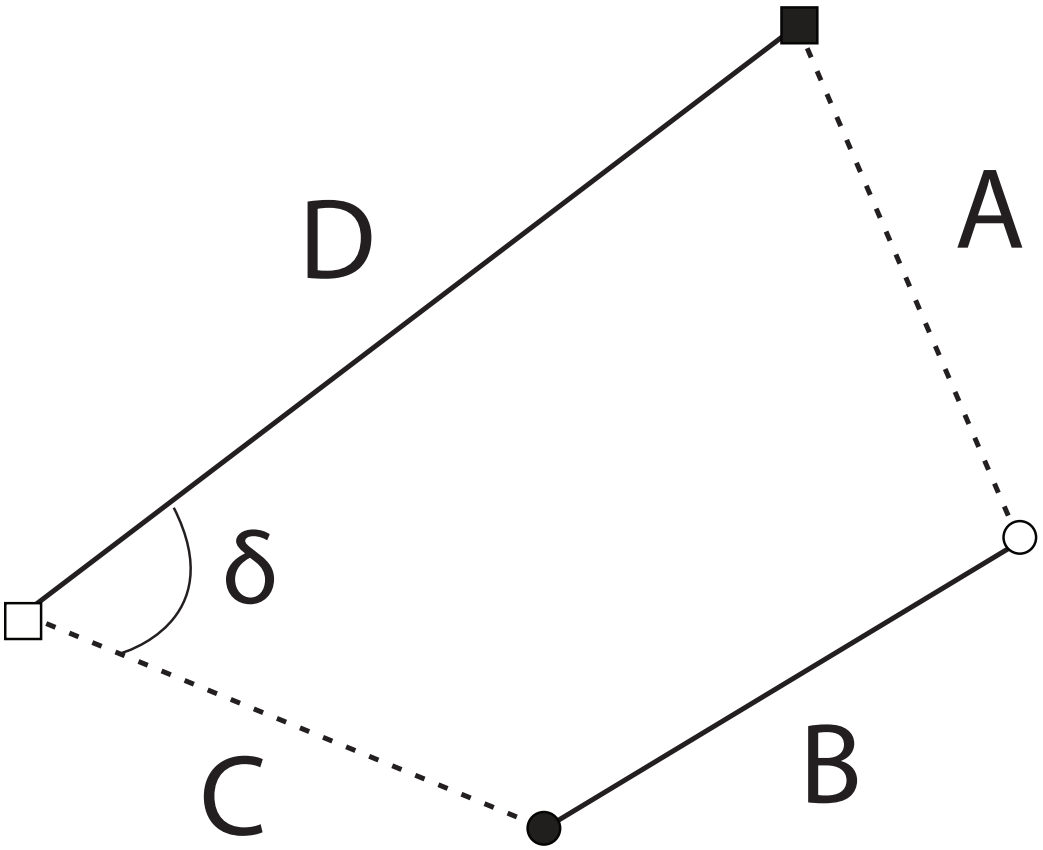

Figure 3.8: Schematic diagram of four-bar linkage with bars and angles labeled. Redrawn after Muller (1996, his Figure 1). The black and white squares and triangles representing the links match the corresponding links in Figure 3.9. The angle between segments C and D is labeled as δ.

The Four Bar Linkage Model

Alexander and Bennett (1987) describe the function of the sheep hock joint in the context of an important mechanical construct, the 2T4l four-bar linkage (see Muller. 1996). Four-bar linkages consist of four elements (bars or rods) connected in a single plane (Hartenberg and Denavit, 1964), and this particular linkage type has bars with lengths A = B = C < D. Figure 3.8 illustrates a schematic diagram of such a linkage with the components labeled with the letters A-D. The angle between segments C and D is

labeled as δ. Because the bars are rigid and the links secure, four-bar linkages can be said to have a single degree of freedom of motion (Alexander and Bennett, 1987; Muller, 1996). That is, for a set of bars with known lengths, moving any component results in a specific, determinable motion in every other element.

Figure 3.9 shows a schematic 4-bar linkage with the bars mapped onto the bones of the sheep hock. The bar D coincides with the collateral ligaments of the hock, which completely traverse the astragalus without attaching to it. These strong ligaments play a critical role; as they cross from the calcaneus to the distal tibia they keep the joint surfaces in tight opposition (Alexander and Bennett, 1987). The bar B consists of the astragalus itself or, more precisely, the functional length of the astragalus between the poles of rotation of the upper ankle joint and the transverse tarsal joint. Bars A and C are "imaginary" in the sense that do not correspond to a specific anatomical structure, but rather they rotate as the astragalus rotates during various stages of the stride cycle.

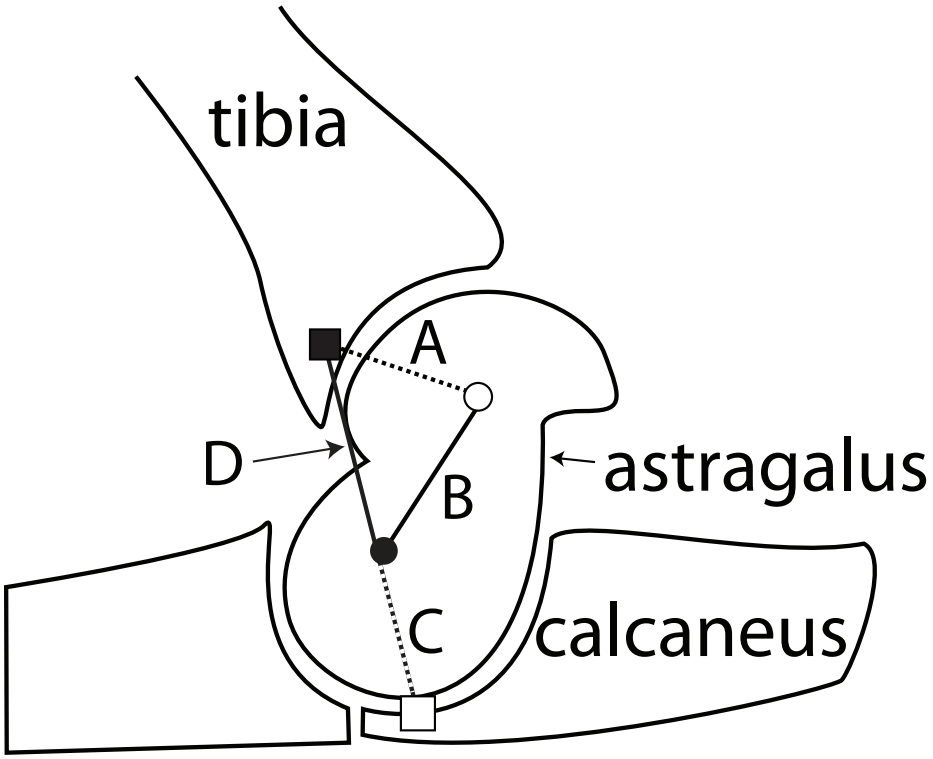

Figure 3.9: Schematic drawing of the bovid hock joint as a four bar linkage. Redrawn after Muller (1996, his Figure 20). Note that in this degree of flexion, segment C appears as superimposed over segment D. Segment D represents the collateral ligaments. The black and white squares and triangles representing the links match the corresponding links in Figure 3.8.

The 4 Bar-Linkage and Hock Angular Excursion

This model of the hock joint as a four-bar linkage is useful because it allows a description of the possible range of angular excursion for the hock. The hock joint is known to be bistable (Alexander and Bennet, 1987), which means that two stable configurations exist. The position of the linkage in Figure 3.9, shows the transition between the two stable configurations which occurs when segments C and D are superimposed and the angle between C and D (δ, not shown in Figure 3.5) equals 0. Thus, there is a stable linkage configuration on either side of this transitory position. The

degree to which δ can be negative is constrained by the angle of segment B with respect to segment D. As the astragalus rotates during plantarflexion, B approaches 90 degrees with respect to segment D, at which point the astragalus reaches a close-packed position with the calcaneus and no further rotation is possible. Figure 3.10 illustrates how the relative length of the astragalus affects the angle of δ at which this contact occurs. As shown in the figure, relatively long astragali reach this point at relatively small negative values of δ, while relatively short astragali can rotate much further before the contact with the calcaneus occurs when B and D are approximately orthogonal.

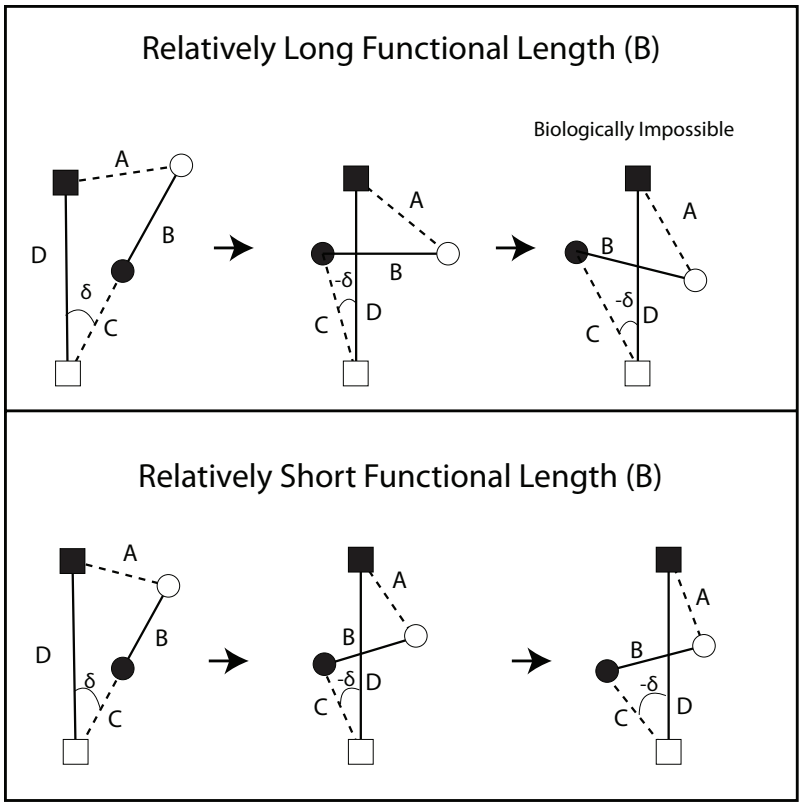

Figure 3.10: Schematic diagrams of long versus short astragali in various configurations. When segment B is long, segments B and D attain biologically unrealistic conformations at small negative values of δ, whereas with shorter B, the larger negative values of δ can be attained without reaching biologically unrealistic conformations.

Thus, this model of the 4-bar linkage provides a direct link between the relative dimensions of the astragalus and the range of angular rotation across the hock joint. Relatively shorter astragali (i.e., systems with relatively short functional lengths (measurement B) will have greater ranges of motion compared to relatively longer astragali. Shorter astragali can rotate through a greater range of negative δ values before this rotation stops. While B can be measured directly, there is no way to directly measure D from an isolated astragalus. However, D is likely to be correlated with the antero-posterior breadth of the distal astragalus. Thus, this study includes a measurement (DistRad in Figure 3.11) that serves as a proxy for the length of D (but note that DistRad is the radius of the distal trochlear margin, not the entire A-P breadth).

Range of angular extension at the hock is related to locomotor speed because speed is a function of stride length and stride frequency (Hildebrand and Goslow, 2001). Bovids (and other cursors) tend to increase stride length by elongating distal limb elements such as metapodials (Scott, 1985) as well as using more extended joint postures (Hildebrand and Goslow, 2001). Apart from lengthening limb elements, strides can be lengthened by increasing the joint ranges of motion (Hildebrand and Goslow, 2001). Therefore, the four-bar linkage model suggests that relatively shorter astragali should result in greater potential range of motion, leading to longer potential stride lengths, while relatively longer astragali should result in shorter potential stride lengths.

Joint Size

Across mammals, as speed of travel increases, the duration of time a limb is in contact with the ground decreases, and peak ground reaction forces increase (Biewener, 1983). Thus, open-country bovids should experience greater ground reaction forces in their limbs compared to closed-country bovids after controlling for body size. Open-

country bovids are predicted to have increased astragalar joint surface areas relative to body size, because dissipating loads over a greater surface area reduces the risk of joint damage (Jungers, 1991; Hamrick, 1996). Furthermore, joints with relatively larger joint surfaces are capable of greater angular excursion during sliding translation (Ruff, 1988), suggesting that joint surfaces which are larger in the direction of joint rotation will also lead to increased range of angular excursion. Therefore, it is expected that open-country bovids will have relatively large joint surface areas for two reasons: transmitting high ground reaction forces and increasing range of angular extension in the direction of limb movement. Areas of all three major articular surfaces are measured in this study: the calcaneal (sustentacular) facet (ACF in Figure 3.11), the large articular surface for the distal tibia (PTArea in Figure 3.11) and the smaller articular surface for the cubonavicular (DTArea in Figure 3.11).

Joint Stability

Cursorial mammals, including bovids, tend to restrict joint mobility outside of the parasagittal plane, because extraneous joint motion results in reduced fore-aft limb velocity and increases the risk of joint dislocation at high speeds (Gambaryan, 1974; Coombs, 1978; Kappelman, 1988; Hildebrand and Goslow, 2001). Hinge joints, such as the bovid hock, may be stabilized by the development of tongue-and-groove mechanisms (Hildebrand and Goslow, 2001, p 445). Examples of these structures can be found in equid (Hildebrand, 1987) and bovid (Kohler, 1993) metapodials. These stabilization structures create opposing joint surfaces that glide past one another parallel to the parasagittal plane of limb motion and thereby inhibit rotation outside this plane. The deeply incised proximal trochlea of the bovid astragalus has been hypothesized to function as a stabilizing structure by interlocking with the distal tibia (Schaeffer, 1947).

To a lesser extent, opposing parasagittal joint surfaces are also observed in the shallower distal trochlea. Thus, open-country bovids are expected to have deeper proximal and distal trochlea than closed-country bovids. Two linear measurements in this study capture the depth of the proximal trochlea. PMTD in Figure 3.11 measures the maximum proximo-distal depth of the trochlea, while APD measures the maximum antero-posterior depth of the trochlea. The proximo-distal depth of the distal trochlea is measured by the measurement DMTD of Figure 3.11.

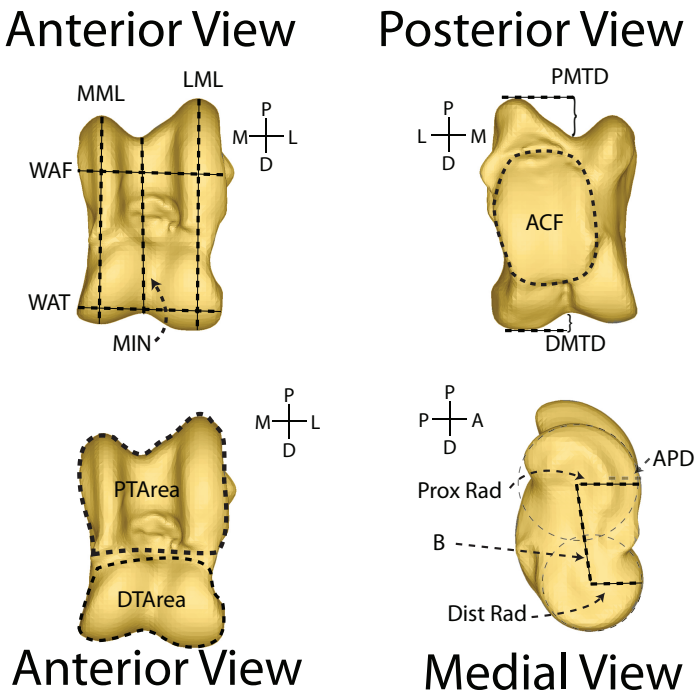

Figure 3.11: Two Anterior views, Posterior, and Medial views of a bovid astragalus, with relevant measurements illustrated. The anterior view is shown twice, once with only linear measurements and again with only area measurements. Abbreviations follow Table 3.1.

Hypotheses and Predictions

Prior work has suggested functional significance for two aspects of astragalar morphology: the minimum proximo-distal length of the astragalus and the antero-posterior depth of the medial portion of the cubonavicular articular surface. The minimum length of the astragalus has been shown to be shorter in open-country bovids, and has been interpreted to reflect a more deeply notched tibial trochlea in open-country bovids (Plummer et al., 2008). In light of the functional framework described above, this variable (MIN) is difficult to interpret because it is very likely related to both the

functional length of the astragalus (implicated in range of angular excursion and the astragalar cam mechanism) and the proximo-distal depths of the proximal and distal trochleae (implicated in joint stability). These distinct variables are more clearly interpretable when measured separately, as they are in the present study.

The antero-posterior width of the distal astragalus has been shown to be greater in open-country bovids, which has been interpreted as reflecting a wider arc for rotation at the distal trochlea and a corresponding greater range of angular excursion (Plummer, 2008:3024). However, prior studies have not corrected this variable to control for body size differences. Thus, in light of the concerns of Klein and colleagues (2010) regarding the confounding effects of body size, the functional importance of this region of the astragalus is currently not well understood.

Employing the functional framework detailed in the previous section, it is possible to expand upon previous interpretations of bovid astragalar function by making the following hypotheses and predictions.

H1 – Joint Excursion: Open-country bovids have a greater range of potential joint excursion compared with closed-country bovids, resulting in longer stride lengths and faster locomotor speed during flight from predators

P1.1: Open-country bovids have a relatively shorter functional length of the astragalus (measurement B in Fig. 3.7), which increases the range of angular excursion possible at the hock following the four-bar linkage model (Alexander and Bennett, 1987; Muller, 1996).

P1.2: Open-country bovids have astragalar joint surfaces with relatively larger radii (ProxRad and DistRad in Fig. 3.7), which increases the range of angular excursion at the hock.

H2 – Joint Surface Area: Open-country bovids have relatively larger joint surface areas for dissipating elevated ground reaction forces experienced during rapid locomotion (Jungers, 1991; Hamrick, 1996).

P2.1: The area of the calcaneal (sustentacular) facet (ACF in Figure 3.11) is relatively larger in open-country bovids.

P2.2: The area of the proximal trochlear articular surface (PTArea in Figure 3.11) is relatively larger in open-country bovids.

P2.3: The area of the distal trochlear articular surface (DTArea in Figure 3.11) is relatively larger in open-country bovids.

H3 - Joint Stability: Open-country bovids have more pronounced "spline and groove" adaptations that augment lateral joint stability during flight from predators.

P3.1: The proximal maximum trochlear depth (PMTD in Figure 3.11) is greater in open-country bovids (Valkenburgh, 1987).

P3.2: The maximum antero-posterior depth of the proximal trochlea (APD in Figure 3.11) is greater in open-country bovids.

P3.3: The distal maximum trochlear depth (DMTD in Figure 3.11) is greater in open-country bovids (Plummer et al, 2008).

H4 – Dynamic Mechanical Advantage of Hock Plantarflexors: Open-country bovids have relatively proximo-distally short astragali to maintain speed during plantarflexion, while bovids from closed country have longer astragali to increase power during plantarflexion through the posterior displacement of the calcaneus by the cam mechanism of the rotating astragalus.

P4.1: The ratio of measurement B / DistRad, (a proxy for the dimensions of the astragalar cam) is smaller in Open-country bovids.

MATERIAL AND METHODS

The extant sample for this project is a taxonomically and ecologically diverse sample of bovids consisting of 181 individuals from the 50 extant species listed in Appendix C. The individuals studied are curated in the osteological collections of the American Museum of Natural History (AMNH), New York, NY, and the National Museum of Natural History (NMNH), Washington, DC. Specimens from the right side of the body were preferred when available. Specimens with visible pathologies were excluded, and efforts were made to sample equal numbers of males and females.

Each species analyzed was classified into one of four habitat categories representing decreasing woody cover: forest, heavy-cover, light-cover, and open (Plummer and Bishop, 1994; Kappelman et al., 1997; DeGusta and Vrba, 2003; Plummer et al., 2008). Habitat preferences were compiled using information from several sources (Kingdon, 1974; Estes, 1992; Kappelman et al., 1997; DeGusta and Vrba, 2003; Skinner and Chimimba, 2006; Kovarovic and Andrews, 2007; Plummer et al., 2008). "Forest" bovids occupy environments where the tree canopy is closed, including rain forest and temperate forest. "Open" habitat bovids include those occupying grasslands, as well as more arid environments. The intermediate habitat groups are more heterogeneous, and include bovids from more diverse habitat types. "Heavy Cover" habitats include bushland and woodland, as well as swampy habitats. "Light Cover" includes bovids from light bushland, as well as bovids that specialize in tall-grass habitats. Any habitat categorization necessarily divides a relatively continuous spectrum of habitat types into discrete analyzable units. However, this 4-part classification scheme is based on published ecological and behavioral studies and has proven useful in prior ecomorphological studies. The habitat for each bovid is given in Appendix C.

All specimens were laser scanned using a NextEngine 3D Desktop Scanner (NextEngine Inc., Santa Monica, CA) to produce point cloud data in the form of X, Y, and Z coordinates, and then exported as .PLY models. Models were oriented manually based on geometric landmarks using RapidForm XOR software. The linear measurements illustrated in Figure 3.11 and detailed in Table 3.1 were obtained for each .PLY model using the "Measure Distance" tool in Rapidform. The radii of the proximal and distal articular surfaces (ProxRad and DistRad of Figure 3.11) were measured by fitting a circle to the proximal and distal margins of the trochlea using the "Perimeter-Circle" tool in RapidForm. Surface area measurements were obtained using the "Select Custom Region" tool in RapidForm. This tool allows the user to define a custom region by repeatedly selecting points on the surface of the model along the border of the articular surface, and subsequently to calculate the surface area of the custom region.

Assessment of Scan Processing and Measurement Precision

Laser scanning introduces additional steps as compared to traditional caliper measurements (*e.g.*, smoothing, merging multiple scan families, and digital alignment). To investigate the repeatability of the laser scanning protocol used in this study, a single specimen of *Ammotragus lervia* (a species not examined in the main part of this study) was laser scanned, processed, and aligned on six separate attempts over three days following the protocol described above. A subset of measurements (MML, MIN, LML, WAF, and WAT) that are obtainable with calipers was measured using the RapidForm "Measure Distance" tool on each of the six scans on three separate occasions. The same measurements were taken with calipers on 18 occasions over the course of 3 days. This process resulted in 18 sets of caliper measurements and 18 sets of laser scan measurements (from six separate scans). The means and coefficients of variation were

compared between the different measurement methods to evaluate the precision of the laser scanning processing procedure. A t-test was performed to test whether or not the two measurement methods differed significantly.

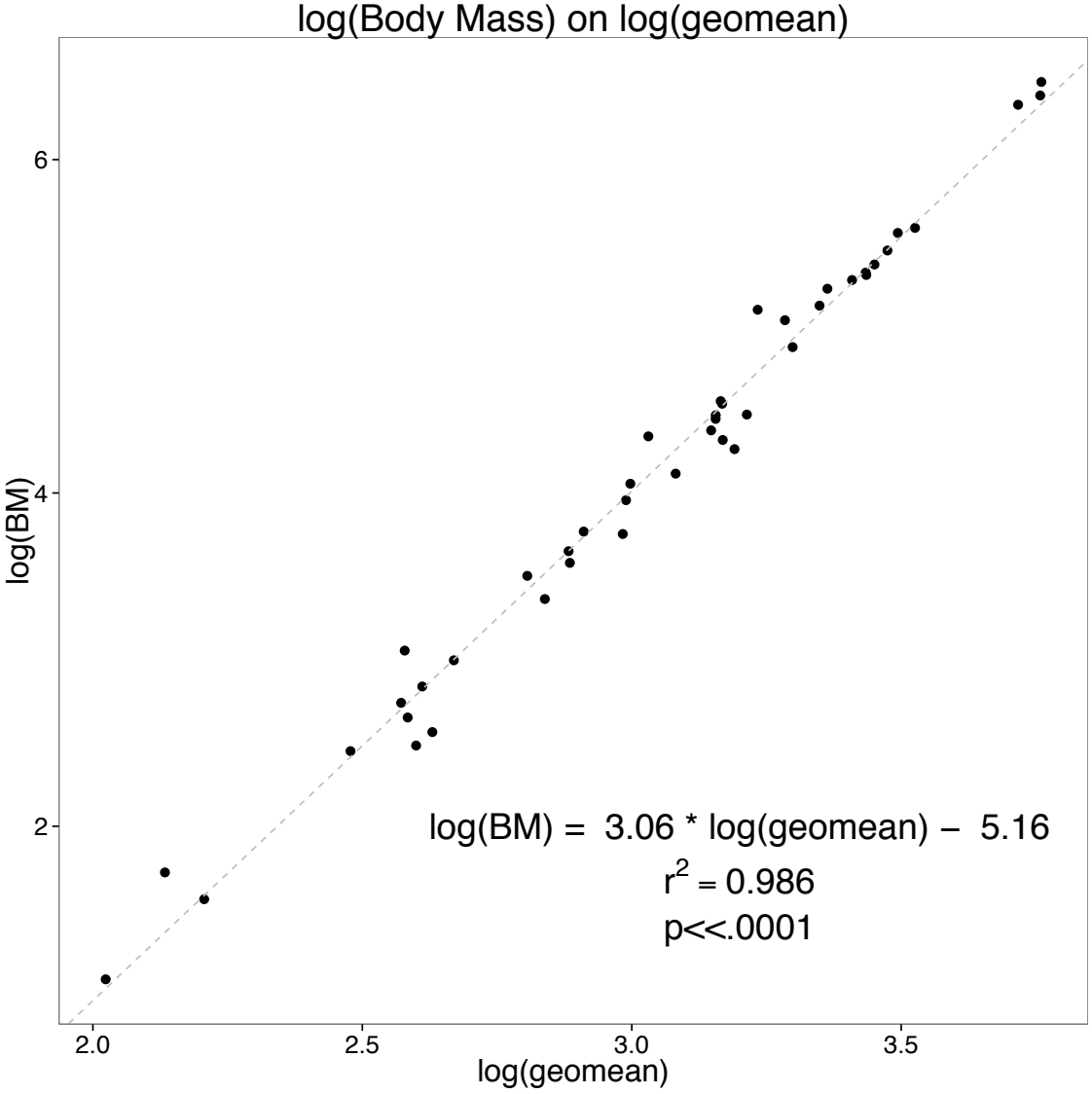

Figure 3.12: Regression of the log of the GEOMEAN size proxy variable on the log of body mass (kg).

Measurement	Description	Sources
ACF	The 2D area of the articular surface for the calcaneus (sustentacular facet).	1
APD	Antero-posterior depth of the proximal trochlea, measured at the anterior-most projection of the medial proximal trochlear margin	1
B	Functional length of the astragalus	2
DistRad	Radius of circle fit to the margin of the distal trochlea	1
DMTD	Distal maximum trochlear depth in proximo-distal plane	1
DTArea	The 2D area of the distal trochlear articular surface	1
LML	Maximum lateral length	3
MIN	Minimum length	3,4
MML	Maximum medial length	3,4
PMTD	Proximal maximum trochlear depth in proximo-distal plane	1
ProxRad	Radius of circle fit to the margin of the proximal trochlea	1
PTArea	The 2D area of the proximal trochlear articular surface	1
WAF	Width of prox trochlea at level of flange on lateral surface (excluding flange)	1
WAT	Greatest width at tarsus	3

Table 3.1: Measurements used in this study. Measurement abbreviations follow Figure 3.11. References: 1 (This Study), 2 (This Study, based on Muller, 1996), 3 (Degusta and Vrba, 2003), 4 (Plummer et al., 2008)

In order to test functional hypotheses regarding the relationship of the measured variables to the categorical habitat variable, I performed Phylogenetic Generalized Least

Squares (PGLS) with the habitat classification represented as a 4-level categorical variable. Each linear measurement was first corrected for isometric size by dividing by the geometric mean size proxy and then calculating the natural log of the resulting ratio to improve normality. Two dimensional area measurements were treated the same as linear measurements, except the square root of each areas was calculated prior to size correction using the geometric mean. The dimensionless ratio B/DistRad was logged, but was not divided by the size proxy variable. This method of size correction follows Jungers et al. (1995). The body size proxy (GEOMEAN) used in this study was calculated using eight of the linear measurements as follows:

$$\text{GEOMEAN} = \sqrt[8]{LML \times MIN \times MML \times WAF \times WAT \times ProxRad \times DistRad \times B}$$

The eight measurements used in the calculation result in a size proxy that correlates extremely well with species-mean body mass (see Figure 3.12). Body mass data comes from the PanTHERIA Database (Jones et al., 2009).

This GEOMEAN variable was included in the PGLS as a covariate to test for the presence of allometric scaling. Because methods for considering individual variation in PGLS analyses are largely experimental and not widely adopted (Revell and Reynolds, 2012) PGLS was conducted on pooled species-means for each variable. PGLS requires a phylogenetic tree; a pruned version of the ruminant supertree published by Fernandez and Vrba (2005) was used in all analyses. Outliers were tested for following the method of Jones and Purvis (1997), but none were discovered. All statistical analyses were conducted using the programming language R (R Development Core Team, 2011). The caper package (version 0.5, Orme et al., 2011) was used to conduct the PGLS analyses. The habitat variable was considered to have a significant effect if the p-value of the overall model was significant at a level of <0.05. Because of the many hypothesis tests against the same habitat variable, the False Discovery Rate (FDR) method of p-value

adjustment for multiple testing was applied (Benjamini and Hochberg, 1995). Post-hoc comparisons were also subjected to the FDR p-value correction. This method of determining significance has been demonstrated to result in acceptable rates of Type I error for PGLS using phylogenetic simulations (Chapter 2; Barr & Scott, 2013).

In addition to examining pairwise comparisons between habitat categories, the habitat category was tested for significance using an F-test. The habitat category term was dropped from the PGLS, and the simplified model (including only the measured variable and the geomean body size proxy) was compared against the full model using an F-test. Habitat was judged to be significant in cases where the full model explained significantly more residual variation, and the F-test indicated that the models were different at a level of $p < 0.05$.

RESULTS

Scanning Precision Results

The summary statistics from the scanning precision analysis are given in Table 3.2. In general, the precision of the laser scanned measurements (as measured by the coefficient of variation) compared favorably with the traditional caliper measurements. The lowest coefficient of variation observed was for the caliper measurement of MML (0.0009), which was less than the corresponding, value for the scanned MML (0.0016). In all other cases, the coefficients of variation for the scanned measurements were either comparable to or slightly lower than the corresponding values for the caliper measurements. As the scanned measurements include six separate scans that were acquired, smoothed, and aligned on separate occasions, the fact that the coefficients of variation are very similar for the caliper and scanned measurements suggests that the

additional processing steps involved in laser scanning are not a major source of measurement imprecision.

	MML	MIN	LML	WAF	WAT
Scan CV	0.0016	0.0012	0.0013	0.0075	0.0025
Scan Range	35.33, 35.55	29.94, 30.08	37.31, 37.44	22.69, 23.38	23.15, 23.40
Caliper CV	0.0009	0.0013	0.0029	0.0090	0.0040
Caliper Range	35.41, 35.52	30.02, 30.16	37.23, 37.6	23.02, 23.81	23.04, 23.4
Scan Mean	35.42	30.03	37.37	23.18	23.27
Caliper Mean	35.47	30.08	37.39	23.26	23.24
T-test results	t = 3.68 df = 33.424 p < 0.001	t = 4.09 df = 28.03 p < 0.001	t = 0.88 df = 23.43 p = 0.389	t = 1.85 df = 24.91 p = 0.076	t = 0.29 df = 30.09 p = 0.768

Table 3.2: Measurement results from the scanning precision analysis.

Results from a t-test for differences between caliper measurements and laser scan measurements are also included in Table 3.2. Three of the measurements (LML, WAF, and WAT) do not show significant differences in the measurements obtained by the two methods. Two measurements (MML and MIN) do show significant differences between the two methods, with the scan method producing length measurements that are slightly shorter than those obtained from calipers. These differences are very small with respect

to the mean differences between habitat groups. For MML, the difference between the caliper and scan means represents 0.52% of the mean difference between the open and closed habitat groups. For MIN, the comparable value is 0.68%.

Thus, while the laser scan measurements have good precision in general, there are some minor differences between the laser scan measurements as compared to traditional caliper measurements. These differences may be attributable to two sources: 1) subtle differences in specimen orientation during measurement with calipers versus the three-dimensional orientation procedure used in this study to orient laser scans and 2) the potential for selecting mesh polygons that are not at the absolute end of the bone during laser scan measurement, which would result in very small underestimates of lengths. The differences between scanned measurements and caliper measurements suggests that care must be taken in attempts to combine data from laser scans with data from caliper measurements. All measurements reported in subsequent sections are obtained from laser scans.

One measurement, WAF, had considerably higher error (CV = 0.0075) than the other measurements. The increased error rate is likely due to the fact that WAF is measured with respect to the flange on the lateral surface of the astragalus, but excludes this flange. Thus, there is inherently some additional error in estimating the level of this measurement. Nonetheless, the mean error for WAF calculated over 18 different scans represents only 1.75% of the mean difference between the open and closed habitat groups for WAF. These results suggest that error rates are comparatively small with respect to the effect size of the habitat variable.

The results from the remaining linear measurements (i.e. those not measurable with calipers) are given in Table 3.3. In general, these measurements showed coefficients of variation that are similar to, or in some cases slightly higher than those obtained using

calipers. B and DistRad have coefficients of variation at or below 0.005, which compare favorably with the precision of caliper measurements. ProxRad and PMTD have slightly elevated coefficients of variation, with DMTD has the highest coefficient of variation observed in this precision analysis.

The specimen examined in this error analysis is near the mean for the entire comparative sample. Slightly different error rates are expected based on the relative size of the triangle mesh compared to the overall size of the astragalus. Slightly larger percentage errors might be expected for the smallest specimens in the sample, for which a single mesh triangle is a relatively larger percentage of the model while slightly smaller percentage errors are expected for the largest specimens.

	PMTD	DMTD	B	ProxRad	DistRad
Mean	5.22	2.10	16.54	10.44	8.73
Range	5.14, 5.26	1.95, 2.21	16.33, 16.68	10.32, 10.62	8.64, 8.82
CV	0.007	0.029	0.005	0.009	0.004

Table 3.3: Summary statistics for measurement precision analysis of linear measurements not obtainable with calipers.

Results of PGLS Analyses

Results from the PGLS analyses are given in Table 3.4. Boxplots of each GEOMEAN corrected variable as well as the dimensionless ratio B/DistRad are plotted against the habitat variable in Figure 3.13. Results are presented in groups according to whether or not variables are significantly related to GEOMEAN, the habitat category, or neither.

Significant habitat effect with no correlation to GEOMEAN

The GEOMEAN corrected variable DistRad showed no statistically significant association with GEOMEAN. Thus, GEOMEAN was removed from the PGLS and the model was recomputed. The PGLS model excluding body mass was highly significant ($F(4,41) = 13.56$, $p<0.001$, $R^2 = 0.499$, lambda = 0.780) and all pairwise comparisons were significant at FDR corrected levels, with the exception of the HC-LC comparison (see Table 3.4).

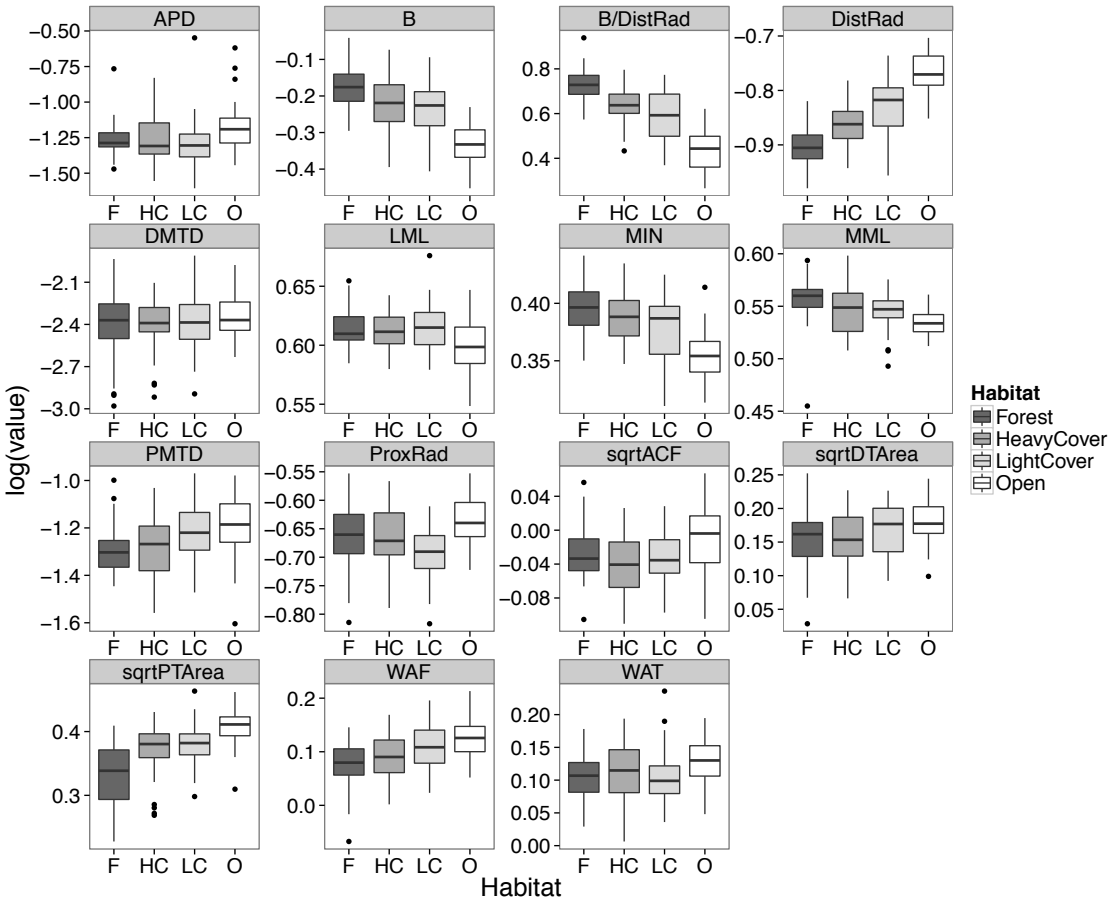

Figure 3.13: Boxplots of the logged and GEOMEAN-corrected value of each variable plotted against the habitat variable. The dimensionless ratio B/DistRad is logged but not corrected by GEOMEAN. The data for the plots are individual specimen values rather than species means. Measurement abbreviations are as in Table 3.1 and Figure 3.11.

Significant habitat effect with significant correlation to GEOMEAN

Four variables, B, MML, ProxRad, and WAF exhibited significant habitat effects in addition to significant correlations with GEOMEAN. After size correction, B and MML had a negative association with GEOMEAN, indicating that larger bovids tended to have relatively smaller values for each of these measurements. Even while controlling for the statistical association between these measurements and GEOMEAN, the effect of the habitat variable was significant for both B ($F(5,40) = 56.2$, $p<0.0001$, $R^2 = 0.85$, lambda < 0.001) and MML ($F(5,40) = 14.3$, $p<0.001$, $R^2 = 0.59$, lambda = <0.001). The R^2 value for B was considerably higher than MML, indicating that B is much better explained by habitat than MML. The dimensionless ratio B/DistRad was also negatively associated with GEOMEAN, and the PGLS was highly statistically significant ($F(5,40) = 31.5$, $p<0.001$, $R^2 = 0.76$, lambda = 0.354). Many, but not all, pairwise comparisons between different habitat levels were highly significant at FDR adjusted levels for these variables (see Table 3.4).

ProxRad and WAF were positively associated with GEOMEAN indicating that larger bovids tend to have relatively wider and relatively antero-posteriorly deeper astragali compared with smaller bovids. PGLS was highly significant for both ProxRad ($F(5,40) = 13.3$, $p<0.0001$, $R^2 = 0.57$, lambda = 0.373) and WAF ($F(5,40) = 7.45$, $p<0.0001$, $R^2 = 0.43$, lambda < 0.001). The significance of ProxRad is largely driven by the significant difference between the LightCover and Open habitat categories (see Table 3.4).

Correlation with GEOMEAN only

Four variables (LML, MIN, WAT and DTArea) were significantly associated with GEOMEAN, but not with the habitat variable. The length variables LML and MIN

show a negative association with GEOMEAN. The width variable WAF and DTArea show a positive relationship to GEOMEAN. No pairwise habitat comparisons were computed for these variables.

No habitat effect and no correlation with GEOMEAN

Four variables, DMTD, PMTD, APD, and ACF showed no statistically significant association with the habitat variable regardless of whether or not GEOMEAN was included as a covariate. Therefore, for these variables, no pairwise comparisons were computed and these variables were not analyzed further.

Phylogenetic Signal

As measured by the lambda parameter, variables exhibit a wide range of residual phylogenetic signal. Lambda values (Table 3.4) range from close to zero (e.g. B, PTArea, MML, WAF) to moderate (e.g. B/DistRad, ProxRad) to relatively high (e.g. DistRad, MIN). There is no obvious pattern regarding which variables exhibit strong versus weak residual phylogenetic signal, but the effects of body size clearly play a role.

When the PGLS analyses are run with only the habitat variable (*i,e.,* excluding the GEOMEAN body size proxy as a covariate), all variables exhibit lambda values greater than 0.4, and all lambda values are significantly different from 1 with the exception of DMTD (results not reported). In the statistics reported in Table 3.4, with the GEOMEAN body size proxy included as a covariate where appropriate, lambda values are all considerably lower than the lambda values obtained from the unreported PGLS with the GEOMEAN variable excluded. Body mass is known to carry high phylogenetic signal in diverse clades of mammals (Blomberg et al., 2003; Kamilar and Cooper, 2013). Thus, by controlling for body size, the result is that residual phylogenetic signal is reduced. Nonetheless, lambda values in the reported PGLS analyses are greater than 0 for many

measurements, which demonstrates that PGLS is necessary in order to obtain accurate parameter estimates.

DISCUSSION

The results of this study demonstrate that statistically significant differences in astragalar morphology exist between bovids occupying structurally distinct habitats. Because PGLS simultaneously controls for body size and phylogenetic signal while testing for habitat differences, significant results provide strong evidence that bovid astragali differ between habitat groups. Demonstrated differences are consistent with some, but not all, of the predictions derived from the functional framework outlined in this paper.

				Post Hoc Habitat Pairwise p-values						GEOMEAN	
Variable	**Overall p**	**ML lambda**	**R^2**	**C-O**	**C-HC**	**C-LC**	**HC-LC**	**HC-O**	**LC-O**	**Effect**	**p-value**
APD	0.712	<0.001	0.055							0.011	0.838
B	<0.001	<0.001	0.849	<0.001	0.454	0.187	0.044	<0.001	<0.001	-0.093	<0.001
(B/DistRad)	<0.001	0.354	0.759	<0.001	0.193	0.002	0.045	<0.001	<0.001	-0.103	<0.001
DistRad	<0.001	0.780	0.499	<0.001	0.031	0.001	0.144	<0.001	0.001	0.014	0.375
DMTD	0.627	0.444	0.07							-0.047	0.463
LML	0.012	0.549	0.266							-0.017	0.008
MIN	0.003	0.652	0.317							-0.025	0.013
MML	<0.001	<0.001	0.589	0.099	0.195	0.642	0.099	0.002	0.1	-0.025	<0.001
PMTD	0.337	0.353	0.113							0.004	0.927
ProxRad	<0.001	0.373	0.572	0.954	0.015	0.001	0.311	0.015	<0.001	0.06	<0.001
sqrt(ACF)	0.144	<0.001	0.16							-0.002	0.838
sqrt(DTArea)	0.009	<0.001	0.277							0.024	0.028
sqrt(PTArea)	<0.001	<0.001	0.746	<0.001	0.57	0.018	0.066	0.001	0.088	0.064	<0.001
WAF	<0.001	<0.001	0.427	0.041	0.507	0.184	0.054	0.008	0.338	0.033	0.011
WAT	<0.001	<0.001	0.49							0.052	<0.001

Table 3.4 Results from PGLS analyses. Post-hoc comparisons between habitat levels are reported only for variables for which a PGLS model including the habitat variable was shown to be significantly better than a model excluding habitat; these variables are also highlighted in grey. P-values for the overall model and the post-hoc comparisons are reported after correction using the False Discovery Rate method.

The first hypothesis tested was that open-country bovids are capable of greater range of angular excursion at the hock joint because increased angular excursion increases stride length and thereby increases maximum running velocity. One prediction from H1 is that open-country bovids have relatively shorter astragali because shorter astragali increase the range of angular excursion possible at the hock joint as predicted by the four-bar linkage model. This prediction finds support in the highly significant effect of the habitat variable on the functional length measurement (B). The length measurement used in previous studies (MIN) did have statistically significant PGLS results, but the PGLS model with the habitat term included was not significantly better at explaining variation than a simpler model including only GEOMEAN as a predictor. This is likely due to the fact that the MIN variable conflates the proximo-distal depth of the proximal trochlea with the functional length of the astragalus, rendering MIN a less effective proxy for functional length than B.

The second prediction of H1 was that trochlear radii would be larger in open-country bovids than in closed-country bovids. This prediction was supported for the distal trochlea (DistRad), but not supported for the proximal trochlea (ProxRad). While the PGLS for the ProxRad variable was significant, the pairwise comparison between the two most extreme habitat groups (Forest and Open) was not significant, which suggests that factors other than adaptation to habitat might be at work.

The predictions of H2 were that open-country bovids should have greater relative joint surface areas compared to closed-country bovids. Of the three joint surfaces measured, only the proximal trochlear articular surface (PTArea) had a significant PGLS that was significantly better than a PGLS excluding the habitat category. Thus, the prediction was supported for PTArea but not for the distal trochlear articular surface (DTArea) or the calcaneal (sustentacular) facet (ACF). These results conform to those

obtained for related linear measurements. The statistical significance of PTArea is expected given the significance of both ProxRad and WAT, two linear measurements that capture aspects of the shape and size of the proximal trochlea quantified by PTArea. Likewise, the lack of significance in DistRad is consistent with the lack of significance for WAT (the width across the distal trochlea). ACF, the area of the calcaneal (sustentacular) facet, also did not exhibit statistically significant differences. This may be due to the fact that this joint surface bears less body weight than the other joints of the hock, and is thus less responsive to the stereotypical loading of the joint by body mass.

Further investigation of joint surface morphology should focus on quantifying relative dimensions in the plane of joint rotation *versus* overall dimensions to help further tease apart the impact of locomotor adaptation on joint shape and size. As discussed in the section on the camming function of the astragalus, the action of the lower ankle joint is fundamentally different than the other two joint surfaces examined. Further study involving a more detailed characterization of the size and shape of this surface is required to fully determine how this joint surface may relate to habitat specific locomotion.

The predictions of H3 were that the trochleae should be deeper in open-country bovids than closed-country bovids due to the operation of a joint stability mechanism. This hypothesis was not supported. While mean values of PMTD followed the predicted trend across habitat categories, these differences were not statistically significant when controlling for GEOMEAN and phylogenetic signal using PGLS. The other measure of the depth of the proximal trochlea (APD) showed no significant differences between habitat groups. For DMTD, the mean values were remarkably uniform across different habitat groups and there were no significant differences between groups. The lack of support for this hypothesis is surprising, given the existence of lateral joint stability mechanisms in other ungulate joint complexes (Hildebrand, 1987; Kohler, 1993). It is

possible that the metrics used in this study, PMTD, APD, and DMTD, do not fully characterize the complex geometry of the trochlear walls. Clarification of the degree to which a stability mechanism is operative in the bovid astragalus must await further study using methods that fully capture the complex three-dimensional surface of the trochleae. Pilot data using Geographic Information Systems (GIS) to characterize the slope of the entire articular surface show strong differences between Open and Forest habitat bovids.

The final hypothesis (H4) was that the dimensions of the astragalar cam mechanism relates to the mechanical advantage of the hock plantarflexors and thereby influences the relative power and speed of hock plantarflexion during locomotion. The ratio B / DistRad served as a proxy for the dimensions of the cam mechanism. Bovids from closed country were predicted to have a higher ratio, because more proximo-distally elongate astragali act to displace the calcaneus further posteriorly during plantarflexion and increase muscular power during plantarflexion. Conversely, cursorial bovids from open country were predicted to have shorter astragali with lower B / DistRad ratios, which augments the speed of hock plantarflexion. This hypothesis was supported by the highly significant differences in B / DistRad, with open country bovids having relatively short astragali and closed country bovids having relatively elongate astragali. The ratio of measurements B / DistRad had the highest R^2 value of any variable in the PGLS and strongly supports the hypothesis that astragalar relative proportions are functionally related to the dynamics of mechanical advantage of the hock plantarflexors during locomotion.

Body Size

Consistent with the findings of previous authors (Klein et al., 2010) most of the measurements examined in this study are very highly correlated with the GEOMEAN

body size proxy. The situation is further complicated by the fact that the allometric effects of size (relatively shorter and wider astragali in larger taxa) are similar to some of the predicted functional effects of habitat specific locomotor adaptation. Nonetheless, using PGLS it is possible to test for the independent effects of size and functional adaptation. The results of this study clearly illustrate that the morphology of the astragalus is related to habitat, independent of the effects of body size and phylogeny.

CONCLUSIONS

Previous studies have examined the ecomorphology of the bovid astragalus, but none has tested explicit functional predictions relating astragalar morphology to habitat. The present study introduces a functional framework for interpreting astragalar morphology, and results in the following four major conclusions.

- Body size is highly correlated with most bovid astragalar metrics, including some allometric effects after controlling for size. However, independent habitat effects are detectable in spite of the body size signal.
- The relatively shorter astragali of open-country bovids likely serve to increase the range of angular excursion at the hock, following the four-bar mechanical linkage model of Muller (1996).
- Open-country bovids have relatively larger proximal trochlear articular surfaces, which likely serve to dissipate increased loads during rapid locomotion.
- The measurements studied do not offer support for the existence of a "spline-in-groove" stability mechanism in the bovid astragalus.

- Astragalar dimensions play a role in the dynamic mechanical advantage of hock plantarflexors, maintaining speed in open country cursors and increasing power in closed country bovids.

The results of this chapter demonstrate that astragalar morphology is related to habitat specific locomotor ecology. The astragalus contains a functional signal that justifies its use in predicting habitats from fossil astragali, which are incredibly common in the fossil record. Thus, the abundance of fossil bovid astragali offer a statistically robust sample of the bovid communities in the past, and comprises a valuable resource for reconstructing past habitats.

Chapter 4: Predicting Habitat Preferences from Astragalar Morphology

In Chapter 3, I used phylogenetic comparative methods to demonstrate that astragalar morphology differs among bovids occupying structurally distinct habitats, and that differences are robust when controlling for phylogenetic signal and body size. The current chapter takes up the related issue of predicting habitat preferences of specimens for which the habitat category is unknown, as is the case with all fossil specimens. As such, this chapter incorporates the methodological framework from the phylogenetic simulations reported in Chapter 2.

This chapter begins with a brief review of the statistical methods for ecomorphological predictions, and then explores the performance of astragalar habitat predictions using a variety of methods. The results of this chapter comprise the basis for habitat predictions of fossil astragali in the Omo Shungura Formation in Chapter 5.

BACKGROUND ON DISCRIMINANT FUNCTION ANALYSIS

Discriminant Function Analysis (hereafter DFA) is discussed in some detail in Chapter 2. The most salient points from that discussion are as follows:

- DFA requires multiple continuous variables as predictors as well as a known "training set" of specimens for which a categorical variable is known *a priori*.
- Once validated with a representative training set, the DFA may be used to classify cases in which the categorical variable is not known *a priori*, such as fossils.

- The predictive success of DFA is correlated with the number of variables used, so care must be taken not to "overfit" the model by including too many variables (Babyak, 2004; Kovarovic et al., 2011).
- DFA is not designed to identify the source of variation between categories. Thus, in ecomorphology, it is advisable to use alternative methods (such as PGLS) to determine whether or not variables are functionally relevant before inclusion in a DFA.

There are two types of DFA: quadratic (QDA) and linear (LDA). The primary distinction between these two methods is the underlying assumption about the within-group covariance matrix. LDA assumes that the within-group covariance matrix is identical for each of the groups (Manly, 2004), while QDA relaxes this assumption. QDA allows an additional term (the square of each variable) to be used when computing discriminant functions (Quinn and Keough, 2002). As such, the classification results from QDA will be higher than classification results from LDA on the same dataset, because statistical models typically fit data better when additional predictors are added, hence the danger of "overfitting" linear models (Babyak, 2004) and the need to correctly count degrees of freedom. Furthermore, because the square of each term is highly correlated with the original term, QDA often suffers from issues of excessive collinearity of predictors (Quinn and Keough, 2002), which can introduce computational errors in actually calculating discriminant functions.

Using LDA when the data set violates assumptions about the homogeneity of within group co-variances primarily affects estimates of the statistical significance of the overall model (Manly, 2004). Because datasets with phylogenetic signal alone (i.e.

datasets lacking any functional signal) quite often produce statistically significant DFAs (as demonstrated in Chapter 2), the statistical significance of ecomorphological DFAs using real-life data (which contain phylogenetic signal plus any functional signal) is not in doubt, especially when variables have been functionally vetted using PGLS. Violations of the assumption of homogeneity of within group co-variances are the primary justification given in the literature for choosing QDA. LDA avoids the issues surrounding over-fitting and collinearity inherent in QDA, and LDA generally provides useful information regarding categorical discriminability, despite the fact that many real-world data-sets violate the underlying assumptions of within-group homogeneity of covariances (Kovarovic et al., 2011).

In publications using DFA, the choice of which DFA model to use (QDA versus LDA) and the number of predictors included rarely receives equal emphasis as the classification accuracy of the overall model, even though the choice of model and the number of predictors are well known to impact classification accuracy (Manly, 2004; Kovarovic et al., 2011). Thus, it is often difficult to compare classification success rates between studies using different numbers of predictors, some of which use LDA and others of which use QDA. In this chapter, QDA results are reported, but LDA results are generally preferred as a reflection of the classification success of analyses.

The success of DFA can be reported using several different methods. The most commonly reported method in ecomorphology is termed "resubstitution" (DeGusta and Vrba, 2003; Plummer et al., 2008). Resubstitution involves computing discriminant functions using a dataset, and then applying the resulting functions to make predictions for each specimen in the original dataset used to create the discriminant functions. There is clearly limited value in making predictions for specimens using equations derived from datasets that include those specimens. Two additional methods exist which base

predictions on subsets of the dataset: cross-validation and test-set withholding. Cross-validation is an iterative process in which each specimen in the dataset is held out and discriminant functions are recomputed. Thus, the prediction for each specimen is based on discriminant functions deriving from all other remaining specimens. In test-set withholding, large groups of specimens are held out, discriminant functions are computed from the remaining specimens, and accuracy is calculated based only on the predictive success of the held out test-set. Test-set withholding is arguably the most conservative method of calculating accuracy, but its performance depends on the composition of the training set, and is not widely implemented in ecomorphology. Therefore, in this chapter, I report standard resubstitution success rates as well as cross-validation results.

METHODS

DFAs were computed using either the raw variables or the GEOMEAN size corrected variables computed using the size correction protocol described in Chapter 3. In these DFAs, variables are included only if they were shown to be significantly related to habitat in the PGLS analyses of Chapter 3. In order to minimize variable collinearity, the dimensionless ratio B/DistRad was not included in the DFAs because it is highly correlated with both B and DistRad. First, simply for comparative purposes, a DFA was conducted on all variables from Chapter 3, including those not demonstrated to relate functionally to habitat. Only the overall classification success rate for this analysis is reported. Three additional data sets were analyzed more completely: 1) all raw variables from the PGLS that were significant (SIGRAW), 2) all geomean corrected variables that were significant in the PGLS (SIGGEO), and 3) all SIGGEO variables with the exception of the PTArea variable. The rationale for excluding PTArea will be explained more completely when those analyses are presented.

DFA results are presented graphically as bivariate plots of individual specimen values for the first, second, and third linear discriminant functions (LD1, LD2, and LD3). Points are color coded by habitat category, and for visual clarity, 95% confidence ellipses for each habitat category are overlaid on the points. Measurement abbreviations follow Figure 3.1.

RESULTS

All Variable Analysis

A DFA including all of the variables from Chapter 3 was conducted, simply in order to obtain the LDA classification accuracy. The classification accuracy using all 14 measured variables was 82.6%, and the cross-validated success rate was 70.4%. However, this classification accuracy is certainly quite inflated. It is included only to demonstrate how including many variables can lead to artificially high classification success rates.

Significant Raw Variables (SIGRAW)

A more appropriate DFA includes only the variables shown to be significant using PGLS. LDA and QDA were first performed on only the raw significant variables (SIGRAW). The proportion of the trace explained by each linear discriminant function was computed from the LDA. The proportion of trace is a measure of the relative contribution of each linear discriminant function to the overall success of the DFA. For the SIGRAW analysis LD1 explains ~ 82% of the total variation, while LD2 explains 12.7%, leaving only ~ 5% for LD3.

Table 4.1 shows the coefficients of each variable for each discriminant function. This table indicates the weighting of each variable's contribution to each discriminant. These results are partially consistent with the findings of the PGLS analyses. B loads heavily negatively on LD1. DistRad loads positively on LD1 (i.e. opposite to the negative loading of DistRad), which is consistent with PGLS results. However, ProxRad also loads heavily negatively on LD1, which is inconsistent with the PGLS results demonstrating opposing effects of these variables on habitat. Confusingly, ProxRad loads equally heavily and negatively on LD2 as on LD1.

	Discriminant Function		
Variable	**LD1**	**LD2**	**LD3**
MML	0.906021	0.29196	-1.21200
WAF	-0.007291	0.25738	0.25918
B	-1.553979	0.09050	1.18355
ProxRad	-1.719018	-1.88558	0.30157
DistRad	0.218764	-0.04885	1.58578
sqrtPTArea	0.293334	0.15795	-0.04783

Table 4.1: Coefficients of linear discriminants from the LDA using SIGRAW variables.

While these variable loadings are sometimes consistent with functional results from PGLS, functional interpretation based on these DFA scores alone would be difficult. A major reason for the difficulty is that, by definition, subsequent discriminant functions are orthogonal to previous functions (Manly, 2004, p 107). This means that if LD1 is functionally related to a particular hypothesis linking morphology to habitat, then LD2 and LD3 **by definition** capture variation that is not functionally related to habitat, at least

not according to the same hypothesis. Thus, subsequent discriminant functions (after LD1), may offer additional discriminatory power for a particular dataset, but this power to discriminate will not be related to the hypothesized functional hypothesis, and may instead be attributable to other factors (such as allometric size differences or individual variation or simple measurement error). Figure 4.1 illustrates how bovid body mass is patterned across habitat categories; this figure will be referenced in subsequent presentation of DFA results.

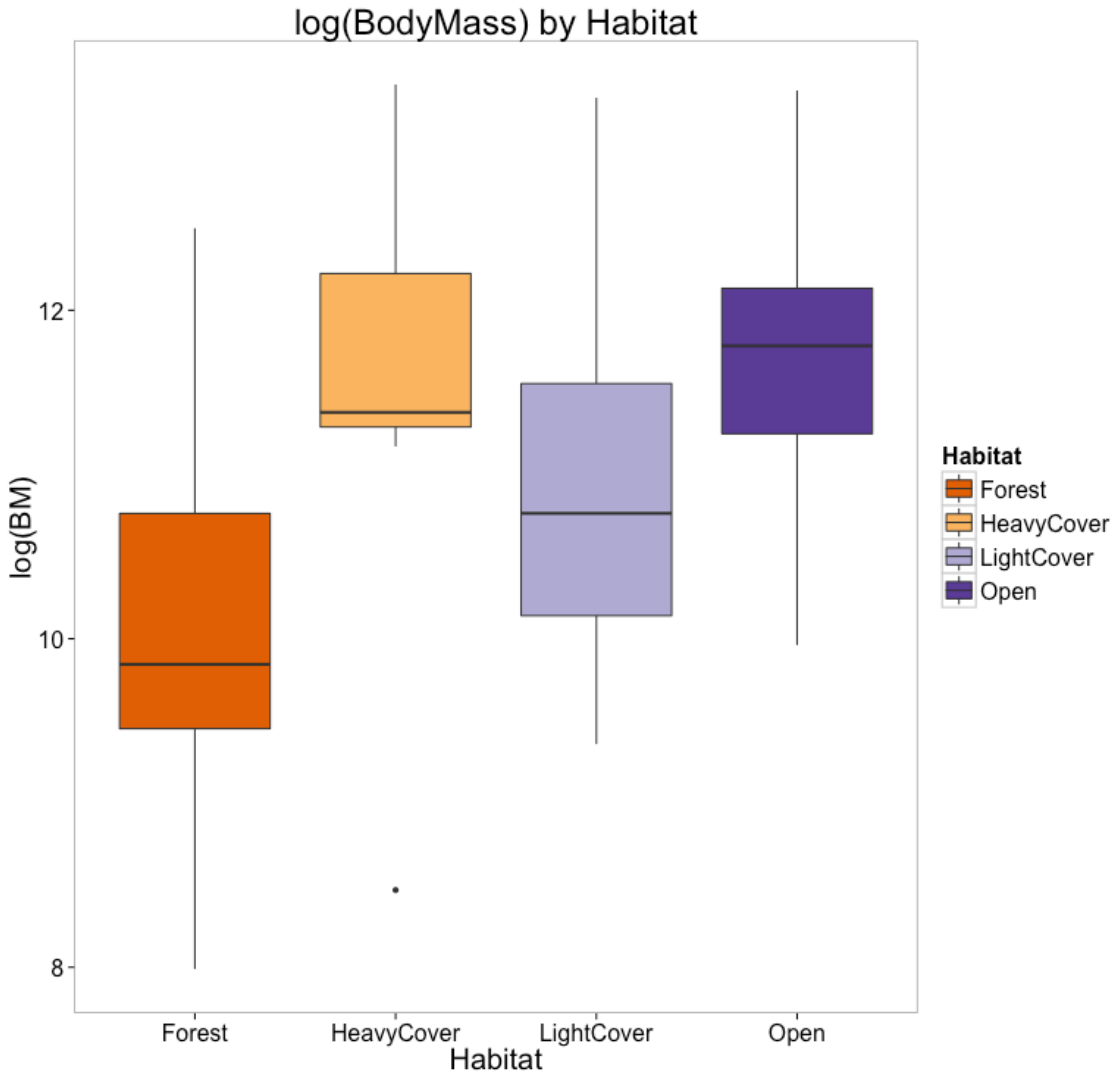

Figure 4.1: Plot of log Body Mass (kg) data from the PanTHERIA dataset (Jones et al., 2009) for species included in this study. Note the typical N-shaped pattern across habitat categories. The outlier is *Madoqua kirkii*.

The scores of the discriminant functions for the SIGRAW analysis are graphically presented in Figure 4.2 and Figure 4.3, which plot scores for each specimen on the three linear discriminants against one another. It is clear that there is much better separation of groups along LD1 and LD2 as compared with LD2 and LD3, which show a great deal of

overlap in the 95% confidence ellipses. Figure 4.4 illustrates LDA scores in a different way, with boxplots of the LD scores by habitat. Figure 4.4 reveals that LD1 most closely follows the pattern of variables shown to have functional signal in Chapter 3, while LD2 has a pattern that is difficult to interpret functionally, because Forest and Open bovids are similar on LD2. It is worth noting that LD1 in this analysis does not discriminate at all among the Forest and Heavy Cover groups. Scores along LD3 are distributed in an *N* – shaped pattern that looks like an inverted version of the boxplot of bovid body mass data across habitats shown in Figure 4.1.

Table 4.2 summarizes the classification accuracies for LDA and QDA using both methods of determining classification success (i.e. resubstitution and cross-validation). The table also includes p-values from four different significance tests for LDA analyses (Wilkes Lambda, Pillai's Trace, Hotelling's T, and Roy's Greatest Root), all of which were highly significant for all LDA analyses.

LDA		**QDA**		**LDA Significance P-values**			
Resub	**C-V**	**Resub**	**C-V**	**Wilkes**	**Pillai**	**Hotelling**	**Roy**
0.6646	0.628	0.6961	0.6159	< 0.0001	< 0.0001	< 0.0001	< 0.0001

Table 4.2: Classification success rates for the SIGRAW dataset. Resubstitution and cross-validation classification rates are shown for LDA and QDA analyses. Four separate methods for determining statistical significance of LDA were used; only their p-values are reported.

The LDA results show that ~66.5% of individuals were correctly classified based on resubstitution rates, and that this accuracy drops to ~62.8% when using leave-one-out cross-validation. The QDA classification results performed slightly better using resubstitution at ~69.6%, but worse when using cross-validation with QDA, at ~61.6%. These results are very similar to those obtained by Degusta and Vrba (2003), who

reported 67% (LDA, resubstitution, 8 variables) and considerably lower than those of Plummer and colleagues (2008), who reported 92% (QDA, resubstitution, 11 variables).

	Predicted Habitat			
Actual Habitat	**Forest**	**HeavyCover**	**LightCover**	**Open**
Forest	0.722	0.200	0.091	0.000
HeavyCover	0.167	0.567	0.205	0.056
LightCover	0.083	0.200	0.523	0.148
Open	0.028	0.033	0.182	0.796

Table 4.3: Confusion matrix giving LDA resubstitution accuracy by habitat category for the SIGRAW analysis.

Table 4.3 breaks down the classification success rates by habitat group. As in prior postcranial ecomorphology studies using DFA on various skeletal elements, the classification success rates are highest for the extreme categories (Forest and Open) and are considerably lower for the intermediate categories (HeavyCover and Light Cover).

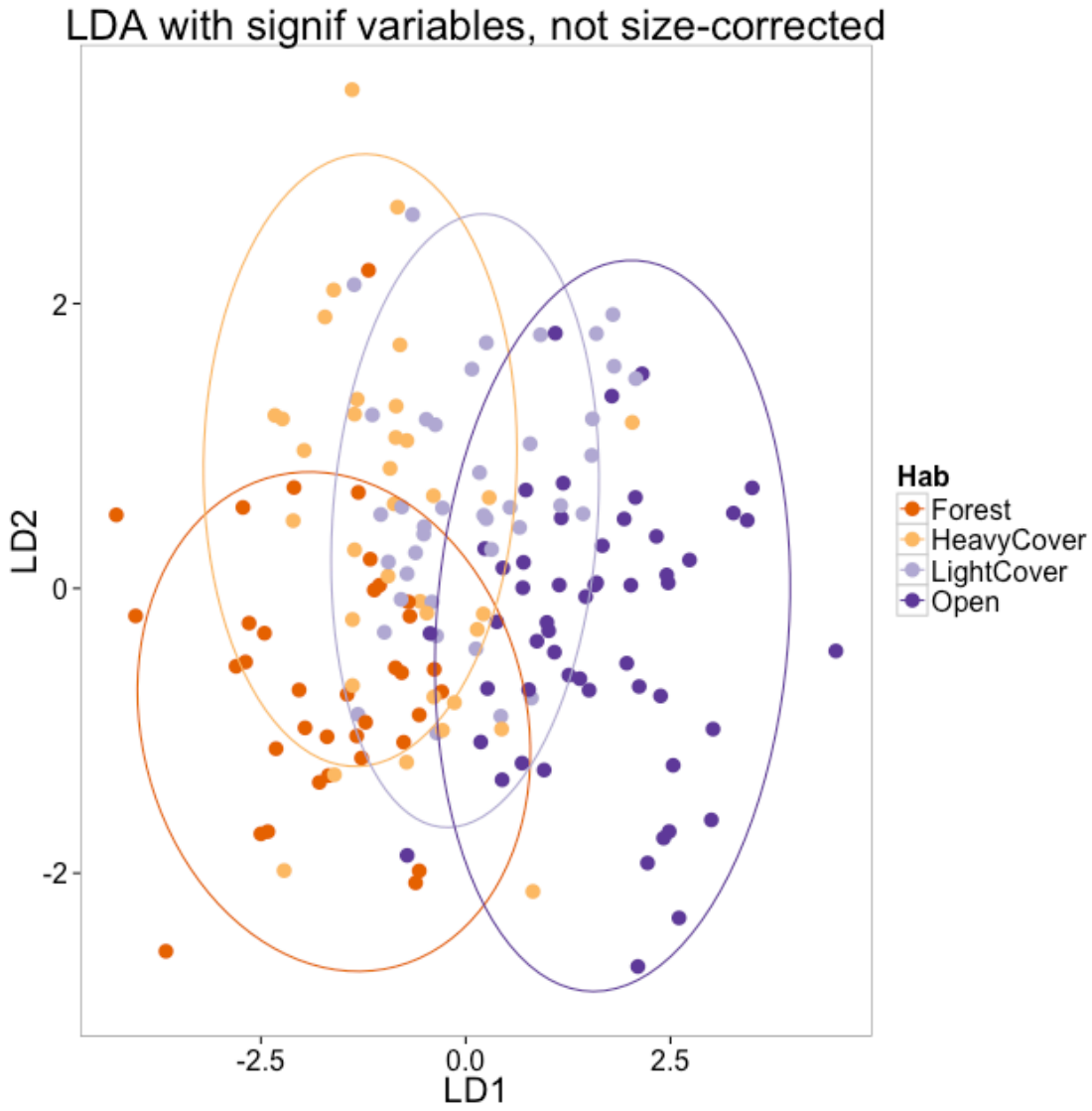

Figure 4.2: LDA results (LD1 and LD2) for SIGRAW analysis.

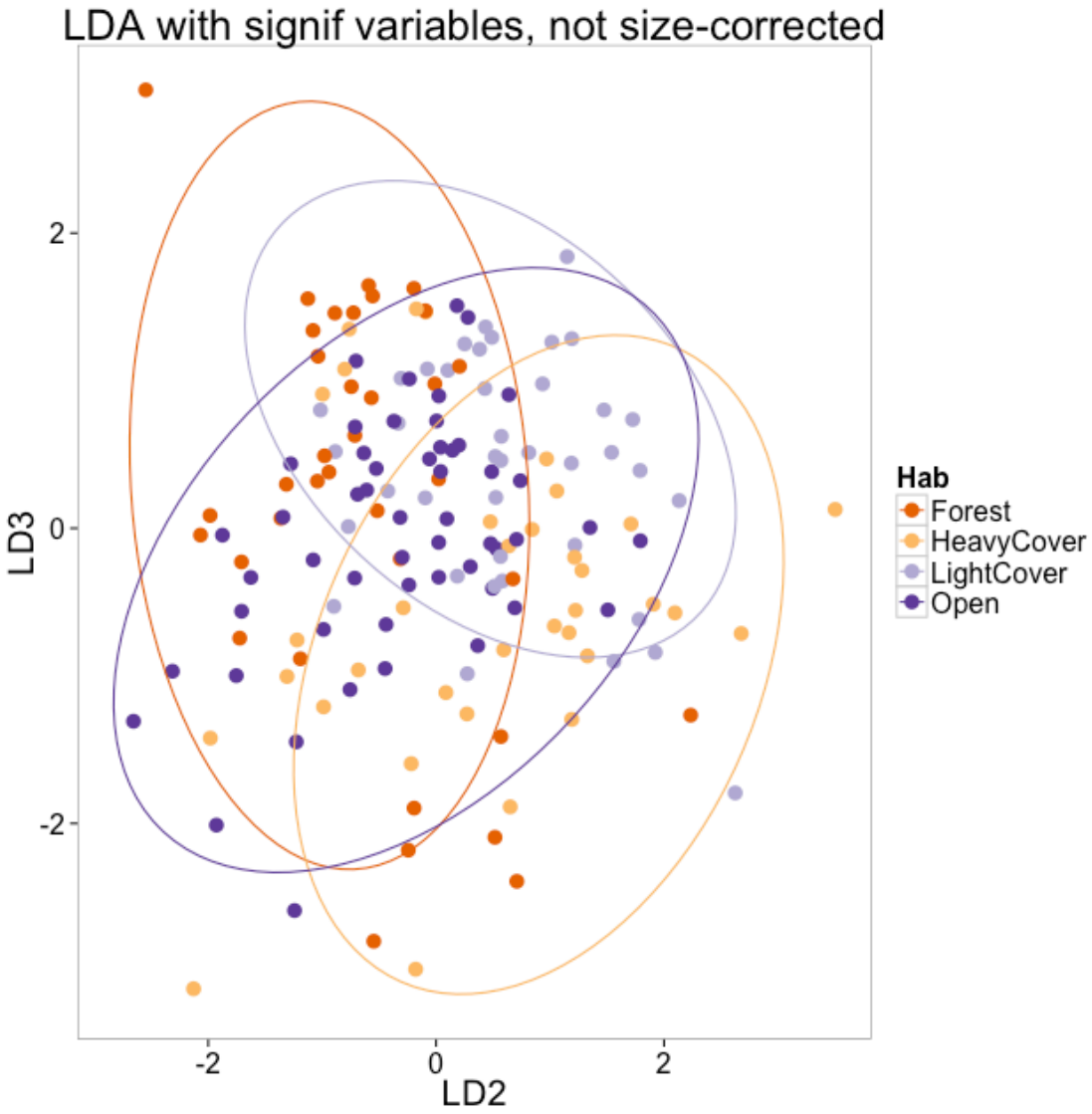

Figure 4.3: LDA results (LD2 and LD3) for SIGRAW analysis.

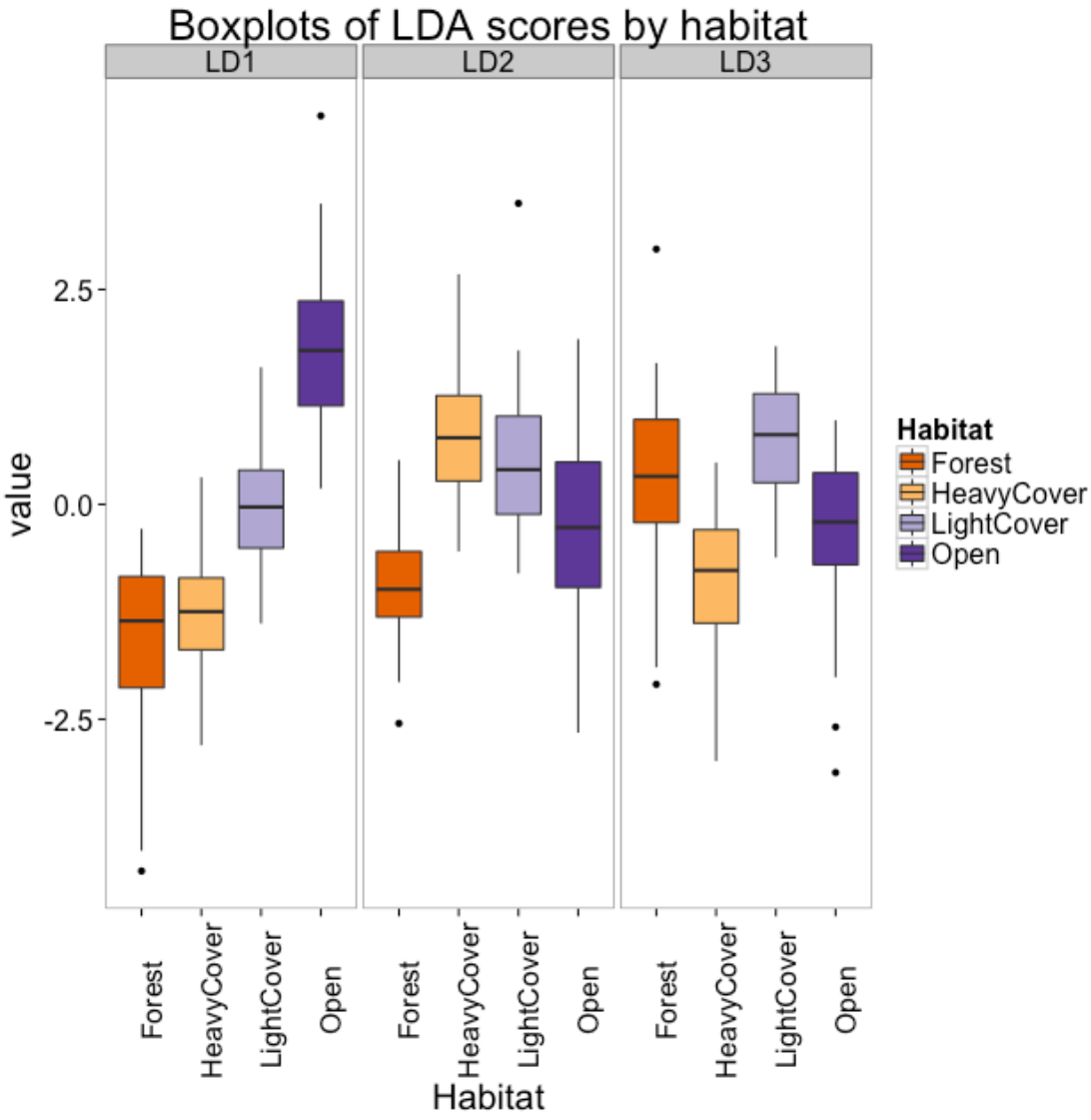

Figure 4.4: Boxplots of LD1, LD2, and LD3 scores across habitat groups for the SIGRAW variables.

Significant geomean corrected variables (SIGGEO)

LDA and QDA were next performed on GEOMEAN corrected significant variables (SIGGEO). The proportion of the trace explained by each linear discriminant function was computed from the LDA. For the SIGGEO analysis LD1 explains ~ 89.7% of the total variation, while LD2 explains ~8.9%, leaving only ~ 1.4% for LD3. These results are better than those from the SIGRAW analysis, for which LDA captured only 82% of the variation. These results suggest that more of the variance in the SIGGEO analysis is captured by LD1, which I interpret to reflect functional differences between habitat groups.

	Discriminant Function		
Variable	**LD1**	**LD2**	**LD3**
MML	-27.461	14.5233	-49.22
WAF	-5.982	-0.5437	23.94
B	10.923	-5.5550	53.11
ProxRad	7.929	19.9038	37.14
DistRad	-15.132	0.1999	42.73
sqrtPTArea	-10.305	-12.8648	-12.75

Table 4.4: Coefficients of linear discriminants from the SIGGEO analysis.

Table 4.4 provides the variable loadings for each of the linear discriminant functions. DistRad and B load heavily in opposite directions on LD1, consistent with functional interpretations from Chapter 3. The sqrtPTArea variable also loads heavily on LD1, with the same sign as DistRad, which is consistent with functional interpretations. MML loads heaviest of all on LD1, but with a sign that is opposite of B, even though

these two measurements were both negatively associated with the habitat category in the PGLS analysis. However, MML also loads heavily in the opposite direction on LD2, and again heavily on LD3. Thus, the variance in MML is effectively being smeared across all the LDs. Overall, as for the SIGRAW analysis, functional interpretations from the DFA are consistent in broad strokes with those from the PGLS, but are rendered more complicated in the multivariate analysis.

LDA		QDA		LDA Significance P-values			
Resub	**C-V**	**Resub**	**C-V**	**Wilkes**	**Pillai**	**Hotelling**	**Roy**
0.6524	0.5915	0.7072	0.615	< 0.0001	< 0.0001	< 0.0001	< 0.0001

Table 4.5: Classification success rates for the SIGGEO dataset. Resubstitution and cross-validation classification rates are shown for LDA and QDA analyses. Four separate methods for determining statistical significance of LDA were used; only their p-values are reported.

Classification accuracies for the SIGGEO analysis are given in Table 4.5. The resubstitution rate for LDA was 65.24%, dropping to 59.15% using cross-validation. The QDA results were somewhat higher, yielding 70.72% using resubstitution and 61.5% using cross-validation. These results are extremely similar to results from SIGRAW analyses. However, the SIGRAW analysis had a lower proportion of variance explained by LD1. Thus, the SIGGEO results are somewhat easier to interpret, and can be more confidently extrapolated outside the predictor dataset, because less of the variance is left unexplained in LD2 and LD3, which are by definition not related to the functional signal reflected in LD1.

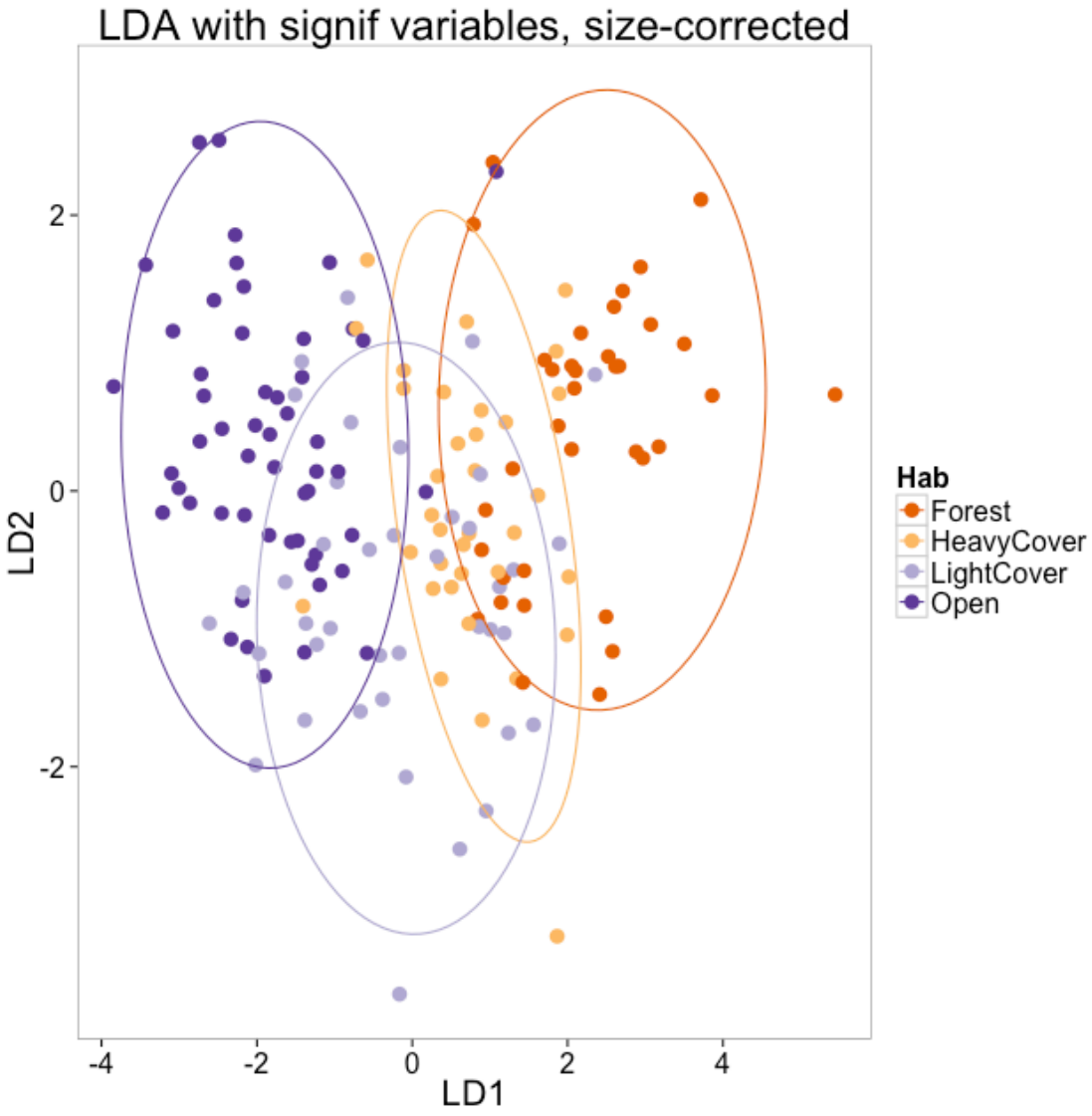

Figure 4.5:DFA (LD1 and LD2) results for all variables after size correction.

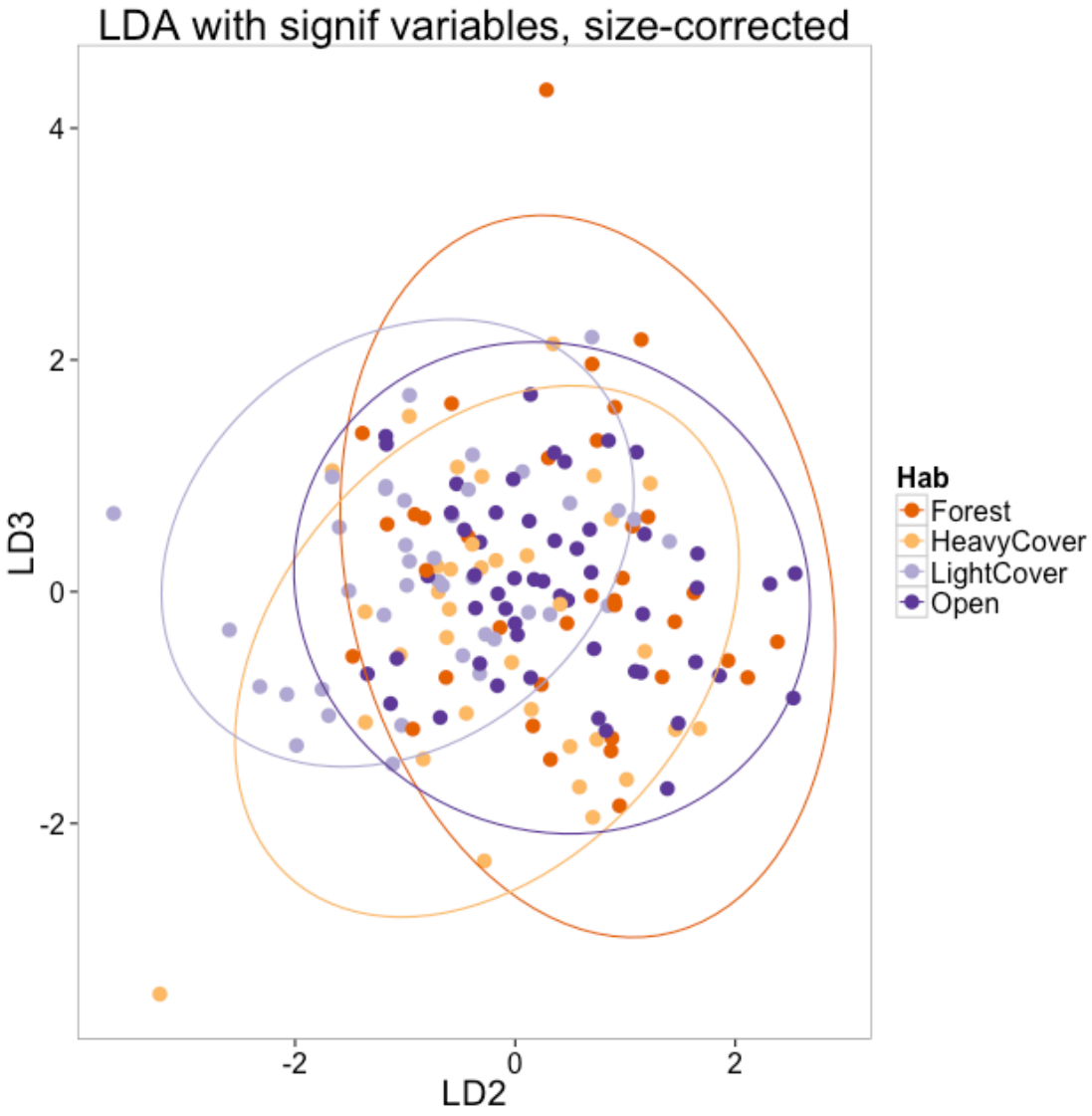

Figure 4.6: DFA (LD2 and LD3) results for all variables after size correction.

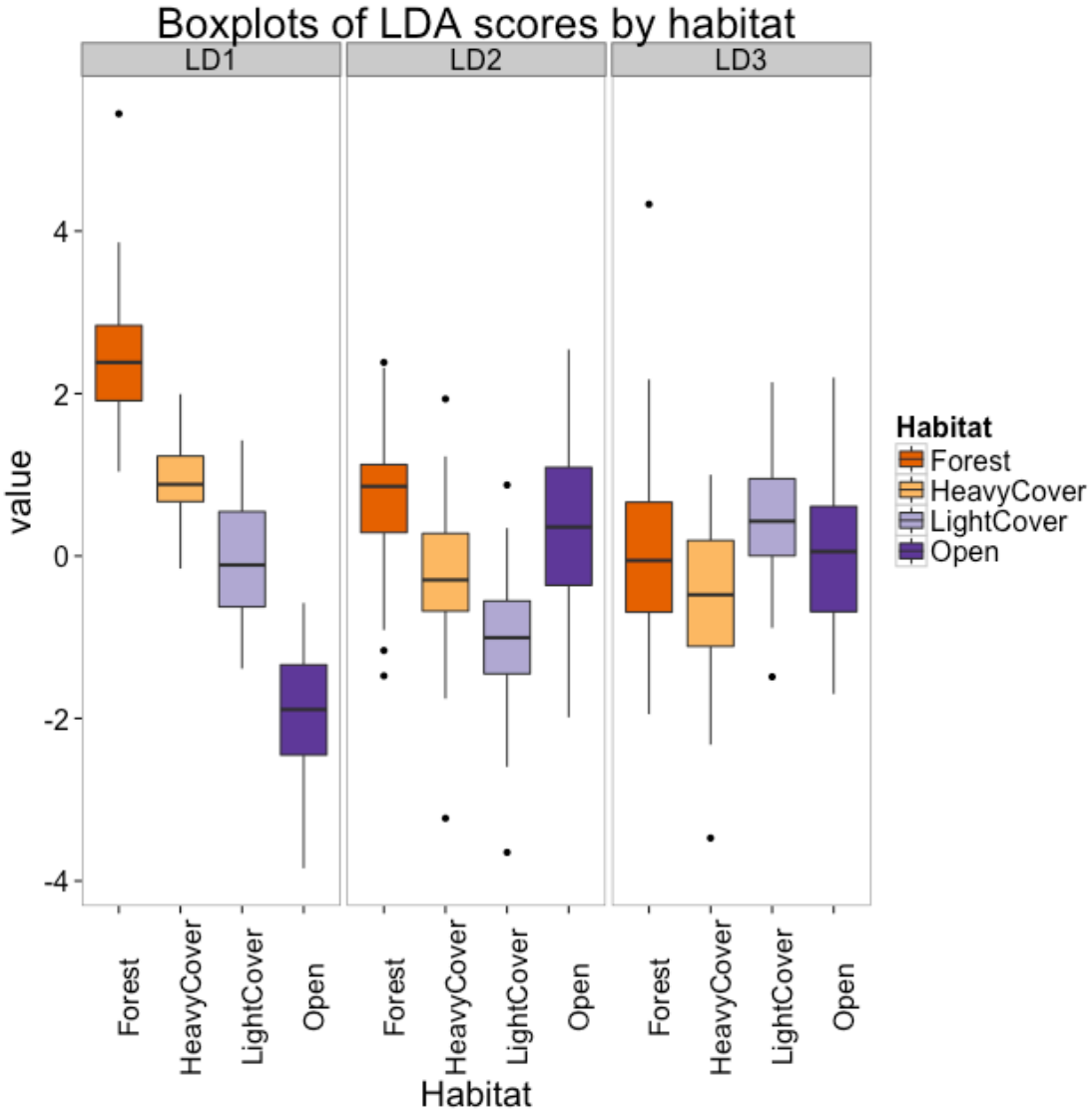

Figure 4.7: Boxplots of LD1, LD2, and LD3 scores across habitat groups for the DFA corrected variables dataset.

Table 4.6 provides a breakdown of the LDA resubstitution accuracies by habitat category. These results are not meaningfully different from the results of the SIGRAW analysis. Once again, Forest and Open categories have the highest predictive accuracies,

with the intermediate categories performing less well, in the neighborhood of 50% accuracy.

	Predicted Habitat			
Actual Habitat	**Forest**	**HeavyCover**	**LightCover**	**Open**
Forest	0.765	0.237	0.032	0.000
HeavyCover	0.147	0.474	0.290	0.049
LightCover	0.059	0.289	0.516	0.180
Open	0.029	0.000	0.161	0.770

Table 4.6: Confusion matrix giving LDA resubstitution accuracy by habitat category for the SIGGEO analysis.

DFA – SIGGEO variables (excluding PTArea)

A final DFA was conducted on the SIGGEO dataset excluding the PTArea variable. This was done because the PTArea measurement is considerably more difficult to obtain, as it depends on collecting high quality 3D models. The remaining variables could be obtained with calipers and high quality photographs of carefully aligned specimens (in the case of B and DistRad). Thus, a DFA including these 5 measurements is easier to apply to fossil collections and thus more likely to be employed by other researchers in future studies. For the LDA on the SIGGEO variables excluding PTArea, the proportion of trace was very similar to the SIGGEO dataset. The proportion explained by LD1 was 90.4%, leaving 8.89% for LD2, and 0.7% for LD3.

Variable loadings for the SIGGEO dataset excluding PTArea are given in Table 4.7. The results are consistent with results from the SIGGEO dataset. Again, DistRad and B load on LD1 in opposite directions, consistent with functional interpretations from Chapter 3. Once again, the variance attributable to MML gets smeared across the three discriminant functions, leading to some difficulty in functionally interpreting loadings.

	Discriminant Function		
Variable	**LD1**	**LD2**	**LD3**
MML	23.619	27.480	-43.27
WAF	10.013	-8.365	20.95
B	-8.837	-7.839	59.47
ProxRad	-1.904	17.176	44.23
DistRad	17.759	-4.535	44.43

Table 4.7: Coefficients of linear discriminants from the LDA for SIGGEO (excluding PTArea).

Classification success rates from the SIGGEO dataset excluding PTArea are given in Table 4.8. These results are nearly indistinguishable from the SIGGEO results.

LDA		**QDA**		**LDA Significance P-values**			
Resub	**C-V**	**Resub**	**C-V**	**Wilkes**	**Pillai**	**Hotelling**	**Roy**
0.6444	0.6056	0.7127	0.6389	< 0.0001	< 0.0001	< 0.0001	< 0.0001

Table 4.8: Classification success rates for SIGGEO analysis (excluding PTArea). Resubstitution and cross-validation classification rates are shown for LDA and QDA analyses. Four separate methods for determining statistical significance of LDA were used; only their p-values are reported.

	Predicted Habitat			
Actual Habitat	**Forest**	**HeavyCover**	**LightCover**	**Open**
Forest	0.733	0.267	0.049	0.000
HeavyCover	0.178	0.400	0.317	0.062
LightCover	0.089	0.267	0.537	0.172
Open	0.000	0.067	0.098	0.766

Table 4.9: Confusion matrix giving LDA classification accuracy by habitat category (SIGGEO excluding PTArea).

Table 4.9 provides the classification accuracy results by habitat. Again, these are largely similar to the SIGGEO, with the exception that discrimination on the Heavy Cover habitat category drops somewhat from 47.4% to 40%. The other categories remain similar or slightly higher in the SIGGEO (excluding PTArea) dataset.

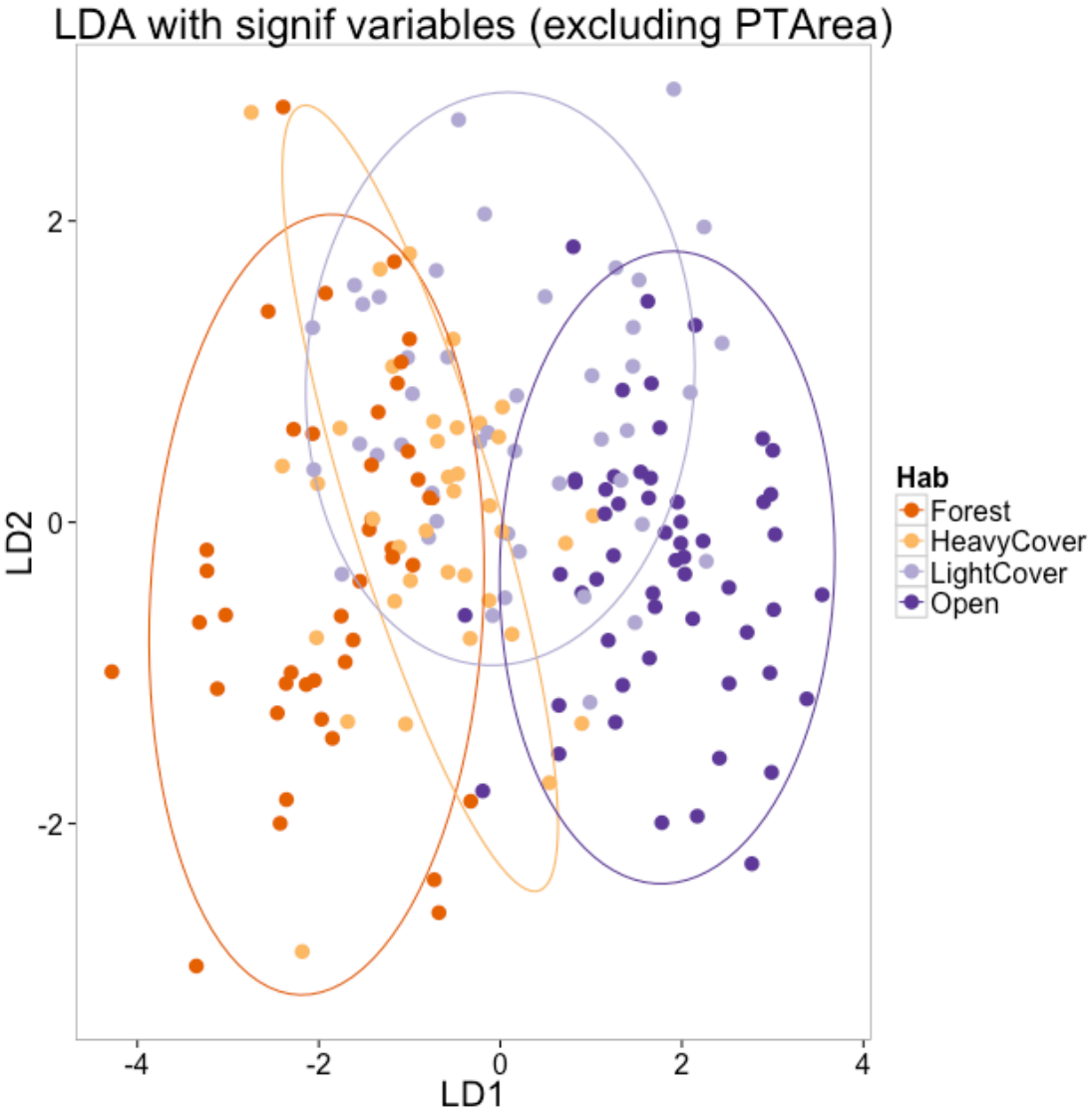

Figure 4.8: DFA results (LD1 and LD2) of SIGGEO analysis (excluding PTArea).

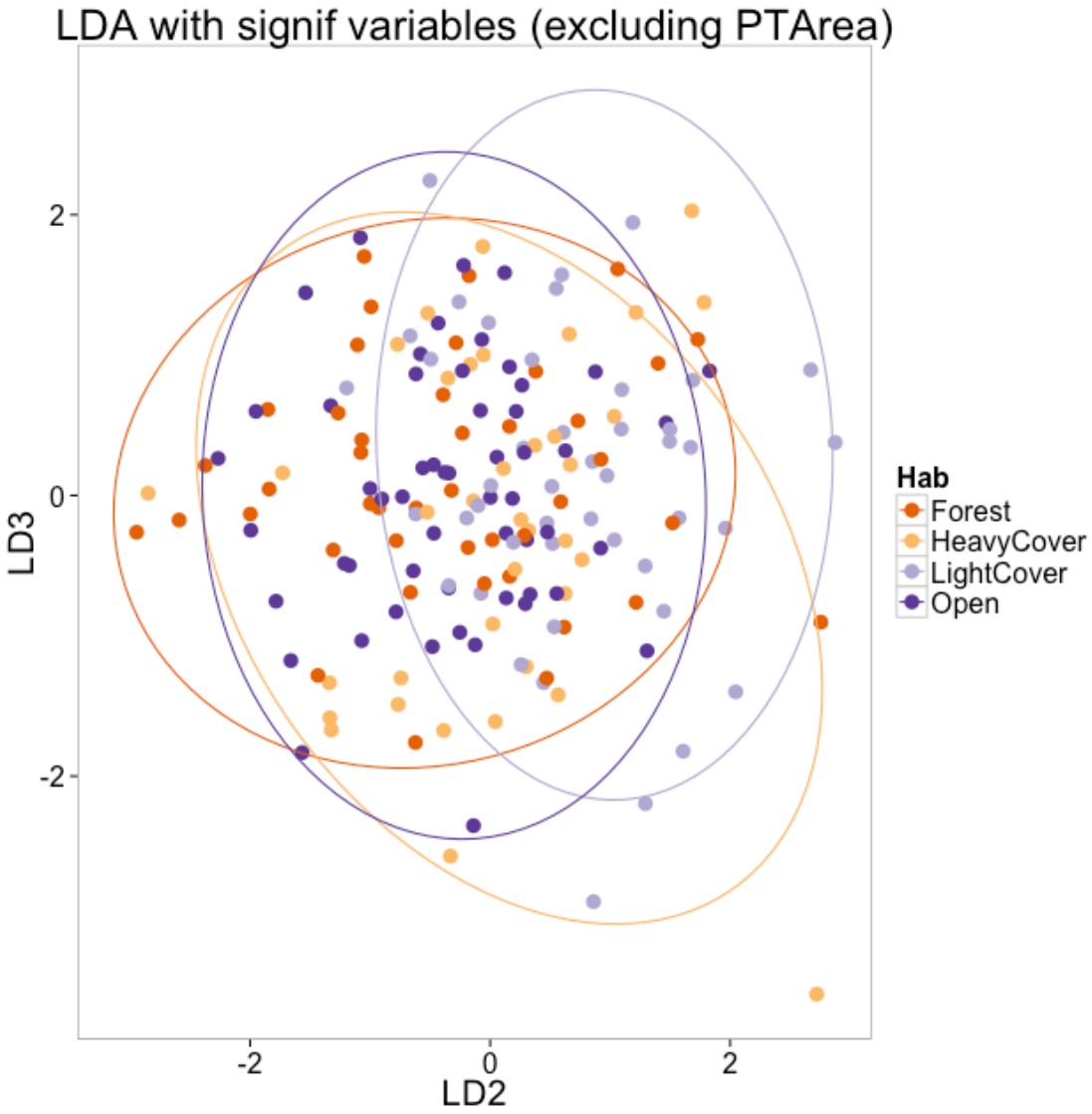

Figure 4.9: DFA results (LD2 and LD3) of SIGGEO analysis (excluding PTArea).

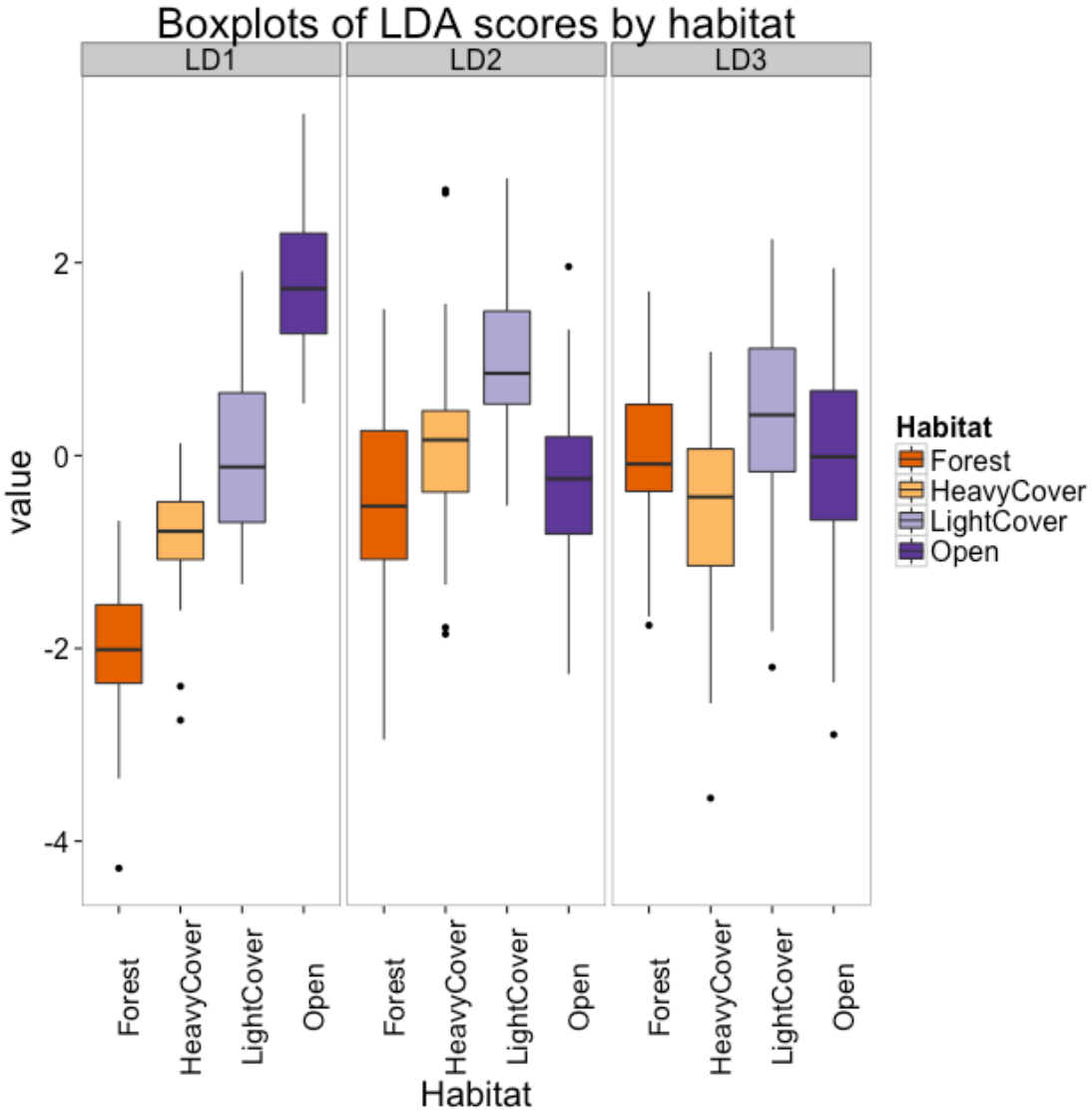

Figure 4.10: Boxplots of LD1, LD2, and LD3 scores across habitat groups for SIGGEO analysis (excluding PTArea).

DISCUSSION

The results from the several DFA analyses in this chapter largely confirm the functional results obtained using PGLS in Chapter 3. It is clear that the morphology of the bovid astragalus holds a functional signal, and that this signal can be exploited to produce habitat classifications at a rate of accuracy far higher than random assignment. The DFA results from this chapter have accuracy rates that are consistently much higher than the simulated data with phylogenetic signal from Chapter 2. This is especially true for the cross-validated results, which hovered around 33% in phylogenetic simulations and were routinely 2X that rate in the astragalar DFAs from this chapter.

Careful selection of functionally relevant measurements results in a small number of measurements that capture the functionally relevant astragalar variation. With only five measurements, the DFA using the SIGGEO variables (excluding PTArea) achieved an LDA classification accuracy of 64.4%, which compares favorably to the 67% LDA accuracy reported by Degusta and Vrba (2003) using 8 measurements.

The results of Plummer and colleagues (2008) in correctly classifying 92% of their extant sample are somewhat difficult to reconcile with the PGLS results from Chapter 3, as well as the DFA classification results from the present chapter. There are several factors that might explain the difference in classification success rates between the Plummer et al. study and this study. First, Plummer et al. used many more variables (11) than were used in this study (5 for the SIGGEO excluding PTArea analysis). These additional variables introduce additional variance that DFA can use to classify extant samples. However, this variance introduced by adding new variables is not necessarily attributable to functional variation related to habitat-specific locomotor ecology. Indeed, the proportion of trace reported by Plummer and colleagues looks quite different than that

obtained in this study. Plummer *et al*.'s first discriminant function explained only 73.4% of the total variance, with 16.7% and 9.9% of the variance left to LD2 and LD3, respectively. The preferred DFA from this chapter (SIGGEO excluding PTArea) explained 90.4% of the sample variation on LD1. Thus, in the analysis of Plummer and colleagues, about 25% of the discriminatory power comes from LD2 and LD3. These secondary and tertiary DFAs are very difficult to interpret functionally because, by definition, they are uncorrelated with the main axis of discrimination related to functional differences between habitats on LD1. It is therefore not clear that the very high classification accuracy reported by Plummer and colleagues reflects only functional differences between habitat groups. As such, the five-variable DFA recommended in this chapter (MML, WAF, B, ProxRad, DistRad) provides a good balance between ease of measurement collection and the functional relevance of the measurements. This five variable DFA will be used to make predictions for fossil taxa in the next chapter.

Chapter 5: Paleoenvironments of the Shungura Formation

This chapter presents paleoenvironmental data for the Shungura Formation based on the ecomorphology of bovid astragali and mesowear evidence from bovid molar teeth. The chapter begins with an overview of the Shungura Formation and a review of previous paleoenvironmental work. Then, paleoenvironmental hypotheses are presented and evaluated using the complementary lines of evidence from astragalar locomotor reconstructions and mesowear-based dietary reconstructions.

BACKGROUND – SHUNGURA FORMATION

The Shungura Formation, located in the Lower Omo Valley of Southwestern Ethiopia, preserves a large sample of hominin fossils that have been attributed to several taxa (Suwa et al., 1996). There is fossil evidence for *P. aethiopicus* at Shungura starting at approximately 2.7Ma (Suwa et al., 1996). Fossils referable to *P. boisei* occur in Member G by approximately 2.3Ma (Suwa *et al*., 1996). There are remains of one or more gracile hominin species from Members B and C, but these fossils are not reliably identifiable to genus. More compelling evidence for the presence of genus *Homo* in the Shungura is established by Member E at ca. 2.4 Ma (Suwa *et al*., 1996). However, the date of the appearance of genus *Homo* at Shungura is difficult to determine with a high degree of accuracy due to the relatively fragmentary nature of the hominin fossils.

In addition to fossil hominins, the Shungura Formation offers one of the richest available collections of mammalian fossils spanning the evolutionary transition from australopiths to early *Homo*. Two research teams: a French team led by Yves Coppens, and an American team led by F. Clark Howell, conducted extensive fieldwork at Shungura during the late 1960s and early 1970s. These assemblages together comprise

one of the most continuous and well-dated fossil collections in Africa for the period from 3.6 to 1.39 Ma.

Beginning in 2006, field research was renewed in the Shungura Formation by the Omo Group Research Expedition (Boisserie et al., 2008, 2010). This ongoing fieldwork will undoubtedly improve our understanding of ecological change through time at Shungura through the application of modern geospatial methods to improve the spatial and temporal precision of the new fossil collections. However, the legacy collections obtained from the earlier work at Shungura to date still offer one of the best available large-scale collections of faunal evolution in East Africa. The examination of the Shungura Formation fauna in this chapter is restricted to the sample collected by the American team in the 1960s and 1970s, which is housed in the Ethiopian National Museum, Addis Ababa.

The Shungura fauna is sampled from a large axial fluvial system, which dominated most of the region around Lake Turkana during the period from approximately 4 Ma to 2 Ma (Brown and Feibel, 1985). The sediments have been divided into 12 members: the Basal member at the bottom of the sequence, followed by members identified by letters A-L (excluding "I"), each of which corresponds to a dated and laterally extensive tuff bearing the same letter (de Heinzelin and Haesaerts, 1983). Members are divided into lithologically defined units (or submembers) bearing a letter and a number (e.g. G-3). Figure 5.1 illustrates a composite geological section from the Omo Shungura. Haesaerts et al. (1983) identify five major depositional episodes in the Shungura Formation, illustrated in Figure 5.1B. The majority of the sediments represent fluvial phases, with three lacustrine episodes interspersed. Most of the mammalian fossils are recovered from coarse sandy deposits representing channel lag deposits (Dechant Boaz, 1994).

As summarized in Figure 5.1 the Shungura sequence begins with a short lacustrine phase in the Basal member, followed by an extensive fluvial phase lasting more than 1.5 Ma from the upper Basal member through Unit G-13. A major lacustrine phase occurs in upper member G from Unit G-14 through G-27. Fluvial conditions dominate the rest of the sequence, except for a short lacustrine phase at the top of the section in units L-7 through L-9. The Shungura Formation is thus overwhelmingly dominated by fluvial depositional conditions, with the lacustrine episode in upper Member G being the major exception. Indeed, depositional and taphonomic conditions are so distinct in upper Member G, that several authors have treated this as a separate member for analytic purposes (Bobe and Eck, 2001; Alemseged, 2003). There is evidence for widespread deep channeling during unit B-10 and in member D, which probably indicates the presence of a large river with the capability of incising older sediments and time-averaging assemblages (Bobe and Eck, 2001).

Paleobotanical evidence for paleoenvironmental reconstruction is rather sparse in the Shungura Formation. Five pollen spectra have been analyzed from the entire formation (Bonnefille and Dechamps, 1983), which evince a decrease in forest pollen and an increase of grass pollen from unit B-10 through Tuff G (although the sample from Tuff G shows a decrease in grass pollen from the previous sample). Macrobotanical samples are likewise sparse, but also support the notion of an aridification trend (Bonnefille and Dechamps, 1983). The nature of paleosol development supports the aridity trend suggested by the pollen, as paleosols in members A and B indicate relatively humid conditions, with dryer conditions prevailing after unit C-3 (Bobe and Eck, 2001). Isotopic analysis of pedogenic carbonates from Shungura clearly indicate an increase in carbon isotope ratios beginning around 2.5 Ma, consistent with an increase in C4 biomass in the floodplain of the ancestral Omo River (Levin et al., 2011).

The microfaunal samples from the Shungura Formation are also relatively sparsely distributed in the formation. The oldest sample from unit B-10 contains three bat species and a shrew species which are allied with extant taxa restricted to rainforests of Western Africa (Wesselman, 1984). The forest dwelling microfauna decrease in importance by unit C-8, and are nearly eliminated altogether in members F and G, replaced by taxa indicative of xeric, open environments including jerboas and gerbils in Members F and G (Wesselman, 1984, 1995). These data have been cited in support for the Turnover Pulse Hypothesis, but they are too sparsely distributed to precisely pinpoint the timing of the faunal transition (Behrensmeyer et al., 1997).

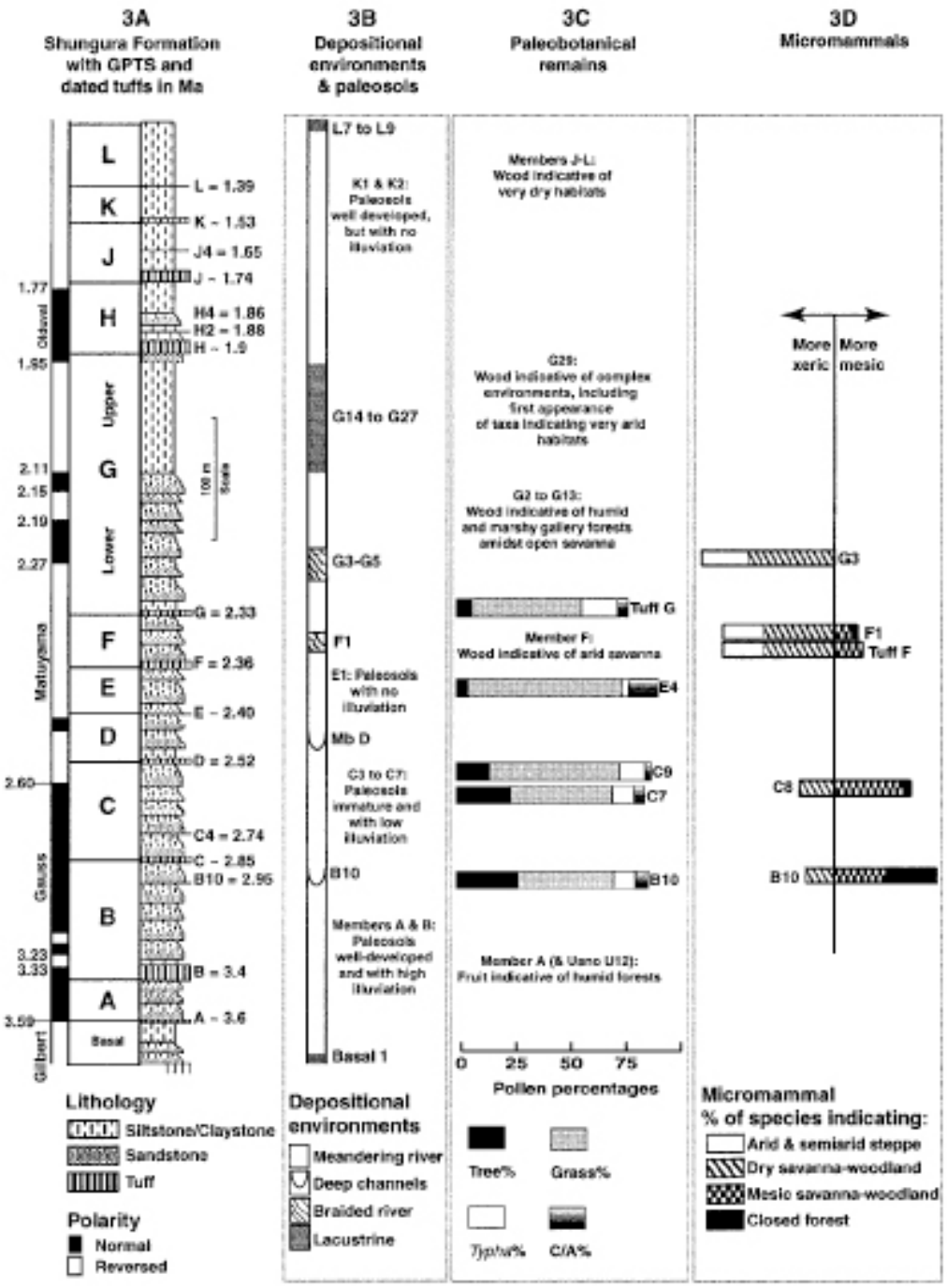

Figure 5.1 **A:** Composite stratigraphic section of the Shungura Formation (Bobe & Eck 2001: their Fig. 3). **B:** Depositional environments and paleosol data (from Haesaerts et al., 1983). **C:** Paleobotanical data (data from Bonnefille and Dechamps, 1983). **D:** Microfaunal remains (data from Wesselman, 1984).

Ecological structure analysis of the Shungura Formation by Reed (1997) is, for the most part, consistent with these various lines of evidence. To summarize, Unit B-10 exhibits a high proportion of arboreal and frugivorous taxa, consistent with woodland / riverine forest / edaphic grassland. Members C and D both indicate a woodland/bushland with some edaphic grasslands. Member E exhibits a reduction in fresh-grass grazers and aquatic animals, but remains consistent with a woodland/bushland. Members F and G have elevated numbers of terrestrial and grazing species, indicative of more open habitat.

While the microfaunal, isotopic, paleobotanical, ecological structure, and paleosol evidence all point to a drying trend over the time period represented at Shungura, these data have not established a consensus on the precise tempo and mode of this transition (Bobe and Eck, 2001). The macrofauna, in particular the bovids, are well preserved in great numbers in every unit at Shungura, and thus provide one of the best sources available for paleoenvironmental reconstruction. Significant research on the Shungura macrofauna has already been published. For his dissertation, Bobe (1997) quantitatively studied the fauna from the American collection. Alemseged studied the independently collected French faunal collection as part of his dissertation (2003). These two datasets, encouragingly, exhibit consistent taphonomic signals (Alemseged et al., 2007). In general, the bovid data point to well-watered, closed environments in the lower Omo valley prior to 2.85 Ma with increasingly arid conditions indicated after 2.85 Ma.

Faunal sample sizes are quite small from member A, but the taxonomic composition is similar to that of the much better sampled member B (Alemseged, 2003). Member B is characterized as relatively moist, with high proportions of reduncine bovids (Bobe and Eck, 2001; Alemseged, 2003). Bobe & Eck (2001) find a major taxonomic change between members B and C (ca. 2.85 Ma) involving a shift towards greater abundance of tragelaphines and bovines, with a reduction of reduncines. Owing to the

absence of apparent major taphonomic shifts between Members B and C, these authors interpret this change as an environmental shift away from closed/wet conditions.

This interpretation finds some support from a recent enamel isotopic study which reported an increase through time in δC13 values in *Tragelaphus nakuae* and *Kolpochoerus limnetes*, two species that persist before and after 2.85 Ma (Bibi et al., 2013). Serial sampling of enamel isotopes from two hippo canines from units B-9 and C-9 (Souron et al., 2012) offers further support for this interpretation, as carbon isotope ratios from the canine from Unit C-9 are consistent with increased consumption of C-4 vegetation and may also indicate more pronounced seasonality (*i.e.*, greater shifts from wet to dry season) as compared with the canine from Unit B-9. However, this shift towards more arid conditions appears less pronounced based on a broad-scale analysis of the French Shungura collection, with members B and C falling relatively close to one another in taxonomic correspondence analysis (Alemseged 2003: Fig 8). Alemseged's major faunal transition occurs after member E (<2.36 Ma), with another major shift occurring between Members F and G. An earlier study of the Shungura fauna using correspondence analysis was in broad agreement, with evidence that the most open and dry conditions occurred during Member F (Geraads and Coppens, 1995).

Several studies have highlighted the major shift in taxonomic abundance in the Shungura Formation at approximately 2.85 Ma (Bobe and Eck, 2001; Bobe et al., 2002). Some of the taxa appearing shortly after this time are indicator taxa heralding the onset of more arid conditions (Bobe and Behrensmeyer, 2004; Bobe, 2006). These patterns may be viewed as support for Vrba's Turnover Pulse, although there is probably less turnover during the 2.85 – 2.5 Ma period than would be predicted based on the TPH (Bobe et al., 2002). After circa 2.5 Ma, taxonomic abundances become more variable over short time

scales on the order of 100ka, which has been suggested to be attributable to eccentricity-induced Milankovitch cycling (Bobe et al., 2002).

In summary, the Shungura Formation presents an invaluable record of faunal evolution across the Plio-Pleistocene boundary. Because of its dense record of deposition over more than two million years of hominin evolution, the Shungura Formation is critical for understanding environmental changes on a regional scale around this time of major climatic reorganization. Prior work in the Shungura has established an overall drying trend accompanied by large-scale faunal turnover. While all authors agree that major faunal changes occurred between 2.85 – 2.3 Ma, the exact timing of these transitions is elusive. This chapter contributes to this discussion by analyzing the dense record of fossil astragali and bovid molar teeth to provide locomotor and dietary reconstructions of the Shungura bovids.

BACKGROUND - METHODS

Molar Morphology and Dietary Ecology

Mammalian tooth form tends to reflect the physical properties of food items habitually consumed. Ungulates have traditionally been categorized either as grazers, which mostly subsist on monocot grass, and browers, which preferentially select dicot leaves and stems, with mixed-feeders consuming significant amounts of vegetation from both categories (Hofmann and Stewart, 1972). However, these gross categories tend to conflate the type of food acquired (grass vs. leaves) with the method of food acquisition (i.e., bulk consumption vs concentrate selection, see Spencer, 1995). Furthermore, additional factors, especially proximity of feeding postures to the ground, tend to have important impacts on dental form due to the amount of included exogenous grit in the diet (Damuth and Janis, 2011) regardless of the type of food consumed. Nonetheless, the

browser/grazer dichotomy persists, and represents a useful generalization that is applicable to characterizing the diets of fossil organisms. The most salient features of bovid teeth related to dietary function are a tooth's mechanical resistance to wear, and tooth crown relief.

A variety of factors influence a tooth's resistance to wear (van Valen, 1960), but by far the most important factor is the quantity of enamel present in a tooth. While some organisms, like hominoids (Martin, 1985) tend to increase tooth resistance by increasing enamel thickness, ungulates tend to increase tooth resistance by increasing tooth height (Fortelius, 1985). The term hypsodonty refers to those teeth that have extremely high crowns allowing the organism to retain a functional dentition in the face of extreme wear. In contrast to low-crowned (brachydont) teeth, hypsodont teeth have tall enamel pillars that are buttressed by cementum, as shown in Figure 5.2B. Hypsodont teeth continue to erupt from the jaw during much of the lifespan of the animal, exposing fresh enamel ridges to preserve tooth function even as an abrasive diet characterized by silica phytoliths in grass and exogenous grit quickly wears down teeth (Janis and Fortelius, 1988; Damuth and Janis, 2011).

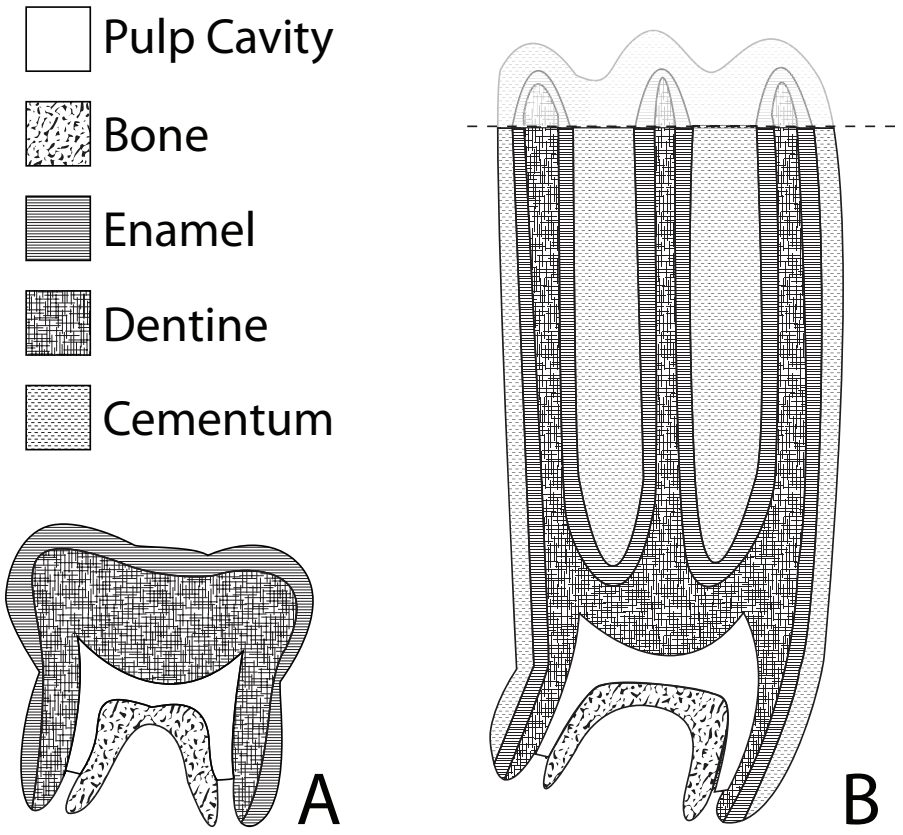

Figure 5.2: Idealized coronal cross-sections through (A) bunodont human molar and (B) hypsodont horse molar. Dotted line on hypsodont molar indicates wear level. Unworn hypsodont teeth are essentially non- functional. Redrawn after Janis & Fortelius (1988, Fig. 8).

Grazers tend to have more hypsodont teeth than browsers, because grazers experience absolutely quicker rates of tooth wear (Solounias et al., 1994), which must be resisted for the organism to maintain a functional dentition. Janis (1988), showed that a simple index of hypsodonty (HI), calculated as M3 height divided by M3 bucco-lingual width, effectively differentiates between browsers and grazers, with exclusive browsers having HI values less than approximately 2, and exclusive grazers having HI values greater than approximately 4.5 (Damuth and Janis, 2011).

The initial intention for this chapter was to measure hypsodonty indices for all isolated lower third molars in the Shungura collection. However, this proved to be infeasible, due to the dramatic differences in wear stages observed in the collections. These differences were so extreme as to render meaningless any comparisons of hypsodonty indices. Figure 5.3 illustrates this problem with three examples of lower third molars of *Aepyceros*. These three individuals would exhibit dramatically different hypsodonty indices, even thought they likely belong to the same species.

Figure 5.3: *Aepyceros* lower M3s in varying stages of wear.

The occlusal relief of a tooth also has great importance for predicting the diet of bovids. In general, browsers have higher occlusal relief than do grazers. Browse is a heterogeneous category, but is generally characterized by softer sheets and thicker rods as compared to the thinner sheets and rods characteristic of mature grass (Fortelius, 1981). Because soft objects resist crack propagation (Lucas, 1979), they can only be divided by blades that are long enough to pass through the entire particle. The particle size of stems

and leaves is usually larger than that of grass, which leads to the need for higher occlusal relief (and consequently longer cutting blades) in browsers to effectively chew their food. Figure 5.4 shows the differences between high relief (browser, large particles) and low relief (grazer, small particles) molars and the maximum particle size these molars can divide.

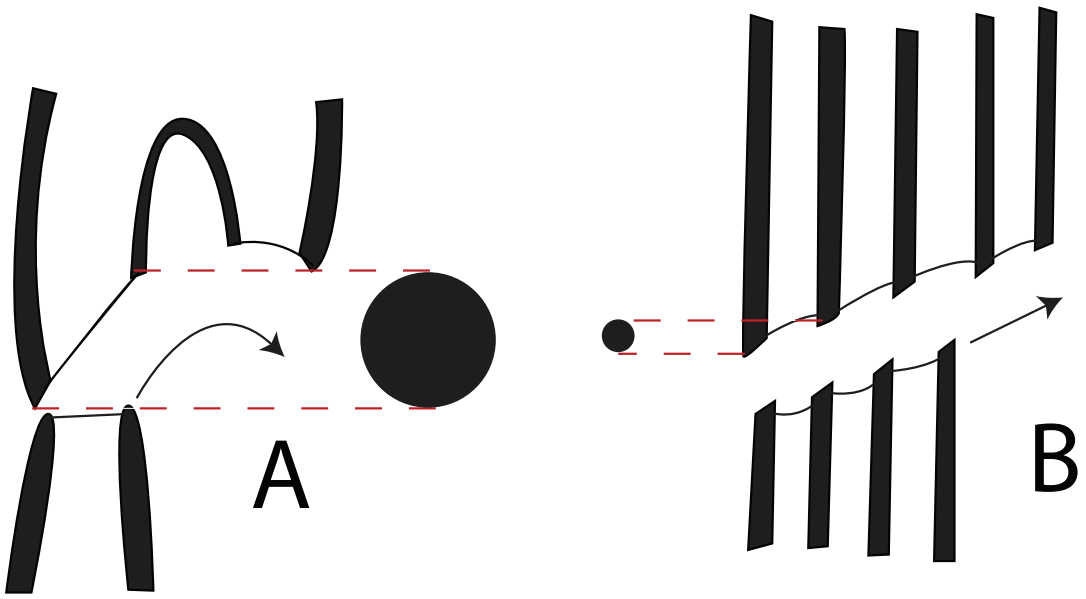

Figure 5.4: Idealized coronal cross sections through high-relief, single bladed molar and low-relief, serially-bladed molar. Arrows indicate stereotyped jaw motion during chewing cycle. Filled circles represent the approximate maximum diameter of food particls which can be divided by these tooth forms. Redrawn after Fortelius (1981, Figure 5.).

The most commonly used method for characterizing molar relief in ungulates is the mesowear method of Fortelius and Solounias (2000). Mesowear is a simple and reliable method of characterizing ungulate molars based on two qualitative variables: cusp shape and cusp relief. Variables are evaluated on upper molars from the buccal aspect of the tooth using the naked eye or a hand lens. Lower molars can also be

evaluated for mesowear, with the caveat that mesowear spectra for lower molars are typically shifted towards a grazing signal (Kaiser and Fortelius, 2003). Uppers and lowers are sometimes analyzed separately, and sometimes are pooled to increase sample size (e.g., Blondel et al., 2010). Cusps shape is scored as sharp, rounded, or blunted, depending on the degree to which wear facets are developed. Cusp relief (either high or low) characterizes the distance from the base of the valley between the tips of the metacone and paracone and the valley between these cusps. Cusp shape and relief can be reliably scored and are maintained throughout an organism's lifespan until the last wear stages (Fortelius and Solounias, 2000). Recent work comparing mesowear variables and stable isotopes of the same individuals in museum collections confirm the utility of mesowear for inferring diet (Louys et al., 2012).

These variables are influenced by the predominant mode of wear: attrition *versus* abrasion. Attrition refers to direct tooth-on-tooth wear, which tends to sharpen cusps and maintain relief (Fortelius and Solounias, 2000). Abrasion refers to tooth-on-food wear, which tends to obliterate the attrition signal and reduce occlusal relief. Committed browsers tend to be attrition dominated, and have high relief and sharp cusps. Committed grazers tend to be abrasion dominated, with low relief and rounded to blunted cusps. A discriminant function analysis using mesowear variables correctly classified 72% of the extant sample as grazers, browsers, or mixed-feeders (Fortelius and Solounias, 2000).

Mesowear reflects mechanical responses to the actual use of teeth during the lifetime of an individual. Thus, while general tooth structure (which is clearly phylogenetically patterned) must affect mesowear to some extent, cusp shape and relief are actively modified during life, which likely mitigates the phylogenetic signal contained in general tooth structure.

Mesowear offers a quasi-independent line of evidence against which astragalar ecomorphic habitat reconstructions of the Shungura Formation may be compared. Molars and astragali are extremely dense and highly resistant to both destruction by carnivores (Brain, 1980) and long distance transport by water (Behrensmeyer, 1975). Thus, these elements are preserved commonly in both low-energy and high-energy depositional settings, whereas more fragile skeletal elements tend to be preserved only in low-energy depositional settings. Astragali and molars are therefore considered to have highly favorable taphonomic properties, and to provide the best available statistical sample of the habitat preferences of the Shungura bovids.

HYPOTHESES

H1: There was a significant drying trend from 4 – 2 Ma (deMenocal, 2004).

P1.1: Mesowear scores will reflect increasingly dry conditions (increase in blunt cusps, low relief) across submembers, and will correlate positively with submember rank order.

P1.2: Percentage of open-country adapted astragali will correlate positively with submember rank order.

H2: There was a sudden environmental change at 2.85 Ma (Vrba, 1995).

P2.2: Changes in mesowear scores will be highest between Members B and C at Shungura (Tuff C = 2.85 Ma).

P2.3: Changes in percentages of astragalar adaptations will be highest between members B and C at Shungura.

MATERIALS AND METHODS

Provenience of the Fossil Sample

The fossils examined in this study all derive from localities in the American collections of the Shungura Formation Members B – G. Fortunately, prior analyses of skeletal part representation indicate that depositional conditions remained relatively constant during the period from the upper Basal member to lower Member G, which corresponds to the period from >3.6 Ma to ~2.1 Ma (Bobe & Eck, 2001). The fossils from the American sectors of the Shungura Formation considered here derive from localities in a relatively constrained ~2Km x ~10Km north-south band (personal observations from original published geological maps and aerial photos). These fossils were collected following rigorously enforced collection criteria and protocols (detailed in Bobe and Eck, 2001), which required collection of all mammalian astragali and isolated molars (the elements considered in this study). These rigorous collection methods help ensure that the fossils examined in this study are representative of the fossils preserved on the surface (Bobe & Eck, 2001). While the nature of the high-energy fluvial depositional setting of the Shungura Formation broadens the inherent spatial and temporal resolution of the paleoenvironmental signal in the Shungura fossil collections, the consistency in depositional setting and in collection methodology suggests that changes in relative abundance of habitats inferred based on ecomorphology are likely to be due to shifting environmental conditions in the region rather than taphonomic bias or collection bias. This interpretation is consistent with prior research examining the American faunal collections (Bobe & Eck, 2001).

Astragalus

I laser scanned 234 bovid astragali from the American collections of the Shungura Formation following the protocol described in Chapter 3. Several astragali were either too covered in matrix, or else too fragmentary to obtain the necessary measurements. While it would have been desirable to scan the French Collections as well, this was not possible given time constraints. In the future, I plan to expand this study to include the French collection, as comparisons between these two collections would be very interesting.

The 11 linear measurements described in Chapter 3 were collected for each fossil astragalus, following the same measurement protocol outlined in Chapter 3. Individual measurements for fossil specimens are given in Appendix D. Joint surface area measurements were collected for a subset of the specimens. While some area measurements were shown in Chapter 3 to be significant predictors of habitat (especially the area of the proximal trochlear articular surface, PTArea) the increased predictive success was modest compared to a Discriminant Function Analysis (DFA) that only included linear variables. Therefore, the DFA applied to the fossil specimens comprises the restricted subset of size-corrected variables shown to be significant in PGLS, excluding PTArea. The variables included in this DFA are MML, WAF, B, ProxRad, and DistRad.

Categorical habitat predictions for each specimen (Forest, Heavy Cover, Light Cover, and Open) are reported. In addition to the categorical predictions, I also present a "Habitat Score" derived from the DFA analysis. This habitat score is distinct from the habitat score of Scott and Maga (2005), whose habitat score is computationally identical to the scores from the first linear discriminant in a linear DFA. The habitat score used in this chapter derives from the probability estimates produced in DFA. For each habitat

category, DFA produces a probability estimate, such that the summed probability across all categories is 1. These probabilities represent the likelihood that each specimen belongs to a given habitat category. The predicted category, then, is simply the category with the highest probability. Using only the predicted category ignores some of the uncertainty inherent in the classification. This approach is similar to the "fuzzy" classification commonly employed to classify remotely-sensed imagery to create land-cover classifications, for example (Wang, 1990; Reed, 2003).

Previous work has advocated only using DFA predictions with very high probabilities (DeGusta and Vrba, 2003). However, because the classification accuracy across habitats is not equal, this may systematically bias results by effectively filtering out intermediate habitats (which have lower classification accuracies than the extreme habitats). The habitat score used in this chapter is computed by assigning an integer value for each habitat category (1=Closed, 2=Heavy Cover, 3=Light Cover, 4=Open). Each classification probability is then multiplied by the corresponding integer, and the results are summed across all habitat categories. For example, a wildebeest specimen might have the following probabilities for each habitat category: Closed=0.001, Heavy Cover = 0.002, Light Cover = 0.1, Open = 0.897. These probabilities are multiplied by their respective integer values and summed to produce the habitat score. In this example, the habitat score is: 0.001 * 1 + 0.002 * 2 + 0.1 * 3 + 0.897 * 4 = 3.893. This habitat score reflects more accurately the inherent "fuzziness" in DFA predictions than simply using the category with the highest probability.

Mesowear

Mesowear scores were calculated for 559 molars from the Shungura Formation (292 upper molars and 267 lower molars). Many teeth showed evidence of post-depositional taphonomic alteration. The most common alteration was breakage on cusp tips, which precluded the observation of cusp shape. Thus, many teeth were rejected for mesowear analysis, and the observed sample represents a subset of the vast number of bovid molars in the American Shungura collections. Because these were isolated teeth, precise taxonomic identifications are typically impossible, which necessitated analyzing mesowear at the level of taxonomic tribe. This method follows previous studies which have demonstrated that tribal level mesowear offers a meaningful ecological signal (Blondel et al., 2010).

Figure 5.5 provides examples of cusp shape and tooth relief variables. Molars in the most extreme wear stages of wear were not scored. Because all cusps will appear rounded with adequate magnification, it is necessary to establish strict criteria for encoding cusp shape. Following Merceron *et al*. (2007 a) cusps were coded as sharp if there was no rounding visible with the naked eye at 20cm. Blunt cusps are easily distinguished by their total lack of distinct wear facets. Cusp height criteria followed Blondel *et al*. (2007) in which cusps are considered low if the horizontal distance between cusp tips is more than twice that of the vertical distance from the bottom of the inter-cusp valley to the cusp tip. Calipers were used to estimate these distances in intermediate cases.

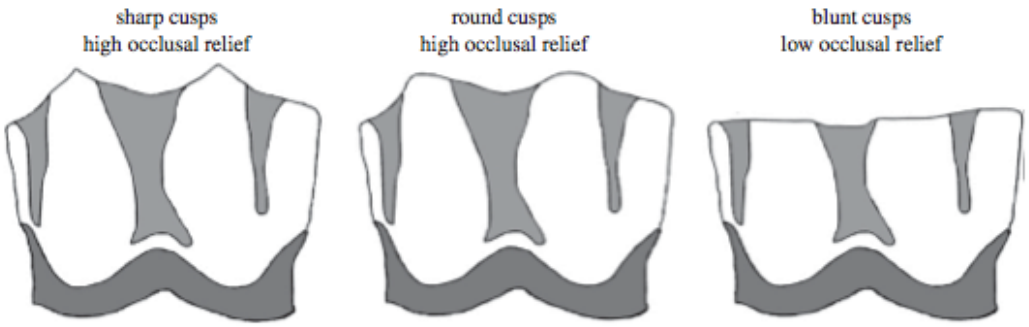

Figure 5.5: Illustration of mesowear variables. Figure is from Louys *et al*. (2012).

Interpreting mesowear requires a set of background data against which scores can be compared. Starting with the original Fortelius and Solounias (2000) mesowear dataset, I subset out all African bovids. This was done because mesowear scores are best compared between taxa with similar overall molar morphology (Solounias and Fortelius, 2000). A series of multivariate ordination methods were employed to visualize the mesowear scores of these taxa. Several previous studies (Fortelius and Solounias, 2000; Kaiser and Fortelius, 2003) have used hierarchical cluster analysis based on Euclidian distances. I prefer not to use hierarchical clustering because it always creates clusters that demand explanation, whether or not these clusters are biologically meaningful. Other methods of ordination do not have the same limitations. Using several packages in R (R Development Core Team, 2011) I performed four types of multivariate ordination on the mesowear data: Correspondence Analysis (CA) (in the vegan package, version 2.0-5, Oksanen et al., 2012), Detrended Correspondence Analysis (vegan 2.0-5), Linear Discriminant Function Analysis (in the MASS package, version 7.3-23, Venables and Ripley, 2002), and Principle Components Analysis (in the base stats package). Because Correspondence Analysis is known to be sensitive to individual outliers, I performed leave-one-out jackknifing to determine whether any one specimen caused significant

reorganization of the CA plot. No major differences were noted during the jackknifing procedure, so the CA was determined to be robust.

There were no major differences in the results of any of the four ordination methods used that would change interpretations of fossil mesowear scores. While axes shifted and the results differed in some details, the major differentiations between dietary groups were preserved across the different methods. Results will be presented visually from CA, because CA allows rows (taxa) and columns (mesowear variables) to be visualized simultaneously on the same plot, thus facilitating visual interpretation.

Predictions from Linear Discriminant Function Analysis were used in a similar fashion as for the astragalar DFA, to produce a "Mesowear Score" for each submember computed by multiplying the categorical probabilities for each diet category (Browser, Mixed Feeder, Grazer) by an integer value (Browser = 1,Mixed Feeder = 2, Grazer = 3) and then summed to produce a single decimal value. Note, however, that in contrast to the astragalar DFA, the mesowear DFA makes predictions for at the level of taxon rather than at the level of individual. As an example, a submember with 15 Tragelaphini upper molars would produce a single DFA prediction of the dietary predictions of Tragelaphini from that submember. This differs from the astragalar DFA predictions, in which a submember with 15 astragali would produce 15 habitat preferences (one per astragalus).

Figure 5.6 shows the results of a Correspondence Analysis of the African bovid subset of the original Fortelius and Solounias (2000) mesowear dataset. This figure forms the background for subsequent interpretation of the fossil mesowear scores. The first CA axis primarily separates dedicated Alcelaphine grazers, characterized by low blunt cusps, from the rest of the sample. The second CA axis pulls out selective, non-frugivorous mixed feeding bovids (Antilopini and some Tragelaphini) in the upper left portion of the plot. These taxa are notable for their high frequency of sharp cusps. Highly selective

browsing bovids that include a significant portion of fruit in their diet are clustered near the origin of the plot. These taxa have a somewhat reduced incidence of sharp cusps compared to the selective mixed feeders and on average a more elevated frequency of high cusps than do the well characterized sharp-cusped mixed feeders. Several taxa in the bottom portion of the plot are characterized by rounded cusps and intermediate frequencies of cusp height variables. These taxa are not well delineated into dietary categories using mesowear.

However, some of these difficult to classify "exceptions" to the broad trends of mesowear are probably ecologically meaningful. For instance, *Hippotragus* has a lower frequency of low and blunt cusps than Alcelaphine grazers, which may be explained by the somewhat higher frequency of dicot vegetation in the *Hippotragus* diet as compared to most Alcelaphines (Gagnon and Chew, 2000). Furthermore, grazing taxa, such as *Alcelaphus (Sigmocerus) lichtensteini,* and fresh grass grazers such as *Redunca redunca* do have a higher frequency of low cusps as compared browers and mixed feeders, but their lack of blunting wear prevents them from clustering with the committed Alcelaphine grazers. Thus, while mesowear is an imperfect proxy for predicting diet, its simplicity and overall utility for characterizing diet explains why it has become a commonly used method (Merceron et al., 2007 b; Rivals et al., 2007; White et al., 2009; Blondel et al., 2010; Kaiser, 2011).

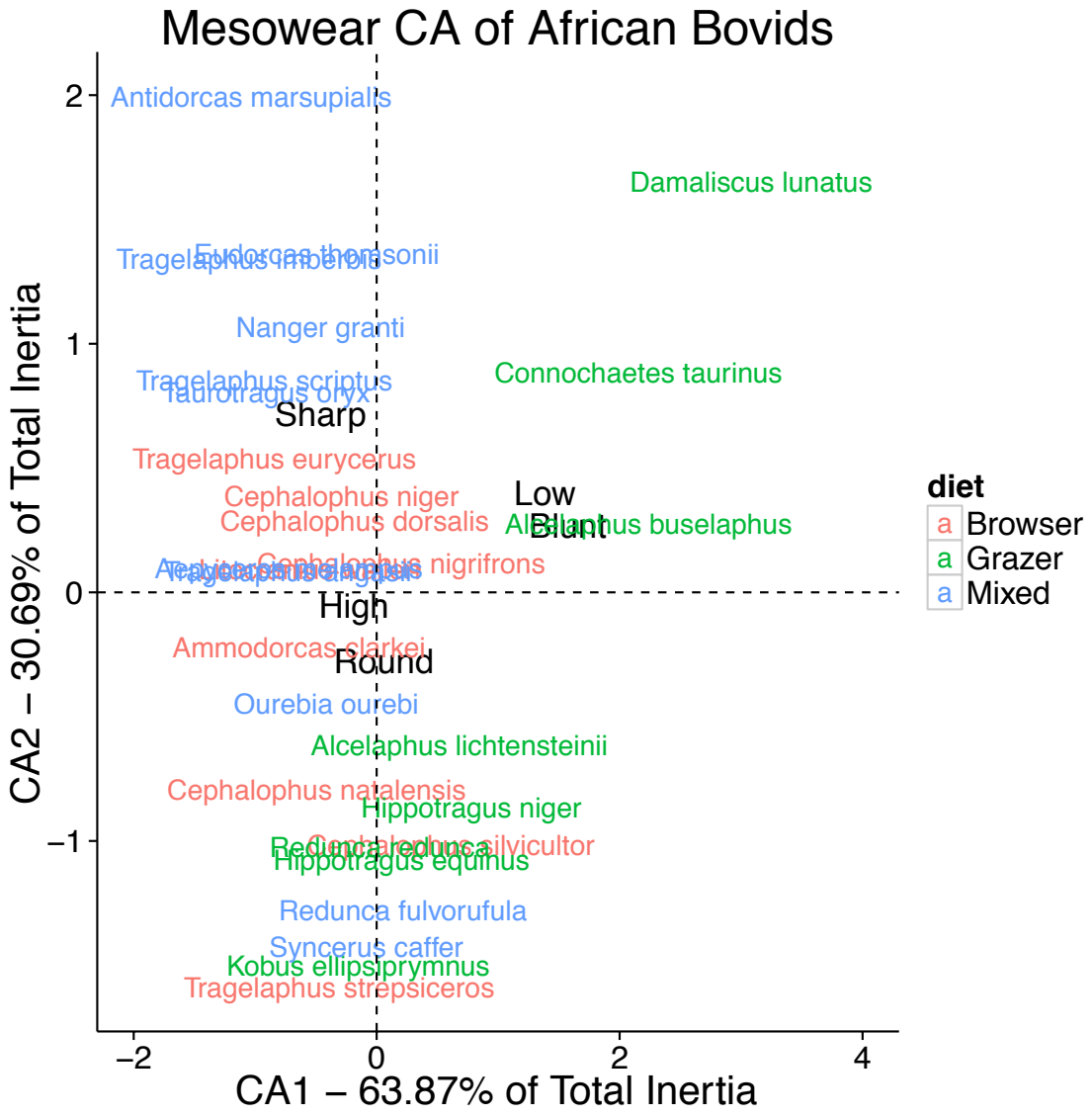

Figure 5.6: Correspondence analysis of the extant African bovid subset from the original Fortelius and Solounias (2000) dataset.

Tests for Uniformity Across Depositional Units

The Chi-Squared test was used to determine whether or not habitat predictions based on astragali changed over time or were constant. A statistically significant result

from the Chi-Squared test ($p < 0.05$) indicates that the observed distribution of astragalar habitat scores departs from a uniform (even) distribution.

Non-Parametric Correlations

In order to test whether or not predicted habitat variables experienced monotonic trends through time, two non-parametric correlation statistics were used: Spearman's rho and Kendall's tau. Both of these correlations are rank-order tests that determine whether or not the dependent variable is a monotonic function of the independent variable (Sokal and Rohlf, 2001). In the analyses here, the independent variable is the rank order of each analytical unit, and the independent variable is the habitat variable being examined.

Pairwise Member and Submember Comparisons

Distributions of astragalar predictions were compared in a pairwise fashion between members and submembers. Mesowear data were not compared in this way because sample sizes were too small for making meaningful comparisons. This is due to the fact that mesowear for each tribe was analyzed separately, which partitions the available sample into several separately analyzed subsamples by tribe, whereas the astragalar sample for each analytical unit is analyzed as a whole.

Pairwise comparisons between astragalar distributions were made using a customized Monte-Carlo procedure that utilizes the Kolmogorov-Smirnov (KS) statistic to characterize the similarity of distributions. The KS statistic compares relative cumulative distribution functions, and is sensitive to differences in location, dispersion and skewness of distributions (Sokal and Rohlf, 2001). Instead of comparing the KS statistic to a table of critical values, the approach taken here is to use a Monte-Carlo resampling technique to compare the KS statistic of two samples against random draws of the same sample size from the entire set of astragalar predictions.

For example, to compare the distribution of astragalar predictions between Member F (n=41) and Member G (n=74), I would first compute the KS statistic between the Member F and Member G distributions. I would then sample the entire set of astragalar predictions across all members to produce a subsample with n=41 and n=74 random astragalar predictions and compute the KS statistic for this subsample. This procedure would then be repeated 10,000 times to determine how often a KS statistic as large as the observed statistic is observed. If the observed KS statistic is larger than 95% of the randomized subsamples, then the observed difference between Member F and Member G would be deemed statistically significant at $\alpha = 0.05$.

RESULTS

Astragali

Individual habitat predictions for each astragalus, along with the constituent habitat scores are given in Appendix E.

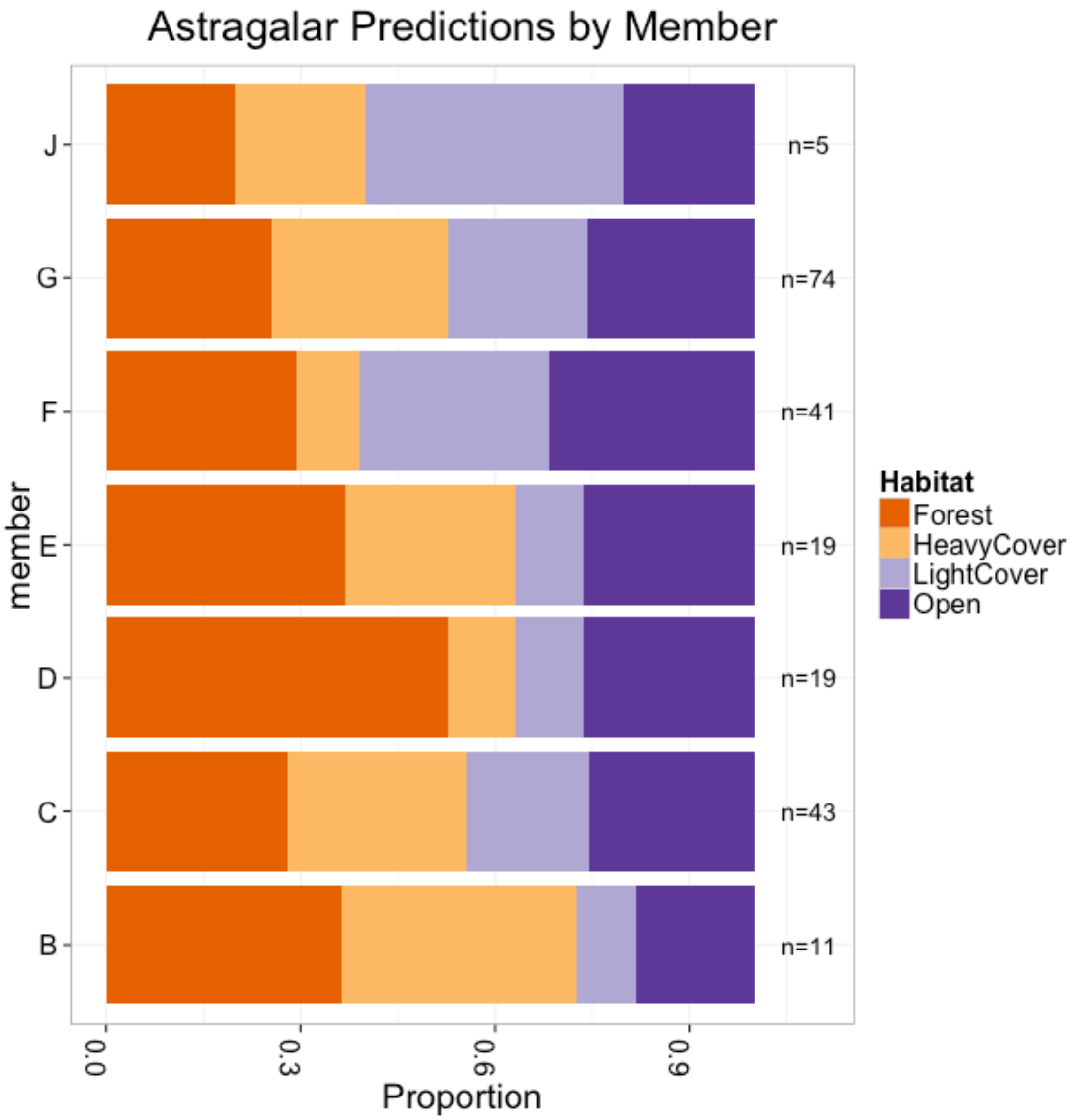

Figure 5.7:Proportion of astragalar predictions by member. The sample size for each member is listed in the right margin.

Astragalar Habitat Predictions by Member

Figure 5.7, provides a set of stacked bar-plots showing the proportions of astragali assigned to each habitat category by geological member. The distribution of astragalar habitat predictions does not remain constant across geological members. Member B has the lowest proportion of open country bovids of any geological member. Member C shows a shift towards more habitat classifications in the Open end of the spectrum and fewer predictions in the Closed end of the spectrum. By Member D, there is a pronounced increase of Closed habitat predictions. The proportion of closed habitat predictions falls monotonically from Member D to Member J. The proportion of Open predictions increases slightly from member D to Member F, and then falls off in Members G and F. The proportion of intermediate habitats predicted through time varied considerably.

A Chi-squared analysis of proportions of astragalar habitat predictions across members lends support to the contention that habitats shift through time at Shungura (Table 5.1). All habitat categories differ significantly from a uniform distribution with p-values <0.0001, suggesting that changes in proportions across members are significant.

Habitat Category	***X*-squared**	**Df**	**p-value**
Forest	22.77	6	<0.0001*
Heavy Cover	40.38	6	<0.0001*
Light Cover	34.65	6	<0.0001*
Open	32.25	6	<0.0001*

Table 5.1: Results of *X*-squared analysis of the proportions of astragalar predictions of Shungura members through time. All habitat categories show statistically significant differences the proportions of habitats predicted through time.

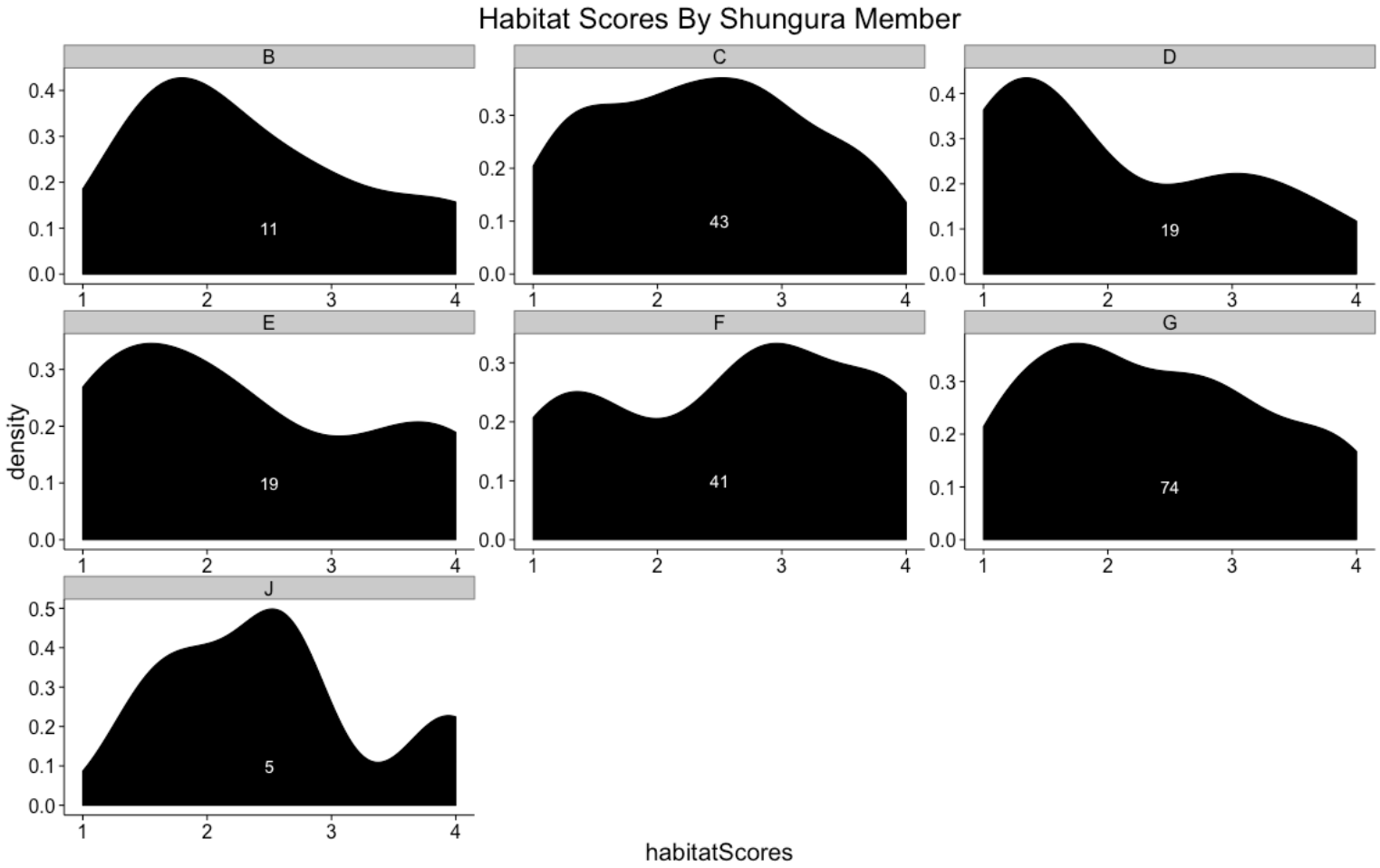

Figure 5.8 : Density plots of habitat scores by Shungura member. The sample size for each member is directly labeled on each density plot. Data are for astragali only.

Figure 5.8 provides a different way of visualizing the astragalar habitat prediction results. This figure displays the distribution of habitat scores using density plots. Density plots encode much the same data as histograms, but whereas histograms show a discrete user-defined number of bins, density plots apply a smoothing function that makes them useful for evaluating general patterns in distribution shape. Additionally, the single geometric shape represented in a density plot makes visual comparison of distribution shape easier than histograms with discrete bins.

The density plots bolster the above characterizations of each member discussed above. Member B has a modal habitat score peak between Forest and Heavy Cover, and very low density in the Open and Light Cover range. The curve for Member C is shifted towards the Heavy Cover / Light Cover portion of the habitat score spectrum, and the shape of the distribution is quite distinct between Members B and C. Member D shows a reversion back to a very strong signal in the Forest end of the spectrum. The shape of the habitat score density distribution in Member E is similar to that of Member D. Member F shows a distribution shape that is quite distinct from any previous member, with a significant peak in the Light Cover range, and with a secondary peak in the Forest / Heavy Cover range. Member G shows a shift towards a unimodal peak in the Forest / Heavy Cover range. Finally, Member J has a modal value squarely in the midrange of the habitat spectrum.

To test the hypothesis regarding sudden environmental change between members B and C, I compared the distribution of habitat scores between each sequential pair of members using a Monte-Carlo procedure and the Kolmogorov-Smirnov statistic. These results are presented in Table 5.2. The only comparison that was statistically significant was the comparison between Member F and Member G, which is undoubtedly related to the fact that the sample sizes are largest for these members. Given the available sample

sizes for the remaining members, it is not possible to exclude the possibility that each member's distribution of habitat scores was sampled from the same distribution as the preceding member. It is interesting to note that the member comparison with the highest value for the KS test statistic (i.e. the member comparison with the greatest statistical distance between distributions) was the comparison between members E and F. The statistical distance between E and F was substantially larger than the statistical distance between B and C. Again, though, it bears repeating that the pairwise differences between these member pairs were not significant.

Comparison	**KS statistic**	**KS p value**
C vs B	0.2326	0.6043
D vs C	0.3060	0.0966
E vs D	0.2105	0.7600
F vs E	0.3184	0.0723
G vs F	0.2314	0.0374*
J vs G	0.2189	0.9303

Table 5.2: Results from Monte-Carlo Kolmogorov-Smirnov tests of habitat score distributions for sequential members. Only the comparison between member F and G was statistically significant.

To test the hypothesis of monotonic change through time, I computed two non-parametric correlations (Spearman's rho and Kendall's tau) between member rank order and the habitat categorical predictions for each habitat category. The results from these correlation analyses are given in Table 5.3. Only the Light Cover category showed a statistically significant correlation with member rank order. This correlation was positive, indicating that Light Cover habitats significantly increase as member rank order

increases. All other habitat categories showed no significant monotonic trend with member rank order. These results do not provide compelling support for the hypothesis of a monotonic drying trend through time, although the increase in Light Cover habitat predictions through time is consistent with this hypothesis.

Spearman Coef	Spearman p-val	Kendall Coef	Kendall p-val	Category
-0.607	0.166	-0.523	0.136	Forest
-0.535	0.235	-0.428	0.238	HeavyCover
0.846	0.016*	0.683	0.033*	LightCover
0.234	0.613	0.195	0.543	Open

Table 5.3: Non parametric correlation coefficients of the percentage of astragali predicted for each category and member rank order. Only the Light Cover habitat category is statistically significant.

Astragalar Habitat Predictions by Submember

Table 5.4 gives a summary of astragalar predictions for each submember.

Submember	Forest	Heavy Cover	Light Cover	Open
B-10	0	3	0	1
B-11	4	1	1	1
C-04	1	0	2	1
C-05	3	1	0	1
C-06	4	5	1	1

Table 5.4: Habitat predictions by submember through time in the Shungura Formation.

Table 5.4 Continued

C-08	2	5	1	5
C-09	2	1	4	3
D-01	3	1	1	2
D-02	1	1	0	1
D-03	4	0	0	1
D-04	2	0	1	1
E-02	1	0	0	2
E-03	2	4	2	3
E-04	4	1	0	0
F-00	1	0	1	3
F-01	6	2	9	8
F-02	0	0	2	1
F-03	5	2	0	1
G-01	1	0	1	1
G-03	1	3	1	0
G-04	2	2	1	4
G-05	1	5	3	2
G-06	1	1	1	0
G-07	1	1	0	2

Table 5.4 Continued

G-08	8	1	2	1
G-09	0	2	1	1
G-12	3	5	5	7
G-13	1	0	1	1
J-06	1	1	2	1

Figure 5.9 depicts the DFA scores for each specimen superimposed over a background plot showing the 95% confidence ellipses of each habitat group from the extant comparative DFA. Each specimen is assigned a habitat prediction corresponding to the group it most closely resembles. These raw predictions are easier to interpret in summary form. Figure 5.10 illustrates a series of stacked bar-plots that illustrate the relative proportions of habitat predictions per submember. Using relative proportions makes it possible to make meaningful comparisons between submembers with different overall numbers of astragali preserved.

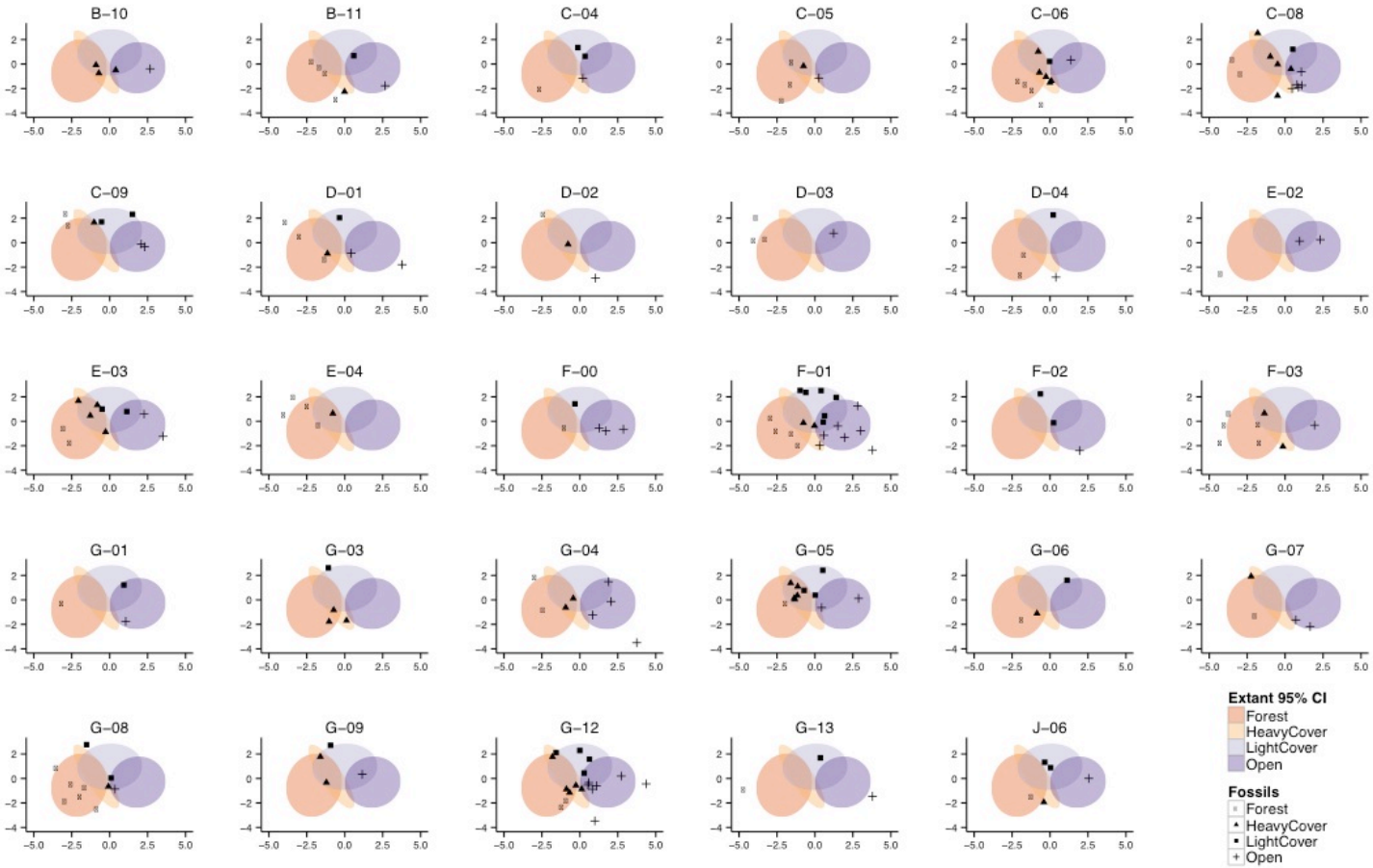

Figure 5.9: Bivariate plots of DFA scores for fossil astragali from Shungura submembers through time. Partially transparent ellipses represent the 95% confidence intervals for each habitat category from the extant DFA. Fossils are plotted as points, with their shape indicating the habitat category with the highest probability.

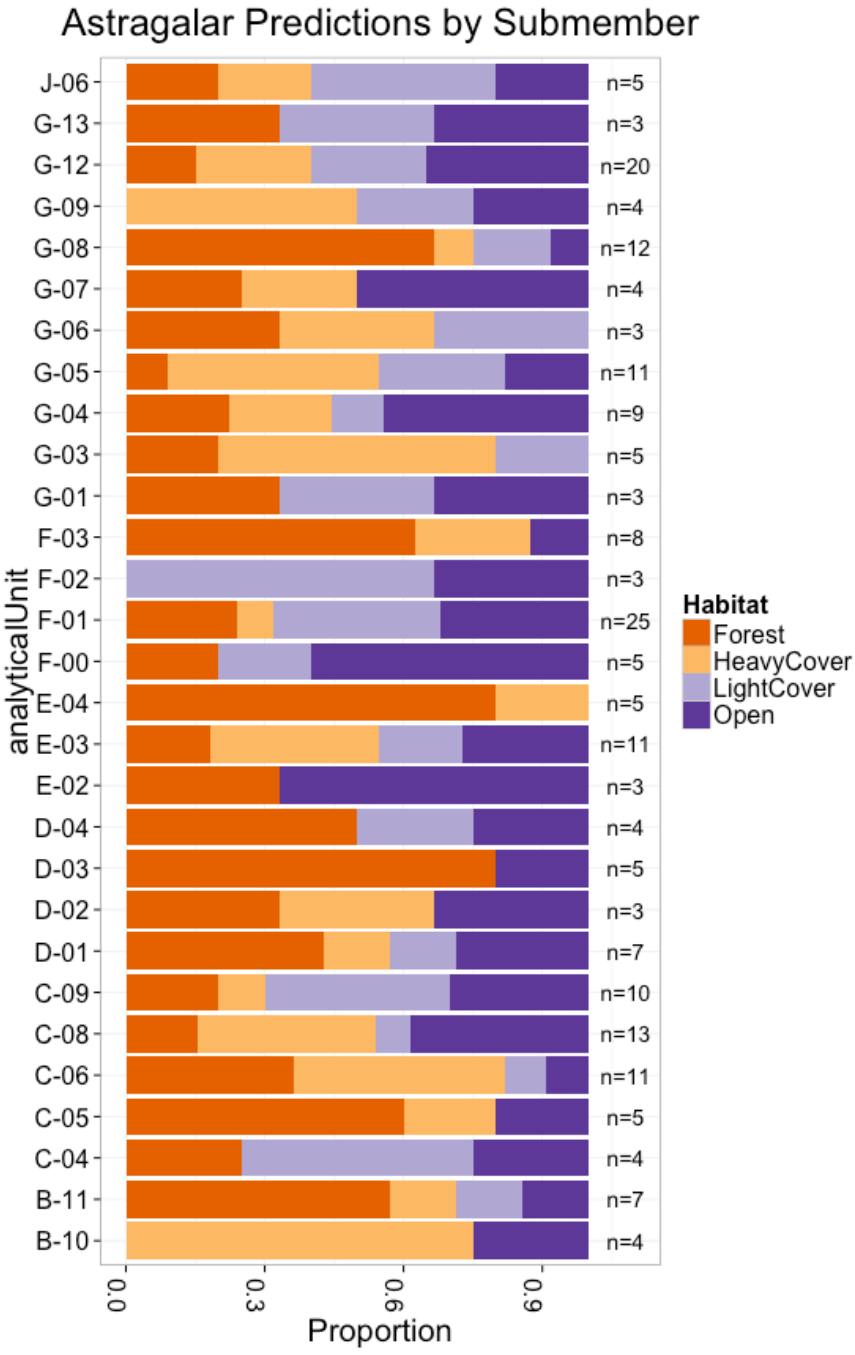

Figure 5.10: Proportion of astragalar predictions by submember. The sample size for each member is listed in the right margin.

Figure 5.10 immediately makes a few observations readily apparent. First is that there is no obvious directional trend in the predicted habitat proportions through time based on the submember data. This is confirmed by the non-parametric correlation analyses, which detect no significant monotonic correlation between the relative proportions of habitat predictions and submember rank order (Table 5.5). The second observation is that, even at the more fine-grained sub-member scale of analysis, all units contain a mosaic of different habitat predictions. Indeed, several submembers contain representatives of all four of the habitat categories.

Spearman Coef	**Spearman p**	**Kendall Coef**	**Kendall p**	**Category**
-0.192	0.317	-0.145	0.302	Forest
0.040	0.835	0.022	0.876	Heavy Cover
0.279	0.142	0.211	0.142	Light Cover
-0.006	0.971	-0.002	0.983	Open

Table 5.5: Non parametric correlation coefficients of the percentage of astragali predicted for each categorgy and submember rank order. None are statistically significant.

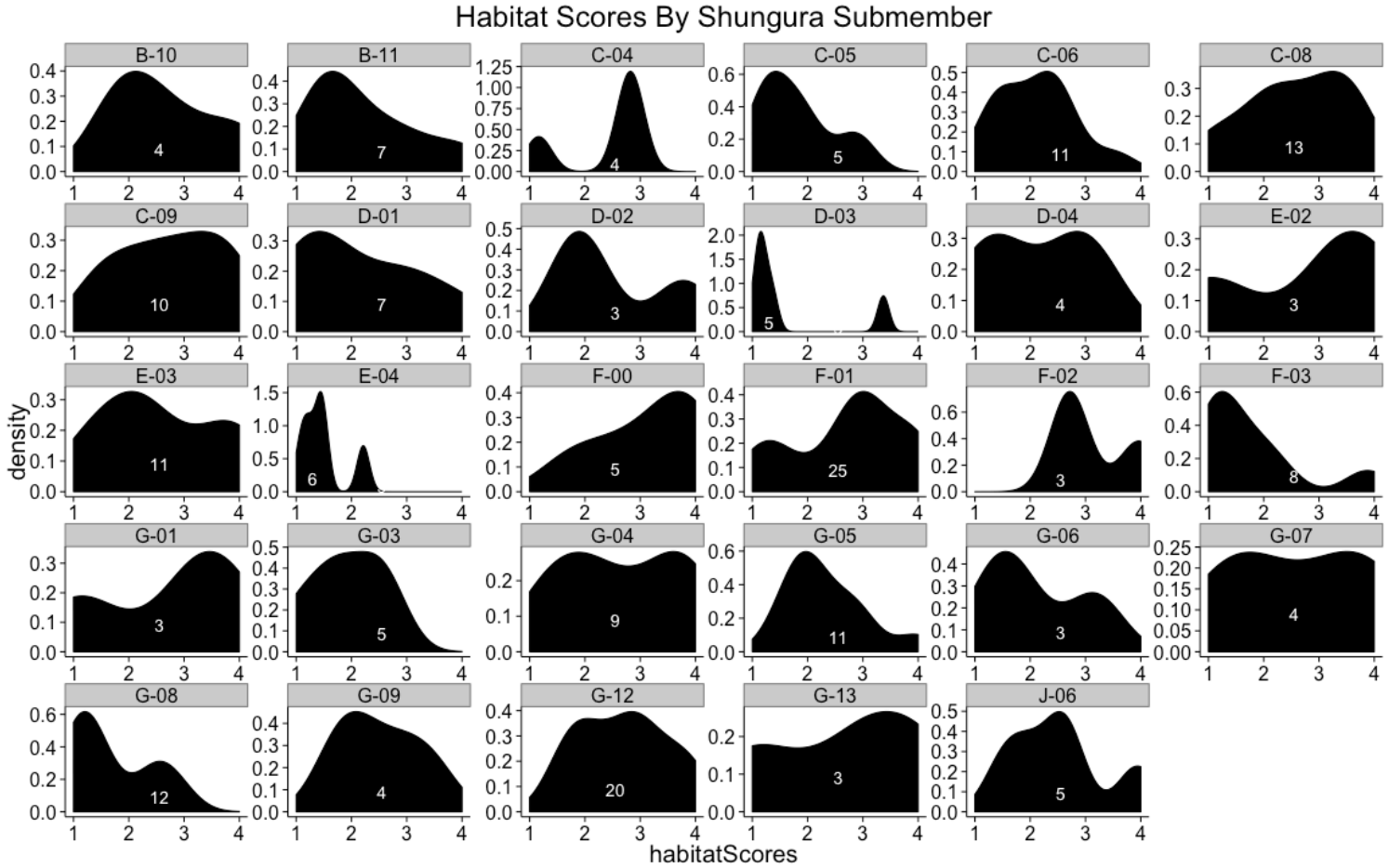

Figure 5.11: Habitat scores for Shungura submembers for which at least three astragalar habitat predictions were possible. The sample size for each submember is directly labeled on each density plot.

Figure 5.11, shows the astragalar habitat scores (as opposed to the categorical predictions) broken down by geological submember. Analyzing this data at the submember level provides additional information regarding fluctuating environment conditions in the Shungura Formation. B-10 and B-11 are very similar to one another, with modal habitat scores near 2, indicating a predominant signal in the range of Heavy Cover. C-4 appears different, with a distinct peak in the Light Cover range. C-5 and C-6 revert to exhibiting similar patterns to the Heavy Cover distributions seen in Member B. Submembers C-8 and C-9 show an altogether different pattern, with relatively robust sample sizes indicating a shift towards the Light Cover / Open end of the habitat score spectrum. Submembers D-1 through D-4 all show distinct peaks in the Forest / Heavy Cover end of the habitat score spectrum. E-2 has a peak in the Open end of the habitat score spectrum (although sample sizes are modest), a trend that is reversed by E-03, with a modal habitat score in the Heavy Cover range. There is a pronounced shift by F-00 and F-01, with very high concentrations of habitat scores in the Light Cover / Open end of the spectrum. This shift is reversed by F-03. Member G contains a somewhat cyclical trend, starting out in G-01 with a distinct peak in the Light Cover / Open range, and shifting to a Heavy Cover / Forest signal by G-05 and G-06, and swinging again in the direction of the Open category by G-13.

The overwhelming picture from this finer scale analysis at the level of submember is that environmental reconstructions at the level of geological member are generalizations of much more dynamic trends at the level of geological submember. A Chi-squared analysis of astragalar predictions by submember (Table 5.6) supports the contention that the astragalar predictions are highly variable throughout the sequence, with all habitat categories evincing significant departures from a uniform distribution.

Habitat Category	*X*-squared	Df	p-value
Forest	45.2	28	0.02*
Heavy Cover	48.67	28	0.009*
Light Cover	66.93	28	<0.0001*
Open	53.79	28	0.002*

Table 5.6: Results of *X*-squared analysis of the proportions of astragalar predictions of Shungura submembers through time. All habitat categories show statistically significant differences in the proportions of habitats predicted through time.

The results of the Monte-Carlo Kolmogorov-Smirnov tests between pairs of sequential submembers are given in Table 5.7. The only submember pair that showed significant differences was the F-03 vs F-02 comparison. Again, as for the member level analysis, these results only compare each submember against the submember immediately preceding it. The comparison between E-04 and F-00 approached significance, and this comparison the highest KS statistic of any submember comparison (tied with the D-02 vs D-03 comparison). Thus, while the results are somewhat equivocal, they are consistent with significant environmental change between members E and F.

Comparison	KS statistic	KS p value
B-11 vs B-10	0.5714	0.3034
C-04 vs B-11	0.4643	0.5200

Table 5.7: Results from Monte-Carlo Kolmogorov-Smirnov tests of habitat score distributions for sequential submembers. Only the comparison between units F-02 and F-03 was significant.

Table 5.7 Continued

C-05 vs C-04	0.5500	0.4190
C-06 vs C-05	0.3455	0.6781
C-08 vs C-06	0.4476	0.1154
C-09 vs C-08	0.2231	0.8423
D-01 vs C-09	0.4286	0.2921
D-02 vs D-01	0.5714	0.3870
D-03 vs D-02	0.8000	0.0878
D-04 vs D-03	0.5500	0.4122
E-02 vs D-04	0.6667	0.3017
E-03 vs E-02	0.3939	0.6467
E-04 vs E-03	0.6364	0.0542
F-00 vs E-04	0.8000	0.0750
F-01 vs F-00	0.3600	0.5668
F-02 vs F-01	0.3600	0.7192
F-03 vs F-02	0.8750	0.0464*
G-01 vs F-03	0.5417	0.3510
G-03 vs G-01	0.6667	0.2077
G-04 vs G-03	0.4444	0.4143
G-05 vs G-04	0.3535	0.3983
G-06 vs G-05	0.4848	0.4881

Table 5.7 Continued

G-07 vs G-06	0.5000	0.6495
G-08 vs G-07	0.5000	0.3355
G-09 vs G-08	0.6667	0.0999
G-12 vs G-09	0.2500	0.9624
G-13 vs G-12	0.3333	0.8387
J-06 vs G-13	0.4667	0.5625

Mesowear

Mesowear scores for each submember are given in Appendix F. As was the case for the astragalar data, results for mesowear are presented both by member and by submember. In every case, only analytical units that contain at least three molars that could be scored for mesowear are included. The mesowear scores are plotted onto the background Correspondence Analysis from Figure 5.6. For clarity, extant taxon names, which are given in Figure 5.6, are eliminated in the fossil mesowear plots. In all fossil mesowear figures, the fossil analytical unit is represented as a black diamond, and the extant comparative sample is represented by symbols that are explained in the legend.

Member	**Tribe**	**Lower n**	**Upper n**
B	Aepycerotini	NA	6
B	Bovini	NA	3
B	Reduncini	3	2
B	Tragelaphini	1	2

Table 5.8: Mesowear ample sizes for both upper and lower molars by tribe and member.

Table 5.8 Continued

C	Aepycerotini	8	8
C	Bovini	7	13
C	Reduncini	7	6
C	Tragelaphini	29	9
D	Aepycerotini	5	12
D	Alcelaphini	1	NA
D	Bovini	2	1
D	Reduncini	3	7
D	Tragelaphini	8	3
E	Aepycerotini	6	11
E	Bovini	4	3
E	Reduncini	6	9
E	Tragelaphini	19	4
F	Aepycerotini	11	15
F	Bovini	3	2
F	Reduncini	5	9
F	Tragelaphini	2	3
G	Aepycerotini	38	63
G	Alcelaphini	NA	4
G	Bovini	10	4
G	Reduncini	52	53
G	Tragelaphini	32	26
H	Reduncini	2	8

Table 5.8 Continued

J	Aepycerotini	NA	3
J	Reduncini	NA	1
K	Reduncini	1	NA
L	Reduncini	1	NA

Mesowear Results By Member

Bovini

Bovini are very large-bodied bovids which include modern cattle and buffalo. The Shungura fossil Bovini are dominated by *Syncerus* sp. (relatives of modern African Buffalo) which are especially common in Member C (Gentry, 1985; Bobe and Eck, 2001). Only relatively few representatives of *Pelorovis*, a lineage of recently extinct long-horned buffalo (Gentry, 1985), are found in the Shungura Formation.

Figure 5.12 shows mesowear results for Bovini upper molars. Bovini upper molars from members C and G plot nearly on top of one another in close proximity to the extant African Buffalo, *Syncerus caffer,* in the CA plot. *Syncerus caffer* is a mixed feeder with a diet composed of approximately 77% monocot forage (Gagnon and Chew, 2000). This diet is distinct from other more selective mixed feeders, such as many Antilopini. However, the diet of *Syncerus caffer* is known to vary considerably in different parts of its geographic range as well as seasonally. Member E bovine uppers fall in a completely different quadrant of the CA plot, aligning much more closely with the more selective Antilopini browsers in the upper left quadrant of the plot.

The lower molar data for Bovini in Figure 5.13 tell a similar story. Members C, F, and G all plot in the general vicinity of modern *Syncerus cafer*, while Member E again is an outlier, with a mesowear signal in the grazing end of the spectrum. This is not unexpected, as previous studies have indicated that lower molar mesowear signatures are often shifted towards a grazing signal compared to upper molar mesowear signatures (Kaiser and Fortelius, 2003).

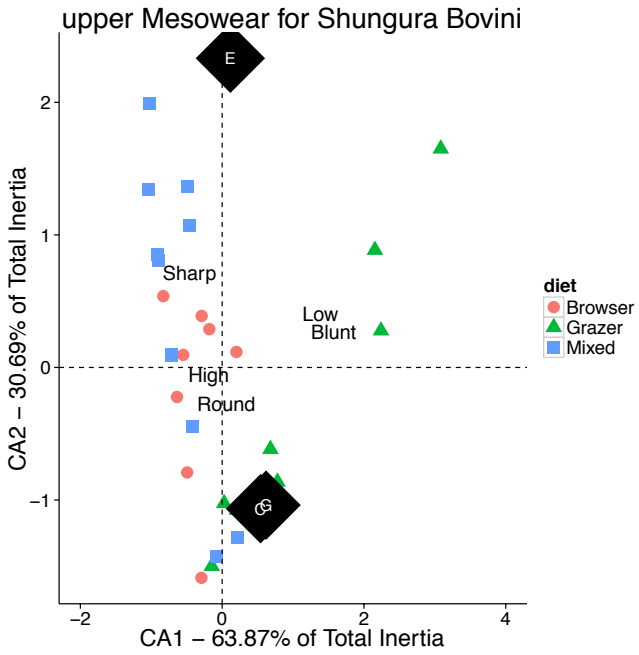

Figure 5.12: Mesowear results for upper molars of Bovini by member. Only members for which three or more observations were possible are included.

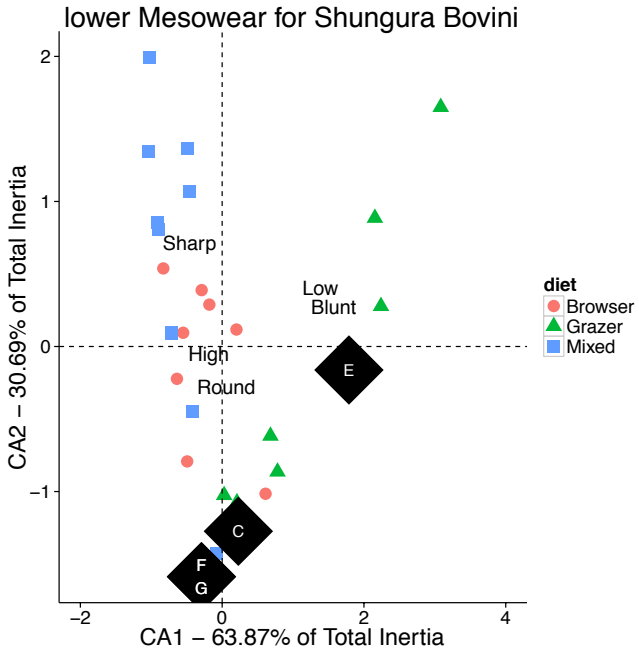

Figure 5.13: Mesowear results for lower molars of Bovini by member. Only members for which three or more observations were possible are included.

Reduncini

Modern Reduncini include the reedbucks, waterbucks, kobs, pukus, and lechwes. On the whole, reduncines are generally water-dependent and subsist almost exclusively on monocot grasses (Gagnon and Chew, 2000). However, this grazing adaptation differs from secondary grassland grazers (such as many Alcelaphini) in that Reduncini specialize on fresh-grass in edaphic grasslands. Reduncini are very common in the Shungura Formation, with several species of *Kobus* represented (Gentry, 1985). Most of these specimens are isolated teeth, which have not typically been identified below the tribal level (Gentry, 1985, Bobe and Eck, 2001).

Figure 5.14 shows the upper mesowear for the Shungura Reduncini by geological member. Reduncines from Members C, D, E, F, and G fall near origin of the plot, in an area that includes taxa with relatively high / round cusps. This region of the plot is not very well characterized by mesowear, as it comprises mixed feeders, browsers, and some fresh grass grazers (including the extant reedbuck, *Redunca redunca*). Member H is something of an outlier, more in the range of the selective mixed feeders.

The lower molar Reduncini mesowear in Figure 5.15 is, as expected, somewhat shifted towards a grazing signal. Members C, F, and G are comfortably in the range expected for modern reduncine fresh-grass grazers, while Members B and E have a higher proportion of high cusps than is common in extant reduncine fresh grass grazers. Member D is something of an outlier, occupying a portion of the CA space that is not occupied by any extant African bovids.

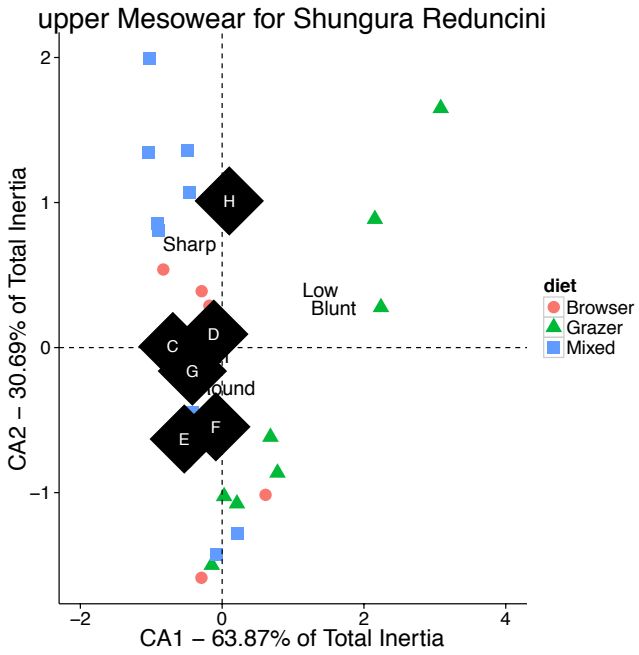

Figure 5.14: Mesowear results for upper molars of Reduncini by member. Only members for which three or more observations were possible are included.

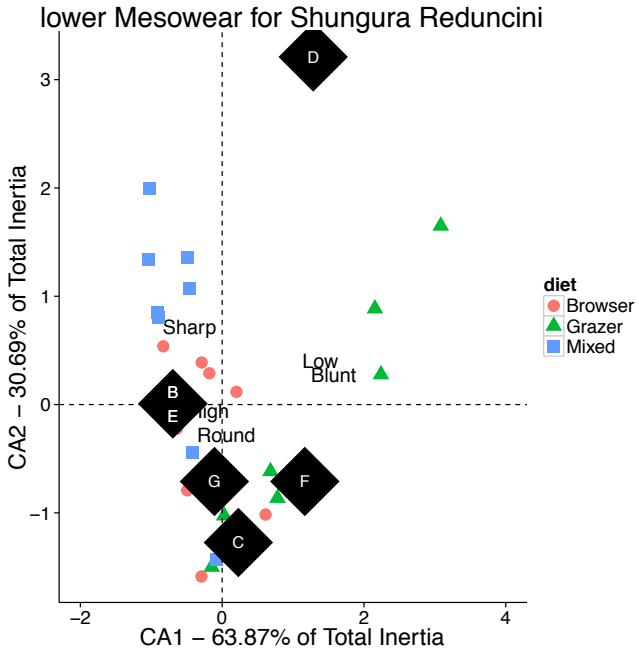

Figure 5.15: Mesowear results for lower molars of Reduncini by member. Only members for which three or more observations were possible are included.

Aepycerotini

The lone extant representative of the Aepycerotini is the impala, *Aepyceros melampus*. Impala are mixed feeders with a diet consisting of nearly equal portions of monocot and dicot forage, with the remaining minor percentage (10%) of their diet coming from fruit (Gagnon and Chew, 2000). In the extant mesowear plot, impala fall just to the left of the plot origin, more in line with the frugivorous browsing taxa than the non-frugivorous open country mixed feeders in the upper left portion of the graph. The very common *Aepyceros* from Shungura is *A. shungurae* (Gentry, 1985), which is somewhat smaller in size than modern impala, but is dentally quite similar.

Upper molar mesowear results for fossil *Aepyceros* by member are given in Figure 5.16. Members B, C, and J fall in with the open country mixed feeders in the upper left portion of the plot, while D, E, F, and G fall much closer to the plot origin, suggesting a diet that is more similar to modern impala.

As expected, the lower molar mesowear data show a shift towards the grazing end of the spectrum for most members, with the exception of Member C. Although Member C is somewhat shifted towards a grazing signal, it falls near the plot origin, in line with modern impala.

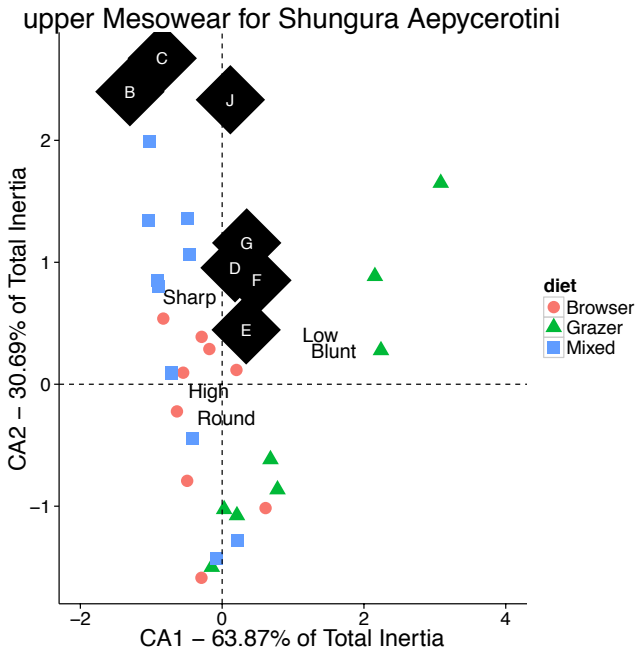

Figure 5.16: Mesowear results for upper molars of Aepycerotini by member. Only members for which three or more observations were possible are included.

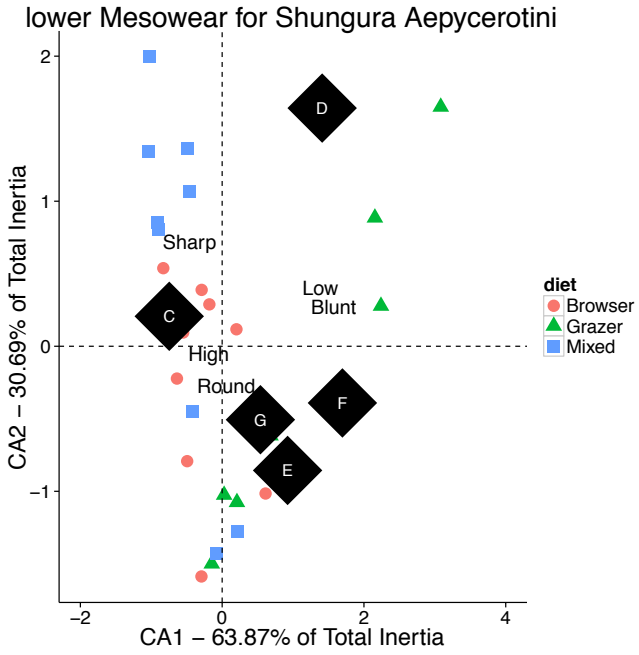

Figure 5.17: Mesowear results for lower molars of Aepycerotini by member. Only members for which three or more observations were possible are included.

Tragelaphini

Tragelaphini are a diverse group that spans the habitat spectrum, from the forest dwelling bongo to the open-country common eland. The remaining Tragelaphini include the kudus, bushbuck, and sitatunga, which occupy a range of heavy-cover habitats including thickets, bushlands, and marshes. In terms of mesowear, extant Tragelaphini generally plot low in the upper left quadrant of the CA plot, which reflects their predominantly browsing and mixed-feeding diets (Gagnon and Chew, 2000). The greater kudu *Tragelaphus strepsiceros* is one browsing Tragelaphini that is poorly characterized by mesowear, appearing in the lower central portion of the plot.

The most common Tragelaphini from the Shungura Formation has long been attributed to *T. nakuae* (Gentry, 1985), but a recent re-evaluation breaks this species into an ancestor - descent lineage of *T. rastafari – T. nakuae* (Bibi, 2011), with the cut-off point occurring at approximately 2.85 Ma. Little is known about the paleoecology of this lineage, but Bibi (2011) suggests that the lineage is associated with modern bongo, which represent the most humid end of the modern Tragelaphini habitat spectrum. Further, Bibi (2011) hinted that the evolutionary transition from *T. rastafari – T. nakuae* might represent an ecological shift towards drier, more open, habitats. Another Tragelaphini species, *T. gaudryi*, becomes common in members F and G.

Upper molar mesowear for Tragelaphini is presented in Figure 5.18. There were inadequate sample sizes to characterize member B. Member C and G fossil Tragelaphini plot nearly on top of extant eland and bushbuck, which are both mixed feeders (although eland consume much more dicot grass than do bushbuck). Member E Tragalaphini are shifted slightly down the graph and plot nearly on top of extand oribi, which are open country mixed feeders which consume large amounts of monocot grasses (Gagnon and Chew, 2000).

Lower molar mesowear for Tragelaphini is presented in Figure 5.19. Again, the lower molars are slightly shifted towards a more grazing signal, but all available members are clustered relatively tightly in the portion of the mesowear CA plot that does not distinguish well between dietary categories.

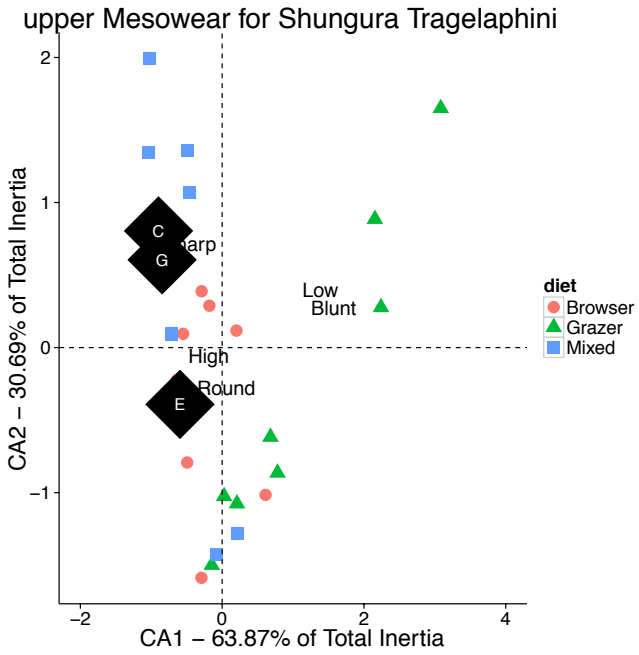

Figure 5.18: Mesowear results for upper molars of Tragelaphini by member. Only members for which three or more observations were possible are included.

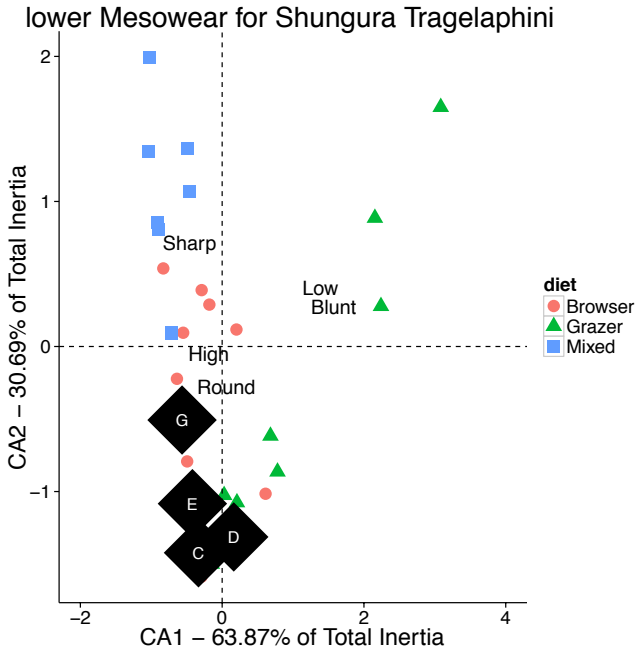

Figure 5.19: Mesowear results for lower molars of Tragelaphini by member. Only members for which three or more observations were possible are included.

Submember	Tribe	Lower N	Upper N
B-03	Bovini	NA	1
B-09	Reduncini	1	NA
B-10	Aepycerotini	NA	2
B-10	Tragelaphini	NA	1
B-11	Aepycerotini	NA	4
B-11	Bovini	NA	2
B-11	Reduncini	2	2
B-11	Tragelaphini	NA	1
B-12	Tragelaphini	1	NA
C-02	Aepycerotini	2	NA
C-03	Tragelaphini	1	NA
C-04	Aepycerotini	1	NA
C-04	Bovini	NA	2
C-04	Reduncini	NA	1
C-04	Tragelaphini	1	NA
C-05	Aepycerotini	NA	4
C-05	Bovini	1	1
C-05	Reduncini	2	NA

Table 5.9: Mesowear sample sizes for upper and lower molars by submember.

Table 5.9 Continued

C-05	Tragelaphini	7	1
C-06	Aepycerotini	2	NA
C-06	Bovini	NA	4
C-06	Reduncini	4	1
C-06	Tragelaphini	6	2
C-07	Aepycerotini	1	NA
C-07	Bovini	1	1
C-07	Reduncini	NA	1
C-07	Tragelaphini	2	2
C-08	1	NA	
C-08	Aepycerotini	1	NA
C-08	Bovini	3	4
C-08	Reduncini	1	2
C-08	Tragelaphini	6	2
C-09	Aepycerotini	1	4
C-09	Bovini	2	1
C-09	Tragelaphini	6	2
C-NA	Reduncini	NA	1
D-01	Aepycerotini	1	NA

Table 5.9 Continued

D-01	Bovini	1	NA
D-01	Reduncini	NA	3
D-02	Aepycerotini	1	4
D-03	Aepycerotini	NA	2
D-03	Bovini	NA	1
D-03	Tragelaphini	3	1
D-04	Aepycerotini	1	2
D-04	Bovini	1	NA
D-04	Reduncini	NA	1
D-04	Tragelaphini	NA	1
D-05	Aepycerotini	2	4
D-05	Alcelaphini	1	NA
D-05	Reduncini	3	3
D-05	Tragelaphini	5	1
E-01	Aepycerotini	1	1
E-01	Bovini	2	NA
E-01	Reduncini	1	3
E-01	Tragelaphini	4	NA
E-02	Aepycerotini	1	NA

Table 5.9 Continued

E-02	Reduncini	2	NA
E-03	Aepycerotini	2	8
E-03	Bovini	1	1
E-03	Reduncini	NA	2
E-03	Tragelaphini	9	3
E-04	Aepycerotini	2	2
E-04	Bovini	1	2
E-04	Reduncini	3	4
E-04	Tragelaphini	6	1
F-00	NA	1	
F-00	Aepycerotini	2	NA
F-00	Bovini	1	NA
F-00	Reduncini	2	1
F-01	NA	1	
F-01	Aepycerotini	8	9
F-01	Bovini	2	NA
F-01	Reduncini	1	1
F-01	Tragelaphini	2	1
F-03	Aepycerotini	1	5

Table 5.9 Continued

F-03	Reduncini	1	6
F-03	Tragelaphini	NA	2
F-04	Aepycerotini	NA	1
F-04	Bovini	NA	2
F-04	Reduncini	NA	1
F-NA	Reduncini	1	NA
G-01	Aepycerotini	1	NA
G-01	Bovini	2	1
G-02	Reduncini	NA	1
G-03	Aepycerotini	4	2
G-03	Bovini	1	1
G-03	Reduncini	1	1
G-03	Tragelaphini	1	1
G-04	Aepycerotini	2	5
G-04	Alcelaphini	NA	1
G-04	Bovini	1	NA
G-04	Reduncini	8	4
G-04	Tragelaphini	5	3
G-05	Aepycerotini	3	9

Table 5.9 Continued

G-05	Alcelaphini	NA	1
G-05	Bovini	2	1
G-05	Reduncini	11	12
G-05	Tragelaphini	7	8
G-06	Aepycerotini	NA	3
G-06	Reduncini	1	3
G-06	Tragelaphini	2	NA
G-07	Reduncini	4	3
G-07	Tragelaphini	1	1
G-08	Aepycerotini	4	6
G-08	Bovini	1	NA
G-08	Reduncini	4	6
G-08	Tragelaphini	4	3
G-09	Aepycerotini	NA	2
G-09	Bovini	1	NA
G-09	Reduncini	NA	4
G-10	Aepycerotini	NA	4
G-10	Reduncini	2	NA
G-10	Tragelaphini	2	NA

Table 5.9 Continued

G-11	Aepycerotini	3	2
G-11	Reduncini	5	2
G-11	Tragelaphini	2	NA
G-12	Aepycerotini	19	22
G-12	Alcelaphini	NA	1
G-12	Bovini	1	1
G-12	Reduncini	13	9
G-12	Tragelaphini	5	9
G-13	Aepycerotini	2	7
G-13	Alcelaphini	NA	1
G-13	Bovini	1	NA
G-13	Reduncini	3	6
G-13	Tragelaphini	3	NA
G-16	Aepycerotini	NA	1
G-16	Reduncini	NA	1
G-19	Tragelaphini	NA	1
G-27	Reduncini	NA	1
H-03	Reduncini	2	8
J-06	Aepycerotini	NA	3

Table 5.9 Continued

J-06	Reduncini	NA	1
K-NA	Reduncini	1	NA
L-05	Reduncini	1	NA

Mesowear Results By Submember

Table 5.9 provides mesowear sample sizes for upper and lower molars by submember. Sample sizes for many submembers were very small, and only submembers with at least three teeth that could be scored for mesowear were deemed reliable enough to attempt interpretations. Even a sample size of three is smaller than would be desirable, but the vagaries of fossil preservation limit the material available for examination.

Bovini

Upper and lower mesowear data are presented in Figure 5.20 and Figure 5.21, respectively. Only 3 submembers preserved adequate sample sizes of Bovini molars that could be scored for mesowear. C-06 and C-08 had adequate sample sizes for upper molars, and these confirm the findings of the analysis by member, with both C-06 and C-08 falling neatly near extant *Syncerus caffer* on the mesowear plot, consistent with a grazing dominated mixed-feeding diet. Lower molars from C-08 evince the expected minor shift towards a more pronounced grazing signature.

Reduncini

The upper molar Reduncini mesowear presented in Figure 5.22 reveals more variability than was observed in the member-level analysis. A cluster of submembers (C-05, D-01,F-03,G-09, and G-12) are located near the origin of the plot, in lie with the member level results. G-08 and H-3 have more of a selective mixed feeder mesowear signal, while E-4 and G-06 plot near extant waterbuck (*Kobus ellipsiprymnus*). D-05 and G-07 exhibit the strongest grazing signature of any submembers. Lower molar mesowear (Figure 5.23) is consistent with the upper results. D-05 is an outlier in a space unoccupied by modern African bovids. G-13 exhibits a pronounced shift towards the grazing end of the mesowear spectrum.

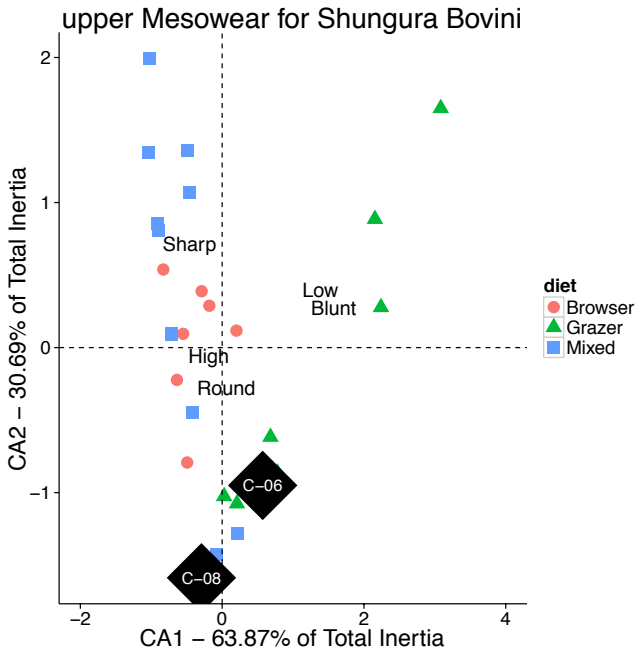

Figure 5.20: Mesowear results for upper molars of Bovini by submember. Only submembers for which >3 observations were possible are included.

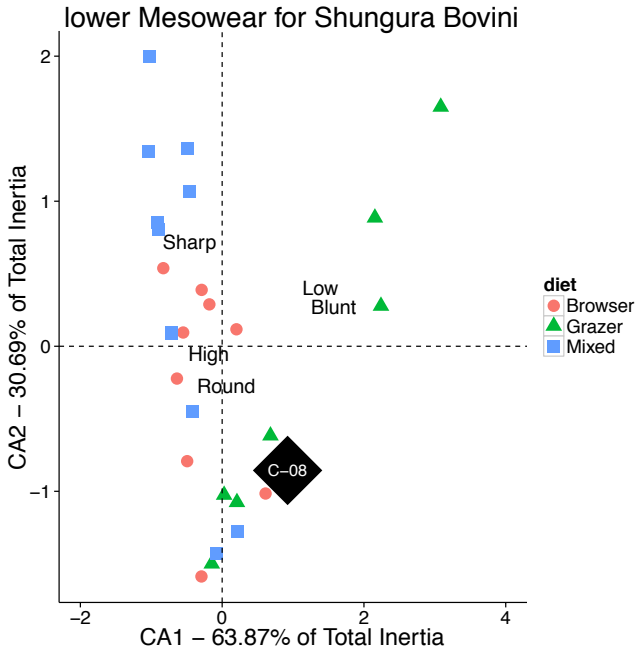

Figure 5.21: Mesowear results for lower molars of Bovini by submember. Only submembers for which >3 observations were possible are included.

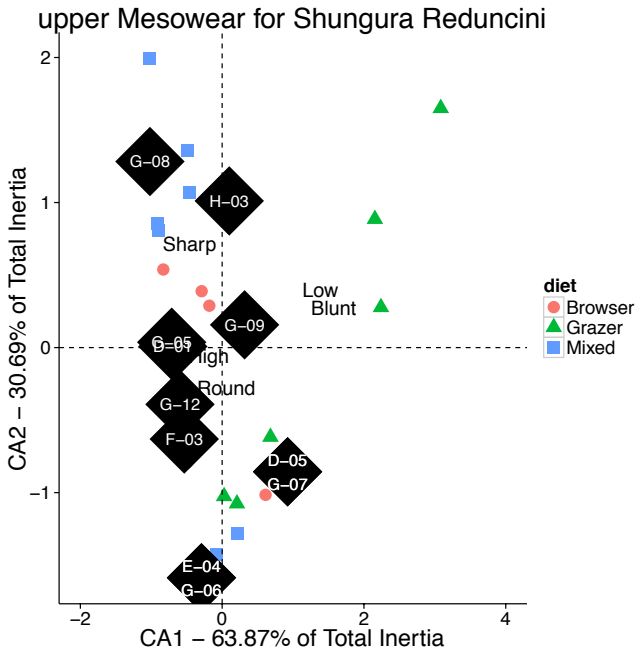

Figure 5.22: Mesowear results for upper molars of Reduncini by submember. Only submembers for which >3 observations were possible are included.

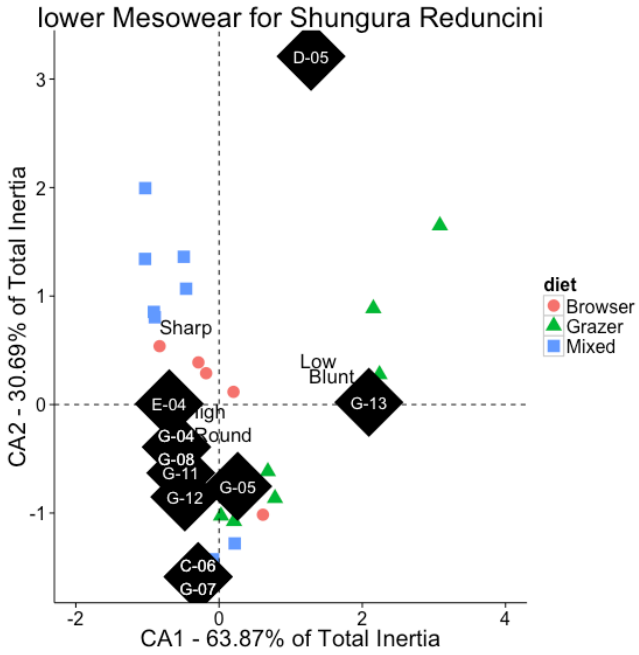

Figure 5.23: Mesowear results for lower molars of Reduncini by submember. Only submembers for which >3 observations were possible are included.

Aepycerotini

Upper molar mesowear for Aepycerotini in Figure 5.24 reveals dramatic variation in mesowear scores across submembers. There appears to be something of a temporal trend in the mesowear scores, with earlier submembers (B-11, C-05, C-09, D-02) occupying the two half of the CA plot, with later submembers (F-01, F-03, and most of member G) occupying the right half of the CA plot. D-05 is, again, an outlier, with this submember occupying a space in the CA plot that is not observed in modern bovids. Lower molar mesowear for Aepycerotini (Figure 5.25) is less variable than upper molar mesowear. D-05 is again an outlier, and G-13 exhibits the strongest grazing signal of any submember.

Tragelaphini

The upper molar Tragelaphini mesowear (Figure 5.26) from all available submembers in member G are in the region of concentrate selectors in the CA plot or on the border of the concentrate selectors and the selective mixed feeders. Member E-03 plots right on top of the greater kudu (*Tragelaphus strepsiceros*) in the lower portion of the CA plot. The lower molar mesowear data (Figure 5.27) largely support the interpretations from the upper molars, with some additional submembers (C-08, E-04, G-08, and G-12) occupying an intermediate position in the CA plot, closest to *Cephalophus natalensis*, the highly frugivorous red forest duiker (Gagnon and Chew, 2000). Neither the upper nor the lower molar mesowear data show any indication of significant grazing in the Shungura Tragelaphini.

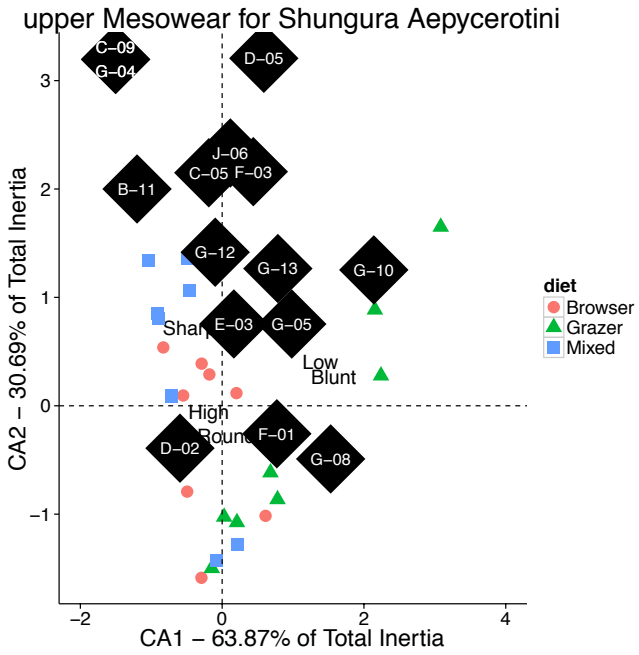

Figure 5.24: Mesowear results for upper molars of Aepycerotini by submember. Only submembers for which >3 observations were possible are included.

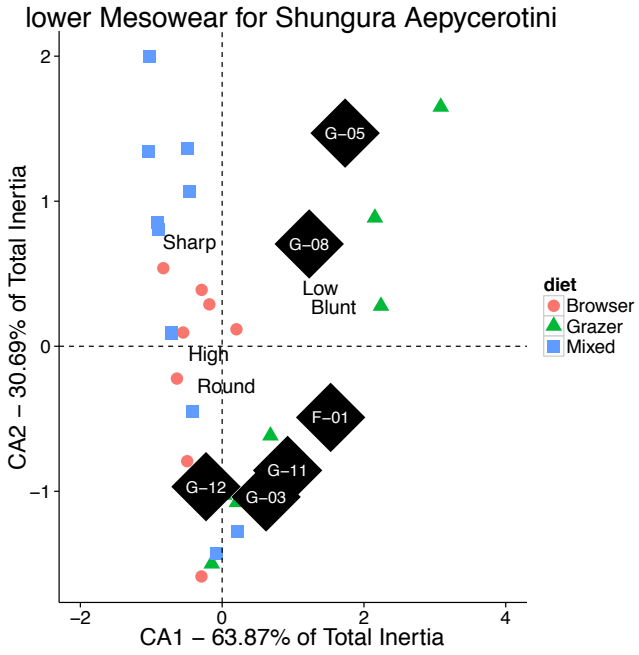

Figure 5.25: Mesowear results for lower molars of Aepycerotini by submember. Only submembers for which >3 observations were possible are included.

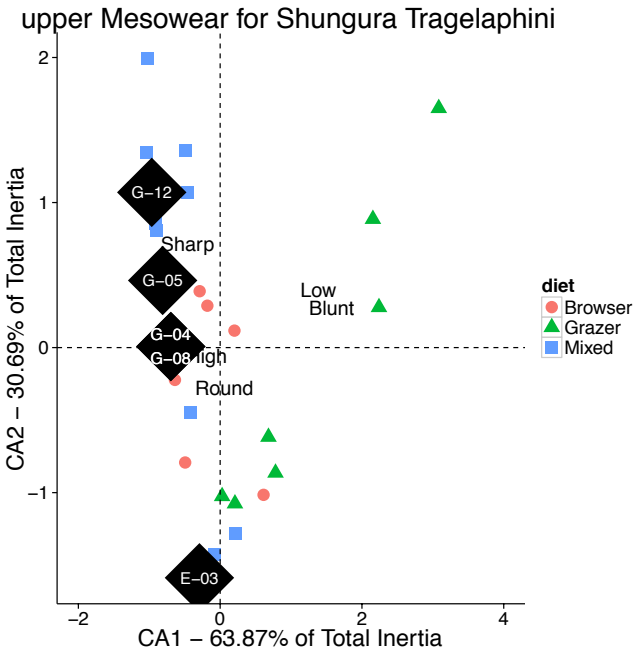

Figure 5.26: Mesowear results for upper molars of Tragelaphini by submember. Only submembers for which >3 observations were possible are included.

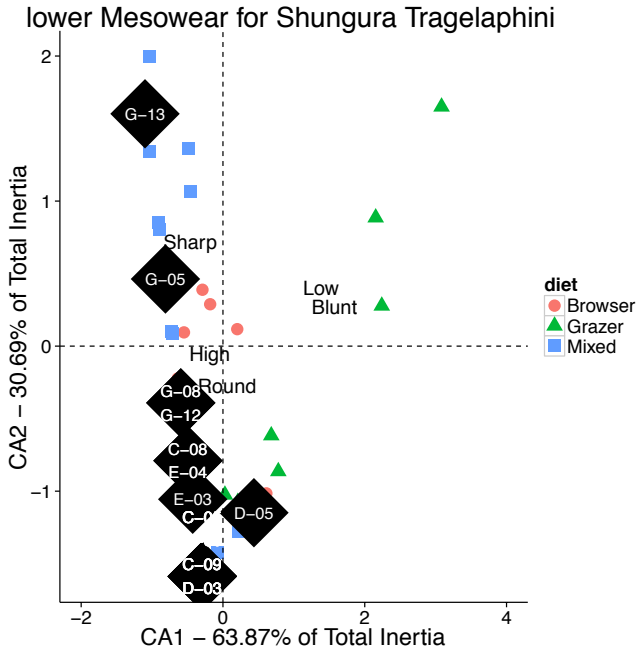

Figure 5.27: Mesowear results for lower molars of Tragelaphini by submember. Only submembers for which >3 observations were possible are included.

Testing Hypotheses with Mesowear

To test the hypothesis of a monotonic trend towards increasing aridity, I calculated the same non-parametric correlation coefficients for the mesowear score data with submember rank order as were previously calculated for the astragalar data. These mesowear scores are derived from a DFA analysis of the mesowear data in exactly the same way as the astragalar scores were calculated (see Materials and Methods). Correlations were computed by tribe, with upper and molars examined separately. Results from the correlation analyses are given in Table 5.10. None of the correlations were statistically significant, though both the Tragelaphini and Aepycerotini lower mesowear had positive correlations that approached significance.

Tribe	Upper/Lower	Spearman Coef	Spearman p	Kendall Coef	Kendall p
Aepycerotini	lower	0.37529	0.06452	0.241627	0.10596
Aepycerotini	upper	-0.15081	0.46211	-0.110445	0.43775
Reduncini	lower	-0.26552	0.18986	-0.197999	0.18403
Reduncini	upper	0.01795	0.92366	-0.004526	0.97252
Tragelaphini	lower	0.38827	0.06081	0.300730	0.06513
Tragelaphini	upper	0.30920	0.17262	0.266199	0.11565

Table 5.10 Non parametric correlation coefficients of submember mesowear scores against submember rank order. None are statistically significant.

The mesowear score data are presented graphically in Figure 5.28. It is clear that there is no strong evidence for a directional trend in any of the mesowear scores. Tragalaphini are notable for exhibiting the least variable mesowear scores. Reduncini and Aepycerotini show much more variability than Tragelaphini, perhaps pointing to

increased dietary variability in these tribes compared to Tragelaphines, according to the mesowear scores.

For reference purposes, Figure 5.29 through Figure 5.31 provide the summarized data which are the source of the CA plots illustrating fossil mesowear data.

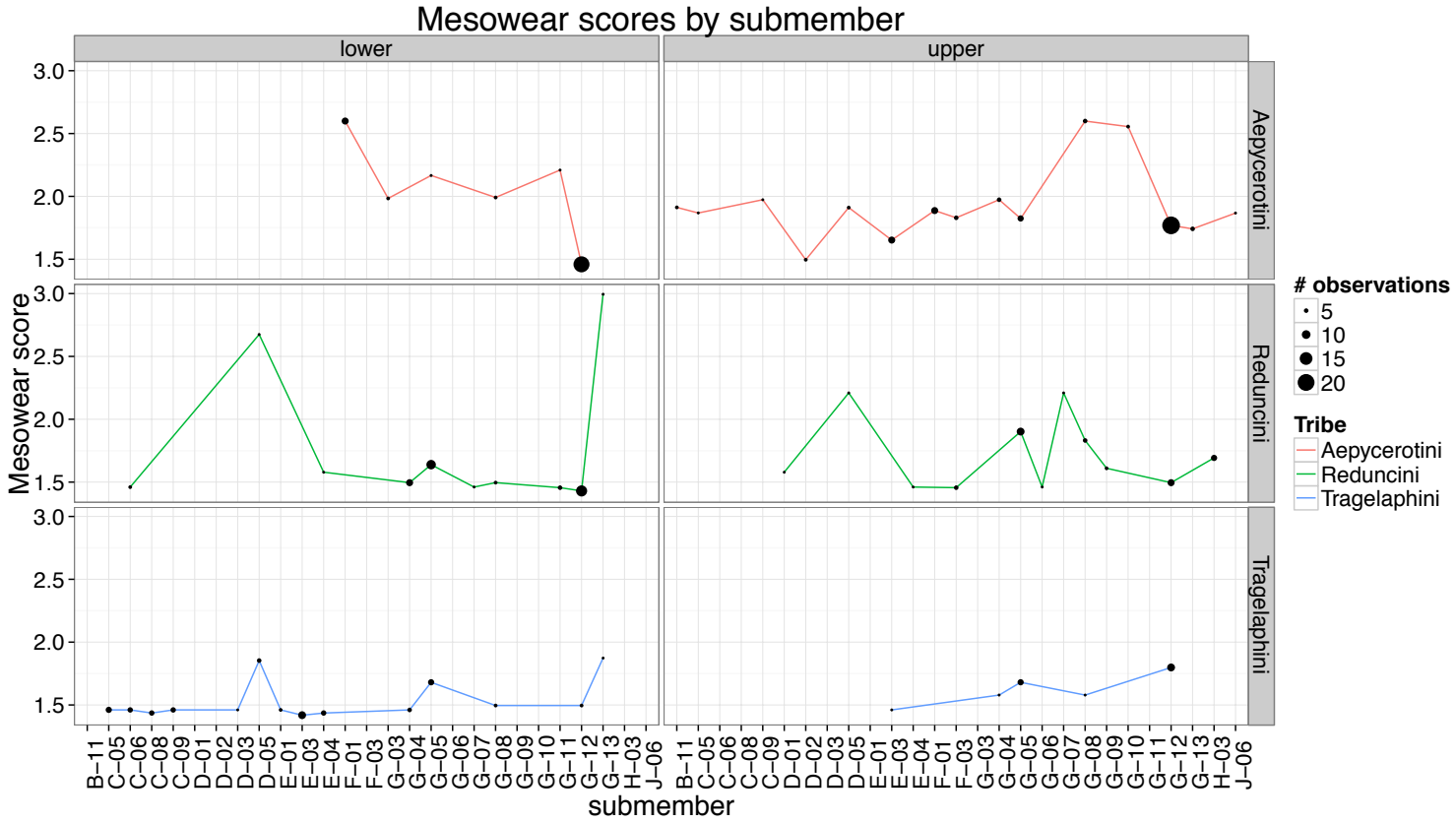

Figure 5.28: Mesowear scores through time in the Shungura Formation by submember. Only Aepycerotini, Reduncini, and Tragelaphini had adequate sample sizes for inclusion in this graph. The size of the plotting symbol indicates the available sample size for that submember, as indicated in the legend. A mesowear score of 1 indicates a 100% confident classification in the browsing category, while a score of 3 would indicate a 100% confident classification as a grazer.

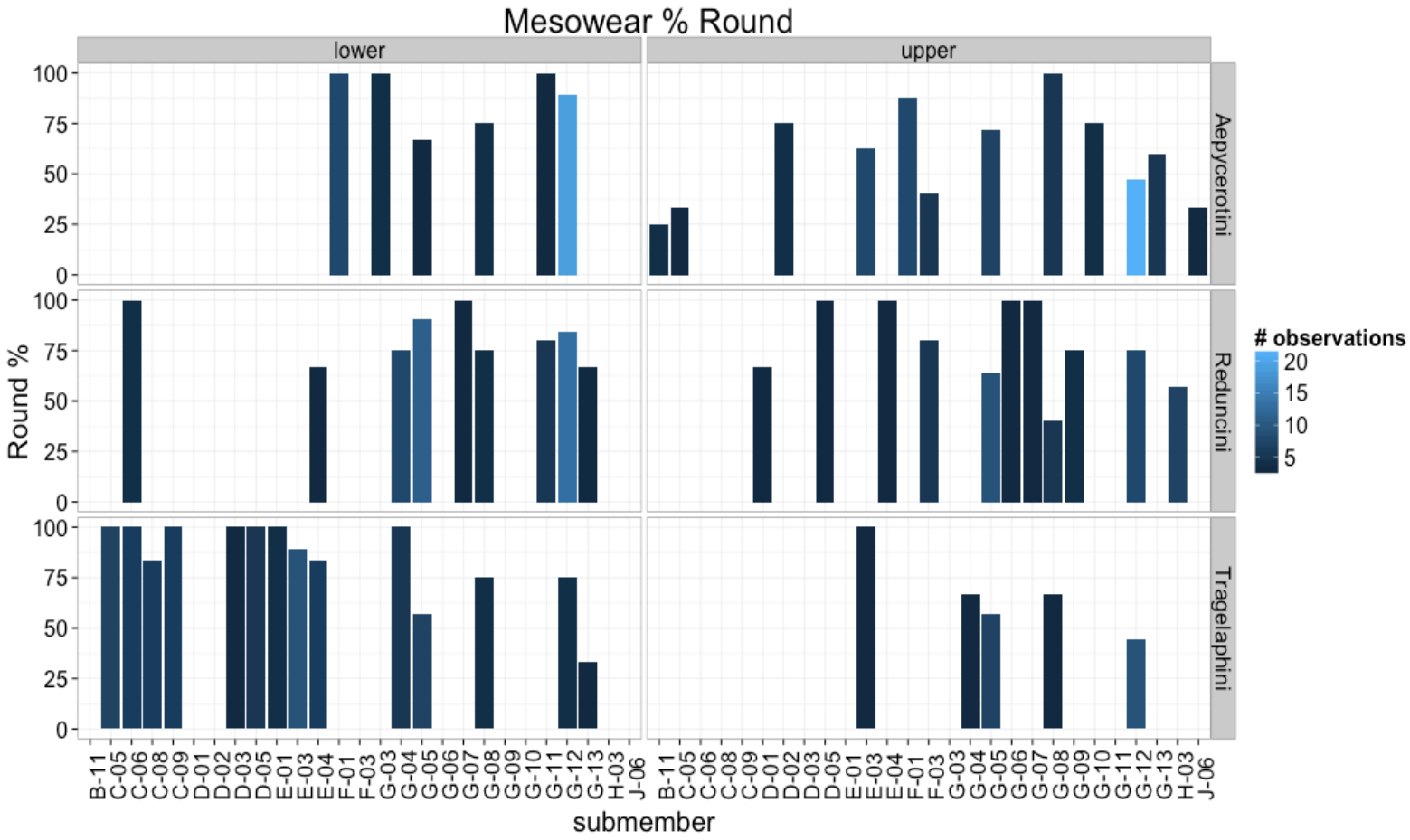

Figure 5.29: Percentage of cusps categorized as round through time. Only submembers with more than three molars that could be scored for mesowear are included.

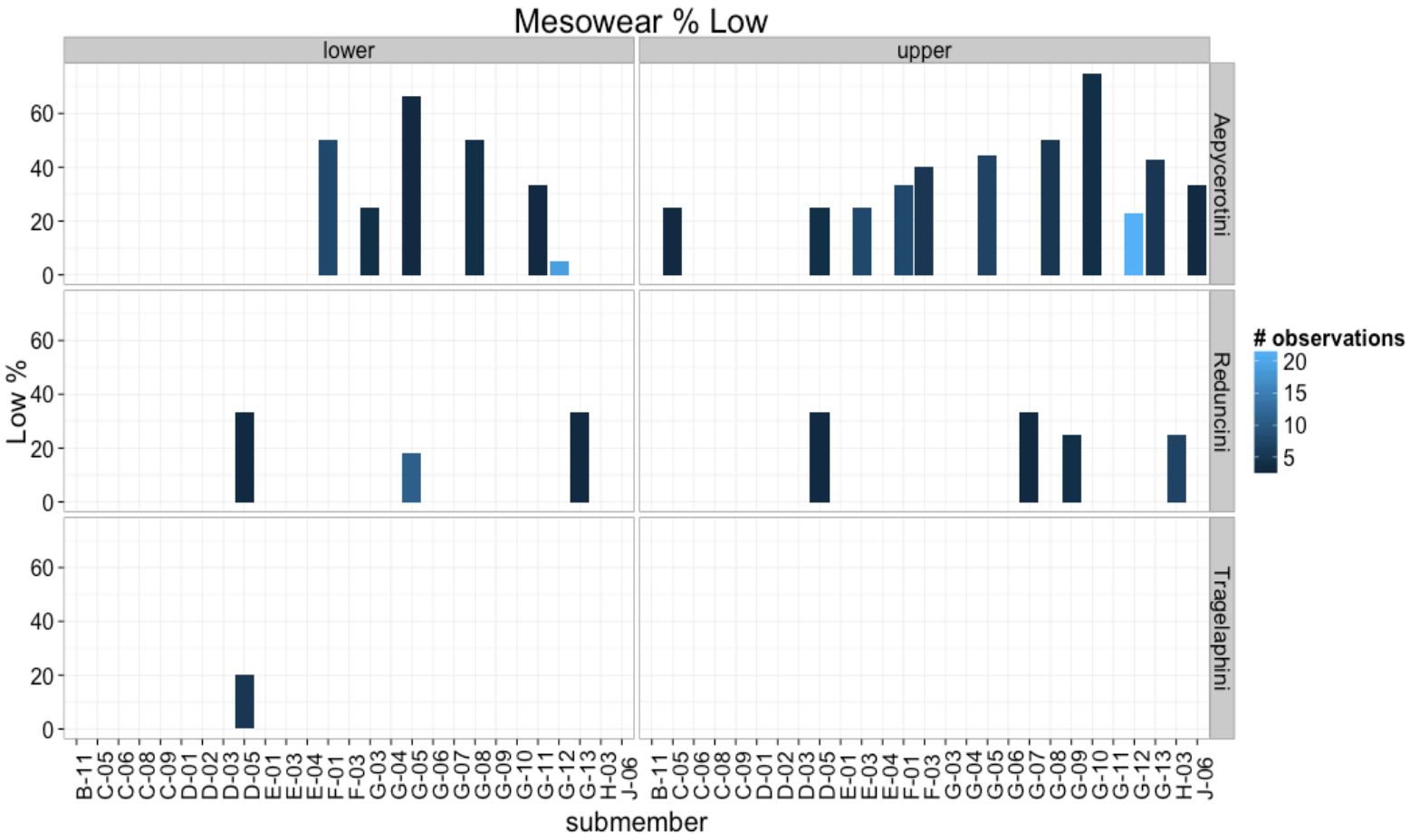

Figure 5.30: Percentage of cusps categorized as low through time. Only submembers with more than three molars that could be scored for mesowear are included.

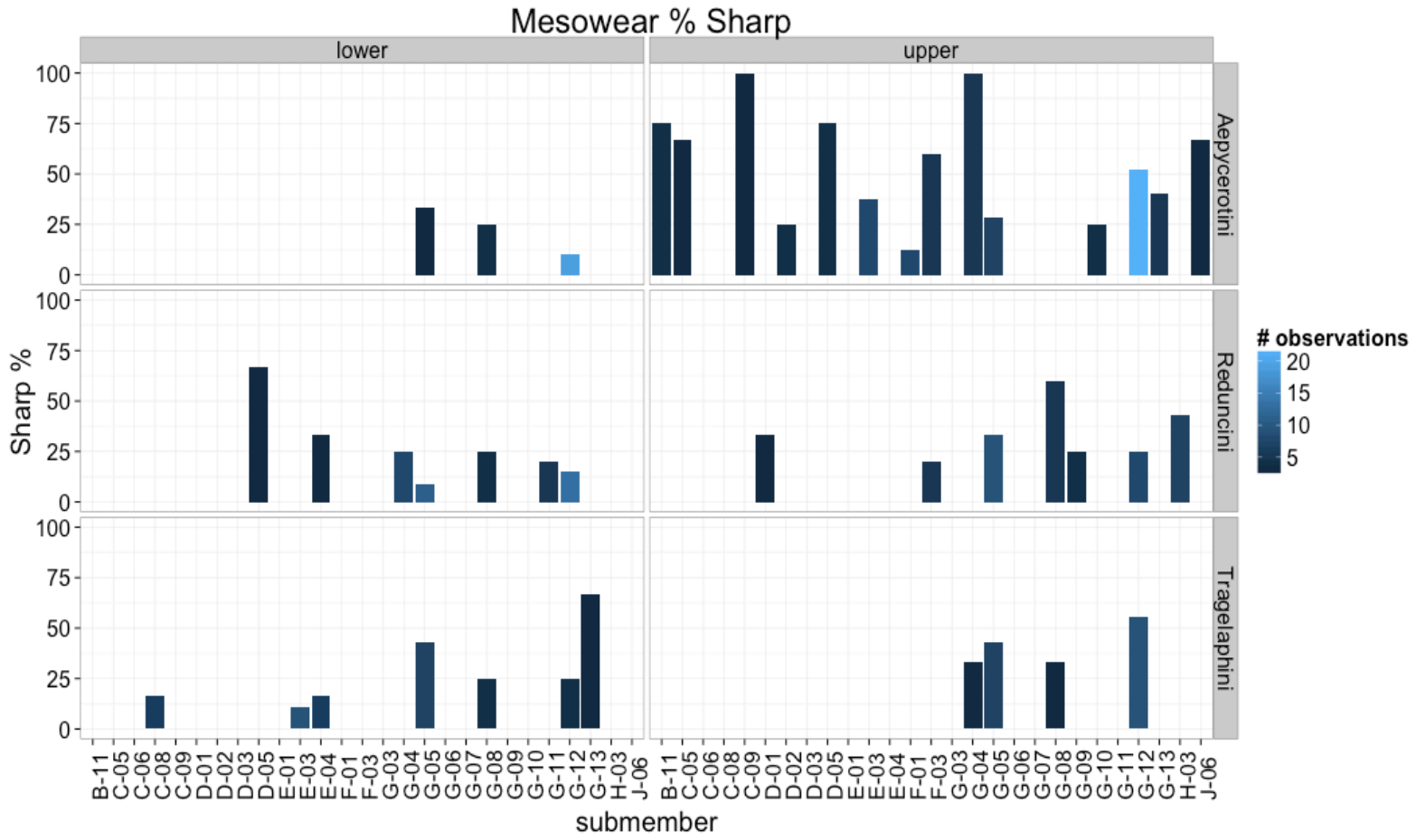

Figure 5.31: Percentage of cusps categorized as sharp through time. Only submembers with more than three molars that could be scored for mesowear are included.

DISCUSSION

Taken together, the results from the astragalar analysis and the exploration of mesowear spectra from the Shungura bovids provide several insights into the fluctuating environmental conditions that faced hominins occupying the lower Omo Valley during the Plio-Pleistocene. Because astragali and molars are extremely taphonomically robust skeletal elements, they are preserved in adequate numbers to allow environmental interpretations on a submember-by-submember basis, which sheds light on environmental conditions at the finest possible temporal scale.

The first hypothesis examined in this chapter was that was a significant drying trend occurred through time in the Shungura Formation. This hypothesis was not strongly supported by the analyses presented here. However, the proportion of Light Cover habitats significantly increases with member rank order (Table 5.3). Furthermore, submembers with astragalar habitat score spectra near the Open end of the range tend to appear later in the section (*e.g.*, F-00, F-01, G-01). There are, however, numerous exceptions to this, for example, the relatively Open astragalar habitat spectra in upper Member C contradicts this trend. There were no statistically significant trends in mesowear scores through time.

In general, the pattern of ecological change through time at Shungura is complex, and the results supported here do not provide strong support for a directional shift in habitats through time. It is clear that several later submembers sample environments with a preponderance of open and light-cover bovid taxa, but there is little evidence that this trend towards open environments occurred in a monotonic fashion. Rather, the submember analyses reveal an environment that changed in fits and starts, with ecological changes occurring between submembers, and then reversing again relatively quickly. This pattern of reversible environmental change may have its roots in variation

in tropical insolation due to cycles of orbital eccentricity with a periodicity of ~ 100 Ka (deMenocal, 1995), which has been suggested to shape the taxonomic community in the Turkana Basin in previous analyses of the large mammal fauna using different methods (Bobe et al., 2002; Bobe and Behrensmeyer, 2004). This environmental variability may have implications for the evolution of hominin cognitive complexity and behavioral flexibility, as has been suggested by Potts (Potts, 1996, 1998 a; b) under the rubric of the Variability Selection Hypothesis.

However, it is not possible with the data presented in this chapter to confidently rule out other factors besides global climate dynamics as the root cause of habitat change in the reconstructed habitats at Shungura. Given that the Shungura fossil collection was recovered from fluvial deposits around the ancestral Omo River, it is highly likely that some of the variation in reconstructed habitats through time in this analysis is due to spatial shifts that occurred as different habitat types migrated across the paleolandscape with fluctuating proximity to the ancestral river. Furthermore, high-energy depositional settings like the Omo River necessarily produce some degree of temporal and spatial averaging of the habitat signal. Despite these caveats, the results presented are broadly consistent with previous results reported on the basis of taxonomic analyses of the mammalian fauna, ecological structure analysis, paleobotanical reconstruction, and stable isotope analysis of mammalian tooth enamel. This concordance of multiple lines of evidence suggests that the data reported here are of sufficient spatial and temporal resolution to be informative with regards to the mix of habitats in the basin through time.

The second hypothesis examined in this study was that a major environmental shift occurred in the Shungura Formation at approximately 2.85 Ma, between Members B and C, as reported in previous research. The analyses presented here partially support this hypothesis, with major differences in astragalar habitat spectra detectable between

Members C and B. However, these differences were not statistically significant, and they were comparable in magnitude to the differences observed between Member E and F (Table 5.2).

The clearest indication from these analyses is that analyzing the Shungura fossils at the level of geological member masks significant variability that is likely related to environmental dynamism *within* members. Member C is a good example of this phenomenon. Analyzed at the level of geological member, the differences between Members B and C are rather pronounced, and accord well with previous work indicating a major shift between these two members. However, the astragalar habitat score spectra in Figure 5.11 suggest that earlier submembers of Member C were ecologically similar to Member B, and that evidence for ecological change in Member C does not occur until later, in units C-08 and C-09. There are no dated tuffs available to precisely date this event, but unit C-09 contains the Gauss- Matuyama paleomagnetic reversal (Feibel et al., 1989) which occurred at approximately 2.58 Ma (Gradstein, 2012). Thus, if major ecological change did not occur until unit C-08 (< 2.58 Ma), as suggested by the astragalar habitat score data, this has significant implications for the timing of this major ecological shift at Shungura. Based on these data, the ecological shift occurred up to 200Ka later than would be indicated based on analysis at the level of geological member. These results are consistent with a previous analysis of the Shunugura faunal database (Fernandez and Vrba, 2006), which divided Member C into upper and lower sections, and reconstructed very different environmental parameters for these submembers. If this characterization is accurate, the relevant environmental shift occurred much closer to the timing of the hypothesized cladogenetic event leading to genus *Homo*. This may lend support to the hypothesis of a causal relationship between the environmental event and the phylogenetic event, as suggested by Vrba's Turnover Pulse Hypothesis (1988).

The results presented in this chapter also lend support to the characterization of major faunal turnover between Member E and Member F discussed in previous work (Alemseged, 2003). In both the member-level and submember-level analyses, the differences between Member E and Member F were among the largest observed anywhere in the Shungura sequence although, given the available sample sizes, these differences were not statistically significant. Thus, based on the analyses presented here, the ecological shift between Member E and Member F must be seen as equally important as the shift occurring between Member B and Member C.

Work on stable isotopic composition of mammalian teeth in the Shungura Formation has suggested that significant dietary flexibility existed among the Tragelaphini through time. Specifically, results from Bibi *et al*. (2013) suggest a major dietary shift in the *T. rastafari – T. nakuae* lineage, with the *T. nakuae* specimens (post 2.85 Ma) exhibiting δ13C values that are higher than any living Tragelaphini. The authors suggest that these results point to significant C4 consumption in the later representatives of this lineage, with specimens from units G4 – G13 having the highest δ13C values. The mesowear data in this chapter do not support a hypothesis of significant dietary flexibility in the Shungura Tragelaphini, at least with regards to the mechanical aspects of the diet reflected in mesowear variables. Specifically, the mesowear spectra presented here are inconsistent with a significant grazing component in the diet of Shungura Tragelaphini at any point in the sequence. This is especially true for units in lower Member G, which exhibit mesowear signatures that are squarely on the browsing end of the range of mesowear seen in modern Tragelaphini. These are the very submembers which for which *T. nakuae* has the highest δ13C values (Bibi et al., 2013). A similar mismatch between isotopic and mesowear data has been documented in the Laetoli Tragelaphini, in which high δ13C values have been observed in species with

browsing mesowear signatures (Kaiser, 2011). This apparent disconnect between mesowear morphology and stable isotope values has been suggested by Kaiser (2011) to reflect the presence of significant amounts of C4 dicots on the paleolandscape, which could explain the browsing-dominated mesowear signature in the face of isotopic evidence for a C4 contribution to the diet. However, this suggestion is quite controversial, as there is no other indication that C4 dicots were a major proportion of plant biomass in Pliocene equatorial Africa (Kingston and Harrison, 2007). Thus, reconstructing the diet of Pliocene Tragelaphini comprises a clear topic for future research in order to resolve this apparent paradox between the isotopic data and the morphological / mesowear data. Overall, the mesowear results argue for careful consideration of multiple proxies of paleoenvironment in order to characterize hominin environments.

CONCLUSION

This chapter made use of the hyper-abundant bovid molars and astragali in order to shed light on the dietary and locomotor adaptions of the Shungura fossil bovids, with a goal of better understanding ecological conditions facing the early hominins occupying the lower Omo Valley. This study differed from previous work in basing habitat reconstructions only on the skeletal elements (astragali and isolated teeth) that are most likely to provide strong statistical samples of the community across different depositional conditions in an effort to mitigate, to the extent possible, the impact of variable taphonomic conditions through time.

The main findings of this chapter are as follows:

- Ecological changes between Members B and C did not fully materialize until the upper submembers of Member C, sometime prior to 2.588 Ma, or some ~260Ka later than reported by some previous studies.
- There is considerable environmental dynamism that is masked by analyzing data at the level of member.
- There is little or no evidence for a monotonic trend in environmental conditions at Shungura. Environmental changes occur in reversible, step-like pattern. However, submembers indicating the greatest importance of open habitats occur later in the sequence, in lower Member F and again in upper Member G.
- Mesowear data offer no support for a significant grazing adaptation in Shungura Tragelaphini, in contrast with data indicating carbon-isotope ratios near the range of modern grazers. The diet of Pliocene Tragelaphini is an important topic needing further research.

Overall, results support the notion that there was significant ecological dynamism in the basin throughout the period sampled by the Shungura fossil assemblage. This suggests one of two possibilities: 1) that the hominins occupying the lower Omo Valley were significantly eurytopic (as suggested by (Reed, 2008) for *A. afarensis* at Hadar), and capable of thriving in diverse habitats or 2) that they may have tracked preferred habitats as these habitats shifted across the paleolandscape. However, the relatively coarse spatial and temporal scale of the Omo Shungura Formation may not be sufficient to distinguish between these two hypotheses.

Shungura Habitat Change and Hominin Evolution

In broad agreement with prior research, the results of this chapter characterize available habitats at Shungura as relatively mesic and closed during the early portion of the sequence (Member B and lower Member C). Later in the sequence, mesic habitats are still represented, but open habitats become more important, first at approximately ~2.58 Ma, and then during lower Member F and again during upper Member G times. The hominin remains from Shungura, though largely fragmentary, indicate that a robust australopith, probably *P. aethiopicus,* was present in the basin by 2.7 Ma, with an evolutionary transition to *P. boisei* occurring by Member G *ca* 2.3 Ma (Suwa *et al*., 1996). The appearance of *P. boisei* therefore occurs in the context of a series of relatively large shifts in the available habitats represented at Shungura. Based on this data, the evolutionary transition towards *P. boisei* is at least temporally coincident with major habitat change at Shungura. However, habitat shifts of comparable magnitude occur at other time periods (e.g. between member B and upper Member C) that are not accompanied by phylogenetic turnover or notable anagenetic change in the robust australopith lineage. Thus, it is difficult to confidently assert a particular environmental cause for the evolutionary appearance of *P. boisei* based on the data presented in this chapter.

The gracile hominins from Members B and C are not reliably identifiable to genus, but there is some evidence for the presence of *Homo* in the Shungura by Member E at approximately 2.4 Ma (Suwa *et al*., 1996). Assuming this date for the origin of *Homo,* the data presented in this chapter would suggest that genus *Homo* appeared in the Shungura Formation some 180Ka after the initial appearance of more open habitats during upper Member C times.

However, dating the appearance of early *Homo* in Africa is a topic of considerable debate and controversy, even in cases where the skeletal evidence is much more complete than the dental sample from Shungura. The earliest fossil that is attributed to *Homo* by many researchers is the A.L. 666 maxilla from Hadar, dated to approximately 2.33 Ma (Kimbel et al., 1997). It is not possible to determine how closely this date coincides with the earliest appearance of *Homo*, because the mammalian fossil record at Hadar is largely absent during the period from 2.9 – 2.35 due to geological disconformities (Reed, 2008). Thus, the first appearance date for genus Homo is not known with a high degree of certainty.

Based on this large uncertainty, it is extremely difficult at present to accurately characterize the ecological context surrounding this event. Resolving the timing and ecological context of the origin of our genus represents one of the most exciting unanswered questions in paleoanthropology. Ultimately, this question must await the discovery of new, more taxonomically diagnostic fossil evidence that more precisely establishes the timing of this event.

Chapter 6: Conclusions

This dissertation explored several aspects of bovid ecomorphology with the goal of shedding light on the environmental context of human evolution in East Africa, specifically in the Omo Shungura Formation in southwestern Ethiopia. The approach taken was to focus on skeletal elements that are very commonly preserved in the fossil record (*i.e.*, astragali and molar teeth), because these elements likely provide the best available statistical sample of bovid communities in the past. Before this ecomorphological study of the Shungura bovids could be completed, however, it was necessary to address several issues that have been recently raised in the literature regarding the influence of phylogeny and body size in ecomorphology, as well as questions regarding whether or not the astragalus holds any functional signal at all (Klein et al., 2010). Accordingly, this dissertation contains methodological contributions in addition to new insights on the functional morphology of the bovid astragalus and Shungura paleoenvironments.

In Chapter 2, I used phylogenetic simulation techniques to explore the performance of statistical methods commonly used in ecomorphology on variables with differing levels of phylogenetic signal. These simulations revealed that, when both predictor variables and predicted categories contain phylogenetic signal, Discriminant Function Analysis (DFA) commonly produces statistically significant results with relatively high classification accuracies, even in cases in which there is no biomechanical relationship between the variables. Critically, this "over-performance" of DFA was only a problem when phylogenetic signal was present in **both** the predictor and predicted variables. Further analysis demonstrated that Phylogenetic Generalized Least Squares (PGLS) has appropriate levels of Type-I error under all simulated conditions. Thus,

PGLS offers a useful tool for functionally validating morphological characters by explicitly testing for evolutionary convergence. The results of Chapter 2 thus provide a methodological framework that explicitly takes into account body size and phylogenetic signal in ecomorphology. These results have been published in the American Journal of Physical Anthropology (Barr and Scott, 2013), and have been applied to the study of bovid metapodials (Scott and Barr, In Press).

The goal of Chapter 3 was to answer unresolved questions regarding the functional morphology of the bovid astragalus. Specifically, previous reports suggested that body-size and phylogeny played the predominant roles in patterning bovid astragalar morphology, and called into question the use of the astragalus as an ecomorphological predictor element. Chapter 3 presented a functional framework for testing explicit hypotheses about the relationship between astragalar morphology and habitat-specific locomotor performance. The results from Chapter 3 unambiguously demonstrate that there is a habitat signal in the morphology of the bovid astragalus, even after controlling for the effects of body size and phylogenetic signal. Chapter 4 used the set of measurements validated in Chapter 3 to evaluate the predictive ability of the astragalus using DFA. The level of predictive success for the astragalus is slightly lower than for some other skeletal elements, but the vast numbers of preserved astragali in the fossil record help to offset this reduction in predictive certainty.

This work on astragalar functional morphology brings some resolution to the literature debate over the use of the astragalus as an ecomorphological predictor, which began with Degusta and Vrba's initial study (2003) and was rekindled by Plummer *et al*. (2008) and Klein and colleagues (2010). The work in Chapters 3 and 4 of this dissertation offers a methodologically rigorous examination of previous claims regarding astragalar functional morphology, offers new functional justification for a measurement scheme

linking astragalar morphology with habitat-specific locomotor function, and validates the use of the astragalus as an ecomorphological predictor element.

Chapter 5 comprised an analysis of a very large sample of astragali and molar teeth from the Shungura Formation with the goal of producing dietary and locomotor reconstructions of the bovid paleo-communities through time at the site. These analyses demonstrated that previously identified ecological shifts between Member B and C likely did not fully materialize until later in time than previously recognized (sometime prior to 2.588 Ma). Further analyses reveal that the differences between Member B and C in Shungura are comparable in magnitude to differences between Member E and F, as has been suggested by Alemseged (2003). Furthermore, considerable environmental dynamism was observed at the level of geological submember. The temporal resolution of the dated submembers is not adequate to uniquely identify the cause of this variability, but it is broadly consistent with the ~100Ka time scale of eccentricity-driven Milankovitch cycles of insolation variation. Reconstructing Shungura environments at the level of geological member masks this variation, but environmental variability on these timescales likely had an impact on hominins occupying the region. Hominins occupying the lower Omo basin may have tracked preferred habitats as they migrated across the landscape through time, or they may have been ecologically eurytopic, as has been suggested for *A. afarensis* at Hadar (Reed, 2008).

Finally, the mesowear results from this chapter offered insight into the dietary adaptation of the Shungura bovids. Previous studies have found exceptionally high carbon isotope ratios in some Shungura Tragelaphini (Bibi et al., 2013), which places these bovids near the range of modern grazers. However, the analysis of mesowear in this dissertation does not offer any evidence for grazing in the Shungura Tragelaphini. Thus,

these results may indicate the existence of some significant C4 browse resource in the region to reconcile the isotopic data with the mesowear data.

FUTURE DIRECTIONS AND REMAINING QUESTIONS

This dissertation offered new data on the habitats available in the Shungura Formation through time, introduced a framework for interpreting the morphology of the astragalus in relation to habitat, and highlighted the importance of phylogenetic statistical methods in ecomorphology. There remains considerable work to be done, however, in illuminating the environmental context of human evolution in East Africa, as well as in refining the methods we use to produce paleoenvironmental reconstructions.

Postcranial Ecomorphology

The Shungura fossil collection is vast, and there is a wide range of bovid skeletal elements represented for which published ecomorphological models exist (*e.g.,* femora, metatarsals, metacarpals, phalanges). Thus, there is considerable future work to be completed to expand the ecomorphological survey of the Shungura collection in this dissertation. Future analyses of the abundant postcranial fossil record at Shungura would contribute to a more robust multi-proxy record of the habitats represented through time at Shungura and these analyses would, no doubt, contribute valuable new data on the environmental context of human evolution in the region. Thus, in the future, I plan to expand my ecomorphological study of the Shungura fossils to include other skeletal elements.

Phylogenetic Statistical Methods

Chapter 2 revealed that PGLS with corrections for multiple comparisons is a useful technique for ecomorphology, but there is work remaining to be done regarding the best practices for statistical methods in ecomorphology. Previous research (Revell,

2010) has demonstrated that phylogenetic signal in multivariate residual space is not necessarily predictable from the levels phylogenetic signal of the univariate predictor variables. This would suggest that the performance of multivariate statistical methods such as DFA might be affected adversely by multivariate residual phylogenetic signal, which could introduce unpredictable errors into classification results. Thus, there is a need for multivariate classification techniques that account for phylogeny directly, rather than using phylogenetic statistical methods to validate each univariate character and then using a multivariate classification technique that does not explicitly account for residual phylogenetic signal. I am aware of one published method, known as phylogenetic DFA (pDFA), which purports to control for phylogenetic signal in DFA (Motani and Schmitz, 2011; Schmitz and Motani, 2011). However, the pDFA method has only been made available in supplementary online material (instead of through typical channels of open-source software distribution), is poorly documented, and produces results that are unstable and difficult to interpret, in my experience. As such, pDFA was not used in this dissertation. In the future, ecomorphology will benefit from the implementation of a robust multivariate method of categorical prediction that includes explicit control of phylogenetic signal.

Hypothesis Testing Framework For Paleoecology

One general observation from this dissertation is that work remains to be done in formalizing a framework for interpreting raw paleoecological data with regards to the implications for human evolution. In my opinion, bridging the gap between the data produced in studies such as Chapter 5 of this dissertation and knowledge about the impact of climate and habitat on hominins requires a clearly articulated framework for testing

hypotheses that is implemented across many independent researchers at many different sites.

Take, for example, a fossil assemblage for which postcranial ecomorphology indicates that 85% of the bovids are open-country adapted and 15% are light-cover adapted. These proportions provide critical primary data regarding the adaptations of the bovid community. However, these proportions are not straightforward to interpret in terms of what they reveal about the habitats available to early hominins, even if we assume perfect fidelity (*i.e.*, 100% accuracy) in habitat predictions for each fossil. Partly, this is due to the relatively coarse habitat categorization scheme commonly used in ecomorphology and employed in this dissertation. To some extent this is unavoidable, because there is an inevitable trade-off between 1) accurately describing the habitat usage of each species (which likely differs from population to population) and 2) lumping variability into a manageable number of habitat categories that is useful for ecomorphological study.

Even in light of ecomorphological data on the relative proportions of locomotor adaptations in the bovid community, questions remain regarding the implications for hominin habitat reconstruction. For instance, what is the likelihood that the hypothetical bovid sample discussed above (15% light-cover adapted individuals) could be drawn from the bovid community in an open-arid environment such as the Etosha National Park in Namibia, a habitat dominated by grassland and low-density mopane savanna (du Plessis, 1999)? Furthermore, what is the likelihood of drawing the same sample from an ecotone community in the Serengetti ecosystem, which presents distinct ecological challenges and affordances as compared to the Etosha ecosystem? Despite the ecological differences between these two real-world examples, the methods currently used in ecomorphology do not offer a formal way of excluding or including either of these

possible modern analogs based on the relative proportions of bovid adaptations in the fossil sample. Some methods currently available (Correspondence Analysis on bovid survey data) provide methods for visualizing this data, but not for formal hypothesis testing.

Another area of ambiguity that remains with current methods relates to the statistical power inherent in ecomorphological habitat reconstructions. For instance, consider a second hypothetical ecomorphological sample of bovids that reflects classifications indicating 80% open cover, 15% light-cover and 5% heavy cover bovids. Does this sample imply a meaningfully different habitat as compared with the previous sample of 85% open and 15% light-cover? There is no way to explicitly address this type of question using current ecomorphological methods, yet these types of comparisons between sites are commonly informed by ecomorphological data.

Much previous research effort in ecomorphology has justifiably been invested in producing ecomorphological habitat reconstructions that maximize the predictive accuracy for each fossil. However, the next link in the chain of inference, which involves testing hypotheses about the specific nature of habitats implied by ecomorphological results and/or comparing multiple samples has received considerably less attention. While the validity of statistical comparisons between sites depend on the accuracy of the habitat reconstruction for each fossil, they also depend on the relative sample sizes available for each element. However, there is no established formal framework for hypothesis testing or statistical power analysis for ecomorphology. Studies have occasionally compared estimated habitat proportions to a few modern analogues (Plummer and Bishop, 1994), but these rare comparisons have been exploratory.

Going forward, ecomorphology would benefit from an explicit framework for testing ecological hypotheses about the habitat predictions that ecomorphological studies

produce. This will involve the creation of a large database of modern analog habitats, with good census data on the relative abundance of bovids present in these habitats. This database would also include information on vegetation physiognomy, precipitation data, elevation data, and other variables that are important for characterizing hominin habitats.

One option for a hypothesis-testing framework would be a Monte-Carlo framework in which a given ecomorphological sample can be compared against the reference database. This framework would create a formal way to bridge the gap between raw ecomorphological data and inferences regarding past hominin environments. As an illustrative example, this framework would provide a means to statistically estimate the likelihood that a given sample was drawn from a habitat with, say, a mean annual precipitation (MAP) less than 500mm. This would be accomplished by resampling bovid census data from communities in the database with MAP less than 500mm and determining -- through resampling -- how often the bovid communities at these sites could produce results similar to those observed in the ecomorphological sample. This technique would provide an explicit numerical estimate of the likelihood of observing an ecomorphological sample in modern analogues with known ecological attributes.

In an analogous manner, ecomorphological results from two separate fossil sites could be compared against sites in the database to produce a list of extant analogues that could produce the observed ecomorphological samples with a given likelihood. These lists could then be compared to determine whether or not the lists of predicted ecological parameters overlap or not, thus offering a way to statistically determine whether two ecomorphological samples point to distinct habitats. If multiple independent researchers adopted such a framework, it would improve the comparability of ecomorphological reconstructions at sites across the continent of Africa.

Understanding the environmental context of human evolution remains a critical research program in paleoanthropology. Like many similar projects, this dissertation focused on site-based reconstructions at particular points in space and time. These reconstructions provide critical background data for characterizing the ecological context of human evolution. However, it is increasingly clear that understanding the "big picture" requires incorporating data from multiple independent research projects across the globe. Indeed, efforts are currently underway to create data-standards and protocols for sharing data across multiple projects (Reed et al., 2013). As data-sharing protocols develop, hypothesis-testing frameworks like the one just described will become more and more important as a way to organize and formalize research inquiries that synthesize data from many sites in many regions. This promises to be a fascinating era in which to study paleoecology as new data, and new ways of sharing and analyzing these data, continue to be amassed. These new data will no doubt resolve many current debates about the environmental context of human evolution as well as raising new unforeseeable questions.

Appendix A

Function to simulate a single character evolving over a given phylogenetic tree (myTree). Resulting trait is correlated with species-average body mass with coefficient correlation r. The full code to simulate all data, perform all analyses, and create all figures is available at https://github.com/wabarr/DFA-phylosim.

```
if(!require(phytools)) install.packages('phytools')

simulateData<-function(r,bodyMass,myTree) {
  #r is correlation between body mass and desired character
  #bodyMass is a vector of species mean body mass values
  #assumes taxon order in bodyMass matches myTree

as.numeric(r*log(bodyMass) +
sqrt(1-r^2) *
fastBM(nsim=1,
       myTree,
       sig2=mean(pic(log(bodyMass),multi2di(myTree))^2)))
```

Appendix B

Code to test a categorical variable for phylogenetic signal. This works by first transforming the existing phylogenetic tree (myTree) into a star phylogeny with lambda = 0. Then, the fitDiscrete() (Harmon et al., 2008) function is used to fit two continuous-time Markov models (Pagel, 1994) of trait evolution: (1) first with the branch lengths from the actual phylogeny and (2) with the transformed equal branch-length star phylogeny. These two models are compared using a likelihood ratio test. If the model using the actual phylogeny fits significantly better than the star phylogeny model, this is taken as evidence for phylogenetic signal in the categorical variable. The same process was repeated with randomized habitat assignments to ensure that this method was capable of detecting situations in which phylogenetic signal was absent.

This example code performs this test using a meristic model, which assumes that character states are ordered, and that character changes can only occur in this order. Several other models of character evolution are included in the full version of the code available online (https://github.com/wabarr/DFA-phylosim). Regardless of which model was used, the likelihood ratio test revealed that a model using the actual phylogeny fit significantly better than the model using the star phylogeny. This suggests that there is strong phylogenetic signal in bovid habitat preference, regardless of the specifics of the character evolution model used. In all models using randomized habitats, the likelihood ratio test showed no significant differences in model fit, which demonstrates that this method is capable of detecting situations in which phylogenetic signal is absent.

```
##Example of how to test for PhyloSignal in categorical variable
#This example uses an ordered states (meristic) model.

require(geiger)
```

```
#assumes myTree is phylogenetic tree, and habs is vector of
habitats
#habs assumed to be in same order as taxa in myTree

zeroTree <- transform(myTree,"lambda",0)


####with Actual hab - meristic model (ordered states)
MeristicActualTree <-
fitDiscrete(multi2di(myTree),habs,model="meristic")
MeristicStarPhylogeny <-
fitDiscrete(multi2di(zeroTree),habs,model="meristic")
pchisq(2 * (MeristicActualTree$opt$lnL -
MeristicStarPhylogeny$opt$lnL),1,lower.tail=FALSE)

#####with random habs  - meristic model (ordered states)
randomHabs <- sample(unique(habs),length(habs),replace=TRUE)
names(randomHabs) <- names(habs)
MeristicActualTree<-
fitDiscrete(multi2di(myTree),randomHabs,model="meristic")
MeristicStarPhylogeny<-
fitDiscrete(multi2di(zeroTree),randomHabs,model="meristic")
pchisq(2 * (MeristicActualTree$opt$lnL -
MeristicStarPhylogeny$opt$lnL),1,lower.tail=FALSE)
```

Appendix C

This appendix contains all the raw measurements of extant bovid astragali from Chapter 3. Measurements definitions can be found in Table 3.1. All linear measurements are in millimeters. All area measurements are in square millimeters.

Individual	Taxon	Habitat	Variable	Value
AMNH113810	*Addax nasomaculatus*	Open	ACF	525.73
AMNH113811	*Addax nasomaculatus*	Open	ACF	446.41
AMNH113812	*Addax nasomaculatus*	Open	ACF	533.34
AMNH113813	*Addax nasomaculatus*	Open	ACF	545.8
AMNH81690	*Aepyceros melampus*	LightCover	ACF	384.72
AMNH82050	*Aepyceros melampus*	LightCover	ACF	NA
AMNH83534	*Aepyceros melampus*	LightCover	ACF	NA
AMNH85150	*Aepyceros melampus*	LightCover	ACF	NA
AMNH233038	*Alcelaphus buselaphus*	Open	ACF	607.83
AMNH34717	*Alcelaphus buselaphus*	Open	ACF	465.91
AMNH34725	*Alcelaphus buselaphus*	Open	ACF	727.85
AMNH82033	*Alcelaphus buselaphus*	Open	ACF	662.8
AMNH82159	*Alcelaphus buselaphus*	Open	ACF	733.39
AMNH16048	*Ammotragus lervia*	NA	ACF	440.11
AMNH81740	*Antidorcas marsupialis*	Open	ACF	NA
AMNH81745	*Antidorcas marsupialis*	Open	ACF	253.21
AMNH83549	*Antidorcas marsupialis*	Open	ACF	NA
AMNH83550	*Antidorcas marsupialis*	Open	ACF	NA
AMNH35527	*Antilope cervicapra*	Open	ACF	298
AMNH35957	*Antilope cervicapra*	Open	ACF	247.31
AMNH54486	*Antilope cervicapra*	Open	ACF	323.46
AMNH88406	*Beatragus hunteri*	Open	ACF	561.05
AMNH88407	*Beatragus hunteri*	Open	ACF	568.98
AMNH88408	*Beatragus hunteri*	Open	ACF	539.23
AMNH54765	*Bubalus bubalis*	NA	ACF	NA
AMNH54766	*Bubalus bubalis*	NA	ACF	NA
AMNH52875	*Cephalophus dorsalis*	Forest	ACF	NA
AMNH52876	*Cephalophus dorsalis*	Forest	ACF	194.55
AMNH52884	*Cephalophus dorsalis*	Forest	ACF	NA
AMNH52888	*Cephalophus dorsalis*	Forest	ACF	NA
AMNH52775	*Cephalophus leucogaster*	Forest	ACF	198.66
AMNH52778	*Cephalophus leucogaster*	Forest	ACF	178.56
AMNH52788	*Cephalophus leucogaster*	Forest	ACF	193.08
AMNH216375	*Cephalophus natalensis*	Forest	ACF	NA
AMNH54391	*Cephalophus natalensis*	Forest	ACF	147.71
AMNH81686	*Cephalophus natalensis*	Forest	ACF	NA
AMNH83387	*Cephalophus natalensis*	Forest	ACF	NA

AMNH52930	*Cephalophus nigrifrons*	Forest	ACF	NA
AMNH52931	*Cephalophus nigrifrons*	Forest	ACF	NA
AMNH52940	*Cephalophus nigrifrons*	Forest	ACF	NA
AMNH52943	*Cephalophus nigrifrons*	Forest	ACF	NA
AMNH53138	*Cephalophus silvicultor*	Forest	ACF	504.11
AMNH53144	*Cephalophus silvicultor*	Forest	ACF	524.81
AMNH53153	*Cephalophus silvicultor*	Forest	ACF	429.42
AMNH52992	*Cephalophus weynsi*	Forest	ACF	197.09
AMNH52995	*Cephalophus weynsi*	Forest	ACF	206.29
AMNH52999	*Cephalophus weynsi*	Forest	ACF	226.3
AMNH88429	*Cephalophus weynsi*	Forest	ACF	155.44
AMNH81716	*Connochaetes gnou*	Open	ACF	666.87
AMNH81720	*Connochaetes gnou*	Open	ACF	720.09
AMNH81722	*Connochaetes gnou*	Open	ACF	NA
AMNH27824	*Connochaetes taurinus*	Open	ACF	830.43
AMNH54133	*Connochaetes taurinus*	Open	ACF	920.67
AMNH83502	*Connochaetes taurinus*	Open	ACF	934.64
AMNH83503	*Connochaetes taurinus*	Open	ACF	843.81
AMNH113781	*Damaliscus lunatus*	Open	ACF	NA
AMNH34729	*Damaliscus lunatus*	Open	ACF	689.95
AMNH34730	*Damaliscus lunatus*	Open	ACF	770.87
AMNH82035	*Damaliscus lunatus*	Open	ACF	763.1
AMNH42953	*Damaliscus pygargus*	Open	ACF	428.02
AMNH81727	*Damaliscus pygargus*	Open	ACF	422.62
AMNH81729	*Damaliscus pygargus*	Open	ACF	393.01
AMNH81787	*Damaliscus pygargus*	Open	ACF	428.4
AMNH81997	*Eudorcas thomsonii*	Open	ACF	203.17
AMNH82059	*Eudorcas thomsonii*	Open	ACF	NA
AMNH82060	*Eudorcas thomsonii*	Open	ACF	NA
AMNH88415	*Eudorcas thomsonii*	Open	ACF	NA
AMNH54506	*Gazella gazella*	Open	ACF	188.86
AMNH54997	*Gazella gazella*	Open	ACF	181.68
AMNH54998	*Gazella gazella*	Open	ACF	160.95
AMNH80143	*Hippotragus equinus*	Open	ACF	924.87
AMNH87217	*Hippotragus equinus*	Open	ACF	1111.37
AMNH216381	*Hippotragus niger*	LightCover	ACF	NA
AMNH80458	*Hippotragus niger*	LightCover	ACF	1088.9
AMNH80461	*Hippotragus niger*	LightCover	ACF	NA

AMNH83476	*Hippotragus niger*	LightCover	ACF	NA
AMNH53492	*Kobus ellipsiprymnus*	HeavyCover	ACF	951.77
NMNH173877	*Kobus ellipsiprymnus*	HeavyCover	ACF	906.94
NMNH21898	*Kobus ellipsiprymnus*	HeavyCover	ACF	858.36
AMNH36396	*Kobus kob*	LightCover	ACF	561.84
AMNH36397	*Kobus kob*	LightCover	ACF	452.34
AMNH82129	*Kobus kob*	LightCover	ACF	NA
AMNH82130	*Kobus kob*	LightCover	ACF	NA
AMNH82173	*Kobus kob*	LightCover	ACF	NA
AMNH70010	*Kobus leche*	HeavyCover	ACF	NA
AMNH99649	*Kobus leche*	HeavyCover	ACF	583.9
NMNH254927	*Kobus leche*	HeavyCover	ACF	530.67
AMNH113784	*Kobus megaceros*	HeavyCover	ACF	531.07
AMNH82135	*Kobus megaceros*	HeavyCover	ACF	NA
AMNH82136	*Kobus megaceros*	HeavyCover	ACF	NA
AMNH82137	*Kobus megaceros*	HeavyCover	ACF	NA
AMNH35323	*Kobus vardonii*	HeavyCover	ACF	567.57
AMNH70057	*Kobus vardonii*	HeavyCover	ACF	NA
AMNH81687	*Kobus vardonii*	HeavyCover	ACF	509.58
AMNH81170	*Litocranius walleri*	LightCover	ACF	NA
NMNH164031	*Litocranius walleri*	LightCover	ACF	289.1
NMNH164033	*Litocranius walleri*	LightCover	ACF	284.68
NMNH259457	*Litocranius walleri*	LightCover	ACF	265.94
AMNH187824	*Madoqua kirkii*	HeavyCover	ACF	NA
AMNH82076	*Madoqua kirkii*	HeavyCover	ACF	NA
NMNH538104	*Madoqua kirkii*	HeavyCover	ACF	NA
NMNH538106	*Madoqua kirkii*	HeavyCover	ACF	74.03
NMNH541419	*Madoqua kirkii*	HeavyCover	ACF	NA
AMNH82051	*Nanger granti*	Open	ACF	NA
AMNH82056	*Nanger granti*	Open	ACF	NA
AMNH82057	*Nanger granti*	Open	ACF	NA
AMNH85152	*Nanger granti*	Open	ACF	368.82
AMNH80111	*Nanger soemmerringii*	Open	ACF	NA
NMNH582229	*Nanger soemmerringii*	Open	ACF	320.21
AMNH53180	*Neotragus batesi*	Forest	ACF	60.78
AMNH53181	*Neotragus batesi*	Forest	ACF	53.8
AMNH53946	*Neotragus batesi*	Forest	ACF	61.79
AMNH88426	*Neotragus moschatus*	Forest	ACF	NA

AMNH88427	*Neotragus moschatus*	Forest	ACF	NA
NMNH367449	*Neotragus moschatus*	Forest	ACF	76.17
AMNH233033	*Oryx gazella*	Open	ACF	NA
AMNH82043	*Oryx gazella*	Open	ACF	NA
AMNH82044	*Oryx gazella*	Open	ACF	NA
AMNH87211	*Oryx gazella*	Open	ACF	868.45
AMNH216387	*Ourebia ourebi*	LightCover	ACF	170.83
AMNH53304	*Ourebia ourebi*	LightCover	ACF	NA
AMNH53328	*Ourebia ourebi*	LightCover	ACF	NA
AMNH269894	*Philantomba monticola*	Forest	ACF	NA
AMNH52726	*Philantomba monticola*	Forest	ACF	NA
AMNH52753	*Philantomba monticola*	Forest	ACF	NA
AMNH52758	*Philantomba monticola*	Forest	ACF	72.42
AMNH216389	*Raphicerus campestris*	LightCover	ACF	NA
AMNH233047	*Raphicerus campestris*	LightCover	ACF	137.24
AMNH34728	*Raphicerus campestris*	LightCover	ACF	NA
AMNH80538	*Raphicerus campestris*	LightCover	ACF	NA
AMNH35493	*Redunca arundinum*	LightCover	ACF	425.65
AMNH80506	*Redunca arundinum*	LightCover	ACF	NA
NMNH367428	*Redunca arundinum*	LightCover	ACF	389.29
NMNH367452	*Redunca arundinum*	LightCover	ACF	NA
NMNH469909	*Redunca arundinum*	LightCover	ACF	267.55
AMNH27803	*Redunca fulvorufula*	LightCover	ACF	312.66
AMNH82063	*Redunca fulvorufula*	LightCover	ACF	245.24
AMNH82066	*Redunca fulvorufula*	LightCover	ACF	253.82
AMNH82067	*Redunca fulvorufula*	LightCover	ACF	261.04
AMNH53294	*Redunca redunca*	LightCover	ACF	352.09
AMNH53296	*Redunca redunca*	LightCover	ACF	358
AMNH90234	*Rupicapra rupicapra*	NA	ACF	274.73
AMNH90235	*Rupicapra rupicapra*	NA	ACF	311.33
AMNH90236	*Rupicapra rupicapra*	NA	ACF	340.43
AMNH17276	*Sigmoceros lichtensteinii*	Open	ACF	810.75
AMNH216382	*Sigmoceros lichtensteinii*	Open	ACF	NA
AMNH216383	*Sigmoceros lichtensteinii*	Open	ACF	NA
AMNH53088	*Sylvicapra grimmia*	LightCover	ACF	164.19
AMNH53092	*Sylvicapra grimmia*	LightCover	ACF	NA
AMNH80562	*Sylvicapra grimmia*	LightCover	ACF	NA
AMNH80563	*Sylvicapra grimmia*	LightCover	ACF	NA

AMNH53583	*Syncerus caffer*	LightCover	ACF	NA
AMNH82005	*Syncerus caffer*	LightCover	ACF	NA
AMNH82006	*Syncerus caffer*	LightCover	ACF	NA
AMNH82009	*Syncerus caffer*	LightCover	ACF	1755.18
AMNH53519	*Taurotragus derbianus*	HeavyCover	ACF	2033.43
AMNH53521	*Taurotragus derbianus*	HeavyCover	ACF	1660.85
AMNH53522	*Taurotragus derbianus*	HeavyCover	ACF	1581.85
AMNH53523	*Taurotragus derbianus*	HeavyCover	ACF	1664.16
AMNH27811	*Taurotragus oryx*	LightCover	ACF	1713.95
AMNH34722	*Taurotragus oryx*	LightCover	ACF	1422.22
AMNH54386	*Tragelaphus angasii*	HeavyCover	ACF	473.29
AMNH54387	*Tragelaphus angasii*	HeavyCover	ACF	622.42
AMNH54390	*Tragelaphus angasii*	HeavyCover	ACF	501.8
AMNH81002	*Tragelaphus buxtoni*	Forest	ACF	1042.27
AMNH81003	*Tragelaphus buxtoni*	Forest	ACF	827.34
AMNH81004	*Tragelaphus buxtoni*	Forest	ACF	1050.43
AMNH81014	*Tragelaphus buxtoni*	Forest	ACF	817.05
AMNH81033	*Tragelaphus buxtoni*	Forest	ACF	NA
AMNH53271	*Tragelaphus eurycerus*	Forest	ACF	980.13
AMNH53279	*Tragelaphus eurycerus*	Forest	ACF	1031.26
AMNH53280	*Tragelaphus eurycerus*	Forest	ACF	1114.05
AMNH36416	*Tragelaphus imberbis*	HeavyCover	ACF	493.53
AMNH36417	*Tragelaphus imberbis*	HeavyCover	ACF	462.19
AMNH82019	*Tragelaphus imberbis*	HeavyCover	ACF	542.22
AMNH82023	*Tragelaphus imberbis*	HeavyCover	ACF	454.12
AMNH187806	*Tragelaphus scriptus*	Forest	ACF	258
AMNH216371	*Tragelaphus scriptus*	Forest	ACF	305.6
AMNH88425	*Tragelaphus scriptus*	Forest	ACF	375.52
AMNH53209	*Tragelaphus spekii*	HeavyCover	ACF	668.87
AMNH53212	*Tragelaphus spekii*	HeavyCover	ACF	647.28
AMNH53213	*Tragelaphus spekii*	HeavyCover	ACF	434.5
AMNH53216	*Tragelaphus spekii*	HeavyCover	ACF	487.76
AMNH233027	*Tragelaphus strepsiceros*	HeavyCover	ACF	1054.36
AMNH70328	*Tragelaphus strepsiceros*	HeavyCover	ACF	733.17
AMNH70328a	*Tragelaphus strepsiceros*	HeavyCover	ACF	NA
AMNH113810	*Addax nasomaculatus*	Open	APD	7.5
AMNH113811	*Addax nasomaculatus*	Open	APD	5.63
AMNH113812	*Addax nasomaculatus*	Open	APD	8.01

AMNH113813	*Addax nasomaculatus*	Open	APD	12.3
AMNH81690	*Aepyceros melampus*	LightCover	APD	6.89
AMNH82050	*Aepyceros melampus*	LightCover	APD	6.09
AMNH83534	*Aepyceros melampus*	LightCover	APD	6.14
AMNH85150	*Aepyceros melampus*	LightCover	APD	5.8
AMNH233038	*Alcelaphus buselaphus*	Open	APD	7.46
AMNH34717	*Alcelaphus buselaphus*	Open	APD	6.56
AMNH34725	*Alcelaphus buselaphus*	Open	APD	8.11
AMNH82033	*Alcelaphus buselaphus*	Open	APD	7.57
AMNH82159	*Alcelaphus buselaphus*	Open	APD	7.59
AMNH16048	*Ammotragus lervia*	NA	APD	12.09
AMNH81740	*Antidorcas marsupialis*	Open	APD	3.98
AMNH81745	*Antidorcas marsupialis*	Open	APD	6.12
AMNH83549	*Antidorcas marsupialis*	Open	APD	5.08
AMNH83550	*Antidorcas marsupialis*	Open	APD	4.07
AMNH35527	*Antilope cervicapra*	Open	APD	5.5
AMNH35957	*Antilope cervicapra*	Open	APD	5.61
AMNH54486	*Antilope cervicapra*	Open	APD	5.04
AMNH88406	*Beatragus hunteri*	Open	APD	7.81
AMNH88407	*Beatragus hunteri*	Open	APD	7.6
AMNH88408	*Beatragus hunteri*	Open	APD	7.9
AMNH54765	*Bubalus bubalis*	NA	APD	39.29
AMNH54766	*Bubalus bubalis*	NA	APD	35.19
AMNH52875	*Cephalophus dorsalis*	Forest	APD	3.91
AMNH52876	*Cephalophus dorsalis*	Forest	APD	4.22
AMNH52884	*Cephalophus dorsalis*	Forest	APD	12.44
AMNH52888	*Cephalophus dorsalis*	Forest	APD	11.38
AMNH52775	*Cephalophus leucogaster*	Forest	APD	3.94
AMNH52778	*Cephalophus leucogaster*	Forest	APD	4.15
AMNH52788	*Cephalophus leucogaster*	Forest	APD	3.8
AMNH216375	*Cephalophus natalensis*	Forest	APD	3.53
AMNH54391	*Cephalophus natalensis*	Forest	APD	3.51
AMNH81686	*Cephalophus natalensis*	Forest	APD	3.44
AMNH83387	*Cephalophus natalensis*	Forest	APD	3.98
AMNH52930	*Cephalophus nigrifrons*	Forest	APD	11.6
AMNH52931	*Cephalophus nigrifrons*	Forest	APD	3.65
AMNH52940	*Cephalophus nigrifrons*	Forest	APD	11.36
AMNH52943	*Cephalophus nigrifrons*	Forest	APD	11.62

AMNH53138	*Cephalophus silvicultor*	Forest	APD	6.94
AMNH53144	*Cephalophus silvicultor*	Forest	APD	6.9
AMNH53153	*Cephalophus silvicultor*	Forest	APD	6.94
AMNH52992	*Cephalophus weynsi*	Forest	APD	4.36
AMNH52995	*Cephalophus weynsi*	Forest	APD	4.21
AMNH52999	*Cephalophus weynsi*	Forest	APD	4.1
AMNH88429	*Cephalophus weynsi*	Forest	APD	4.08
AMNH81716	*Connochaetes gnou*	Open	APD	7.18
AMNH81720	*Connochaetes gnou*	Open	APD	8.51
AMNH81722	*Connochaetes gnou*	Open	APD	7.89
AMNH27824	*Connochaetes taurinus*	Open	APD	10.04
AMNH54133	*Connochaetes taurinus*	Open	APD	11.09
AMNH83502	*Connochaetes taurinus*	Open	APD	9.51
AMNH83503	*Connochaetes taurinus*	Open	APD	9.02
AMNH113781	*Damaliscus lunatus*	Open	APD	7.56
AMNH34729	*Damaliscus lunatus*	Open	APD	11.54
AMNH34730	*Damaliscus lunatus*	Open	APD	13.27
AMNH82035	*Damaliscus lunatus*	Open	APD	8.69
AMNH42953	*Damaliscus pygargus*	Open	APD	6.47
AMNH81727	*Damaliscus pygargus*	Open	APD	5.89
AMNH81729	*Damaliscus pygargus*	Open	APD	6.69
AMNH81787	*Damaliscus pygargus*	Open	APD	5.73
AMNH81997	*Eudorcas thomsonii*	Open	APD	3.56
AMNH82059	*Eudorcas thomsonii*	Open	APD	4.63
AMNH82060	*Eudorcas thomsonii*	Open	APD	4.4
AMNH88415	*Eudorcas thomsonii*	Open	APD	4.68
AMNH54506	*Gazella gazella*	Open	APD	3.21
AMNH54997	*Gazella gazella*	Open	APD	3.58
AMNH54998	*Gazella gazella*	Open	APD	4.68
AMNH80143	*Hippotragus equinus*	Open	APD	9
AMNH87217	*Hippotragus equinus*	Open	APD	9.01
AMNH216381	*Hippotragus niger*	LightCover	APD	9.04
AMNH80458	*Hippotragus niger*	LightCover	APD	9.1
AMNH80461	*Hippotragus niger*	LightCover	APD	9.18
AMNH83476	*Hippotragus niger*	LightCover	APD	8.47
AMNH53492	*Kobus ellipsiprymnus*	HeavyCover	APD	10.17
NMNH173877	*Kobus ellipsiprymnus*	HeavyCover	APD	6.81
NMNH21898	*Kobus ellipsiprymnus*	HeavyCover	APD	7.67

AMNH36396	*Kobus kob*	LightCover	APD	6.01
AMNH36397	*Kobus kob*	LightCover	APD	5.58
AMNH82129	*Kobus kob*	LightCover	APD	6.49
AMNH82130	*Kobus kob*	LightCover	APD	6.21
AMNH82173	*Kobus kob*	LightCover	APD	6.32
AMNH70010	*Kobus leche*	HeavyCover	APD	23.3
AMNH99649	*Kobus leche*	HeavyCover	APD	6.41
NMNH254927	*Kobus leche*	HeavyCover	APD	5.02
AMNH113784	*Kobus megaceros*	HeavyCover	APD	5.62
AMNH82135	*Kobus megaceros*	HeavyCover	APD	6.95
AMNH82136	*Kobus megaceros*	HeavyCover	APD	6.49
AMNH82137	*Kobus megaceros*	HeavyCover	APD	5.37
AMNH35323	*Kobus vardonii*	HeavyCover	APD	11.06
AMNH70057	*Kobus vardonii*	HeavyCover	APD	6.46
AMNH81687	*Kobus vardonii*	HeavyCover	APD	9.23
AMNH81170	*Litocranius walleri*	LightCover	APD	5.51
NMNH164031	*Litocranius walleri*	LightCover	APD	NA
NMNH164033	*Litocranius walleri*	LightCover	APD	4.97
NMNH259457	*Litocranius walleri*	LightCover	APD	3.6
AMNH187824	*Madoqua kirkii*	HeavyCover	APD	2.21
AMNH82076	*Madoqua kirkii*	HeavyCover	APD	2.49
NMNH538104	*Madoqua kirkii*	HeavyCover	APD	2.33
NMNH538106	*Madoqua kirkii*	HeavyCover	APD	2.6
NMNH541419	*Madoqua kirkii*	HeavyCover	APD	2.51
AMNH82051	*Nanger granti*	Open	APD	5.58
AMNH82056	*Nanger granti*	Open	APD	5.59
AMNH82057	*Nanger granti*	Open	APD	5.49
AMNH85152	*Nanger granti*	Open	APD	4.69
AMNH80111	*Nanger soemmerringii*	Open	APD	5.17
NMNH582229	*Nanger soemmerringii*	Open	APD	3.94
AMNH53180	*Neotragus batesi*	Forest	APD	2.12
AMNH53181	*Neotragus batesi*	Forest	APD	1.77
AMNH53946	*Neotragus batesi*	Forest	APD	2.26
AMNH88426	*Neotragus moschatus*	Forest	APD	2.44
AMNH88427	*Neotragus moschatus*	Forest	APD	1.88
NMNH367449	*Neotragus moschatus*	Forest	APD	2.61
AMNH233033	*Oryx gazella*	Open	APD	19.19
AMNH82043	*Oryx gazella*	Open	APD	7.71

AMNH82044	*Oryx gazella*	Open	APD	7.31
AMNH87211	*Oryx gazella*	Open	APD	8.77
AMNH216387	*Ourebia ourebi*	LightCover	APD	8.32
AMNH53304	*Ourebia ourebi*	LightCover	APD	3.15
AMNH53328	*Ourebia ourebi*	LightCover	APD	3.31
AMNH269894	*Philantomba monticola*	Forest	APD	2.36
AMNH52726	*Philantomba monticola*	Forest	APD	2.13
AMNH52753	*Philantomba monticola*	Forest	APD	2.34
AMNH52758	*Philantomba monticola*	Forest	APD	4.12
AMNH216389	*Raphicerus campestris*	LightCover	APD	3.87
AMNH233047	*Raphicerus campestris*	LightCover	APD	4
AMNH34728	*Raphicerus campestris*	LightCover	APD	3.12
AMNH80538	*Raphicerus campestris*	LightCover	APD	4.34
AMNH35493	*Redunca arundinum*	LightCover	APD	5.81
AMNH80506	*Redunca arundinum*	LightCover	APD	5.19
NMNH367428	*Redunca arundinum*	LightCover	APD	5.59
NMNH367452	*Redunca arundinum*	LightCover	APD	16.75
NMNH469909	*Redunca arundinum*	LightCover	APD	3.92
AMNH27803	*Redunca fulvorufula*	LightCover	APD	4.68
AMNH82063	*Redunca fulvorufula*	LightCover	APD	3.7
AMNH82066	*Redunca fulvorufula*	LightCover	APD	3.96
AMNH82067	*Redunca fulvorufula*	LightCover	APD	3.99
AMNH53294	*Redunca redunca*	LightCover	APD	4.46
AMNH53296	*Redunca redunca*	LightCover	APD	5.39
AMNH90234	*Rupicapra rupicapra*	NA	APD	4.92
AMNH90235	*Rupicapra rupicapra*	NA	APD	5.14
AMNH90236	*Rupicapra rupicapra*	NA	APD	4.83
AMNH17276	*Sigmoceros lichtensteinii*	Open	APD	7.22
AMNH216382	*Sigmoceros lichtensteinii*	Open	APD	6.9
AMNH216383	*Sigmoceros lichtensteinii*	Open	APD	7.75
AMNH53088	*Sylvicapra grimmia*	LightCover	APD	3.67
AMNH53092	*Sylvicapra grimmia*	LightCover	APD	2.93
AMNH80562	*Sylvicapra grimmia*	LightCover	APD	3.65
AMNH80563	*Sylvicapra grimmia*	LightCover	APD	3.48
AMNH53583	*Syncerus caffer*	LightCover	APD	30.17
AMNH82005	*Syncerus caffer*	LightCover	APD	30.16
AMNH82006	*Syncerus caffer*	LightCover	APD	32.66
AMNH82009	*Syncerus caffer*	LightCover	APD	15.01

AMNH53519	*Taurotragus derbianus*	HeavyCover	APD	NA
AMNH53521	*Taurotragus derbianus*	HeavyCover	APD	NA
AMNH53522	*Taurotragus derbianus*	HeavyCover	APD	NA
AMNH53523	*Taurotragus derbianus*	HeavyCover	APD	NA
AMNH27811	*Taurotragus oryx*	LightCover	APD	NA
AMNH34722	*Taurotragus oryx*	LightCover	APD	NA
AMNH54386	*Tragelaphus angasii*	HeavyCover	APD	8.41
AMNH54387	*Tragelaphus angasii*	HeavyCover	APD	7.84
AMNH54390	*Tragelaphus angasii*	HeavyCover	APD	7.12
AMNH81002	*Tragelaphus buxtoni*	Forest	APD	NA
AMNH81003	*Tragelaphus buxtoni*	Forest	APD	NA
AMNH81004	*Tragelaphus buxtoni*	Forest	APD	NA
AMNH81014	*Tragelaphus buxtoni*	Forest	APD	8.03
AMNH81033	*Tragelaphus buxtoni*	Forest	APD	26.04
AMNH53271	*Tragelaphus eurycerus*	Forest	APD	NA
AMNH53279	*Tragelaphus eurycerus*	Forest	APD	NA
AMNH53280	*Tragelaphus eurycerus*	Forest	APD	NA
AMNH36416	*Tragelaphus imberbis*	HeavyCover	APD	7.67
AMNH36417	*Tragelaphus imberbis*	HeavyCover	APD	6.17
AMNH82019	*Tragelaphus imberbis*	HeavyCover	APD	8.44
AMNH82023	*Tragelaphus imberbis*	HeavyCover	APD	6.3
AMNH187806	*Tragelaphus scriptus*	Forest	APD	4.37
AMNH216371	*Tragelaphus scriptus*	Forest	APD	4.84
AMNH88425	*Tragelaphus scriptus*	Forest	APD	5.12
AMNH53209	*Tragelaphus spekii*	HeavyCover	APD	7.15
AMNH53212	*Tragelaphus spekii*	HeavyCover	APD	5.24
AMNH53213	*Tragelaphus spekii*	HeavyCover	APD	5.61
AMNH53216	*Tragelaphus spekii*	HeavyCover	APD	7.18
AMNH233027	*Tragelaphus strepsiceros*	HeavyCover	APD	NA
AMNH70328	*Tragelaphus strepsiceros*	HeavyCover	APD	NA
AMNH70328a	*Tragelaphus strepsiceros*	HeavyCover	APD	22.27
AMNH113810	*Addax nasomaculatus*	Open	B	18.51
AMNH113811	*Addax nasomaculatus*	Open	B	16.48
AMNH113812	*Addax nasomaculatus*	Open	B	18.75
AMNH113813	*Addax nasomaculatus*	Open	B	15.06
AMNH81690	*Aepyceros melampus*	LightCover	B	15.16
AMNH82050	*Aepyceros melampus*	LightCover	B	14
AMNH83534	*Aepyceros melampus*	LightCover	B	17.22

AMNH85150	*Aepyceros melampus*	LightCover	B	15.27
AMNH233038	*Alcelaphus buselaphus*	Open	B	18.47
AMNH34717	*Alcelaphus buselaphus*	Open	B	15.47
AMNH34725	*Alcelaphus buselaphus*	Open	B	18.48
AMNH82033	*Alcelaphus buselaphus*	Open	B	15.97
AMNH82159	*Alcelaphus buselaphus*	Open	B	18.13
AMNH16048	*Ammotragus lervia*	NA	B	15.54
AMNH81740	*Antidorcas marsupialis*	Open	B	11.78
AMNH81745	*Antidorcas marsupialis*	Open	B	12.78
AMNH83549	*Antidorcas marsupialis*	Open	B	11.94
AMNH83550	*Antidorcas marsupialis*	Open	B	11.86
AMNH35527	*Antilope cervicapra*	Open	B	13.03
AMNH35957	*Antilope cervicapra*	Open	B	13.31
AMNH54486	*Antilope cervicapra*	Open	B	14.52
AMNH88406	*Beatragus hunteri*	Open	B	15.07
AMNH88407	*Beatragus hunteri*	Open	B	15.62
AMNH88408	*Beatragus hunteri*	Open	B	15.76
AMNH54765	*Bubalus bubalis*	NA	B	23
AMNH54766	*Bubalus bubalis*	NA	B	21.5
AMNH52875	*Cephalophus dorsalis*	Forest	B	11.17
AMNH52876	*Cephalophus dorsalis*	Forest	B	10.73
AMNH52884	*Cephalophus dorsalis*	Forest	B	6.11
AMNH52888	*Cephalophus dorsalis*	Forest	B	5.92
AMNH52775	*Cephalophus leucogaster*	Forest	B	12.31
AMNH52778	*Cephalophus leucogaster*	Forest	B	11.88
AMNH52788	*Cephalophus leucogaster*	Forest	B	11.47
AMNH216375	*Cephalophus natalensis*	Forest	B	12.16
AMNH54391	*Cephalophus natalensis*	Forest	B	9.91
AMNH81686	*Cephalophus natalensis*	Forest	B	10.03
AMNH83387	*Cephalophus natalensis*	Forest	B	11.84
AMNH52930	*Cephalophus nigrifrons*	Forest	B	5.36
AMNH52931	*Cephalophus nigrifrons*	Forest	B	11.3
AMNH52940	*Cephalophus nigrifrons*	Forest	B	5.29
AMNH52943	*Cephalophus nigrifrons*	Forest	B	5.77
AMNH53138	*Cephalophus silvicultor*	Forest	B	16.2
AMNH53144	*Cephalophus silvicultor*	Forest	B	18.98
AMNH53153	*Cephalophus silvicultor*	Forest	B	16.38
AMNH52992	*Cephalophus weynsi*	Forest	B	12.51

AMNH52995	*Cephalophus weynsi*	Forest	B	12.18
AMNH52999	*Cephalophus weynsi*	Forest	B	13.88
AMNH88429	*Cephalophus weynsi*	Forest	B	11.89
AMNH81716	*Connochaetes gnou*	Open	B	18.8
AMNH81720	*Connochaetes gnou*	Open	B	18.74
AMNH81722	*Connochaetes gnou*	Open	B	19.05
AMNH27824	*Connochaetes taurinus*	Open	B	22.12
AMNH54133	*Connochaetes taurinus*	Open	B	22.41
AMNH83502	*Connochaetes taurinus*	Open	B	20.55
AMNH83503	*Connochaetes taurinus*	Open	B	18.92
AMNH113781	*Damaliscus lunatus*	Open	B	19.18
AMNH34729	*Damaliscus lunatus*	Open	B	19.21
AMNH34730	*Damaliscus lunatus*	Open	B	20.27
AMNH82035	*Damaliscus lunatus*	Open	B	18.77
AMNH42953	*Damaliscus pygargus*	Open	B	14.8
AMNH81727	*Damaliscus pygargus*	Open	B	15.06
AMNH81729	*Damaliscus pygargus*	Open	B	14.81
AMNH81787	*Damaliscus pygargus*	Open	B	14.49
AMNH81997	*Eudorcas thomsonii*	Open	B	10.77
AMNH82059	*Eudorcas thomsonii*	Open	B	10.21
AMNH82060	*Eudorcas thomsonii*	Open	B	9.76
AMNH88415	*Eudorcas thomsonii*	Open	B	10.59
AMNH54506	*Gazella gazella*	Open	B	10.38
AMNH54997	*Gazella gazella*	Open	B	10.46
AMNH54998	*Gazella gazella*	Open	B	9.91
AMNH80143	*Hippotragus equinus*	Open	B	20.73
AMNH87217	*Hippotragus equinus*	Open	B	25.41
AMNH216381	*Hippotragus niger*	LightCover	B	23.1
AMNH80458	*Hippotragus niger*	LightCover	B	25.16
AMNH80461	*Hippotragus niger*	LightCover	B	24.18
AMNH83476	*Hippotragus niger*	LightCover	B	23.1
AMNH53492	*Kobus ellipsiprymnus*	HeavyCover	B	23.01
NMNH173877	*Kobus ellipsiprymnus*	HeavyCover	B	23.38
NMNH21898	*Kobus ellipsiprymnus*	HeavyCover	B	25.83
AMNH36396	*Kobus kob*	LightCover	B	18.69
AMNH36397	*Kobus kob*	LightCover	B	19.22
AMNH82129	*Kobus kob*	LightCover	B	18.56
AMNH82130	*Kobus kob*	LightCover	B	20.62

AMNH82173	*Kobus kob*	LightCover	B	17.62
AMNH70010	*Kobus leche*	HeavyCover	B	11
AMNH99649	*Kobus leche*	HeavyCover	B	21.09
NMNH254927	*Kobus leche*	HeavyCover	B	19.91
AMNH113784	*Kobus megaceros*	HeavyCover	B	19.13
AMNH82135	*Kobus megaceros*	HeavyCover	B	17.75
AMNH82136	*Kobus megaceros*	HeavyCover	B	19.31
AMNH82137	*Kobus megaceros*	HeavyCover	B	17.21
AMNH35323	*Kobus vardonii*	HeavyCover	B	21.53
AMNH70057	*Kobus vardonii*	HeavyCover	B	21.66
AMNH81687	*Kobus vardonii*	HeavyCover	B	16.68
AMNH81170	*Litocranius walleri*	LightCover	B	14.24
NMNH164031	*Litocranius walleri*	LightCover	B	14.24
NMNH164033	*Litocranius walleri*	LightCover	B	13.56
NMNH259457	*Litocranius walleri*	LightCover	B	13.79
AMNH187824	*Madoqua kirkii*	HeavyCover	B	7.73
AMNH82076	*Madoqua kirkii*	HeavyCover	B	8.27
NMNH538104	*Madoqua kirkii*	HeavyCover	B	7.59
NMNH538106	*Madoqua kirkii*	HeavyCover	B	7.93
NMNH541419	*Madoqua kirkii*	HeavyCover	B	7.85
AMNH82051	*Nanger granti*	Open	B	14.81
AMNH82056	*Nanger granti*	Open	B	14.06
AMNH82057	*Nanger granti*	Open	B	13.73
AMNH85152	*Nanger granti*	Open	B	14.25
AMNH80111	*Nanger soemmerringii*	Open	B	12.47
NMNH582229	*Nanger soemmerringii*	Open	B	14.08
AMNH53180	*Neotragus batesi*	Forest	B	7.28
AMNH53181	*Neotragus batesi*	Forest	B	6.42
AMNH53946	*Neotragus batesi*	Forest	B	6.77
AMNH88426	*Neotragus moschatus*	Forest	B	6.6
AMNH88427	*Neotragus moschatus*	Forest	B	7.09
NMNH367449	*Neotragus moschatus*	Forest	B	8.16
AMNH233033	*Oryx gazella*	Open	B	13.38
AMNH82043	*Oryx gazella*	Open	B	22.64
AMNH82044	*Oryx gazella*	Open	B	20.53
AMNH87211	*Oryx gazella*	Open	B	19.6
AMNH216387	*Ourebia ourebi*	LightCover	B	11.61
AMNH53304	*Ourebia ourebi*	LightCover	B	10.91

AMNH53328	*Ourebia ourebi*	LightCover	B	10.57
AMNH269894	*Philantomba monticola*	Forest	B	7.69
AMNH52726	*Philantomba monticola*	Forest	B	8.26
AMNH52753	*Philantomba monticola*	Forest	B	7.07
AMNH52758	*Philantomba monticola*	Forest	B	7.42
AMNH216389	*Raphicerus campestris*	LightCover	B	11.09
AMNH233047	*Raphicerus campestris*	LightCover	B	10.25
AMNH34728	*Raphicerus campestris*	LightCover	B	10.03
AMNH80538	*Raphicerus campestris*	LightCover	B	10.58
AMNH35493	*Redunca arundinum*	LightCover	B	15.65
AMNH80506	*Redunca arundinum*	LightCover	B	15.34
NMNH367428	*Redunca arundinum*	LightCover	B	17.05
NMNH367452	*Redunca arundinum*	LightCover	B	9.91
NMNH469909	*Redunca arundinum*	LightCover	B	12.96
AMNH27803	*Redunca fulvorufula*	LightCover	B	15.01
AMNH82063	*Redunca fulvorufula*	LightCover	B	14.24
AMNH82066	*Redunca fulvorufula*	LightCover	B	12.86
AMNH82067	*Redunca fulvorufula*	LightCover	B	13.55
AMNH53294	*Redunca redunca*	LightCover	B	15.79
AMNH53296	*Redunca redunca*	LightCover	B	16.91
AMNH90234	*Rupicapra rupicapra*	NA	B	14.57
AMNH90235	*Rupicapra rupicapra*	NA	B	12.41
AMNH90236	*Rupicapra rupicapra*	NA	B	14.8
AMNH17276	*Sigmoceros lichtensteinii*	Open	B	18.44
AMNH216382	*Sigmoceros lichtensteinii*	Open	B	20.31
AMNH216383	*Sigmoceros lichtensteinii*	Open	B	19.4
AMNH53088	*Sylvicapra grimmia*	LightCover	B	9.84
AMNH53092	*Sylvicapra grimmia*	LightCover	B	10.65
AMNH80562	*Sylvicapra grimmia*	LightCover	B	11.18
AMNH80563	*Sylvicapra grimmia*	LightCover	B	11.06
AMNH53583	*Syncerus caffer*	LightCover	B	14
AMNH82005	*Syncerus caffer*	LightCover	B	20.86
AMNH82006	*Syncerus caffer*	LightCover	B	20.82
AMNH82009	*Syncerus caffer*	LightCover	B	33.43
AMNH53519	*Taurotragus derbianus*	HeavyCover	B	29.69
AMNH53521	*Taurotragus derbianus*	HeavyCover	B	31.78
AMNH53522	*Taurotragus derbianus*	HeavyCover	B	30.47
AMNH53523	*Taurotragus derbianus*	HeavyCover	B	31.84

AMNH27811	*Taurotragus oryx*	LightCover	B	30.61
AMNH34722	*Taurotragus oryx*	LightCover	B	28.45
AMNH54386	*Tragelaphus angasii*	HeavyCover	B	18.57
AMNH54387	*Tragelaphus angasii*	HeavyCover	B	17.91
AMNH54390	*Tragelaphus angasii*	HeavyCover	B	17.82
AMNH81002	*Tragelaphus buxtoni*	Forest	B	26.11
AMNH81003	*Tragelaphus buxtoni*	Forest	B	25.89
AMNH81004	*Tragelaphus buxtoni*	Forest	B	26.18
AMNH81014	*Tragelaphus buxtoni*	Forest	B	25.21
AMNH81033	*Tragelaphus buxtoni*	Forest	B	11.33
AMNH53271	*Tragelaphus eurycerus*	Forest	B	26.84
AMNH53279	*Tragelaphus eurycerus*	Forest	B	26.44
AMNH53280	*Tragelaphus eurycerus*	Forest	B	28.1
AMNH36416	*Tragelaphus imberbis*	HeavyCover	B	19.83
AMNH36417	*Tragelaphus imberbis*	HeavyCover	B	18.29
AMNH82019	*Tragelaphus imberbis*	HeavyCover	B	20.89
AMNH82023	*Tragelaphus imberbis*	HeavyCover	B	19.45
AMNH187806	*Tragelaphus scriptus*	Forest	B	13.97
AMNH216371	*Tragelaphus scriptus*	Forest	B	15.66
AMNH88425	*Tragelaphus scriptus*	Forest	B	15.67
AMNH53209	*Tragelaphus spekii*	HeavyCover	B	22.77
AMNH53212	*Tragelaphus spekii*	HeavyCover	B	21.58
AMNH53213	*Tragelaphus spekii*	HeavyCover	B	16.59
AMNH53216	*Tragelaphus spekii*	HeavyCover	B	17.61
AMNH233027	*Tragelaphus strepsiceros*	HeavyCover	B	24.51
AMNH70328	*Tragelaphus strepsiceros*	HeavyCover	B	23.37
AMNH70328a	*Tragelaphus strepsiceros*	HeavyCover	B	12.21
AMNH113810	*Addax nasomaculatus*	Open	DistRad	11.04
AMNH113811	*Addax nasomaculatus*	Open	DistRad	11.19
AMNH113812	*Addax nasomaculatus*	Open	DistRad	11.38
AMNH113813	*Addax nasomaculatus*	Open	DistRad	11
AMNH81690	*Aepyceros melampus*	LightCover	DistRad	9.22
AMNH82050	*Aepyceros melampus*	LightCover	DistRad	8.73
AMNH83534	*Aepyceros melampus*	LightCover	DistRad	9.19
AMNH85150	*Aepyceros melampus*	LightCover	DistRad	8.85
AMNH233038	*Alcelaphus buselaphus*	Open	DistRad	11.33
AMNH34717	*Alcelaphus buselaphus*	Open	DistRad	9.79
AMNH34725	*Alcelaphus buselaphus*	Open	DistRad	13.53

AMNH82033	*Alcelaphus buselaphus*	Open	DistRad	12.12
AMNH82159	*Alcelaphus buselaphus*	Open	DistRad	13.13
AMNH16048	*Ammotragus lervia*	NA	DistRad	9.8
AMNH81740	*Antidorcas marsupialis*	Open	DistRad	7.72
AMNH81745	*Antidorcas marsupialis*	Open	DistRad	7.61
AMNH83549	*Antidorcas marsupialis*	Open	DistRad	7.32
AMNH83550	*Antidorcas marsupialis*	Open	DistRad	7.42
AMNH35527	*Antilope cervicapra*	Open	DistRad	8.37
AMNH35957	*Antilope cervicapra*	Open	DistRad	7.83
AMNH54486	*Antilope cervicapra*	Open	DistRad	7.8
AMNH88406	*Beatragus hunteri*	Open	DistRad	11.5
AMNH88407	*Beatragus hunteri*	Open	DistRad	11
AMNH88408	*Beatragus hunteri*	Open	DistRad	11.1
AMNH54765	*Bubalus bubalis*	NA	DistRad	6.06
AMNH54766	*Bubalus bubalis*	NA	DistRad	5.25
AMNH52875	*Cephalophus dorsalis*	Forest	DistRad	5.36
AMNH52876	*Cephalophus dorsalis*	Forest	DistRad	6
AMNH52884	*Cephalophus dorsalis*	Forest	DistRad	2.01
AMNH52888	*Cephalophus dorsalis*	Forest	DistRad	1.61
AMNH52775	*Cephalophus leucogaster*	Forest	DistRad	5.71
AMNH52778	*Cephalophus leucogaster*	Forest	DistRad	5.71
AMNH52788	*Cephalophus leucogaster*	Forest	DistRad	5.7
AMNH216375	*Cephalophus natalensis*	Forest	DistRad	5.84
AMNH54391	*Cephalophus natalensis*	Forest	DistRad	5.58
AMNH81686	*Cephalophus natalensis*	Forest	DistRad	5.28
AMNH83387	*Cephalophus natalensis*	Forest	DistRad	5.67
AMNH52930	*Cephalophus nigrifrons*	Forest	DistRad	1.32
AMNH52931	*Cephalophus nigrifrons*	Forest	DistRad	5.7
AMNH52940	*Cephalophus nigrifrons*	Forest	DistRad	1.24
AMNH52943	*Cephalophus nigrifrons*	Forest	DistRad	1.42
AMNH53138	*Cephalophus silvicultor*	Forest	DistRad	9.13
AMNH53144	*Cephalophus silvicultor*	Forest	DistRad	9.5
AMNH53153	*Cephalophus silvicultor*	Forest	DistRad	8
AMNH52992	*Cephalophus weynsi*	Forest	DistRad	5.72
AMNH52995	*Cephalophus weynsi*	Forest	DistRad	5.87
AMNH52999	*Cephalophus weynsi*	Forest	DistRad	6
AMNH88429	*Cephalophus weynsi*	Forest	DistRad	5.56
AMNH81716	*Connochaetes gnou*	Open	DistRad	11.78

AMNH81720	*Connochaetes gnou*	Open	DistRad	12.5
AMNH81722	*Connochaetes gnou*	Open	DistRad	13
AMNH27824	*Connochaetes taurinus*	Open	DistRad	13.65
AMNH54133	*Connochaetes taurinus*	Open	DistRad	14.74
AMNH83502	*Connochaetes taurinus*	Open	DistRad	14
AMNH83503	*Connochaetes taurinus*	Open	DistRad	14.5
AMNH113781	*Damaliscus lunatus*	Open	DistRad	12.19
AMNH34729	*Damaliscus lunatus*	Open	DistRad	12.5
AMNH34730	*Damaliscus lunatus*	Open	DistRad	12.78
AMNH82035	*Damaliscus lunatus*	Open	DistRad	12
AMNH42953	*Damaliscus pygargus*	Open	DistRad	9.5
AMNH81727	*Damaliscus pygargus*	Open	DistRad	10.5
AMNH81729	*Damaliscus pygargus*	Open	DistRad	9.6
AMNH81787	*Damaliscus pygargus*	Open	DistRad	10.14
AMNH81997	*Eudorcas thomsonii*	Open	DistRad	6.5
AMNH82059	*Eudorcas thomsonii*	Open	DistRad	6.21
AMNH82060	*Eudorcas thomsonii*	Open	DistRad	6.25
AMNH88415	*Eudorcas thomsonii*	Open	DistRad	6.09
AMNH54506	*Gazella gazella*	Open	DistRad	5.77
AMNH54997	*Gazella gazella*	Open	DistRad	6.27
AMNH54998	*Gazella gazella*	Open	DistRad	5.88
AMNH80143	*Hippotragus equinus*	Open	DistRad	14.5
AMNH87217	*Hippotragus equinus*	Open	DistRad	17.3
AMNH216381	*Hippotragus niger*	LightCover	DistRad	14.27
AMNH80458	*Hippotragus niger*	LightCover	DistRad	15.28
AMNH80461	*Hippotragus niger*	LightCover	DistRad	14.5
AMNH83476	*Hippotragus niger*	LightCover	DistRad	13.73
AMNH53492	*Kobus ellipsiprymnus*	HeavyCover	DistRad	14.32
NMNH173877	*Kobus ellipsiprymnus*	HeavyCover	DistRad	12.82
NMNH21898	*Kobus ellipsiprymnus*	HeavyCover	DistRad	13.11
AMNH36396	*Kobus kob*	LightCover	DistRad	10.61
AMNH36397	*Kobus kob*	LightCover	DistRad	9.68
AMNH82129	*Kobus kob*	LightCover	DistRad	10.19
AMNH82130	*Kobus kob*	LightCover	DistRad	10
AMNH82173	*Kobus kob*	LightCover	DistRad	9.26
AMNH70010	*Kobus leche*	HeavyCover	DistRad	1.41
AMNH99649	*Kobus leche*	HeavyCover	DistRad	10.68
NMNH254927	*Kobus leche*	HeavyCover	DistRad	10.14

AMNH113784	*Kobus megaceros*	HeavyCover	DistRad	10.16
AMNH82135	*Kobus megaceros*	HeavyCover	DistRad	10.66
AMNH82136	*Kobus megaceros*	HeavyCover	DistRad	10
AMNH82137	*Kobus megaceros*	HeavyCover	DistRad	9.72
AMNH35323	*Kobus vardonii*	HeavyCover	DistRad	10.71
AMNH70057	*Kobus vardonii*	HeavyCover	DistRad	10.5
AMNH81687	*Kobus vardonii*	HeavyCover	DistRad	9.18
AMNH81170	*Litocranius walleri*	LightCover	DistRad	9
NMNH164031	*Litocranius walleri*	LightCover	DistRad	7.23
NMNH164033	*Litocranius walleri*	LightCover	DistRad	7.84
NMNH259457	*Litocranius walleri*	LightCover	DistRad	8.6
AMNH187824	*Madoqua kirkii*	HeavyCover	DistRad	3.5
AMNH82076	*Madoqua kirkii*	HeavyCover	DistRad	4.08
NMNH538104	*Madoqua kirkii*	HeavyCover	DistRad	4.04
NMNH538106	*Madoqua kirkii*	HeavyCover	DistRad	4.2
NMNH541419	*Madoqua kirkii*	HeavyCover	DistRad	4.17
AMNH82051	*Nanger granti*	Open	DistRad	9
AMNH82056	*Nanger granti*	Open	DistRad	9
AMNH82057	*Nanger granti*	Open	DistRad	9
AMNH85152	*Nanger granti*	Open	DistRad	8.32
AMNH80111	*Nanger soemmerringii*	Open	DistRad	7.27
NMNH582229	*Nanger soemmerringii*	Open	DistRad	8.2
AMNH53180	*Neotragus batesi*	Forest	DistRad	3.15
AMNH53181	*Neotragus batesi*	Forest	DistRad	3.1
AMNH53946	*Neotragus batesi*	Forest	DistRad	2.9
AMNH88426	*Neotragus moschatus*	Forest	DistRad	3.25
AMNH88427	*Neotragus moschatus*	Forest	DistRad	3.27
NMNH367449	*Neotragus moschatus*	Forest	DistRad	3.85
AMNH233033	*Oryx gazella*	Open	DistRad	2.4
AMNH82043	*Oryx gazella*	Open	DistRad	13.5
AMNH82044	*Oryx gazella*	Open	DistRad	12.24
AMNH87211	*Oryx gazella*	Open	DistRad	13.76
AMNH216387	*Ourebia ourebi*	LightCover	DistRad	5.78
AMNH53304	*Ourebia ourebi*	LightCover	DistRad	5.71
AMNH53328	*Ourebia ourebi*	LightCover	DistRad	5.66
AMNH269894	*Philantomba monticola*	Forest	DistRad	3.35
AMNH52726	*Philantomba monticola*	Forest	DistRad	3.23
AMNH52753	*Philantomba monticola*	Forest	DistRad	3.63

AMNH52758	*Philantomba monticola*	Forest	DistRad	3.72
AMNH216389	*Raphicerus campestris*	LightCover	DistRad	5.36
AMNH233047	*Raphicerus campestris*	LightCover	DistRad	4.84
AMNH34728	*Raphicerus campestris*	LightCover	DistRad	4.63
AMNH80538	*Raphicerus campestris*	LightCover	DistRad	5
AMNH35493	*Redunca arundinum*	LightCover	DistRad	9.77
AMNH80506	*Redunca arundinum*	LightCover	DistRad	9.32
NMNH367428	*Redunca arundinum*	LightCover	DistRad	9.32
NMNH367452	*Redunca arundinum*	LightCover	DistRad	1.47
NMNH469909	*Redunca arundinum*	LightCover	DistRad	7.39
AMNH27803	*Redunca fulvorufula*	LightCover	DistRad	7.5
AMNH82063	*Redunca fulvorufula*	LightCover	DistRad	7.13
AMNH82066	*Redunca fulvorufula*	LightCover	DistRad	7.5
AMNH82067	*Redunca fulvorufula*	LightCover	DistRad	7.12
AMNH53294	*Redunca redunca*	LightCover	DistRad	8.73
AMNH53296	*Redunca redunca*	LightCover	DistRad	8.78
AMNH90234	*Rupicapra rupicapra*	NA	DistRad	7.61
AMNH90235	*Rupicapra rupicapra*	NA	DistRad	8.18
AMNH90236	*Rupicapra rupicapra*	NA	DistRad	7.42
AMNH17276	*Sigmoceros lichtensteinii*	Open	DistRad	13.31
AMNH216382	*Sigmoceros lichtensteinii*	Open	DistRad	13.5
AMNH216383	*Sigmoceros lichtensteinii*	Open	DistRad	13.75
AMNH53088	*Sylvicapra grimmia*	LightCover	DistRad	5.5
AMNH53092	*Sylvicapra grimmia*	LightCover	DistRad	5.2
AMNH80562	*Sylvicapra grimmia*	LightCover	DistRad	5.62
AMNH80563	*Sylvicapra grimmia*	LightCover	DistRad	5.5
AMNH53583	*Syncerus caffer*	LightCover	DistRad	3.83
AMNH82005	*Syncerus caffer*	LightCover	DistRad	4.48
AMNH82006	*Syncerus caffer*	LightCover	DistRad	5.51
AMNH82009	*Syncerus caffer*	LightCover	DistRad	18.5
AMNH53519	*Taurotragus derbianus*	HeavyCover	DistRad	19.25
AMNH53521	*Taurotragus derbianus*	HeavyCover	DistRad	17.65
AMNH53522	*Taurotragus derbianus*	HeavyCover	DistRad	18.13
AMNH53523	*Taurotragus derbianus*	HeavyCover	DistRad	19
AMNH27811	*Taurotragus oryx*	LightCover	DistRad	20
AMNH34722	*Taurotragus oryx*	LightCover	DistRad	17.38
AMNH54386	*Tragelaphus angasii*	HeavyCover	DistRad	8.87
AMNH54387	*Tragelaphus angasii*	HeavyCover	DistRad	10.22

AMNH54390	*Tragelaphus angasii*	HeavyCover	DistRad	9.38
AMNH81002	*Tragelaphus buxtoni*	Forest	DistRad	13.28
AMNH81003	*Tragelaphus buxtoni*	Forest	DistRad	11.5
AMNH81004	*Tragelaphus buxtoni*	Forest	DistRad	13.5
AMNH81014	*Tragelaphus buxtoni*	Forest	DistRad	11.79
AMNH81033	*Tragelaphus buxtoni*	Forest	DistRad	2.68
AMNH53271	*Tragelaphus eurycerus*	Forest	DistRad	13.5
AMNH53279	*Tragelaphus eurycerus*	Forest	DistRad	13.23
AMNH53280	*Tragelaphus eurycerus*	Forest	DistRad	14.68
AMNH36416	*Tragelaphus imberbis*	HeavyCover	DistRad	10.2
AMNH36417	*Tragelaphus imberbis*	HeavyCover	DistRad	9.57
AMNH82019	*Tragelaphus imberbis*	HeavyCover	DistRad	11.13
AMNH82023	*Tragelaphus imberbis*	HeavyCover	DistRad	8.79
AMNH187806	*Tragelaphus scriptus*	Forest	DistRad	6.86
AMNH216371	*Tragelaphus scriptus*	Forest	DistRad	7
AMNH88425	*Tragelaphus scriptus*	Forest	DistRad	8.07
AMNH53209	*Tragelaphus spekii*	HeavyCover	DistRad	11
AMNH53212	*Tragelaphus spekii*	HeavyCover	DistRad	9.73
AMNH53213	*Tragelaphus spekii*	HeavyCover	DistRad	8.35
AMNH53216	*Tragelaphus spekii*	HeavyCover	DistRad	8.86
AMNH233027	*Tragelaphus strepsiceros*	HeavyCover	DistRad	13.38
AMNH70328	*Tragelaphus strepsiceros*	HeavyCover	DistRad	12.5
AMNH70328a	*Tragelaphus strepsiceros*	HeavyCover	DistRad	2.64
AMNH113810	*Addax nasomaculatus*	Open	DMTD	1.75
AMNH113811	*Addax nasomaculatus*	Open	DMTD	2.45
AMNH113812	*Addax nasomaculatus*	Open	DMTD	2.36
AMNH113813	*Addax nasomaculatus*	Open	DMTD	2.14
AMNH81690	*Aepyceros melampus*	LightCover	DMTD	1.78
AMNH82050	*Aepyceros melampus*	LightCover	DMTD	1.64
AMNH83534	*Aepyceros melampus*	LightCover	DMTD	1.7
AMNH85150	*Aepyceros melampus*	LightCover	DMTD	1.72
AMNH233038	*Alcelaphus buselaphus*	Open	DMTD	2.26
AMNH34717	*Alcelaphus buselaphus*	Open	DMTD	1.78
AMNH34725	*Alcelaphus buselaphus*	Open	DMTD	3.03
AMNH82033	*Alcelaphus buselaphus*	Open	DMTD	3.07
AMNH82159	*Alcelaphus buselaphus*	Open	DMTD	2.76
AMNH16048	*Ammotragus lervia*	NA	DMTD	1.84
AMNH81740	*Antidorcas marsupialis*	Open	DMTD	1.29

AMNH81745	*Antidorcas marsupialis*	Open	DMTD	1.81
AMNH83549	*Antidorcas marsupialis*	Open	DMTD	1.65
AMNH83550	*Antidorcas marsupialis*	Open	DMTD	1.28
AMNH35527	*Antilope cervicapra*	Open	DMTD	1.5
AMNH35957	*Antilope cervicapra*	Open	DMTD	1.6
AMNH54486	*Antilope cervicapra*	Open	DMTD	1.68
AMNH88406	*Beatragus hunteri*	Open	DMTD	2.13
AMNH88407	*Beatragus hunteri*	Open	DMTD	2.23
AMNH88408	*Beatragus hunteri*	Open	DMTD	2.13
AMNH54765	*Bubalus bubalis*	NA	DMTD	NA
AMNH54766	*Bubalus bubalis*	NA	DMTD	NA
AMNH52875	*Cephalophus dorsalis*	Forest	DMTD	1.2
AMNH52876	*Cephalophus dorsalis*	Forest	DMTD	2.08
AMNH52884	*Cephalophus dorsalis*	Forest	DMTD	NA
AMNH52888	*Cephalophus dorsalis*	Forest	DMTD	NA
AMNH52775	*Cephalophus leucogaster*	Forest	DMTD	1.23
AMNH52778	*Cephalophus leucogaster*	Forest	DMTD	1.34
AMNH52788	*Cephalophus leucogaster*	Forest	DMTD	1.56
AMNH216375	*Cephalophus natalensis*	Forest	DMTD	1.19
AMNH54391	*Cephalophus natalensis*	Forest	DMTD	0.95
AMNH81686	*Cephalophus natalensis*	Forest	DMTD	1.34
AMNH83387	*Cephalophus natalensis*	Forest	DMTD	1.36
AMNH52930	*Cephalophus nigrifrons*	Forest	DMTD	NA
AMNH52931	*Cephalophus nigrifrons*	Forest	DMTD	1.37
AMNH52940	*Cephalophus nigrifrons*	Forest	DMTD	NA
AMNH52943	*Cephalophus nigrifrons*	Forest	DMTD	NA
AMNH53138	*Cephalophus silvicultor*	Forest	DMTD	2.04
AMNH53144	*Cephalophus silvicultor*	Forest	DMTD	2.11
AMNH53153	*Cephalophus silvicultor*	Forest	DMTD	1.97
AMNH52992	*Cephalophus weynsi*	Forest	DMTD	1.75
AMNH52995	*Cephalophus weynsi*	Forest	DMTD	1.38
AMNH52999	*Cephalophus weynsi*	Forest	DMTD	1.29
AMNH88429	*Cephalophus weynsi*	Forest	DMTD	1.26
AMNH81716	*Connochaetes gnou*	Open	DMTD	2.16
AMNH81720	*Connochaetes gnou*	Open	DMTD	2.11
AMNH81722	*Connochaetes gnou*	Open	DMTD	2.52
AMNH27824	*Connochaetes taurinus*	Open	DMTD	2.86
AMNH54133	*Connochaetes taurinus*	Open	DMTD	2.27

AMNH83502	*Connochaetes taurinus*	Open	DMTD	3.08
AMNH83503	*Connochaetes taurinus*	Open	DMTD	2.6
AMNH113781	*Damaliscus lunatus*	Open	DMTD	2.39
AMNH34729	*Damaliscus lunatus*	Open	DMTD	3.7
AMNH34730	*Damaliscus lunatus*	Open	DMTD	2.46
AMNH82035	*Damaliscus lunatus*	Open	DMTD	2.52
AMNH42953	*Damaliscus pygargus*	Open	DMTD	1.81
AMNH81727	*Damaliscus pygargus*	Open	DMTD	1.97
AMNH81729	*Damaliscus pygargus*	Open	DMTD	1.86
AMNH81787	*Damaliscus pygargus*	Open	DMTD	2.34
AMNH81997	*Eudorcas thomsonii*	Open	DMTD	1.58
AMNH82059	*Eudorcas thomsonii*	Open	DMTD	1.32
AMNH82060	*Eudorcas thomsonii*	Open	DMTD	1.58
AMNH88415	*Eudorcas thomsonii*	Open	DMTD	1.57
AMNH54506	*Gazella gazella*	Open	DMTD	1.15
AMNH54997	*Gazella gazella*	Open	DMTD	1.45
AMNH54998	*Gazella gazella*	Open	DMTD	1.31
AMNH80143	*Hippotragus equinus*	Open	DMTD	3.08
AMNH87217	*Hippotragus equinus*	Open	DMTD	4.08
AMNH216381	*Hippotragus niger*	LightCover	DMTD	4.16
AMNH80458	*Hippotragus niger*	LightCover	DMTD	3.07
AMNH80461	*Hippotragus niger*	LightCover	DMTD	2.4
AMNH83476	*Hippotragus niger*	LightCover	DMTD	3.23
AMNH53492	*Kobus ellipsiprymnus*	HeavyCover	DMTD	2.12
NMNH173877	*Kobus ellipsiprymnus*	HeavyCover	DMTD	2.9
NMNH21898	*Kobus ellipsiprymnus*	HeavyCover	DMTD	3.14
AMNH36396	*Kobus kob*	LightCover	DMTD	1.68
AMNH36397	*Kobus kob*	LightCover	DMTD	2.16
AMNH82129	*Kobus kob*	LightCover	DMTD	1.26
AMNH82130	*Kobus kob*	LightCover	DMTD	2.71
AMNH82173	*Kobus kob*	LightCover	DMTD	1.7
AMNH70010	*Kobus leche*	HeavyCover	DMTD	NA
AMNH99649	*Kobus leche*	HeavyCover	DMTD	2.28
NMNH254927	*Kobus leche*	HeavyCover	DMTD	2.61
AMNH113784	*Kobus megaceros*	HeavyCover	DMTD	2.04
AMNH82135	*Kobus megaceros*	HeavyCover	DMTD	2.21
AMNH82136	*Kobus megaceros*	HeavyCover	DMTD	2.29
AMNH82137	*Kobus megaceros*	HeavyCover	DMTD	2.25

AMNH35323	*Kobus vardonii*	HeavyCover	DMTD	2.06
AMNH70057	*Kobus vardonii*	HeavyCover	DMTD	2.24
AMNH81687	*Kobus vardonii*	HeavyCover	DMTD	1.52
AMNH81170	*Litocranius walleri*	LightCover	DMTD	2.35
NMNH164031	*Litocranius walleri*	LightCover	DMTD	1.93
NMNH164033	*Litocranius walleri*	LightCover	DMTD	1.91
NMNH259457	*Litocranius walleri*	LightCover	DMTD	2.65
AMNH187824	*Madoqua kirkii*	HeavyCover	DMTD	0.85
AMNH82076	*Madoqua kirkii*	HeavyCover	DMTD	1.09
NMNH538104	*Madoqua kirkii*	HeavyCover	DMTD	1.04
NMNH538106	*Madoqua kirkii*	HeavyCover	DMTD	1.14
NMNH541419	*Madoqua kirkii*	HeavyCover	DMTD	1.11
AMNH82051	*Nanger granti*	Open	DMTD	1.52
AMNH82056	*Nanger granti*	Open	DMTD	1.6
AMNH82057	*Nanger granti*	Open	DMTD	1.85
AMNH85152	*Nanger granti*	Open	DMTD	1.45
AMNH80111	*Nanger soemmerringii*	Open	DMTD	1.55
NMNH582229	*Nanger soemmerringii*	Open	DMTD	2.14
AMNH53180	*Neotragus batesi*	Forest	DMTD	0.76
AMNH53181	*Neotragus batesi*	Forest	DMTD	0.68
AMNH53946	*Neotragus batesi*	Forest	DMTD	0.66
AMNH88426	*Neotragus moschatus*	Forest	DMTD	0.72
AMNH88427	*Neotragus moschatus*	Forest	DMTD	0.61
NMNH367449	*Neotragus moschatus*	Forest	DMTD	0.51
AMNH233033	*Oryx gazella*	Open	DMTD	NA
AMNH82043	*Oryx gazella*	Open	DMTD	3.46
AMNH82044	*Oryx gazella*	Open	DMTD	2.94
AMNH87211	*Oryx gazella*	Open	DMTD	3.73
AMNH216387	*Ourebia ourebi*	LightCover	DMTD	1.2
AMNH53304	*Ourebia ourebi*	LightCover	DMTD	1.24
AMNH53328	*Ourebia ourebi*	LightCover	DMTD	1.07
AMNH269894	*Philantomba monticola*	Forest	DMTD	0.91
AMNH52726	*Philantomba monticola*	Forest	DMTD	0.56
AMNH52753	*Philantomba monticola*	Forest	DMTD	0.91
AMNH52758	*Philantomba monticola*	Forest	DMTD	0.74
AMNH216389	*Raphicerus campestris*	LightCover	DMTD	1.41
AMNH233047	*Raphicerus campestris*	LightCover	DMTD	1.11
AMNH34728	*Raphicerus campestris*	LightCover	DMTD	1.09

AMNH80538	*Raphicerus campestris*	LightCover	DMTD	0.97
AMNH35493	*Redunca arundinum*	LightCover	DMTD	1.81
AMNH80506	*Redunca arundinum*	LightCover	DMTD	1.92
NMNH367428	*Redunca arundinum*	LightCover	DMTD	1.73
NMNH367452	*Redunca arundinum*	LightCover	DMTD	NA
NMNH469909	*Redunca arundinum*	LightCover	DMTD	1.9
AMNH27803	*Redunca fulvorufula*	LightCover	DMTD	1.42
AMNH82063	*Redunca fulvorufula*	LightCover	DMTD	1.46
AMNH82066	*Redunca fulvorufula*	LightCover	DMTD	1.62
AMNH82067	*Redunca fulvorufula*	LightCover	DMTD	1.69
AMNH53294	*Redunca redunca*	LightCover	DMTD	1.59
AMNH53296	*Redunca redunca*	LightCover	DMTD	1.58
AMNH90234	*Rupicapra rupicapra*	NA	DMTD	1.88
AMNH90235	*Rupicapra rupicapra*	NA	DMTD	1.98
AMNH90236	*Rupicapra rupicapra*	NA	DMTD	1.39
AMNH17276	*Sigmoceros lichtensteinii*	Open	DMTD	2.43
AMNH216382	*Sigmoceros lichtensteinii*	Open	DMTD	3.18
AMNH216383	*Sigmoceros lichtensteinii*	Open	DMTD	3
AMNH53088	*Sylvicapra grimmia*	LightCover	DMTD	1.01
AMNH53092	*Sylvicapra grimmia*	LightCover	DMTD	1.03
AMNH80562	*Sylvicapra grimmia*	LightCover	DMTD	1.37
AMNH80563	*Sylvicapra grimmia*	LightCover	DMTD	1.25
AMNH53583	*Syncerus caffer*	LightCover	DMTD	NA
AMNH82005	*Syncerus caffer*	LightCover	DMTD	NA
AMNH82006	*Syncerus caffer*	LightCover	DMTD	NA
AMNH82009	*Syncerus caffer*	LightCover	DMTD	2.84
AMNH53519	*Taurotragus derbianus*	HeavyCover	DMTD	3.35
AMNH53521	*Taurotragus derbianus*	HeavyCover	DMTD	3.57
AMNH53522	*Taurotragus derbianus*	HeavyCover	DMTD	3.81
AMNH53523	*Taurotragus derbianus*	HeavyCover	DMTD	4.14
AMNH27811	*Taurotragus oryx*	LightCover	DMTD	4.87
AMNH34722	*Taurotragus oryx*	LightCover	DMTD	3.77
AMNH54386	*Tragelaphus angasii*	HeavyCover	DMTD	1.34
AMNH54387	*Tragelaphus angasii*	HeavyCover	DMTD	1.85
AMNH54390	*Tragelaphus angasii*	HeavyCover	DMTD	2.09
AMNH81002	*Tragelaphus buxtoni*	Forest	DMTD	2.28
AMNH81003	*Tragelaphus buxtoni*	Forest	DMTD	1.55
AMNH81004	*Tragelaphus buxtoni*	Forest	DMTD	2.36

AMNH81014	*Tragelaphus buxtoni*	Forest	DMTD	1.66
AMNH81033	*Tragelaphus buxtoni*	Forest	DMTD	NA
AMNH53271	*Tragelaphus eurycerus*	Forest	DMTD	3.52
AMNH53279	*Tragelaphus eurycerus*	Forest	DMTD	3.63
AMNH53280	*Tragelaphus eurycerus*	Forest	DMTD	3.63
AMNH36416	*Tragelaphus imberbis*	HeavyCover	DMTD	2.53
AMNH36417	*Tragelaphus imberbis*	HeavyCover	DMTD	2.25
AMNH82019	*Tragelaphus imberbis*	HeavyCover	DMTD	2.69
AMNH82023	*Tragelaphus imberbis*	HeavyCover	DMTD	2.02
AMNH187806	*Tragelaphus scriptus*	Forest	DMTD	1.79
AMNH216371	*Tragelaphus scriptus*	Forest	DMTD	1.18
AMNH88425	*Tragelaphus scriptus*	Forest	DMTD	1.16
AMNH53209	*Tragelaphus spekii*	HeavyCover	DMTD	2.46
AMNH53212	*Tragelaphus spekii*	HeavyCover	DMTD	1.48
AMNH53213	*Tragelaphus spekii*	HeavyCover	DMTD	2.06
AMNH53216	*Tragelaphus spekii*	HeavyCover	DMTD	2.62
AMNH233027	*Tragelaphus strepsiceros*	HeavyCover	DMTD	2.51
AMNH70328	*Tragelaphus strepsiceros*	HeavyCover	DMTD	2.74
AMNH70328a	*Tragelaphus strepsiceros*	HeavyCover	DMTD	NA
AMNH113810	*Addax nasomaculatus*	Open	DTArea	843.25
AMNH113811	*Addax nasomaculatus*	Open	DTArea	765.98
AMNH113812	*Addax nasomaculatus*	Open	DTArea	856.38
AMNH113813	*Addax nasomaculatus*	Open	DTArea	685.38
AMNH81690	*Aepyceros melampus*	LightCover	DTArea	553.14
AMNH82050	*Aepyceros melampus*	LightCover	DTArea	558.17
AMNH83534	*Aepyceros melampus*	LightCover	DTArea	554
AMNH85150	*Aepyceros melampus*	LightCover	DTArea	498.67
AMNH233038	*Alcelaphus buselaphus*	Open	DTArea	900.76
AMNH34717	*Alcelaphus buselaphus*	Open	DTArea	649.47
AMNH34725	*Alcelaphus buselaphus*	Open	DTArea	1267.33
AMNH82033	*Alcelaphus buselaphus*	Open	DTArea	1015.48
AMNH82159	*Alcelaphus buselaphus*	Open	DTArea	1051.47
AMNH16048	*Ammotragus lervia*	NA	DTArea	585.32
AMNH81740	*Antidorcas marsupialis*	Open	DTArea	416.43
AMNH81745	*Antidorcas marsupialis*	Open	DTArea	414.86
AMNH83549	*Antidorcas marsupialis*	Open	DTArea	350.41
AMNH83550	*Antidorcas marsupialis*	Open	DTArea	377.72
AMNH35527	*Antilope cervicapra*	Open	DTArea	463.99

AMNH35957	*Antilope cervicapra*	Open	DTArea	428.49
AMNH54486	*Antilope cervicapra*	Open	DTArea	482.38
AMNH88406	*Beatragus hunteri*	Open	DTArea	766.58
AMNH88407	*Beatragus hunteri*	Open	DTArea	747.09
AMNH88408	*Beatragus hunteri*	Open	DTArea	767.03
AMNH54765	*Bubalus bubalis*	NA	DTArea	97.12
AMNH54766	*Bubalus bubalis*	NA	DTArea	91.4
AMNH52875	*Cephalophus dorsalis*	Forest	DTArea	272.17
AMNH52876	*Cephalophus dorsalis*	Forest	DTArea	291.75
AMNH52884	*Cephalophus dorsalis*	Forest	DTArea	27.78
AMNH52888	*Cephalophus dorsalis*	Forest	DTArea	26.34
AMNH52775	*Cephalophus leucogaster*	Forest	DTArea	270.38
AMNH52778	*Cephalophus leucogaster*	Forest	DTArea	305.35
AMNH52788	*Cephalophus leucogaster*	Forest	DTArea	301.14
AMNH216375	*Cephalophus natalensis*	Forest	DTArea	286.98
AMNH54391	*Cephalophus natalensis*	Forest	DTArea	236.58
AMNH81686	*Cephalophus natalensis*	Forest	DTArea	188.32
AMNH83387	*Cephalophus natalensis*	Forest	DTArea	258.32
AMNH52930	*Cephalophus nigrifrons*	Forest	DTArea	24.05
AMNH52931	*Cephalophus nigrifrons*	Forest	DTArea	244.27
AMNH52940	*Cephalophus nigrifrons*	Forest	DTArea	24.72
AMNH52943	*Cephalophus nigrifrons*	Forest	DTArea	24.44
AMNH53138	*Cephalophus silvicultor*	Forest	DTArea	771.28
AMNH53144	*Cephalophus silvicultor*	Forest	DTArea	803.95
AMNH53153	*Cephalophus silvicultor*	Forest	DTArea	566.49
AMNH52992	*Cephalophus weynsi*	Forest	DTArea	286.36
AMNH52995	*Cephalophus weynsi*	Forest	DTArea	318.75
AMNH52999	*Cephalophus weynsi*	Forest	DTArea	298.86
AMNH88429	*Cephalophus weynsi*	Forest	DTArea	265.18
AMNH81716	*Connochaetes gnou*	Open	DTArea	884.39
AMNH81720	*Connochaetes gnou*	Open	DTArea	975.93
AMNH81722	*Connochaetes gnou*	Open	DTArea	1279.99
AMNH27824	*Connochaetes taurinus*	Open	DTArea	1168.62
AMNH54133	*Connochaetes taurinus*	Open	DTArea	1437.42
AMNH83502	*Connochaetes taurinus*	Open	DTArea	1300.37
AMNH83503	*Connochaetes taurinus*	Open	DTArea	1385.45
AMNH113781	*Damaliscus lunatus*	Open	DTArea	984.22
AMNH34729	*Damaliscus lunatus*	Open	DTArea	1124.34

AMNH34730	*Damaliscus lunatus*	Open	DTArea	1084.13
AMNH82035	*Damaliscus lunatus*	Open	DTArea	1029.66
AMNH42953	*Damaliscus pygargus*	Open	DTArea	575.67
AMNH81727	*Damaliscus pygargus*	Open	DTArea	686.85
AMNH81729	*Damaliscus pygargus*	Open	DTArea	651.2
AMNH81787	*Damaliscus pygargus*	Open	DTArea	668.74
AMNH81997	*Eudorcas thomsonii*	Open	DTArea	298.57
AMNH82059	*Eudorcas thomsonii*	Open	DTArea	255.73
AMNH82060	*Eudorcas thomsonii*	Open	DTArea	263.93
AMNH88415	*Eudorcas thomsonii*	Open	DTArea	218.75
AMNH54506	*Gazella gazella*	Open	DTArea	253.23
AMNH54997	*Gazella gazella*	Open	DTArea	252.81
AMNH54998	*Gazella gazella*	Open	DTArea	247.24
AMNH80143	*Hippotragus equinus*	Open	DTArea	1393.84
AMNH87217	*Hippotragus equinus*	Open	DTArea	1743.21
AMNH216381	*Hippotragus niger*	LightCover	DTArea	1589.88
AMNH80458	*Hippotragus niger*	LightCover	DTArea	1619.13
AMNH80461	*Hippotragus niger*	LightCover	DTArea	1631.64
AMNH83476	*Hippotragus niger*	LightCover	DTArea	1417.6
AMNH53492	*Kobus ellipsiprymnus*	HeavyCover	DTArea	1543.31
NMNH173877	*Kobus ellipsiprymnus*	HeavyCover	DTArea	1259.97
NMNH21898	*Kobus ellipsiprymnus*	HeavyCover	DTArea	1311.68
AMNH36396	*Kobus kob*	LightCover	DTArea	886.65
AMNH36397	*Kobus kob*	LightCover	DTArea	776.42
AMNH82129	*Kobus kob*	LightCover	DTArea	737.87
AMNH82130	*Kobus kob*	LightCover	DTArea	905.48
AMNH82173	*Kobus kob*	LightCover	DTArea	633.84
AMNH70010	*Kobus leche*	HeavyCover	DTArea	47.03
AMNH99649	*Kobus leche*	HeavyCover	DTArea	811.73
NMNH254927	*Kobus leche*	HeavyCover	DTArea	668.08
AMNH113784	*Kobus megaceros*	HeavyCover	DTArea	767.83
AMNH82135	*Kobus megaceros*	HeavyCover	DTArea	696.47
AMNH82136	*Kobus megaceros*	HeavyCover	DTArea	785.74
AMNH82137	*Kobus megaceros*	HeavyCover	DTArea	681.7
AMNH35323	*Kobus vardonii*	HeavyCover	DTArea	846.6
AMNH70057	*Kobus vardonii*	HeavyCover	DTArea	864.33
AMNH81687	*Kobus vardonii*	HeavyCover	DTArea	685.03
AMNH81170	*Litocranius walleri*	LightCover	DTArea	502.91

NMNH164031	*Litocranius walleri*	LightCover	DTArea	NA
NMNH164033	*Litocranius walleri*	LightCover	DTArea	427.83
NMNH259457	*Litocranius walleri*	LightCover	DTArea	432.96
AMNH187824	*Madoqua kirkii*	HeavyCover	DTArea	83.88
AMNH82076	*Madoqua kirkii*	HeavyCover	DTArea	112.71
NMNH538104	*Madoqua kirkii*	HeavyCover	DTArea	97.1
NMNH538106	*Madoqua kirkii*	HeavyCover	DTArea	120.43
NMNH541419	*Madoqua kirkii*	HeavyCover	DTArea	109.21
AMNH82051	*Nanger granti*	Open	DTArea	530.88
AMNH82056	*Nanger granti*	Open	DTArea	528.96
AMNH82057	*Nanger granti*	Open	DTArea	529.93
AMNH85152	*Nanger granti*	Open	DTArea	492.6
AMNH80111	*Nanger soemmerringii*	Open	DTArea	456.37
NMNH582229	*Nanger soemmerringii*	Open	DTArea	463.46
AMNH53180	*Neotragus batesi*	Forest	DTArea	86.79
AMNH53181	*Neotragus batesi*	Forest	DTArea	87.8
AMNH53946	*Neotragus batesi*	Forest	DTArea	77.17
AMNH88426	*Neotragus moschatus*	Forest	DTArea	83.7
AMNH88427	*Neotragus moschatus*	Forest	DTArea	97.35
NMNH367449	*Neotragus moschatus*	Forest	DTArea	99.47
AMNH233033	*Oryx gazella*	Open	DTArea	52.72
AMNH82043	*Oryx gazella*	Open	DTArea	1345.61
AMNH82044	*Oryx gazella*	Open	DTArea	1000.99
AMNH87211	*Oryx gazella*	Open	DTArea	1236.25
AMNH216387	*Ourebia ourebi*	LightCover	DTArea	274.38
AMNH53304	*Ourebia ourebi*	LightCover	DTArea	262.1
AMNH53328	*Ourebia ourebi*	LightCover	DTArea	239.87
AMNH269894	*Philantomba monticola*	Forest	DTArea	100.51
AMNH52726	*Philantomba monticola*	Forest	DTArea	108.7
AMNH52753	*Philantomba monticola*	Forest	DTArea	92.17
AMNH52758	*Philantomba monticola*	Forest	DTArea	99.92
AMNH216389	*Raphicerus campestris*	LightCover	DTArea	178.64
AMNH233047	*Raphicerus campestris*	LightCover	DTArea	201.13
AMNH34728	*Raphicerus campestris*	LightCover	DTArea	170.29
AMNH80538	*Raphicerus campestris*	LightCover	DTArea	201.48
AMNH35493	*Redunca arundinum*	LightCover	DTArea	685.63
AMNH80506	*Redunca arundinum*	LightCover	DTArea	561.34
NMNH367428	*Redunca arundinum*	LightCover	DTArea	559.29

NMNH367452	*Redunca arundinum*	LightCover	DTArea	37.96
NMNH469909	*Redunca arundinum*	LightCover	DTArea	366.44
AMNH27803	*Redunca fulvorufula*	LightCover	DTArea	482.79
AMNH82063	*Redunca fulvorufula*	LightCover	DTArea	384.32
AMNH82066	*Redunca fulvorufula*	LightCover	DTArea	379.71
AMNH82067	*Redunca fulvorufula*	LightCover	DTArea	411.1
AMNH53294	*Redunca redunca*	LightCover	DTArea	589.25
AMNH53296	*Redunca redunca*	LightCover	DTArea	594.95
AMNH90234	*Rupicapra rupicapra*	NA	DTArea	475.9
AMNH90235	*Rupicapra rupicapra*	NA	DTArea	380.04
AMNH90236	*Rupicapra rupicapra*	NA	DTArea	497.19
AMNH17276	*Sigmoceros lichtensteinii*	Open	DTArea	1311.7
AMNH216382	*Sigmoceros lichtensteinii*	Open	DTArea	1130.59
AMNH216383	*Sigmoceros lichtensteinii*	Open	DTArea	1141.29
AMNH53088	*Sylvicapra grimmia*	LightCover	DTArea	219.31
AMNH53092	*Sylvicapra grimmia*	LightCover	DTArea	241.35
AMNH80562	*Sylvicapra grimmia*	LightCover	DTArea	233.32
AMNH80563	*Sylvicapra grimmia*	LightCover	DTArea	233.62
AMNH53583	*Syncerus caffer*	LightCover	DTArea	66.16
AMNH82005	*Syncerus caffer*	LightCover	DTArea	82.58
AMNH82006	*Syncerus caffer*	LightCover	DTArea	85.08
AMNH82009	*Syncerus caffer*	LightCover	DTArea	2756.81
AMNH53519	*Taurotragus derbianus*	HeavyCover	DTArea	NA
AMNH53521	*Taurotragus derbianus*	HeavyCover	DTArea	NA
AMNH53522	*Taurotragus derbianus*	HeavyCover	DTArea	2374.88
AMNH53523	*Taurotragus derbianus*	HeavyCover	DTArea	2239.98
AMNH27811	*Taurotragus oryx*	LightCover	DTArea	2779.18
AMNH34722	*Taurotragus oryx*	LightCover	DTArea	2178.15
AMNH54386	*Tragelaphus angasii*	HeavyCover	DTArea	702.24
AMNH54387	*Tragelaphus angasii*	HeavyCover	DTArea	879.26
AMNH54390	*Tragelaphus angasii*	HeavyCover	DTArea	717.95
AMNH81002	*Tragelaphus buxtoni*	Forest	DTArea	1464
AMNH81003	*Tragelaphus buxtoni*	Forest	DTArea	985.83
AMNH81004	*Tragelaphus buxtoni*	Forest	DTArea	1655.98
AMNH81014	*Tragelaphus buxtoni*	Forest	DTArea	1289.64
AMNH81033	*Tragelaphus buxtoni*	Forest	DTArea	54.32
AMNH53271	*Tragelaphus eurycerus*	Forest	DTArea	1518.47
AMNH53279	*Tragelaphus eurycerus*	Forest	DTArea	1383.78

AMNH53280	*Tragelaphus eurycerus*	Forest	DTArea	1464.37
AMNH36416	*Tragelaphus imberbis*	HeavyCover	DTArea	881.56
AMNH36417	*Tragelaphus imberbis*	HeavyCover	DTArea	766.77
AMNH82019	*Tragelaphus imberbis*	HeavyCover	DTArea	805.1
AMNH82023	*Tragelaphus imberbis*	HeavyCover	DTArea	690.02
AMNH187806	*Tragelaphus scriptus*	Forest	DTArea	337.02
AMNH216371	*Tragelaphus scriptus*	Forest	DTArea	401.89
AMNH88425	*Tragelaphus scriptus*	Forest	DTArea	538.71
AMNH53209	*Tragelaphus spekii*	HeavyCover	DTArea	1132.15
AMNH53212	*Tragelaphus spekii*	HeavyCover	DTArea	950.17
AMNH53213	*Tragelaphus spekii*	HeavyCover	DTArea	653.81
AMNH53216	*Tragelaphus spekii*	HeavyCover	DTArea	710.38
AMNH233027	*Tragelaphus strepsiceros*	HeavyCover	DTArea	1580.77
AMNH70328	*Tragelaphus strepsiceros*	HeavyCover	DTArea	1050.71
AMNH70328a	*Tragelaphus strepsiceros*	HeavyCover	DTArea	54.57
AMNH113810	*Addax nasomaculatus*	Open	LML	44.76
AMNH113811	*Addax nasomaculatus*	Open	LML	42.61
AMNH113812	*Addax nasomaculatus*	Open	LML	45.35
AMNH113813	*Addax nasomaculatus*	Open	LML	41.64
AMNH81690	*Aepyceros melampus*	LightCover	LML	35.78
AMNH82050	*Aepyceros melampus*	LightCover	LML	35.46
AMNH83534	*Aepyceros melampus*	LightCover	LML	39.15
AMNH85150	*Aepyceros melampus*	LightCover	LML	36.61
AMNH233038	*Alcelaphus buselaphus*	Open	LML	45.25
AMNH34717	*Alcelaphus buselaphus*	Open	LML	36.81
AMNH34725	*Alcelaphus buselaphus*	Open	LML	50.48
AMNH82033	*Alcelaphus buselaphus*	Open	LML	45.01
AMNH82159	*Alcelaphus buselaphus*	Open	LML	48.56
AMNH16048	*Ammotragus lervia*	NA	LML	36.72
AMNH81740	*Antidorcas marsupialis*	Open	LML	30.66
AMNH81745	*Antidorcas marsupialis*	Open	LML	30.55
AMNH83549	*Antidorcas marsupialis*	Open	LML	31.02
AMNH83550	*Antidorcas marsupialis*	Open	LML	28.7
AMNH35527	*Antilope cervicapra*	Open	LML	32.49
AMNH35957	*Antilope cervicapra*	Open	LML	32.5
AMNH54486	*Antilope cervicapra*	Open	LML	33.9
AMNH88406	*Beatragus hunteri*	Open	LML	42.22
AMNH88407	*Beatragus hunteri*	Open	LML	41.99

AMNH88408	*Beatragus hunteri*	Open	LML	42.13
AMNH54765	*Bubalus bubalis*	NA	LML	72.79
AMNH54766	*Bubalus bubalis*	NA	LML	70.13
AMNH52875	*Cephalophus dorsalis*	Forest	LML	25.37
AMNH52876	*Cephalophus dorsalis*	Forest	LML	27.13
AMNH52884	*Cephalophus dorsalis*	Forest	LML	21.54
AMNH52888	*Cephalophus dorsalis*	Forest	LML	20.77
AMNH52775	*Cephalophus leucogaster*	Forest	LML	25.97
AMNH52778	*Cephalophus leucogaster*	Forest	LML	25.76
AMNH52788	*Cephalophus leucogaster*	Forest	LML	25.54
AMNH216375	*Cephalophus natalensis*	Forest	LML	26.72
AMNH54391	*Cephalophus natalensis*	Forest	LML	23.65
AMNH81686	*Cephalophus natalensis*	Forest	LML	23.32
AMNH83387	*Cephalophus natalensis*	Forest	LML	24.93
AMNH52930	*Cephalophus nigrifrons*	Forest	LML	19.7
AMNH52931	*Cephalophus nigrifrons*	Forest	LML	25.29
AMNH52940	*Cephalophus nigrifrons*	Forest	LML	19.65
AMNH52943	*Cephalophus nigrifrons*	Forest	LML	20.05
AMNH53138	*Cephalophus silvicultor*	Forest	LML	40.03
AMNH53144	*Cephalophus silvicultor*	Forest	LML	42.49
AMNH53153	*Cephalophus silvicultor*	Forest	LML	38.1
AMNH52992	*Cephalophus weynsi*	Forest	LML	27.51
AMNH52995	*Cephalophus weynsi*	Forest	LML	27.52
AMNH52999	*Cephalophus weynsi*	Forest	LML	28.42
AMNH88429	*Cephalophus weynsi*	Forest	LML	25.71
AMNH81716	*Connochaetes gnou*	Open	LML	45.01
AMNH81720	*Connochaetes gnou*	Open	LML	47.21
AMNH81722	*Connochaetes gnou*	Open	LML	50.11
AMNH27824	*Connochaetes taurinus*	Open	LML	53.56
AMNH54133	*Connochaetes taurinus*	Open	LML	55.8
AMNH83502	*Connochaetes taurinus*	Open	LML	54.38
AMNH83503	*Connochaetes taurinus*	Open	LML	51.98
AMNH113781	*Damaliscus lunatus*	Open	LML	48.57
AMNH34729	*Damaliscus lunatus*	Open	LML	49.17
AMNH34730	*Damaliscus lunatus*	Open	LML	51.08
AMNH82035	*Damaliscus lunatus*	Open	LML	46.56
AMNH42953	*Damaliscus pygargus*	Open	LML	36.23
AMNH81727	*Damaliscus pygargus*	Open	LML	38.14

AMNH81729	*Damaliscus pygargus*	Open	LML	36.81
AMNH81787	*Damaliscus pygargus*	Open	LML	37.44
AMNH81997	*Eudorcas thomsonii*	Open	LML	26.33
AMNH82059	*Eudorcas thomsonii*	Open	LML	25.74
AMNH82060	*Eudorcas thomsonii*	Open	LML	26.05
AMNH88415	*Eudorcas thomsonii*	Open	LML	25.58
AMNH54506	*Gazella gazella*	Open	LML	24.71
AMNH54997	*Gazella gazella*	Open	LML	24.95
AMNH54998	*Gazella gazella*	Open	LML	23.76
AMNH80143	*Hippotragus equinus*	Open	LML	53.56
AMNH87217	*Hippotragus equinus*	Open	LML	65.93
AMNH216381	*Hippotragus niger*	LightCover	LML	57.8
AMNH80458	*Hippotragus niger*	LightCover	LML	61.16
AMNH80461	*Hippotragus niger*	LightCover	LML	60.51
AMNH83476	*Hippotragus niger*	LightCover	LML	56.21
AMNH53492	*Kobus ellipsiprymnus*	HeavyCover	LML	58.64
NMNH173877	*Kobus ellipsiprymnus*	HeavyCover	LML	53.57
NMNH21898	*Kobus ellipsiprymnus*	HeavyCover	LML	59.39
AMNH36396	*Kobus kob*	LightCover	LML	44.15
AMNH36397	*Kobus kob*	LightCover	LML	43.25
AMNH82129	*Kobus kob*	LightCover	LML	41.45
AMNH82130	*Kobus kob*	LightCover	LML	45.17
AMNH82173	*Kobus kob*	LightCover	LML	40.95
AMNH70010	*Kobus leche*	HeavyCover	LML	39.94
AMNH99649	*Kobus leche*	HeavyCover	LML	45.49
NMNH254927	*Kobus leche*	HeavyCover	LML	43.12
AMNH113784	*Kobus megaceros*	HeavyCover	LML	43.65
AMNH82135	*Kobus megaceros*	HeavyCover	LML	43.02
AMNH82136	*Kobus megaceros*	HeavyCover	LML	45.7
AMNH82137	*Kobus megaceros*	HeavyCover	LML	41.33
AMNH35323	*Kobus vardonii*	HeavyCover	LML	46.05
AMNH70057	*Kobus vardonii*	HeavyCover	LML	46.17
AMNH81687	*Kobus vardonii*	HeavyCover	LML	40.99
AMNH81170	*Litocranius walleri*	LightCover	LML	35.07
NMNH164031	*Litocranius walleri*	LightCover	LML	32.21
NMNH164033	*Litocranius walleri*	LightCover	LML	32.33
NMNH259457	*Litocranius walleri*	LightCover	LML	33.77
AMNH187824	*Madoqua kirkii*	HeavyCover	LML	15.13

AMNH82076	*Madoqua kirkii*	HeavyCover	LML	17.01
NMNH538104	*Madoqua kirkii*	HeavyCover	LML	17.48
NMNH538106	*Madoqua kirkii*	HeavyCover	LML	17.58
NMNH541419	*Madoqua kirkii*	HeavyCover	LML	17.81
AMNH82051	*Nanger granti*	Open	LML	36.8
AMNH82056	*Nanger granti*	Open	LML	36.13
AMNH82057	*Nanger granti*	Open	LML	36.01
AMNH85152	*Nanger granti*	Open	LML	34.58
AMNH80111	*Nanger soemmerringii*	Open	LML	31.81
NMNH582229	*Nanger soemmerringii*	Open	LML	34.48
AMNH53180	*Neotragus batesi*	Forest	LML	14.72
AMNH53181	*Neotragus batesi*	Forest	LML	13.68
AMNH53946	*Neotragus batesi*	Forest	LML	13.67
AMNH88426	*Neotragus moschatus*	Forest	LML	15.06
AMNH88427	*Neotragus moschatus*	Forest	LML	14.82
NMNH367449	*Neotragus moschatus*	Forest	LML	16.91
AMNH233033	*Oryx gazella*	Open	LML	41.94
AMNH82043	*Oryx gazella*	Open	LML	54.81
AMNH82044	*Oryx gazella*	Open	LML	50
AMNH87211	*Oryx gazella*	Open	LML	52.7
AMNH216387	*Ourebia ourebi*	LightCover	LML	27.17
AMNH53304	*Ourebia ourebi*	LightCover	LML	24.98
AMNH53328	*Ourebia ourebi*	LightCover	LML	25.66
AMNH269894	*Philantomba monticola*	Forest	LML	16.52
AMNH52726	*Philantomba monticola*	Forest	LML	15.74
AMNH52753	*Philantomba monticola*	Forest	LML	15.81
AMNH52758	*Philantomba monticola*	Forest	LML	16.27
AMNH216389	*Raphicerus campestris*	LightCover	LML	23.27
AMNH233047	*Raphicerus campestris*	LightCover	LML	21.88
AMNH34728	*Raphicerus campestris*	LightCover	LML	21.58
AMNH80538	*Raphicerus campestris*	LightCover	LML	23.49
AMNH35493	*Redunca arundinum*	LightCover	LML	39.68
AMNH80506	*Redunca arundinum*	LightCover	LML	37.89
NMNH367428	*Redunca arundinum*	LightCover	LML	38.95
NMNH367452	*Redunca arundinum*	LightCover	LML	31.06
NMNH469909	*Redunca arundinum*	LightCover	LML	31.7
AMNH27803	*Redunca fulvorufula*	LightCover	LML	32.27
AMNH82063	*Redunca fulvorufula*	LightCover	LML	31.4

AMNH82066	*Redunca fulvorufula*	LightCover	LML	30.41
AMNH82067	*Redunca fulvorufula*	LightCover	LML	31.45
AMNH53294	*Redunca redunca*	LightCover	LML	36.48
AMNH53296	*Redunca redunca*	LightCover	LML	37.12
AMNH90234	*Rupicapra rupicapra*	NA	LML	31.59
AMNH90235	*Rupicapra rupicapra*	NA	LML	31.63
AMNH90236	*Rupicapra rupicapra*	NA	LML	32.23
AMNH17276	*Sigmoceros lichtensteinii*	Open	LML	51.83
AMNH216382	*Sigmoceros lichtensteinii*	Open	LML	52.89
AMNH216383	*Sigmoceros lichtensteinii*	Open	LML	51.81
AMNH53088	*Sylvicapra grimmia*	LightCover	LML	22.68
AMNH53092	*Sylvicapra grimmia*	LightCover	LML	22.9
AMNH80562	*Sylvicapra grimmia*	LightCover	LML	25.06
AMNH80563	*Sylvicapra grimmia*	LightCover	LML	24.89
AMNH53583	*Syncerus caffer*	LightCover	LML	51.54
AMNH82005	*Syncerus caffer*	LightCover	LML	62.79
AMNH82006	*Syncerus caffer*	LightCover	LML	64.88
AMNH82009	*Syncerus caffer*	LightCover	LML	79.42
AMNH53519	*Taurotragus derbianus*	HeavyCover	LML	78.65
AMNH53521	*Taurotragus derbianus*	HeavyCover	LML	74.96
AMNH53522	*Taurotragus derbianus*	HeavyCover	LML	78.28
AMNH53523	*Taurotragus derbianus*	HeavyCover	LML	79.26
AMNH27811	*Taurotragus oryx*	LightCover	LML	76.96
AMNH34722	*Taurotragus oryx*	LightCover	LML	70.3
AMNH54386	*Tragelaphus angasii*	HeavyCover	LML	42.39
AMNH54387	*Tragelaphus angasii*	HeavyCover	LML	45.18
AMNH54390	*Tragelaphus angasii*	HeavyCover	LML	43.98
AMNH81002	*Tragelaphus buxtoni*	Forest	LML	59.68
AMNH81003	*Tragelaphus buxtoni*	Forest	LML	54.83
AMNH81004	*Tragelaphus buxtoni*	Forest	LML	61.29
AMNH81014	*Tragelaphus buxtoni*	Forest	LML	54.17
AMNH81033	*Tragelaphus buxtoni*	Forest	LML	44.55
AMNH53271	*Tragelaphus eurycerus*	Forest	LML	61.24
AMNH53279	*Tragelaphus eurycerus*	Forest	LML	61.56
AMNH53280	*Tragelaphus eurycerus*	Forest	LML	64.97
AMNH36416	*Tragelaphus imberbis*	HeavyCover	LML	45.67
AMNH36417	*Tragelaphus imberbis*	HeavyCover	LML	41.27
AMNH82019	*Tragelaphus imberbis*	HeavyCover	LML	48.33

AMNH82023	*Tragelaphus imberbis*	HeavyCover	LML	41.85
AMNH187806	*Tragelaphus scriptus*	Forest	LML	31.53
AMNH216371	*Tragelaphus scriptus*	Forest	LML	33.59
AMNH88425	*Tragelaphus scriptus*	Forest	LML	37.22
AMNH53209	*Tragelaphus spekii*	HeavyCover	LML	48.93
AMNH53212	*Tragelaphus spekii*	HeavyCover	LML	46.74
AMNH53213	*Tragelaphus spekii*	HeavyCover	LML	38.76
AMNH53216	*Tragelaphus spekii*	HeavyCover	LML	40.58
AMNH233027	*Tragelaphus strepsiceros*	HeavyCover	LML	60.85
AMNH70328	*Tragelaphus strepsiceros*	HeavyCover	LML	54.79
AMNH70328a	*Tragelaphus strepsiceros*	HeavyCover	LML	43.49
AMNH113810	*Addax nasomaculatus*	Open	MIN	36.82
AMNH113811	*Addax nasomaculatus*	Open	MIN	33.35
AMNH113812	*Addax nasomaculatus*	Open	MIN	35.64
AMNH113813	*Addax nasomaculatus*	Open	MIN	33.06
AMNH81690	*Aepyceros melampus*	LightCover	MIN	28.04
AMNH82050	*Aepyceros melampus*	LightCover	MIN	27.28
AMNH83534	*Aepyceros melampus*	LightCover	MIN	29.99
AMNH85150	*Aepyceros melampus*	LightCover	MIN	28.02
AMNH233038	*Alcelaphus buselaphus*	Open	MIN	36.03
AMNH34717	*Alcelaphus buselaphus*	Open	MIN	30.8
AMNH34725	*Alcelaphus buselaphus*	Open	MIN	39.8
AMNH82033	*Alcelaphus buselaphus*	Open	MIN	35.54
AMNH82159	*Alcelaphus buselaphus*	Open	MIN	37.24
AMNH16048	*Ammotragus lervia*	NA	MIN	30.74
AMNH81740	*Antidorcas marsupialis*	Open	MIN	23.72
AMNH81745	*Antidorcas marsupialis*	Open	MIN	23.83
AMNH83549	*Antidorcas marsupialis*	Open	MIN	24.06
AMNH83550	*Antidorcas marsupialis*	Open	MIN	23.61
AMNH35527	*Antilope cervicapra*	Open	MIN	25.98
AMNH35957	*Antilope cervicapra*	Open	MIN	25.43
AMNH54486	*Antilope cervicapra*	Open	MIN	27.03
AMNH88406	*Beatragus hunteri*	Open	MIN	32.56
AMNH88407	*Beatragus hunteri*	Open	MIN	31.86
AMNH88408	*Beatragus hunteri*	Open	MIN	32.06
AMNH54765	*Bubalus bubalis*	NA	MIN	88.19
AMNH54766	*Bubalus bubalis*	NA	MIN	82.84
AMNH52875	*Cephalophus dorsalis*	Forest	MIN	20.15

AMNH52876	*Cephalophus dorsalis*	Forest	MIN	20.49
AMNH52884	*Cephalophus dorsalis*	Forest	MIN	26.46
AMNH52888	*Cephalophus dorsalis*	Forest	MIN	24.58
AMNH52775	*Cephalophus leucogaster*	Forest	MIN	20.95
AMNH52778	*Cephalophus leucogaster*	Forest	MIN	20.62
AMNH52788	*Cephalophus leucogaster*	Forest	MIN	20.64
AMNH216375	*Cephalophus natalensis*	Forest	MIN	22.47
AMNH54391	*Cephalophus natalensis*	Forest	MIN	19.35
AMNH81686	*Cephalophus natalensis*	Forest	MIN	18.29
AMNH83387	*Cephalophus natalensis*	Forest	MIN	20.39
AMNH52930	*Cephalophus nigrifrons*	Forest	MIN	23.12
AMNH52931	*Cephalophus nigrifrons*	Forest	MIN	20.31
AMNH52940	*Cephalophus nigrifrons*	Forest	MIN	23.11
AMNH52943	*Cephalophus nigrifrons*	Forest	MIN	23.35
AMNH53138	*Cephalophus silvicultor*	Forest	MIN	31.09
AMNH53144	*Cephalophus silvicultor*	Forest	MIN	34
AMNH53153	*Cephalophus silvicultor*	Forest	MIN	29.27
AMNH52992	*Cephalophus weynsi*	Forest	MIN	22.12
AMNH52995	*Cephalophus weynsi*	Forest	MIN	22.26
AMNH52999	*Cephalophus weynsi*	Forest	MIN	23.64
AMNH88429	*Cephalophus weynsi*	Forest	MIN	20.89
AMNH81716	*Connochaetes gnou*	Open	MIN	36.63
AMNH81720	*Connochaetes gnou*	Open	MIN	36.64
AMNH81722	*Connochaetes gnou*	Open	MIN	39.94
AMNH27824	*Connochaetes taurinus*	Open	MIN	41.78
AMNH54133	*Connochaetes taurinus*	Open	MIN	45.55
AMNH83502	*Connochaetes taurinus*	Open	MIN	42.84
AMNH83503	*Connochaetes taurinus*	Open	MIN	41.55
AMNH113781	*Damaliscus lunatus*	Open	MIN	37.33
AMNH34729	*Damaliscus lunatus*	Open	MIN	37.13
AMNH34730	*Damaliscus lunatus*	Open	MIN	40.66
AMNH82035	*Damaliscus lunatus*	Open	MIN	36.19
AMNH42953	*Damaliscus pygargus*	Open	MIN	28.38
AMNH81727	*Damaliscus pygargus*	Open	MIN	29.84
AMNH81729	*Damaliscus pygargus*	Open	MIN	29.69
AMNH81787	*Damaliscus pygargus*	Open	MIN	29.43
AMNH81997	*Eudorcas thomsonii*	Open	MIN	20.29
AMNH82059	*Eudorcas thomsonii*	Open	MIN	19.6

AMNH82060	*Eudorcas thomsonii*	Open	MIN	19.64
AMNH88415	*Eudorcas thomsonii*	Open	MIN	19.47
AMNH54506	*Gazella gazella*	Open	MIN	18.85
AMNH54997	*Gazella gazella*	Open	MIN	19.53
AMNH54998	*Gazella gazella*	Open	MIN	18.23
AMNH80143	*Hippotragus equinus*	Open	MIN	41.7
AMNH87217	*Hippotragus equinus*	Open	MIN	51.4
AMNH216381	*Hippotragus niger*	LightCover	MIN	44.49
AMNH80458	*Hippotragus niger*	LightCover	MIN	48.55
AMNH80461	*Hippotragus niger*	LightCover	MIN	48.48
AMNH83476	*Hippotragus niger*	LightCover	MIN	44.1
AMNH53492	*Kobus ellipsiprymnus*	HeavyCover	MIN	46.49
NMNH173877	*Kobus ellipsiprymnus*	HeavyCover	MIN	42.82
NMNH21898	*Kobus ellipsiprymnus*	HeavyCover	MIN	47.6
AMNH36396	*Kobus kob*	LightCover	MIN	36.59
AMNH36397	*Kobus kob*	LightCover	MIN	34.88
AMNH82129	*Kobus kob*	LightCover	MIN	34.75
AMNH82130	*Kobus kob*	LightCover	MIN	36.29
AMNH82173	*Kobus kob*	LightCover	MIN	32.97
AMNH70010	*Kobus leche*	HeavyCover	MIN	46.37
AMNH99649	*Kobus leche*	HeavyCover	MIN	37.22
NMNH254927	*Kobus leche*	HeavyCover	MIN	34.95
AMNH113784	*Kobus megaceros*	HeavyCover	MIN	34.93
AMNH82135	*Kobus megaceros*	HeavyCover	MIN	35.49
AMNH82136	*Kobus megaceros*	HeavyCover	MIN	36.32
AMNH82137	*Kobus megaceros*	HeavyCover	MIN	32.86
AMNH35323	*Kobus vardonii*	HeavyCover	MIN	37.84
AMNH70057	*Kobus vardonii*	HeavyCover	MIN	37.99
AMNH81687	*Kobus vardonii*	HeavyCover	MIN	32.88
AMNH81170	*Litocranius walleri*	LightCover	MIN	26.57
NMNH164031	*Litocranius walleri*	LightCover	MIN	25.11
NMNH164033	*Litocranius walleri*	LightCover	MIN	25
NMNH259457	*Litocranius walleri*	LightCover	MIN	24.48
AMNH187824	*Madoqua kirkii*	HeavyCover	MIN	12.54
AMNH82076	*Madoqua kirkii*	HeavyCover	MIN	14.13
NMNH538104	*Madoqua kirkii*	HeavyCover	MIN	13.86
NMNH538106	*Madoqua kirkii*	HeavyCover	MIN	14.11
NMNH541419	*Madoqua kirkii*	HeavyCover	MIN	14.35

AMNH82051	*Nanger granti*	Open	MIN	28.58
AMNH82056	*Nanger granti*	Open	MIN	28.17
AMNH82057	*Nanger granti*	Open	MIN	27.49
AMNH85152	*Nanger granti*	Open	MIN	26.73
AMNH80111	*Nanger soemmerringii*	Open	MIN	24.17
NMNH582229	*Nanger soemmerringii*	Open	MIN	26.79
AMNH53180	*Neotragus batesi*	Forest	MIN	11.87
AMNH53181	*Neotragus batesi*	Forest	MIN	10.94
AMNH53946	*Neotragus batesi*	Forest	MIN	10.82
AMNH88426	*Neotragus moschatus*	Forest	MIN	11.48
AMNH88427	*Neotragus moschatus*	Forest	MIN	11.95
NMNH367449	*Neotragus moschatus*	Forest	MIN	13.85
AMNH233033	*Oryx gazella*	Open	MIN	49.38
AMNH82043	*Oryx gazella*	Open	MIN	42.27
AMNH82044	*Oryx gazella*	Open	MIN	38.81
AMNH87211	*Oryx gazella*	Open	MIN	40.2
AMNH216387	*Ourebia ourebi*	LightCover	MIN	21.43
AMNH53304	*Ourebia ourebi*	LightCover	MIN	20.3
AMNH53328	*Ourebia ourebi*	LightCover	MIN	19.69
AMNH269894	*Philantomba monticola*	Forest	MIN	12.95
AMNH52726	*Philantomba monticola*	Forest	MIN	13.01
AMNH52753	*Philantomba monticola*	Forest	MIN	12.7
AMNH52758	*Philantomba monticola*	Forest	MIN	13.25
AMNH216389	*Raphicerus campestris*	LightCover	MIN	18.17
AMNH233047	*Raphicerus campestris*	LightCover	MIN	17.06
AMNH34728	*Raphicerus campestris*	LightCover	MIN	17.17
AMNH80538	*Raphicerus campestris*	LightCover	MIN	18.4
AMNH35493	*Redunca arundinum*	LightCover	MIN	30.44
AMNH80506	*Redunca arundinum*	LightCover	MIN	29.79
NMNH367428	*Redunca arundinum*	LightCover	MIN	30.48
NMNH367452	*Redunca arundinum*	LightCover	MIN	36.24
NMNH469909	*Redunca arundinum*	LightCover	MIN	24.95
AMNH27803	*Redunca fulvorufula*	LightCover	MIN	26.49
AMNH82063	*Redunca fulvorufula*	LightCover	MIN	25.85
AMNH82066	*Redunca fulvorufula*	LightCover	MIN	23.84
AMNH82067	*Redunca fulvorufula*	LightCover	MIN	25.11
AMNH53294	*Redunca redunca*	LightCover	MIN	29.5
AMNH53296	*Redunca redunca*	LightCover	MIN	30.05

AMNH90234	*Rupicapra rupicapra*	NA	MIN	25.08
AMNH90235	*Rupicapra rupicapra*	NA	MIN	25.51
AMNH90236	*Rupicapra rupicapra*	NA	MIN	26.1
AMNH17276	*Sigmoceros lichtensteinii*	Open	MIN	40.85
AMNH216382	*Sigmoceros lichtensteinii*	Open	MIN	39.73
AMNH216383	*Sigmoceros lichtensteinii*	Open	MIN	39.69
AMNH53088	*Sylvicapra grimmia*	LightCover	MIN	18.44
AMNH53092	*Sylvicapra grimmia*	LightCover	MIN	18.78
AMNH80562	*Sylvicapra grimmia*	LightCover	MIN	20.29
AMNH80563	*Sylvicapra grimmia*	LightCover	MIN	19.94
AMNH53583	*Syncerus caffer*	LightCover	MIN	62.95
AMNH82005	*Syncerus caffer*	LightCover	MIN	74.11
AMNH82006	*Syncerus caffer*	LightCover	MIN	76.27
AMNH82009	*Syncerus caffer*	LightCover	MIN	63.37
AMNH53519	*Taurotragus derbianus*	HeavyCover	MIN	63.28
AMNH53521	*Taurotragus derbianus*	HeavyCover	MIN	59.94
AMNH53522	*Taurotragus derbianus*	HeavyCover	MIN	61.57
AMNH53523	*Taurotragus derbianus*	HeavyCover	MIN	63.23
AMNH27811	*Taurotragus oryx*	LightCover	MIN	60.22
AMNH34722	*Taurotragus oryx*	LightCover	MIN	55.54
AMNH54386	*Tragelaphus angasii*	HeavyCover	MIN	33.47
AMNH54387	*Tragelaphus angasii*	HeavyCover	MIN	36.13
AMNH54390	*Tragelaphus angasii*	HeavyCover	MIN	34.35
AMNH81002	*Tragelaphus buxtoni*	Forest	MIN	49.18
AMNH81003	*Tragelaphus buxtoni*	Forest	MIN	45.94
AMNH81004	*Tragelaphus buxtoni*	Forest	MIN	50.1
AMNH81014	*Tragelaphus buxtoni*	Forest	MIN	44.81
AMNH81033	*Tragelaphus buxtoni*	Forest	MIN	52.47
AMNH53271	*Tragelaphus eurycerus*	Forest	MIN	48.51
AMNH53279	*Tragelaphus eurycerus*	Forest	MIN	48.32
AMNH53280	*Tragelaphus eurycerus*	Forest	MIN	52.4
AMNH36416	*Tragelaphus imberbis*	HeavyCover	MIN	34.64
AMNH36417	*Tragelaphus imberbis*	HeavyCover	MIN	31.83
AMNH82019	*Tragelaphus imberbis*	HeavyCover	MIN	36.97
AMNH82023	*Tragelaphus imberbis*	HeavyCover	MIN	32.55
AMNH187806	*Tragelaphus scriptus*	Forest	MIN	24.12
AMNH216371	*Tragelaphus scriptus*	Forest	MIN	27.77
AMNH88425	*Tragelaphus scriptus*	Forest	MIN	30.35

AMNH53209	*Tragelaphus spekii*	HeavyCover	MIN	40.05
AMNH53212	*Tragelaphus spekii*	HeavyCover	MIN	37.18
AMNH53213	*Tragelaphus spekii*	HeavyCover	MIN	31.06
AMNH53216	*Tragelaphus spekii*	HeavyCover	MIN	31.84
AMNH233027	*Tragelaphus strepsiceros*	HeavyCover	MIN	48.33
AMNH70328	*Tragelaphus strepsiceros*	HeavyCover	MIN	43.61
AMNH70328a	*Tragelaphus strepsiceros*	HeavyCover	MIN	49.83
AMNH113810	*Addax nasomaculatus*	Open	MML	41.85
AMNH113811	*Addax nasomaculatus*	Open	MML	39.54
AMNH113812	*Addax nasomaculatus*	Open	MML	42
AMNH113813	*Addax nasomaculatus*	Open	MML	38.47
AMNH81690	*Aepyceros melampus*	LightCover	MML	34.39
AMNH82050	*Aepyceros melampus*	LightCover	MML	33.18
AMNH83534	*Aepyceros melampus*	LightCover	MML	36.94
AMNH85150	*Aepyceros melampus*	LightCover	MML	34.09
AMNH233038	*Alcelaphus buselaphus*	Open	MML	43.55
AMNH34717	*Alcelaphus buselaphus*	Open	MML	35.95
AMNH34725	*Alcelaphus buselaphus*	Open	MML	47.71
AMNH82033	*Alcelaphus buselaphus*	Open	MML	42.3
AMNH82159	*Alcelaphus buselaphus*	Open	MML	46.06
AMNH16048	*Ammotragus lervia*	NA	MML	35.94
AMNH81740	*Antidorcas marsupialis*	Open	MML	28.52
AMNH81745	*Antidorcas marsupialis*	Open	MML	28.69
AMNH83549	*Antidorcas marsupialis*	Open	MML	28.2
AMNH83550	*Antidorcas marsupialis*	Open	MML	27.46
AMNH35527	*Antilope cervicapra*	Open	MML	30.83
AMNH35957	*Antilope cervicapra*	Open	MML	30.6
AMNH54486	*Antilope cervicapra*	Open	MML	31.75
AMNH88406	*Beatragus hunteri*	Open	MML	39.69
AMNH88407	*Beatragus hunteri*	Open	MML	38.5
AMNH88408	*Beatragus hunteri*	Open	MML	38.83
AMNH54765	*Bubalus bubalis*	NA	MML	18.52
AMNH54766	*Bubalus bubalis*	NA	MML	15.94
AMNH52875	*Cephalophus dorsalis*	Forest	MML	23.91
AMNH52876	*Cephalophus dorsalis*	Forest	MML	24.79
AMNH52884	*Cephalophus dorsalis*	Forest	MML	4.22
AMNH52888	*Cephalophus dorsalis*	Forest	MML	3.99
AMNH52775	*Cephalophus leucogaster*	Forest	MML	24.87

AMNH52778	*Cephalophus leucogaster*	Forest	MML	24.21
AMNH52788	*Cephalophus leucogaster*	Forest	MML	24.33
AMNH216375	*Cephalophus natalensis*	Forest	MML	25.59
AMNH54391	*Cephalophus natalensis*	Forest	MML	22.61
AMNH81686	*Cephalophus natalensis*	Forest	MML	21.56
AMNH83387	*Cephalophus natalensis*	Forest	MML	24.15
AMNH52930	*Cephalophus nigrifrons*	Forest	MML	3.11
AMNH52931	*Cephalophus nigrifrons*	Forest	MML	23.6
AMNH52940	*Cephalophus nigrifrons*	Forest	MML	3.84
AMNH52943	*Cephalophus nigrifrons*	Forest	MML	3.16
AMNH53138	*Cephalophus silvicultor*	Forest	MML	34.01
AMNH53144	*Cephalophus silvicultor*	Forest	MML	40.06
AMNH53153	*Cephalophus silvicultor*	Forest	MML	35.42
AMNH52992	*Cephalophus weynsi*	Forest	MML	25.75
AMNH52995	*Cephalophus weynsi*	Forest	MML	25.68
AMNH52999	*Cephalophus weynsi*	Forest	MML	27.52
AMNH88429	*Cephalophus weynsi*	Forest	MML	24.44
AMNH81716	*Connochaetes gnou*	Open	MML	43.55
AMNH81720	*Connochaetes gnou*	Open	MML	44.8
AMNH81722	*Connochaetes gnou*	Open	MML	47.61
AMNH27824	*Connochaetes taurinus*	Open	MML	50.93
AMNH54133	*Connochaetes taurinus*	Open	MML	53.61
AMNH83502	*Connochaetes taurinus*	Open	MML	51.58
AMNH83503	*Connochaetes taurinus*	Open	MML	49.21
AMNH113781	*Damaliscus lunatus*	Open	MML	46.13
AMNH34729	*Damaliscus lunatus*	Open	MML	45.56
AMNH34730	*Damaliscus lunatus*	Open	MML	48.72
AMNH82035	*Damaliscus lunatus*	Open	MML	44.12
AMNH42953	*Damaliscus pygargus*	Open	MML	34.52
AMNH81727	*Damaliscus pygargus*	Open	MML	36.55
AMNH81729	*Damaliscus pygargus*	Open	MML	35.51
AMNH81787	*Damaliscus pygargus*	Open	MML	35.44
AMNH81997	*Eudorcas thomsonii*	Open	MML	24.61
AMNH82059	*Eudorcas thomsonii*	Open	MML	23.54
AMNH82060	*Eudorcas thomsonii*	Open	MML	23.68
AMNH88415	*Eudorcas thomsonii*	Open	MML	23.3
AMNH54506	*Gazella gazella*	Open	MML	22.5
AMNH54997	*Gazella gazella*	Open	MML	23.13

AMNH54998	*Gazella gazella*	Open	MML	22.25
AMNH80143	*Hippotragus equinus*	Open	MML	50.66
AMNH87217	*Hippotragus equinus*	Open	MML	62.35
AMNH216381	*Hippotragus niger*	LightCover	MML	53.2
AMNH80458	*Hippotragus niger*	LightCover	MML	57.27
AMNH80461	*Hippotragus niger*	LightCover	MML	55.3
AMNH83476	*Hippotragus niger*	LightCover	MML	52.99
AMNH53492	*Kobus ellipsiprymnus*	HeavyCover	MML	52.96
NMNH173877	*Kobus ellipsiprymnus*	HeavyCover	MML	51.33
NMNH21898	*Kobus ellipsiprymnus*	HeavyCover	MML	54.91
AMNH36396	*Kobus kob*	LightCover	MML	41.45
AMNH36397	*Kobus kob*	LightCover	MML	39.82
AMNH82129	*Kobus kob*	LightCover	MML	39.42
AMNH82130	*Kobus kob*	LightCover	MML	42.38
AMNH82173	*Kobus kob*	LightCover	MML	38.22
AMNH70010	*Kobus leche*	HeavyCover	MML	5.86
AMNH99649	*Kobus leche*	HeavyCover	MML	44.16
NMNH254927	*Kobus leche*	HeavyCover	MML	41.35
AMNH113784	*Kobus megaceros*	HeavyCover	MML	40.8
AMNH82135	*Kobus megaceros*	HeavyCover	MML	41.13
AMNH82136	*Kobus megaceros*	HeavyCover	MML	42.31
AMNH82137	*Kobus megaceros*	HeavyCover	MML	38.24
AMNH35323	*Kobus vardonii*	HeavyCover	MML	44.99
AMNH70057	*Kobus vardonii*	HeavyCover	MML	44.76
AMNH81687	*Kobus vardonii*	HeavyCover	MML	37.74
AMNH81170	*Litocranius walleri*	LightCover	MML	32.23
NMNH164031	*Litocranius walleri*	LightCover	MML	30
NMNH164033	*Litocranius walleri*	LightCover	MML	29.73
NMNH259457	*Litocranius walleri*	LightCover	MML	31.25
AMNH187824	*Madoqua kirkii*	HeavyCover	MML	15.13
AMNH82076	*Madoqua kirkii*	HeavyCover	MML	16.54
NMNH538104	*Madoqua kirkii*	HeavyCover	MML	16.32
NMNH538106	*Madoqua kirkii*	HeavyCover	MML	16.66
NMNH541419	*Madoqua kirkii*	HeavyCover	MML	16.9
AMNH82051	*Nanger granti*	Open	MML	34.35
AMNH82056	*Nanger granti*	Open	MML	33.03
AMNH82057	*Nanger granti*	Open	MML	32.36
AMNH85152	*Nanger granti*	Open	MML	31.86

AMNH80111	*Nanger soemmerringii*	Open	MML	28.74
NMNH582229	*Nanger soemmerringii*	Open	MML	32.19
AMNH53180	*Neotragus batesi*	Forest	MML	14.06
AMNH53181	*Neotragus batesi*	Forest	MML	13.2
AMNH53946	*Neotragus batesi*	Forest	MML	13.17
AMNH88426	*Neotragus moschatus*	Forest	MML	13.68
AMNH88427	*Neotragus moschatus*	Forest	MML	14.17
NMNH367449	*Neotragus moschatus*	Forest	MML	16.32
AMNH233033	*Oryx gazella*	Open	MML	9.58
AMNH82043	*Oryx gazella*	Open	MML	51.45
AMNH82044	*Oryx gazella*	Open	MML	47.29
AMNH87211	*Oryx gazella*	Open	MML	48.01
AMNH216387	*Ourebia ourebi*	LightCover	MML	24.8
AMNH53304	*Ourebia ourebi*	LightCover	MML	23.34
AMNH53328	*Ourebia ourebi*	LightCover	MML	22.37
AMNH269894	*Philantomba monticola*	Forest	MML	15.38
AMNH52726	*Philantomba monticola*	Forest	MML	15.31
AMNH52753	*Philantomba monticola*	Forest	MML	15.04
AMNH52758	*Philantomba monticola*	Forest	MML	15.48
AMNH216389	*Raphicerus campestris*	LightCover	MML	21.54
AMNH233047	*Raphicerus campestris*	LightCover	MML	20.31
AMNH34728	*Raphicerus campestris*	LightCover	MML	20.25
AMNH80538	*Raphicerus campestris*	LightCover	MML	21.44
AMNH35493	*Redunca arundinum*	LightCover	MML	35.39
AMNH80506	*Redunca arundinum*	LightCover	MML	35.74
NMNH367428	*Redunca arundinum*	LightCover	MML	36.22
NMNH367452	*Redunca arundinum*	LightCover	MML	5.37
NMNH469909	*Redunca arundinum*	LightCover	MML	29.14
AMNH27803	*Redunca fulvorufula*	LightCover	MML	31.14
AMNH82063	*Redunca fulvorufula*	LightCover	MML	29.77
AMNH82066	*Redunca fulvorufula*	LightCover	MML	28.42
AMNH82067	*Redunca fulvorufula*	LightCover	MML	29.39
AMNH53294	*Redunca redunca*	LightCover	MML	33.82
AMNH53296	*Redunca redunca*	LightCover	MML	35.38
AMNH90234	*Rupicapra rupicapra*	NA	MML	30.79
AMNH90235	*Rupicapra rupicapra*	NA	MML	30.53
AMNH90236	*Rupicapra rupicapra*	NA	MML	31.08
AMNH17276	*Sigmoceros lichtensteinii*	Open	MML	47.63

AMNH216382	*Sigmoceros lichtensteinii*	Open	MML	48.63
AMNH216383	*Sigmoceros lichtensteinii*	Open	MML	47.71
AMNH53088	*Sylvicapra grimmia*	LightCover	MML	21.69
AMNH53092	*Sylvicapra grimmia*	LightCover	MML	21.96
AMNH80562	*Sylvicapra grimmia*	LightCover	MML	23.45
AMNH80563	*Sylvicapra grimmia*	LightCover	MML	23.31
AMNH53583	*Syncerus caffer*	LightCover	MML	10.86
AMNH82005	*Syncerus caffer*	LightCover	MML	14.86
AMNH82006	*Syncerus caffer*	LightCover	MML	14.62
AMNH82009	*Syncerus caffer*	LightCover	MML	73.97
AMNH53519	*Taurotragus derbianus*	HeavyCover	MML	73.19
AMNH53521	*Taurotragus derbianus*	HeavyCover	MML	69.76
AMNH53522	*Taurotragus derbianus*	HeavyCover	MML	71.43
AMNH53523	*Taurotragus derbianus*	HeavyCover	MML	73.75
AMNH27811	*Taurotragus oryx*	LightCover	MML	72.37
AMNH34722	*Taurotragus oryx*	LightCover	MML	65.82
AMNH54386	*Tragelaphus angasii*	HeavyCover	MML	38.77
AMNH54387	*Tragelaphus angasii*	HeavyCover	MML	40.66
AMNH54390	*Tragelaphus angasii*	HeavyCover	MML	39.63
AMNH81002	*Tragelaphus buxtoni*	Forest	MML	56.59
AMNH81003	*Tragelaphus buxtoni*	Forest	MML	53.27
AMNH81004	*Tragelaphus buxtoni*	Forest	MML	57.54
AMNH81014	*Tragelaphus buxtoni*	Forest	MML	52.67
AMNH81033	*Tragelaphus buxtoni*	Forest	MML	7.21
AMNH53271	*Tragelaphus eurycerus*	Forest	MML	57.72
AMNH53279	*Tragelaphus eurycerus*	Forest	MML	57.87
AMNH53280	*Tragelaphus eurycerus*	Forest	MML	60.18
AMNH36416	*Tragelaphus imberbis*	HeavyCover	MML	42.21
AMNH36417	*Tragelaphus imberbis*	HeavyCover	MML	38.93
AMNH82019	*Tragelaphus imberbis*	HeavyCover	MML	45.41
AMNH82023	*Tragelaphus imberbis*	HeavyCover	MML	39.2
AMNH187806	*Tragelaphus scriptus*	Forest	MML	29.3
AMNH216371	*Tragelaphus scriptus*	Forest	MML	32.04
AMNH88425	*Tragelaphus scriptus*	Forest	MML	34.62
AMNH53209	*Tragelaphus spekii*	HeavyCover	MML	46.97
AMNH53212	*Tragelaphus spekii*	HeavyCover	MML	42.67
AMNH53213	*Tragelaphus spekii*	HeavyCover	MML	36.35
AMNH53216	*Tragelaphus spekii*	HeavyCover	MML	38.41

AMNH233027	*Tragelaphus strepsiceros*	HeavyCover	MML	55.28
AMNH70328	*Tragelaphus strepsiceros*	HeavyCover	MML	50.29
AMNH70328a	*Tragelaphus strepsiceros*	HeavyCover	MML	8.64
AMNH113810	*Addax nasomaculatus*	Open	PMTD	6.35
AMNH113811	*Addax nasomaculatus*	Open	PMTD	6.83
AMNH113812	*Addax nasomaculatus*	Open	PMTD	7.41
AMNH113813	*Addax nasomaculatus*	Open	PMTD	6.5
AMNH81690	*Aepyceros melampus*	LightCover	PMTD	6.33
AMNH82050	*Aepyceros melampus*	LightCover	PMTD	6.54
AMNH83534	*Aepyceros melampus*	LightCover	PMTD	7.63
AMNH85150	*Aepyceros melampus*	LightCover	PMTD	6.97
AMNH233038	*Alcelaphus buselaphus*	Open	PMTD	6.83
AMNH34717	*Alcelaphus buselaphus*	Open	PMTD	4.28
AMNH34725	*Alcelaphus buselaphus*	Open	PMTD	7.69
AMNH82033	*Alcelaphus buselaphus*	Open	PMTD	6.56
AMNH82159	*Alcelaphus buselaphus*	Open	PMTD	8.61
AMNH16048	*Ammotragus lervia*	NA	PMTD	4.13
AMNH81740	*Antidorcas marsupialis*	Open	PMTD	5.71
AMNH81745	*Antidorcas marsupialis*	Open	PMTD	5.03
AMNH83549	*Antidorcas marsupialis*	Open	PMTD	5.48
AMNH83550	*Antidorcas marsupialis*	Open	PMTD	3.85
AMNH35527	*Antilope cervicapra*	Open	PMTD	4.91
AMNH35957	*Antilope cervicapra*	Open	PMTD	5.44
AMNH54486	*Antilope cervicapra*	Open	PMTD	5.22
AMNH88406	*Beatragus hunteri*	Open	PMTD	7.8
AMNH88407	*Beatragus hunteri*	Open	PMTD	7.95
AMNH88408	*Beatragus hunteri*	Open	PMTD	7.77
AMNH54765	*Bubalus bubalis*	NA	PMTD	26.5
AMNH54766	*Bubalus bubalis*	NA	PMTD	26.65
AMNH52875	*Cephalophus dorsalis*	Forest	PMTD	4.19
AMNH52876	*Cephalophus dorsalis*	Forest	PMTD	4.81
AMNH52884	*Cephalophus dorsalis*	Forest	PMTD	8
AMNH52888	*Cephalophus dorsalis*	Forest	PMTD	7.42
AMNH52775	*Cephalophus leucogaster*	Forest	PMTD	3.78
AMNH52778	*Cephalophus leucogaster*	Forest	PMTD	3.86
AMNH52788	*Cephalophus leucogaster*	Forest	PMTD	3.45
AMNH216375	*Cephalophus natalensis*	Forest	PMTD	3.48
AMNH54391	*Cephalophus natalensis*	Forest	PMTD	3.3

AMNH81686	*Cephalophus natalensis*	Forest	PMTD	3.87
AMNH83387	*Cephalophus natalensis*	Forest	PMTD	3.32
AMNH52930	*Cephalophus nigrifrons*	Forest	PMTD	6.38
AMNH52931	*Cephalophus nigrifrons*	Forest	PMTD	3.81
AMNH52940	*Cephalophus nigrifrons*	Forest	PMTD	6.59
AMNH52943	*Cephalophus nigrifrons*	Forest	PMTD	6
AMNH53138	*Cephalophus silvicultor*	Forest	PMTD	6.81
AMNH53144	*Cephalophus silvicultor*	Forest	PMTD	6.59
AMNH53153	*Cephalophus silvicultor*	Forest	PMTD	6.82
AMNH52992	*Cephalophus weynsi*	Forest	PMTD	3.66
AMNH52995	*Cephalophus weynsi*	Forest	PMTD	3.92
AMNH52999	*Cephalophus weynsi*	Forest	PMTD	3.58
AMNH88429	*Cephalophus weynsi*	Forest	PMTD	3.58
AMNH81716	*Connochaetes gnou*	Open	PMTD	6.35
AMNH81720	*Connochaetes gnou*	Open	PMTD	8.2
AMNH81722	*Connochaetes gnou*	Open	PMTD	8.3
AMNH27824	*Connochaetes taurinus*	Open	PMTD	8.91
AMNH54133	*Connochaetes taurinus*	Open	PMTD	7.95
AMNH83502	*Connochaetes taurinus*	Open	PMTD	8.46
AMNH83503	*Connochaetes taurinus*	Open	PMTD	7.83
AMNH113781	*Damaliscus lunatus*	Open	PMTD	8.91
AMNH34729	*Damaliscus lunatus*	Open	PMTD	8.29
AMNH34730	*Damaliscus lunatus*	Open	PMTD	8.04
AMNH82035	*Damaliscus lunatus*	Open	PMTD	7.64
AMNH42953	*Damaliscus pygargus*	Open	PMTD	6.06
AMNH81727	*Damaliscus pygargus*	Open	PMTD	6.41
AMNH81729	*Damaliscus pygargus*	Open	PMTD	5.28
AMNH81787	*Damaliscus pygargus*	Open	PMTD	5.7
AMNH81997	*Eudorcas thomsonii*	Open	PMTD	4.47
AMNH82059	*Eudorcas thomsonii*	Open	PMTD	4.89
AMNH82060	*Eudorcas thomsonii*	Open	PMTD	4.82
AMNH88415	*Eudorcas thomsonii*	Open	PMTD	4.71
AMNH54506	*Gazella gazella*	Open	PMTD	4.59
AMNH54997	*Gazella gazella*	Open	PMTD	4.11
AMNH54998	*Gazella gazella*	Open	PMTD	4.29
AMNH80143	*Hippotragus equinus*	Open	PMTD	8.57
AMNH87217	*Hippotragus equinus*	Open	PMTD	10.21
AMNH216381	*Hippotragus niger*	LightCover	PMTD	9.48

AMNH80458	*Hippotragus niger*	LightCover	PMTD	9.58
AMNH80461	*Hippotragus niger*	LightCover	PMTD	9.87
AMNH83476	*Hippotragus niger*	LightCover	PMTD	8.92
AMNH53492	*Kobus ellipsiprymnus*	HeavyCover	PMTD	9.96
NMNH173877	*Kobus ellipsiprymnus*	HeavyCover	PMTD	7.83
NMNH21898	*Kobus ellipsiprymnus*	HeavyCover	PMTD	8.79
AMNH36396	*Kobus kob*	LightCover	PMTD	5.61
AMNH36397	*Kobus kob*	LightCover	PMTD	6.27
AMNH82129	*Kobus kob*	LightCover	PMTD	5.3
AMNH82130	*Kobus kob*	LightCover	PMTD	6.34
AMNH82173	*Kobus kob*	LightCover	PMTD	6.28
AMNH70010	*Kobus leche*	HeavyCover	PMTD	12.2
AMNH99649	*Kobus leche*	HeavyCover	PMTD	6.05
NMNH254927	*Kobus leche*	HeavyCover	PMTD	5.63
AMNH113784	*Kobus megaceros*	HeavyCover	PMTD	6.73
AMNH82135	*Kobus megaceros*	HeavyCover	PMTD	5.31
AMNH82136	*Kobus megaceros*	HeavyCover	PMTD	7.4
AMNH82137	*Kobus megaceros*	HeavyCover	PMTD	6.42
AMNH35323	*Kobus vardonii*	HeavyCover	PMTD	6.08
AMNH70057	*Kobus vardonii*	HeavyCover	PMTD	6.13
AMNH81687	*Kobus vardonii*	HeavyCover	PMTD	6.59
AMNH81170	*Litocranius walleri*	LightCover	PMTD	6.08
NMNH164031	*Litocranius walleri*	LightCover	PMTD	5.1
NMNH164033	*Litocranius walleri*	LightCover	PMTD	5.36
NMNH259457	*Litocranius walleri*	LightCover	PMTD	6.64
AMNH187824	*Madoqua kirkii*	HeavyCover	PMTD	1.75
AMNH82076	*Madoqua kirkii*	HeavyCover	PMTD	1.93
NMNH538104	*Madoqua kirkii*	HeavyCover	PMTD	2.73
NMNH538106	*Madoqua kirkii*	HeavyCover	PMTD	2.35
NMNH541419	*Madoqua kirkii*	HeavyCover	PMTD	2.39
AMNH82051	*Nanger granti*	Open	PMTD	6.71
AMNH82056	*Nanger granti*	Open	PMTD	6.62
AMNH82057	*Nanger granti*	Open	PMTD	6.85
AMNH85152	*Nanger granti*	Open	PMTD	6.26
AMNH80111	*Nanger soemmerringii*	Open	PMTD	6.29
NMNH582229	*Nanger soemmerringii*	Open	PMTD	5.65
AMNH53180	*Neotragus batesi*	Forest	PMTD	2.08
AMNH53181	*Neotragus batesi*	Forest	PMTD	2.05

AMNH53946	*Neotragus batesi*	Forest	PMTD	2.15
AMNH88426	*Neotragus moschatus*	Forest	PMTD	2.88
AMNH88427	*Neotragus moschatus*	Forest	PMTD	2.27
NMNH367449	*Neotragus moschatus*	Forest	PMTD	2.6
AMNH233033	*Oryx gazella*	Open	PMTD	16
AMNH82043	*Oryx gazella*	Open	PMTD	9.59
AMNH82044	*Oryx gazella*	Open	PMTD	9.46
AMNH87211	*Oryx gazella*	Open	PMTD	8.74
AMNH216387	*Ourebia ourebi*	LightCover	PMTD	4.26
AMNH53304	*Ourebia ourebi*	LightCover	PMTD	3.58
AMNH53328	*Ourebia ourebi*	LightCover	PMTD	4.95
AMNH269894	*Philantomba monticola*	Forest	PMTD	2.71
AMNH52726	*Philantomba monticola*	Forest	PMTD	2.23
AMNH52753	*Philantomba monticola*	Forest	PMTD	2.23
AMNH52758	*Philantomba monticola*	Forest	PMTD	2.26
AMNH216389	*Raphicerus campestris*	LightCover	PMTD	3.76
AMNH233047	*Raphicerus campestris*	LightCover	PMTD	3.73
AMNH34728	*Raphicerus campestris*	LightCover	PMTD	3.38
AMNH80538	*Raphicerus campestris*	LightCover	PMTD	4.18
AMNH35493	*Redunca arundinum*	LightCover	PMTD	7.5
AMNH80506	*Redunca arundinum*	LightCover	PMTD	6.21
NMNH367428	*Redunca arundinum*	LightCover	PMTD	6.83
NMNH367452	*Redunca arundinum*	LightCover	PMTD	9.64
NMNH469909	*Redunca arundinum*	LightCover	PMTD	4.89
AMNH27803	*Redunca fulvorufula*	LightCover	PMTD	4.4
AMNH82063	*Redunca fulvorufula*	LightCover	PMTD	3.93
AMNH82066	*Redunca fulvorufula*	LightCover	PMTD	4.89
AMNH82067	*Redunca fulvorufula*	LightCover	PMTD	4.64
AMNH53294	*Redunca redunca*	LightCover	PMTD	5.39
AMNH53296	*Redunca redunca*	LightCover	PMTD	5.53
AMNH90234	*Rupicapra rupicapra*	NA	PMTD	4.64
AMNH90235	*Rupicapra rupicapra*	NA	PMTD	4.13
AMNH90236	*Rupicapra rupicapra*	NA	PMTD	4.73
AMNH17276	*Sigmoceros lichtensteinii*	Open	PMTD	8.55
AMNH216382	*Sigmoceros lichtensteinii*	Open	PMTD	9.87
AMNH216383	*Sigmoceros lichtensteinii*	Open	PMTD	9.15
AMNH53088	*Sylvicapra grimmia*	LightCover	PMTD	3.24
AMNH53092	*Sylvicapra grimmia*	LightCover	PMTD	3.21

AMNH80562	*Sylvicapra grimmia*	LightCover	PMTD	3.67
AMNH80563	*Sylvicapra grimmia*	LightCover	PMTD	3.71
AMNH53583	*Syncerus caffer*	LightCover	PMTD	19.15
AMNH82005	*Syncerus caffer*	LightCover	PMTD	23.5
AMNH82006	*Syncerus caffer*	LightCover	PMTD	23
AMNH82009	*Syncerus caffer*	LightCover	PMTD	12.91
AMNH53519	*Taurotragus derbianus*	HeavyCover	PMTD	11.84
AMNH53521	*Taurotragus derbianus*	HeavyCover	PMTD	11.51
AMNH53522	*Taurotragus derbianus*	HeavyCover	PMTD	12.88
AMNH53523	*Taurotragus derbianus*	HeavyCover	PMTD	11.95
AMNH27811	*Taurotragus oryx*	LightCover	PMTD	11.94
AMNH34722	*Taurotragus oryx*	LightCover	PMTD	10.92
AMNH54386	*Tragelaphus angasii*	HeavyCover	PMTD	7.33
AMNH54387	*Tragelaphus angasii*	HeavyCover	PMTD	7.2
AMNH54390	*Tragelaphus angasii*	HeavyCover	PMTD	7.48
AMNH81002	*Tragelaphus buxtoni*	Forest	PMTD	8.53
AMNH81003	*Tragelaphus buxtoni*	Forest	PMTD	7.34
AMNH81004	*Tragelaphus buxtoni*	Forest	PMTD	8.98
AMNH81014	*Tragelaphus buxtoni*	Forest	PMTD	7.12
AMNH81033	*Tragelaphus buxtoni*	Forest	PMTD	15.5
AMNH53271	*Tragelaphus eurycerus*	Forest	PMTD	9.07
AMNH53279	*Tragelaphus eurycerus*	Forest	PMTD	9.61
AMNH53280	*Tragelaphus eurycerus*	Forest	PMTD	9.02
AMNH36416	*Tragelaphus imberbis*	HeavyCover	PMTD	8.65
AMNH36417	*Tragelaphus imberbis*	HeavyCover	PMTD	7.25
AMNH82019	*Tragelaphus imberbis*	HeavyCover	PMTD	8.78
AMNH82023	*Tragelaphus imberbis*	HeavyCover	PMTD	7.42
AMNH187806	*Tragelaphus scriptus*	Forest	PMTD	5.69
AMNH216371	*Tragelaphus scriptus*	Forest	PMTD	4.66
AMNH88425	*Tragelaphus scriptus*	Forest	PMTD	5.72
AMNH53209	*Tragelaphus spekii*	HeavyCover	PMTD	6.45
AMNH53212	*Tragelaphus spekii*	HeavyCover	PMTD	7.87
AMNH53213	*Tragelaphus spekii*	HeavyCover	PMTD	5.72
AMNH53216	*Tragelaphus spekii*	HeavyCover	PMTD	6.16
AMNH233027	*Tragelaphus strepsiceros*	HeavyCover	PMTD	10.05
AMNH70328	*Tragelaphus strepsiceros*	HeavyCover	PMTD	8.46
AMNH70328a	*Tragelaphus strepsiceros*	HeavyCover	PMTD	15.65
AMNH113810	*Addax nasomaculatus*	Open	ProxRad	12.5

AMNH113811	*Addax nasomaculatus*	Open	ProxRad	12
AMNH113812	*Addax nasomaculatus*	Open	ProxRad	12
AMNH113813	*Addax nasomaculatus*	Open	ProxRad	12.62
AMNH81690	*Aepyceros melampus*	LightCover	ProxRad	10
AMNH82050	*Aepyceros melampus*	LightCover	ProxRad	10.5
AMNH83534	*Aepyceros melampus*	LightCover	ProxRad	10.65
AMNH85150	*Aepyceros melampus*	LightCover	ProxRad	10
AMNH233038	*Alcelaphus buselaphus*	Open	ProxRad	13.85
AMNH34717	*Alcelaphus buselaphus*	Open	ProxRad	10.91
AMNH34725	*Alcelaphus buselaphus*	Open	ProxRad	16.14
AMNH82033	*Alcelaphus buselaphus*	Open	ProxRad	14.26
AMNH82159	*Alcelaphus buselaphus*	Open	ProxRad	15
AMNH16048	*Ammotragus lervia*	NA	ProxRad	10.87
AMNH81740	*Antidorcas marsupialis*	Open	ProxRad	9
AMNH81745	*Antidorcas marsupialis*	Open	ProxRad	8.43
AMNH83549	*Antidorcas marsupialis*	Open	ProxRad	9.06
AMNH83550	*Antidorcas marsupialis*	Open	ProxRad	8.16
AMNH35527	*Antilope cervicapra*	Open	ProxRad	9.5
AMNH35957	*Antilope cervicapra*	Open	ProxRad	9.5
AMNH54486	*Antilope cervicapra*	Open	ProxRad	9.63
AMNH88406	*Beatragus hunteri*	Open	ProxRad	13.32
AMNH88407	*Beatragus hunteri*	Open	ProxRad	12
AMNH88408	*Beatragus hunteri*	Open	ProxRad	12.15
AMNH54765	*Bubalus bubalis*	NA	ProxRad	NA
AMNH54766	*Bubalus bubalis*	NA	ProxRad	NA
AMNH52875	*Cephalophus dorsalis*	Forest	ProxRad	7.5
AMNH52876	*Cephalophus dorsalis*	Forest	ProxRad	8.29
AMNH52884	*Cephalophus dorsalis*	Forest	ProxRad	NA
AMNH52888	*Cephalophus dorsalis*	Forest	ProxRad	NA
AMNH52775	*Cephalophus leucogaster*	Forest	ProxRad	7.17
AMNH52778	*Cephalophus leucogaster*	Forest	ProxRad	6.88
AMNH52788	*Cephalophus leucogaster*	Forest	ProxRad	7.28
AMNH216375	*Cephalophus natalensis*	Forest	ProxRad	7.84
AMNH54391	*Cephalophus natalensis*	Forest	ProxRad	7.21
AMNH81686	*Cephalophus natalensis*	Forest	ProxRad	6.33
AMNH83387	*Cephalophus natalensis*	Forest	ProxRad	6.79
AMNH52930	*Cephalophus nigrifrons*	Forest	ProxRad	NA
AMNH52931	*Cephalophus nigrifrons*	Forest	ProxRad	6.87

AMNH52940	*Cephalophus nigrifrons*	Forest	ProxRad	NA
AMNH52943	*Cephalophus nigrifrons*	Forest	ProxRad	NA
AMNH53138	*Cephalophus silvicultor*	Forest	ProxRad	12.14
AMNH53144	*Cephalophus silvicultor*	Forest	ProxRad	11.84
AMNH53153	*Cephalophus silvicultor*	Forest	ProxRad	11.64
AMNH52992	*Cephalophus weynsi*	Forest	ProxRad	7.8
AMNH52995	*Cephalophus weynsi*	Forest	ProxRad	7.87
AMNH52999	*Cephalophus weynsi*	Forest	ProxRad	7.8
AMNH88429	*Cephalophus weynsi*	Forest	ProxRad	7.24
AMNH81716	*Connochaetes gnou*	Open	ProxRad	13.2
AMNH81720	*Connochaetes gnou*	Open	ProxRad	13.88
AMNH81722	*Connochaetes gnou*	Open	ProxRad	15.5
AMNH27824	*Connochaetes taurinus*	Open	ProxRad	15.32
AMNH54133	*Connochaetes taurinus*	Open	ProxRad	16.77
AMNH83502	*Connochaetes taurinus*	Open	ProxRad	17.34
AMNH83503	*Connochaetes taurinus*	Open	ProxRad	15.84
AMNH113781	*Damaliscus lunatus*	Open	ProxRad	14.88
AMNH34729	*Damaliscus lunatus*	Open	ProxRad	13.85
AMNH34730	*Damaliscus lunatus*	Open	ProxRad	15.79
AMNH82035	*Damaliscus lunatus*	Open	ProxRad	13.63
AMNH42953	*Damaliscus pygargus*	Open	ProxRad	10.5
AMNH81727	*Damaliscus pygargus*	Open	ProxRad	11.24
AMNH81729	*Damaliscus pygargus*	Open	ProxRad	11.07
AMNH81787	*Damaliscus pygargus*	Open	ProxRad	11
AMNH81997	*Eudorcas thomsonii*	Open	ProxRad	7.34
AMNH82059	*Eudorcas thomsonii*	Open	ProxRad	7.17
AMNH82060	*Eudorcas thomsonii*	Open	ProxRad	7.67
AMNH88415	*Eudorcas thomsonii*	Open	ProxRad	6.71
AMNH54506	*Gazella gazella*	Open	ProxRad	6.4
AMNH54997	*Gazella gazella*	Open	ProxRad	6.57
AMNH54998	*Gazella gazella*	Open	ProxRad	6.7
AMNH80143	*Hippotragus equinus*	Open	ProxRad	15.76
AMNH87217	*Hippotragus equinus*	Open	ProxRad	19.78
AMNH216381	*Hippotragus niger*	LightCover	ProxRad	16.5
AMNH80458	*Hippotragus niger*	LightCover	ProxRad	17
AMNH80461	*Hippotragus niger*	LightCover	ProxRad	17
AMNH83476	*Hippotragus niger*	LightCover	ProxRad	16.5
AMNH53492	*Kobus ellipsiprymnus*	HeavyCover	ProxRad	16

NMNH173877	*Kobus ellipsiprymnus*	HeavyCover	ProxRad	15.5
NMNH21898	*Kobus ellipsiprymnus*	HeavyCover	ProxRad	16.26
AMNH36396	*Kobus kob*	LightCover	ProxRad	12.27
AMNH36397	*Kobus kob*	LightCover	ProxRad	11.09
AMNH82129	*Kobus kob*	LightCover	ProxRad	11
AMNH82130	*Kobus kob*	LightCover	ProxRad	12
AMNH82173	*Kobus kob*	LightCover	ProxRad	11.44
AMNH70010	*Kobus leche*	HeavyCover	ProxRad	NA
AMNH99649	*Kobus leche*	HeavyCover	ProxRad	12.5
NMNH254927	*Kobus leche*	HeavyCover	ProxRad	11.5
AMNH113784	*Kobus megaceros*	HeavyCover	ProxRad	11.72
AMNH82135	*Kobus megaceros*	HeavyCover	ProxRad	12.72
AMNH82136	*Kobus megaceros*	HeavyCover	ProxRad	13
AMNH82137	*Kobus megaceros*	HeavyCover	ProxRad	11.24
AMNH35323	*Kobus vardonii*	HeavyCover	ProxRad	12.79
AMNH70057	*Kobus vardonii*	HeavyCover	ProxRad	12.28
AMNH81687	*Kobus vardonii*	HeavyCover	ProxRad	12.31
AMNH81170	*Litocranius walleri*	LightCover	ProxRad	9
NMNH164031	*Litocranius walleri*	LightCover	ProxRad	8.5
NMNH164033	*Litocranius walleri*	LightCover	ProxRad	8.5
NMNH259457	*Litocranius walleri*	LightCover	ProxRad	8.81
AMNH187824	*Madoqua kirkii*	HeavyCover	ProxRad	3.85
AMNH82076	*Madoqua kirkii*	HeavyCover	ProxRad	4.21
NMNH538104	*Madoqua kirkii*	HeavyCover	ProxRad	4.54
NMNH538106	*Madoqua kirkii*	HeavyCover	ProxRad	4.62
NMNH541419	*Madoqua kirkii*	HeavyCover	ProxRad	4.74
AMNH82051	*Nanger granti*	Open	ProxRad	10.5
AMNH82056	*Nanger granti*	Open	ProxRad	10
AMNH82057	*Nanger granti*	Open	ProxRad	9.66
AMNH85152	*Nanger granti*	Open	ProxRad	9.42
AMNH80111	*Nanger soemmerringii*	Open	ProxRad	9.2
NMNH582229	*Nanger soemmerringii*	Open	ProxRad	NA
AMNH53180	*Neotragus batesi*	Forest	ProxRad	3.45
AMNH53181	*Neotragus batesi*	Forest	ProxRad	3.67
AMNH53946	*Neotragus batesi*	Forest	ProxRad	3.58
AMNH88426	*Neotragus moschatus*	Forest	ProxRad	3.85
AMNH88427	*Neotragus moschatus*	Forest	ProxRad	3.95
NMNH367449	*Neotragus moschatus*	Forest	ProxRad	4.45

AMNH233033	*Oryx gazella*	Open	ProxRad	NA
AMNH82043	*Oryx gazella*	Open	ProxRad	15.5
AMNH82044	*Oryx gazella*	Open	ProxRad	14.5
AMNH87211	*Oryx gazella*	Open	ProxRad	14.81
AMNH216387	*Ourebia ourebi*	LightCover	ProxRad	7.57
AMNH53304	*Ourebia ourebi*	LightCover	ProxRad	6.72
AMNH53328	*Ourebia ourebi*	LightCover	ProxRad	6.14
AMNH269894	*Philantomba monticola*	Forest	ProxRad	4.45
AMNH52726	*Philantomba monticola*	Forest	ProxRad	4.39
AMNH52753	*Philantomba monticola*	Forest	ProxRad	4.26
AMNH52758	*Philantomba monticola*	Forest	ProxRad	4.5
AMNH216389	*Raphicerus campestris*	LightCover	ProxRad	5.38
AMNH233047	*Raphicerus campestris*	LightCover	ProxRad	5.38
AMNH34728	*Raphicerus campestris*	LightCover	ProxRad	5.61
AMNH80538	*Raphicerus campestris*	LightCover	ProxRad	6
AMNH35493	*Redunca arundinum*	LightCover	ProxRad	10
AMNH80506	*Redunca arundinum*	LightCover	ProxRad	11
NMNH367428	*Redunca arundinum*	LightCover	ProxRad	9.91
NMNH367452	*Redunca arundinum*	LightCover	ProxRad	NA
NMNH469909	*Redunca arundinum*	LightCover	ProxRad	8.77
AMNH27803	*Redunca fulvorufula*	LightCover	ProxRad	8.78
AMNH82063	*Redunca fulvorufula*	LightCover	ProxRad	8.5
AMNH82066	*Redunca fulvorufula*	LightCover	ProxRad	8.14
AMNH82067	*Redunca fulvorufula*	LightCover	ProxRad	8.71
AMNH53294	*Redunca redunca*	LightCover	ProxRad	9.5
AMNH53296	*Redunca redunca*	LightCover	ProxRad	9.88
AMNH90234	*Rupicapra rupicapra*	NA	ProxRad	8.64
AMNH90235	*Rupicapra rupicapra*	NA	ProxRad	10.12
AMNH90236	*Rupicapra rupicapra*	NA	ProxRad	9
AMNH17276	*Sigmoceros lichtensteinii*	Open	ProxRad	16.09
AMNH216382	*Sigmoceros lichtensteinii*	Open	ProxRad	14.82
AMNH216383	*Sigmoceros lichtensteinii*	Open	ProxRad	14.72
AMNH53088	*Sylvicapra grimmia*	LightCover	ProxRad	6.42
AMNH53092	*Sylvicapra grimmia*	LightCover	ProxRad	6.26
AMNH80562	*Sylvicapra grimmia*	LightCover	ProxRad	6.75
AMNH80563	*Sylvicapra grimmia*	LightCover	ProxRad	6.88
AMNH53583	*Syncerus caffer*	LightCover	ProxRad	NA
AMNH82005	*Syncerus caffer*	LightCover	ProxRad	NA

AMNH82006	*Syncerus caffer*	LightCover	ProxRad	NA
AMNH82009	*Syncerus caffer*	LightCover	ProxRad	22.5
AMNH53519	*Taurotragus derbianus*	HeavyCover	ProxRad	25
AMNH53521	*Taurotragus derbianus*	HeavyCover	ProxRad	21.23
AMNH53522	*Taurotragus derbianus*	HeavyCover	ProxRad	23.19
AMNH53523	*Taurotragus derbianus*	HeavyCover	ProxRad	23.5
AMNH27811	*Taurotragus oryx*	LightCover	ProxRad	23.2
AMNH34722	*Taurotragus oryx*	LightCover	ProxRad	20.5
AMNH54386	*Tragelaphus angasii*	HeavyCover	ProxRad	11.88
AMNH54387	*Tragelaphus angasii*	HeavyCover	ProxRad	12.88
AMNH54390	*Tragelaphus angasii*	HeavyCover	ProxRad	12.82
AMNH81002	*Tragelaphus buxtoni*	Forest	ProxRad	17.61
AMNH81003	*Tragelaphus buxtoni*	Forest	ProxRad	16.15
AMNH81004	*Tragelaphus buxtoni*	Forest	ProxRad	18.15
AMNH81014	*Tragelaphus buxtoni*	Forest	ProxRad	16.18
AMNH81033	*Tragelaphus buxtoni*	Forest	ProxRad	NA
AMNH53271	*Tragelaphus eurycerus*	Forest	ProxRad	17.5
AMNH53279	*Tragelaphus eurycerus*	Forest	ProxRad	18.5
AMNH53280	*Tragelaphus eurycerus*	Forest	ProxRad	17.78
AMNH36416	*Tragelaphus imberbis*	HeavyCover	ProxRad	12.23
AMNH36417	*Tragelaphus imberbis*	HeavyCover	ProxRad	11.25
AMNH82019	*Tragelaphus imberbis*	HeavyCover	ProxRad	13.5
AMNH82023	*Tragelaphus imberbis*	HeavyCover	ProxRad	11.23
AMNH187806	*Tragelaphus scriptus*	Forest	ProxRad	8.65
AMNH216371	*Tragelaphus scriptus*	Forest	ProxRad	9.62
AMNH88425	*Tragelaphus scriptus*	Forest	ProxRad	11
AMNH53209	*Tragelaphus spekii*	HeavyCover	ProxRad	13.5
AMNH53212	*Tragelaphus spekii*	HeavyCover	ProxRad	11.26
AMNH53213	*Tragelaphus spekii*	HeavyCover	ProxRad	11.36
AMNH53216	*Tragelaphus spekii*	HeavyCover	ProxRad	12.5
AMNH233027	*Tragelaphus strepsiceros*	HeavyCover	ProxRad	17.86
AMNH70328	*Tragelaphus strepsiceros*	HeavyCover	ProxRad	15.5
AMNH70328a	*Tragelaphus strepsiceros*	HeavyCover	ProxRad	NA
AMNH113810	*Addax nasomaculatus*	Open	PTArea	1401.48
AMNH113811	*Addax nasomaculatus*	Open	PTArea	1237.05
AMNH113812	*Addax nasomaculatus*	Open	PTArea	1378.74
AMNH113813	*Addax nasomaculatus*	Open	PTArea	1213.05
AMNH81690	*Aepyceros melampus*	LightCover	PTArea	915.5

AMNH82050	*Aepyceros melampus*	LightCover	PTArea	841.79
AMNH83534	*Aepyceros melampus*	LightCover	PTArea	976.25
AMNH85150	*Aepyceros melampus*	LightCover	PTArea	841.71
AMNH233038	*Alcelaphus buselaphus*	Open	PTArea	1557.05
AMNH34717	*Alcelaphus buselaphus*	Open	PTArea	1139.5
AMNH34725	*Alcelaphus buselaphus*	Open	PTArea	1765.78
AMNH82033	*Alcelaphus buselaphus*	Open	PTArea	1372.77
AMNH82159	*Alcelaphus buselaphus*	Open	PTArea	1762.3
AMNH16048	*Ammotragus lervia*	NA	PTArea	1121.71
AMNH81740	*Antidorcas marsupialis*	Open	PTArea	651.28
AMNH81745	*Antidorcas marsupialis*	Open	PTArea	605.17
AMNH83549	*Antidorcas marsupialis*	Open	PTArea	613.04
AMNH83550	*Antidorcas marsupialis*	Open	PTArea	557.37
AMNH35527	*Antilope cervicapra*	Open	PTArea	729.66
AMNH35957	*Antilope cervicapra*	Open	PTArea	671.99
AMNH54486	*Antilope cervicapra*	Open	PTArea	756.46
AMNH88406	*Beatragus hunteri*	Open	PTArea	1343.08
AMNH88407	*Beatragus hunteri*	Open	PTArea	1158.33
AMNH88408	*Beatragus hunteri*	Open	PTArea	1259.46
AMNH54765	*Bubalus bubalis*	NA	PTArea	62.16
AMNH54766	*Bubalus bubalis*	NA	PTArea	59.68
AMNH52875	*Cephalophus dorsalis*	Forest	PTArea	358.75
AMNH52876	*Cephalophus dorsalis*	Forest	PTArea	471.34
AMNH52884	*Cephalophus dorsalis*	Forest	PTArea	17
AMNH52888	*Cephalophus dorsalis*	Forest	PTArea	16.36
AMNH52775	*Cephalophus leucogaster*	Forest	PTArea	347.19
AMNH52778	*Cephalophus leucogaster*	Forest	PTArea	393.16
AMNH52788	*Cephalophus leucogaster*	Forest	PTArea	367.75
AMNH216375	*Cephalophus natalensis*	Forest	PTArea	424.42
AMNH54391	*Cephalophus natalensis*	Forest	PTArea	327.79
AMNH81686	*Cephalophus natalensis*	Forest	PTArea	312.42
AMNH83387	*Cephalophus natalensis*	Forest	PTArea	363.17
AMNH52930	*Cephalophus nigrifrons*	Forest	PTArea	13.7
AMNH52931	*Cephalophus nigrifrons*	Forest	PTArea	302.57
AMNH52940	*Cephalophus nigrifrons*	Forest	PTArea	14.36
AMNH52943	*Cephalophus nigrifrons*	Forest	PTArea	12.88
AMNH53138	*Cephalophus silvicultor*	Forest	PTArea	1039.18
AMNH53144	*Cephalophus silvicultor*	Forest	PTArea	1174.81

AMNH53153	*Cephalophus silvicultor*	Forest	PTArea	940.4
AMNH52992	*Cephalophus weynsi*	Forest	PTArea	370.71
AMNH52995	*Cephalophus weynsi*	Forest	PTArea	409.34
AMNH52999	*Cephalophus weynsi*	Forest	PTArea	398.92
AMNH88429	*Cephalophus weynsi*	Forest	PTArea	340.52
AMNH81716	*Connochaetes gnou*	Open	PTArea	1400.92
AMNH81720	*Connochaetes gnou*	Open	PTArea	1558.15
AMNH81722	*Connochaetes gnou*	Open	PTArea	1841.1
AMNH27824	*Connochaetes taurinus*	Open	PTArea	2176.18
AMNH54133	*Connochaetes taurinus*	Open	PTArea	2322.19
AMNH83502	*Connochaetes taurinus*	Open	PTArea	2315.56
AMNH83503	*Connochaetes taurinus*	Open	PTArea	2068.94
AMNH113781	*Damaliscus lunatus*	Open	PTArea	1634.64
AMNH34729	*Damaliscus lunatus*	Open	PTArea	1467.76
AMNH34730	*Damaliscus lunatus*	Open	PTArea	1769.59
AMNH82035	*Damaliscus lunatus*	Open	PTArea	1534.64
AMNH42953	*Damaliscus pygargus*	Open	PTArea	946.73
AMNH81727	*Damaliscus pygargus*	Open	PTArea	974.27
AMNH81729	*Damaliscus pygargus*	Open	PTArea	974.33
AMNH81787	*Damaliscus pygargus*	Open	PTArea	961.07
AMNH81997	*Eudorcas thomsonii*	Open	PTArea	464.71
AMNH82059	*Eudorcas thomsonii*	Open	PTArea	429.5
AMNH82060	*Eudorcas thomsonii*	Open	PTArea	462.36
AMNH88415	*Eudorcas thomsonii*	Open	PTArea	384.13
AMNH54506	*Gazella gazella*	Open	PTArea	356.57
AMNH54997	*Gazella gazella*	Open	PTArea	380.63
AMNH54998	*Gazella gazella*	Open	PTArea	356.71
AMNH80143	*Hippotragus equinus*	Open	PTArea	2108.99
AMNH87217	*Hippotragus equinus*	Open	PTArea	2872.32
AMNH216381	*Hippotragus niger*	LightCover	PTArea	2448.57
AMNH80458	*Hippotragus niger*	LightCover	PTArea	2566.2
AMNH80461	*Hippotragus niger*	LightCover	PTArea	2724.97
AMNH83476	*Hippotragus niger*	LightCover	PTArea	2125.74
AMNH53492	*Kobus ellipsiprymnus*	HeavyCover	PTArea	2318.97
NMNH173877	*Kobus ellipsiprymnus*	HeavyCover	PTArea	1934.89
NMNH21898	*Kobus ellipsiprymnus*	HeavyCover	PTArea	2020.46
AMNH36396	*Kobus kob*	LightCover	PTArea	1248.81
AMNH36397	*Kobus kob*	LightCover	PTArea	1040.56

AMNH82129	*Kobus kob*	LightCover	PTArea	1107.86
AMNH82130	*Kobus kob*	LightCover	PTArea	1314.36
AMNH82173	*Kobus kob*	LightCover	PTArea	1010.56
AMNH70010	*Kobus leche*	HeavyCover	PTArea	28.44
AMNH99649	*Kobus leche*	HeavyCover	PTArea	1271.03
NMNH254927	*Kobus leche*	HeavyCover	PTArea	1188.18
AMNH113784	*Kobus megaceros*	HeavyCover	PTArea	1082.97
AMNH82135	*Kobus megaceros*	HeavyCover	PTArea	1204.09
AMNH82136	*Kobus megaceros*	HeavyCover	PTArea	1350.28
AMNH82137	*Kobus megaceros*	HeavyCover	PTArea	1040.22
AMNH35323	*Kobus vardonii*	HeavyCover	PTArea	1384.85
AMNH70057	*Kobus vardonii*	HeavyCover	PTArea	1208.32
AMNH81687	*Kobus vardonii*	HeavyCover	PTArea	1174
AMNH81170	*Litocranius walleri*	LightCover	PTArea	713.32
NMNH164031	*Litocranius walleri*	LightCover	PTArea	NA
NMNH164033	*Litocranius walleri*	LightCover	PTArea	683.43
NMNH259457	*Litocranius walleri*	LightCover	PTArea	702.85
AMNH187824	*Madoqua kirkii*	HeavyCover	PTArea	131.65
AMNH82076	*Madoqua kirkii*	HeavyCover	PTArea	143.26
NMNH538104	*Madoqua kirkii*	HeavyCover	PTArea	149.02
NMNH538106	*Madoqua kirkii*	HeavyCover	PTArea	154.67
NMNH541419	*Madoqua kirkii*	HeavyCover	PTArea	151.13
AMNH82051	*Nanger granti*	Open	PTArea	910.73
AMNH82056	*Nanger granti*	Open	PTArea	858.96
AMNH82057	*Nanger granti*	Open	PTArea	860.86
AMNH85152	*Nanger granti*	Open	PTArea	735.36
AMNH80111	*Nanger soemmerringii*	Open	PTArea	520.12
NMNH582229	*Nanger soemmerringii*	Open	PTArea	777.71
AMNH53180	*Neotragus batesi*	Forest	PTArea	95.68
AMNH53181	*Neotragus batesi*	Forest	PTArea	94.12
AMNH53946	*Neotragus batesi*	Forest	PTArea	105.05
AMNH88426	*Neotragus moschatus*	Forest	PTArea	122.09
AMNH88427	*Neotragus moschatus*	Forest	PTArea	122.09
NMNH367449	*Neotragus moschatus*	Forest	PTArea	167.4
AMNH233033	*Oryx gazella*	Open	PTArea	35.3
AMNH82043	*Oryx gazella*	Open	PTArea	2058.98
AMNH82044	*Oryx gazella*	Open	PTArea	1666.91
AMNH87211	*Oryx gazella*	Open	PTArea	1921.99

AMNH216387	*Ourebia ourebi*	LightCover	PTArea	392.9
AMNH53304	*Ourebia ourebi*	LightCover	PTArea	360.38
AMNH53328	*Ourebia ourebi*	LightCover	PTArea	357.56
AMNH269894	*Philantomba monticola*	Forest	PTArea	131.69
AMNH52726	*Philantomba monticola*	Forest	PTArea	122.42
AMNH52753	*Philantomba monticola*	Forest	PTArea	NA
AMNH52758	*Philantomba monticola*	Forest	PTArea	137.09
AMNH216389	*Raphicerus campestris*	LightCover	PTArea	318.55
AMNH233047	*Raphicerus campestris*	LightCover	PTArea	291.58
AMNH34728	*Raphicerus campestris*	LightCover	PTArea	285.59
AMNH80538	*Raphicerus campestris*	LightCover	PTArea	355.25
AMNH35493	*Redunca arundinum*	LightCover	PTArea	995.84
AMNH80506	*Redunca arundinum*	LightCover	PTArea	862.6
NMNH367428	*Redunca arundinum*	LightCover	PTArea	900.7
NMNH367452	*Redunca arundinum*	LightCover	PTArea	24.26
NMNH469909	*Redunca arundinum*	LightCover	PTArea	596.04
AMNH27803	*Redunca fulvorufula*	LightCover	PTArea	628.68
AMNH82063	*Redunca fulvorufula*	LightCover	PTArea	615.89
AMNH82066	*Redunca fulvorufula*	LightCover	PTArea	584.19
AMNH82067	*Redunca fulvorufula*	LightCover	PTArea	614.91
AMNH53294	*Redunca redunca*	LightCover	PTArea	807.12
AMNH53296	*Redunca redunca*	LightCover	PTArea	871.68
AMNH90234	*Rupicapra rupicapra*	NA	PTArea	649.53
AMNH90235	*Rupicapra rupicapra*	NA	PTArea	686.98
AMNH90236	*Rupicapra rupicapra*	NA	PTArea	662.01
AMNH17276	*Sigmoceros lichtensteinii*	Open	PTArea	1848.67
AMNH216382	*Sigmoceros lichtensteinii*	Open	PTArea	NA
AMNH216383	*Sigmoceros lichtensteinii*	Open	PTArea	1842.76
AMNH53088	*Sylvicapra grimmia*	LightCover	PTArea	281.6
AMNH53092	*Sylvicapra grimmia*	LightCover	PTArea	302.17
AMNH80562	*Sylvicapra grimmia*	LightCover	PTArea	378.17
AMNH80563	*Sylvicapra grimmia*	LightCover	PTArea	381.05
AMNH53583	*Syncerus caffer*	LightCover	PTArea	43.45
AMNH82005	*Syncerus caffer*	LightCover	PTArea	54.19
AMNH82006	*Syncerus caffer*	LightCover	PTArea	53.64
AMNH82009	*Syncerus caffer*	LightCover	PTArea	4187.03
AMNH53519	*Taurotragus derbianus*	HeavyCover	PTArea	4413.41
AMNH53521	*Taurotragus derbianus*	HeavyCover	PTArea	3783.87

AMNH53522	*Taurotragus derbianus*	HeavyCover	PTArea	4109.68
AMNH53523	*Taurotragus derbianus*	HeavyCover	PTArea	4011.52
AMNH27811	*Taurotragus oryx*	LightCover	PTArea	4082.54
AMNH34722	*Taurotragus oryx*	LightCover	PTArea	3350.05
AMNH54386	*Tragelaphus angasii*	HeavyCover	PTArea	1164.27
AMNH54387	*Tragelaphus angasii*	HeavyCover	PTArea	1387.05
AMNH54390	*Tragelaphus angasii*	HeavyCover	PTArea	1174.23
AMNH81002	*Tragelaphus buxtoni*	Forest	PTArea	2260.62
AMNH81003	*Tragelaphus buxtoni*	Forest	PTArea	1931.86
AMNH81004	*Tragelaphus buxtoni*	Forest	PTArea	2319.87
AMNH81014	*Tragelaphus buxtoni*	Forest	PTArea	1845.88
AMNH81033	*Tragelaphus buxtoni*	Forest	PTArea	32.48
AMNH53271	*Tragelaphus eurycerus*	Forest	PTArea	2411.93
AMNH53279	*Tragelaphus eurycerus*	Forest	PTArea	2520.69
AMNH53280	*Tragelaphus eurycerus*	Forest	PTArea	2719.16
AMNH36416	*Tragelaphus imberbis*	HeavyCover	PTArea	1263.27
AMNH36417	*Tragelaphus imberbis*	HeavyCover	PTArea	1035.2
AMNH82019	*Tragelaphus imberbis*	HeavyCover	PTArea	1438.96
AMNH82023	*Tragelaphus imberbis*	HeavyCover	PTArea	1083.11
AMNH187806	*Tragelaphus scriptus*	Forest	PTArea	624.43
AMNH216371	*Tragelaphus scriptus*	Forest	PTArea	688.77
AMNH88425	*Tragelaphus scriptus*	Forest	PTArea	882.33
AMNH53209	*Tragelaphus spekii*	HeavyCover	PTArea	1627.85
AMNH53212	*Tragelaphus spekii*	HeavyCover	PTArea	1309.3
AMNH53213	*Tragelaphus spekii*	HeavyCover	PTArea	948.72
AMNH53216	*Tragelaphus spekii*	HeavyCover	PTArea	1108.21
AMNH233027	*Tragelaphus strepsiceros*	HeavyCover	PTArea	2401.12
AMNH70328	*Tragelaphus strepsiceros*	HeavyCover	PTArea	1859.71
AMNH70328a	*Tragelaphus strepsiceros*	HeavyCover	PTArea	35.08
AMNH113810	*Addax nasomaculatus*	Open	WAF	25.89
AMNH113811	*Addax nasomaculatus*	Open	WAF	25.42
AMNH113812	*Addax nasomaculatus*	Open	WAF	25.55
AMNH113813	*Addax nasomaculatus*	Open	WAF	24.89
AMNH81690	*Aepyceros melampus*	LightCover	WAF	21.39
AMNH82050	*Aepyceros melampus*	LightCover	WAF	22.47
AMNH83534	*Aepyceros melampus*	LightCover	WAF	22.07
AMNH85150	*Aepyceros melampus*	LightCover	WAF	22.55
AMNH233038	*Alcelaphus buselaphus*	Open	WAF	28.98

AMNH34717	*Alcelaphus buselaphus*	Open	WAF	24.04
AMNH34725	*Alcelaphus buselaphus*	Open	WAF	31.37
AMNH82033	*Alcelaphus buselaphus*	Open	WAF	28.7
AMNH82159	*Alcelaphus buselaphus*	Open	WAF	31.41
AMNH16048	*Ammotragus lervia*	NA	WAF	23.71
AMNH81740	*Antidorcas marsupialis*	Open	WAF	20.03
AMNH81745	*Antidorcas marsupialis*	Open	WAF	18.3
AMNH83549	*Antidorcas marsupialis*	Open	WAF	18.41
AMNH83550	*Antidorcas marsupialis*	Open	WAF	18.72
AMNH35527	*Antilope cervicapra*	Open	WAF	19.93
AMNH35957	*Antilope cervicapra*	Open	WAF	18.84
AMNH54486	*Antilope cervicapra*	Open	WAF	20.09
AMNH88406	*Beatragus hunteri*	Open	WAF	27.92
AMNH88407	*Beatragus hunteri*	Open	WAF	27.35
AMNH88408	*Beatragus hunteri*	Open	WAF	27.77
AMNH54765	*Bubalus bubalis*	NA	WAF	60.58
AMNH54766	*Bubalus bubalis*	NA	WAF	59.46
AMNH52875	*Cephalophus dorsalis*	Forest	WAF	15.43
AMNH52876	*Cephalophus dorsalis*	Forest	WAF	15.9
AMNH52884	*Cephalophus dorsalis*	Forest	WAF	17.17
AMNH52888	*Cephalophus dorsalis*	Forest	WAF	16.38
AMNH52775	*Cephalophus leucogaster*	Forest	WAF	14.15
AMNH52778	*Cephalophus leucogaster*	Forest	WAF	14.92
AMNH52788	*Cephalophus leucogaster*	Forest	WAF	14.57
AMNH216375	*Cephalophus natalensis*	Forest	WAF	15.8
AMNH54391	*Cephalophus natalensis*	Forest	WAF	13.14
AMNH81686	*Cephalophus natalensis*	Forest	WAF	13.55
AMNH83387	*Cephalophus natalensis*	Forest	WAF	15.58
AMNH52930	*Cephalophus nigrifrons*	Forest	WAF	14.81
AMNH52931	*Cephalophus nigrifrons*	Forest	WAF	14.35
AMNH52940	*Cephalophus nigrifrons*	Forest	WAF	15.26
AMNH52943	*Cephalophus nigrifrons*	Forest	WAF	14.59
AMNH53138	*Cephalophus silvicultor*	Forest	WAF	23.99
AMNH53144	*Cephalophus silvicultor*	Forest	WAF	25.26
AMNH53153	*Cephalophus silvicultor*	Forest	WAF	22.63
AMNH52992	*Cephalophus weynsi*	Forest	WAF	13.41
AMNH52995	*Cephalophus weynsi*	Forest	WAF	14.9
AMNH52999	*Cephalophus weynsi*	Forest	WAF	15.17

AMNH88429	*Cephalophus weynsi*	Forest	WAF	14.31
AMNH81716	*Connochaetes gnou*	Open	WAF	30.08
AMNH81720	*Connochaetes gnou*	Open	WAF	29.73
AMNH81722	*Connochaetes gnou*	Open	WAF	33.3
AMNH27824	*Connochaetes taurinus*	Open	WAF	33.75
AMNH54133	*Connochaetes taurinus*	Open	WAF	36.02
AMNH83502	*Connochaetes taurinus*	Open	WAF	34.14
AMNH83503	*Connochaetes taurinus*	Open	WAF	33.96
AMNH113781	*Damaliscus lunatus*	Open	WAF	33.76
AMNH34729	*Damaliscus lunatus*	Open	WAF	30.31
AMNH34730	*Damaliscus lunatus*	Open	WAF	32.41
AMNH82035	*Damaliscus lunatus*	Open	WAF	28.78
AMNH42953	*Damaliscus pygargus*	Open	WAF	22.5
AMNH81727	*Damaliscus pygargus*	Open	WAF	23.64
AMNH81729	*Damaliscus pygargus*	Open	WAF	22.79
AMNH81787	*Damaliscus pygargus*	Open	WAF	22.77
AMNH81997	*Eudorcas thomsonii*	Open	WAF	15.88
AMNH82059	*Eudorcas thomsonii*	Open	WAF	15.14
AMNH82060	*Eudorcas thomsonii*	Open	WAF	16.19
AMNH88415	*Eudorcas thomsonii*	Open	WAF	14.5
AMNH54506	*Gazella gazella*	Open	WAF	15.55
AMNH54997	*Gazella gazella*	Open	WAF	15.35
AMNH54998	*Gazella gazella*	Open	WAF	14.37
AMNH80143	*Hippotragus equinus*	Open	WAF	34.58
AMNH87217	*Hippotragus equinus*	Open	WAF	38.06
AMNH216381	*Hippotragus niger*	LightCover	WAF	38.95
AMNH80458	*Hippotragus niger*	LightCover	WAF	37.27
AMNH80461	*Hippotragus niger*	LightCover	WAF	37.34
AMNH83476	*Hippotragus niger*	LightCover	WAF	35.27
AMNH53492	*Kobus ellipsiprymnus*	HeavyCover	WAF	34
NMNH173877	*Kobus ellipsiprymnus*	HeavyCover	WAF	33.83
NMNH21898	*Kobus ellipsiprymnus*	HeavyCover	WAF	34.53
AMNH36396	*Kobus kob*	LightCover	WAF	25.86
AMNH36397	*Kobus kob*	LightCover	WAF	23.35
AMNH82129	*Kobus kob*	LightCover	WAF	24.09
AMNH82130	*Kobus kob*	LightCover	WAF	27.78
AMNH82173	*Kobus kob*	LightCover	WAF	24.44
AMNH70010	*Kobus leche*	HeavyCover	WAF	27.57

AMNH99649	*Kobus leche*	HeavyCover	WAF	26.22
NMNH254927	*Kobus leche*	HeavyCover	WAF	25.01
AMNH113784	*Kobus megaceros*	HeavyCover	WAF	25.15
AMNH82135	*Kobus megaceros*	HeavyCover	WAF	24.47
AMNH82136	*Kobus megaceros*	HeavyCover	WAF	27.38
AMNH82137	*Kobus megaceros*	HeavyCover	WAF	24.69
AMNH35323	*Kobus vardonii*	HeavyCover	WAF	26.7
AMNH70057	*Kobus vardonii*	HeavyCover	WAF	27.59
AMNH81687	*Kobus vardonii*	HeavyCover	WAF	24.73
AMNH81170	*Litocranius walleri*	LightCover	WAF	21.56
NMNH164031	*Litocranius walleri*	LightCover	WAF	19.53
NMNH164033	*Litocranius walleri*	LightCover	WAF	20.42
NMNH259457	*Litocranius walleri*	LightCover	WAF	20.48
AMNH187824	*Madoqua kirkii*	HeavyCover	WAF	8.84
AMNH82076	*Madoqua kirkii*	HeavyCover	WAF	9.21
NMNH538104	*Madoqua kirkii*	HeavyCover	WAF	9.53
NMNH538106	*Madoqua kirkii*	HeavyCover	WAF	9.62
NMNH541419	*Madoqua kirkii*	HeavyCover	WAF	9.39
AMNH82051	*Nanger granti*	Open	WAF	22.03
AMNH82056	*Nanger granti*	Open	WAF	21.98
AMNH82057	*Nanger granti*	Open	WAF	22.71
AMNH85152	*Nanger granti*	Open	WAF	20.6
AMNH80111	*Nanger soemmerringii*	Open	WAF	17.76
NMNH582229	*Nanger soemmerringii*	Open	WAF	20.71
AMNH53180	*Neotragus batesi*	Forest	WAF	8.24
AMNH53181	*Neotragus batesi*	Forest	WAF	8.09
AMNH53946	*Neotragus batesi*	Forest	WAF	8.25
AMNH88426	*Neotragus moschatus*	Forest	WAF	8.64
AMNH88427	*Neotragus moschatus*	Forest	WAF	9.17
NMNH367449	*Neotragus moschatus*	Forest	WAF	10.5
AMNH233033	*Oryx gazella*	Open	WAF	34.99
AMNH82043	*Oryx gazella*	Open	WAF	36.16
AMNH82044	*Oryx gazella*	Open	WAF	32.57
AMNH87211	*Oryx gazella*	Open	WAF	32.85
AMNH216387	*Ourebia ourebi*	LightCover	WAF	15.95
AMNH53304	*Ourebia ourebi*	LightCover	WAF	14.35
AMNH53328	*Ourebia ourebi*	LightCover	WAF	14.54
AMNH269894	*Philantomba monticola*	Forest	WAF	9.27

AMNH52726	*Philantomba monticola*	Forest	WAF	8.58
AMNH52753	*Philantomba monticola*	Forest	WAF	9.08
AMNH52758	*Philantomba monticola*	Forest	WAF	9.37
AMNH216389	*Raphicerus campestris*	LightCover	WAF	12.9
AMNH233047	*Raphicerus campestris*	LightCover	WAF	12.15
AMNH34728	*Raphicerus campestris*	LightCover	WAF	12.76
AMNH80538	*Raphicerus campestris*	LightCover	WAF	14.03
AMNH35493	*Redunca arundinum*	LightCover	WAF	23.07
AMNH80506	*Redunca arundinum*	LightCover	WAF	22.16
NMNH367428	*Redunca arundinum*	LightCover	WAF	22.82
NMNH367452	*Redunca arundinum*	LightCover	WAF	23.54
NMNH469909	*Redunca arundinum*	LightCover	WAF	18.65
AMNH27803	*Redunca fulvorufula*	LightCover	WAF	18.99
AMNH82063	*Redunca fulvorufula*	LightCover	WAF	19.09
AMNH82066	*Redunca fulvorufula*	LightCover	WAF	18.42
AMNH82067	*Redunca fulvorufula*	LightCover	WAF	18.72
AMNH53294	*Redunca redunca*	LightCover	WAF	20.31
AMNH53296	*Redunca redunca*	LightCover	WAF	21.71
AMNH90234	*Rupicapra rupicapra*	NA	WAF	19.03
AMNH90235	*Rupicapra rupicapra*	NA	WAF	19.66
AMNH90236	*Rupicapra rupicapra*	NA	WAF	19.37
AMNH17276	*Sigmoceros lichtensteinii*	Open	WAF	33.94
AMNH216382	*Sigmoceros lichtensteinii*	Open	WAF	31.27
AMNH216383	*Sigmoceros lichtensteinii*	Open	WAF	32.28
AMNH53088	*Sylvicapra grimmia*	LightCover	WAF	13.06
AMNH53092	*Sylvicapra grimmia*	LightCover	WAF	13.59
AMNH80562	*Sylvicapra grimmia*	LightCover	WAF	16.24
AMNH80563	*Sylvicapra grimmia*	LightCover	WAF	16.12
AMNH53583	*Syncerus caffer*	LightCover	WAF	41.08
AMNH82005	*Syncerus caffer*	LightCover	WAF	57.32
AMNH82006	*Syncerus caffer*	LightCover	WAF	55.45
AMNH82009	*Syncerus caffer*	LightCover	WAF	50.42
AMNH53519	*Taurotragus derbianus*	HeavyCover	WAF	51.55
AMNH53521	*Taurotragus derbianus*	HeavyCover	WAF	48.52
AMNH53522	*Taurotragus derbianus*	HeavyCover	WAF	48.8
AMNH53523	*Taurotragus derbianus*	HeavyCover	WAF	51.82
AMNH27811	*Taurotragus oryx*	LightCover	WAF	51.2
AMNH34722	*Taurotragus oryx*	LightCover	WAF	47.47

AMNH54386	*Tragelaphus angasii*	HeavyCover	WAF	26.41
AMNH54387	*Tragelaphus angasii*	HeavyCover	WAF	27.12
AMNH54390	*Tragelaphus angasii*	HeavyCover	WAF	25.62
AMNH81002	*Tragelaphus buxtoni*	Forest	WAF	38.47
AMNH81003	*Tragelaphus buxtoni*	Forest	WAF	33.26
AMNH81004	*Tragelaphus buxtoni*	Forest	WAF	37.8
AMNH81014	*Tragelaphus buxtoni*	Forest	WAF	32.34
AMNH81033	*Tragelaphus buxtoni*	Forest	WAF	33.63
AMNH53271	*Tragelaphus eurycerus*	Forest	WAF	35.73
AMNH53279	*Tragelaphus eurycerus*	Forest	WAF	37.41
AMNH53280	*Tragelaphus eurycerus*	Forest	WAF	38.83
AMNH36416	*Tragelaphus imberbis*	HeavyCover	WAF	27.13
AMNH36417	*Tragelaphus imberbis*	HeavyCover	WAF	25.27
AMNH82019	*Tragelaphus imberbis*	HeavyCover	WAF	28.44
AMNH82023	*Tragelaphus imberbis*	HeavyCover	WAF	24.45
AMNH187806	*Tragelaphus scriptus*	Forest	WAF	18.57
AMNH216371	*Tragelaphus scriptus*	Forest	WAF	19.84
AMNH88425	*Tragelaphus scriptus*	Forest	WAF	21.73
AMNH53209	*Tragelaphus spekii*	HeavyCover	WAF	29.6
AMNH53212	*Tragelaphus spekii*	HeavyCover	WAF	27
AMNH53213	*Tragelaphus spekii*	HeavyCover	WAF	23.44
AMNH53216	*Tragelaphus spekii*	HeavyCover	WAF	22.61
AMNH233027	*Tragelaphus strepsiceros*	HeavyCover	WAF	38.35
AMNH70328	*Tragelaphus strepsiceros*	HeavyCover	WAF	35.21
AMNH70328a	*Tragelaphus strepsiceros*	HeavyCover	WAF	34.01
AMNH113810	*Addax nasomaculatus*	Open	WAT	26.97
AMNH113811	*Addax nasomaculatus*	Open	WAT	27.25
AMNH113812	*Addax nasomaculatus*	Open	WAT	26.98
AMNH113813	*Addax nasomaculatus*	Open	WAT	26.87
AMNH81690	*Aepyceros melampus*	LightCover	WAT	21.83
AMNH82050	*Aepyceros melampus*	LightCover	WAT	21.11
AMNH83534	*Aepyceros melampus*	LightCover	WAT	21.54
AMNH85150	*Aepyceros melampus*	LightCover	WAT	21.03
AMNH233038	*Alcelaphus buselaphus*	Open	WAT	27.07
AMNH34717	*Alcelaphus buselaphus*	Open	WAT	25.84
AMNH34725	*Alcelaphus buselaphus*	Open	WAT	31.66
AMNH82033	*Alcelaphus buselaphus*	Open	WAT	29.39
AMNH82159	*Alcelaphus buselaphus*	Open	WAT	32.21

AMNH16048	*Ammotragus lervia*	NA	WAT	25.56
AMNH81740	*Antidorcas marsupialis*	Open	WAT	19.13
AMNH81745	*Antidorcas marsupialis*	Open	WAT	18.55
AMNH83549	*Antidorcas marsupialis*	Open	WAT	18.21
AMNH83550	*Antidorcas marsupialis*	Open	WAT	18.59
AMNH35527	*Antilope cervicapra*	Open	WAT	20.19
AMNH35957	*Antilope cervicapra*	Open	WAT	18.32
AMNH54486	*Antilope cervicapra*	Open	WAT	19.54
AMNH88406	*Beatragus hunteri*	Open	WAT	28.04
AMNH88407	*Beatragus hunteri*	Open	WAT	26.42
AMNH88408	*Beatragus hunteri*	Open	WAT	27.73
AMNH54765	*Bubalus bubalis*	NA	WAT	52.33
AMNH54766	*Bubalus bubalis*	NA	WAT	49.83
AMNH52875	*Cephalophus dorsalis*	Forest	WAT	15.47
AMNH52876	*Cephalophus dorsalis*	Forest	WAT	15.95
AMNH52884	*Cephalophus dorsalis*	Forest	WAT	15.17
AMNH52888	*Cephalophus dorsalis*	Forest	WAT	14.35
AMNH52775	*Cephalophus leucogaster*	Forest	WAT	14.53
AMNH52778	*Cephalophus leucogaster*	Forest	WAT	14.83
AMNH52788	*Cephalophus leucogaster*	Forest	WAT	15.53
AMNH216375	*Cephalophus natalensis*	Forest	WAT	15.88
AMNH54391	*Cephalophus natalensis*	Forest	WAT	14.31
AMNH81686	*Cephalophus natalensis*	Forest	WAT	14.05
AMNH83387	*Cephalophus natalensis*	Forest	WAT	14.74
AMNH52930	*Cephalophus nigrifrons*	Forest	WAT	13.13
AMNH52931	*Cephalophus nigrifrons*	Forest	WAT	14.08
AMNH52940	*Cephalophus nigrifrons*	Forest	WAT	13.29
AMNH52943	*Cephalophus nigrifrons*	Forest	WAT	13.1
AMNH53138	*Cephalophus silvicultor*	Forest	WAT	25.79
AMNH53144	*Cephalophus silvicultor*	Forest	WAT	26.36
AMNH53153	*Cephalophus silvicultor*	Forest	WAT	23.97
AMNH52992	*Cephalophus weynsi*	Forest	WAT	15.33
AMNH52995	*Cephalophus weynsi*	Forest	WAT	15.53
AMNH52999	*Cephalophus weynsi*	Forest	WAT	15.65
AMNH88429	*Cephalophus weynsi*	Forest	WAT	15.06
AMNH81716	*Connochaetes gnou*	Open	WAT	30.09
AMNH81720	*Connochaetes gnou*	Open	WAT	29.36
AMNH81722	*Connochaetes gnou*	Open	WAT	32.91

AMNH27824	*Connochaetes taurinus*	Open	WAT	33.52
AMNH54133	*Connochaetes taurinus*	Open	WAT	36.28
AMNH83502	*Connochaetes taurinus*	Open	WAT	35.32
AMNH83503	*Connochaetes taurinus*	Open	WAT	34.65
AMNH113781	*Damaliscus lunatus*	Open	WAT	31.23
AMNH34729	*Damaliscus lunatus*	Open	WAT	31.07
AMNH34730	*Damaliscus lunatus*	Open	WAT	31.72
AMNH82035	*Damaliscus lunatus*	Open	WAT	30.18
AMNH42953	*Damaliscus pygargus*	Open	WAT	23.01
AMNH81727	*Damaliscus pygargus*	Open	WAT	24.26
AMNH81729	*Damaliscus pygargus*	Open	WAT	23.75
AMNH81787	*Damaliscus pygargus*	Open	WAT	23.96
AMNH81997	*Eudorcas thomsonii*	Open	WAT	16.05
AMNH82059	*Eudorcas thomsonii*	Open	WAT	15.01
AMNH82060	*Eudorcas thomsonii*	Open	WAT	16.05
AMNH88415	*Eudorcas thomsonii*	Open	WAT	14.21
AMNH54506	*Gazella gazella*	Open	WAT	14.04
AMNH54997	*Gazella gazella*	Open	WAT	14.97
AMNH54998	*Gazella gazella*	Open	WAT	14.08
AMNH80143	*Hippotragus equinus*	Open	WAT	34.3
AMNH87217	*Hippotragus equinus*	Open	WAT	39.6
AMNH216381	*Hippotragus niger*	LightCover	WAT	38.2
AMNH80458	*Hippotragus niger*	LightCover	WAT	36.8
AMNH80461	*Hippotragus niger*	LightCover	WAT	37.47
AMNH83476	*Hippotragus niger*	LightCover	WAT	34.27
AMNH53492	*Kobus ellipsiprymnus*	HeavyCover	WAT	35.64
NMNH173877	*Kobus ellipsiprymnus*	HeavyCover	WAT	35
NMNH21898	*Kobus ellipsiprymnus*	HeavyCover	WAT	35.71
AMNH36396	*Kobus kob*	LightCover	WAT	26.58
AMNH36397	*Kobus kob*	LightCover	WAT	25.31
AMNH82129	*Kobus kob*	LightCover	WAT	25.14
AMNH82130	*Kobus kob*	LightCover	WAT	28.52
AMNH82173	*Kobus kob*	LightCover	WAT	24.07
AMNH70010	*Kobus leche*	HeavyCover	WAT	26.07
AMNH99649	*Kobus leche*	HeavyCover	WAT	27.03
NMNH254927	*Kobus leche*	HeavyCover	WAT	26.45
AMNH113784	*Kobus megaceros*	HeavyCover	WAT	26.18
AMNH82135	*Kobus megaceros*	HeavyCover	WAT	25.46

AMNH82136	*Kobus megaceros*	HeavyCover	WAT	26.4
AMNH82137	*Kobus megaceros*	HeavyCover	WAT	25.76
AMNH35323	*Kobus vardonii*	HeavyCover	WAT	27.62
AMNH70057	*Kobus vardonii*	HeavyCover	WAT	27.06
AMNH81687	*Kobus vardonii*	HeavyCover	WAT	25.82
AMNH81170	*Litocranius walleri*	LightCover	WAT	21.66
NMNH164031	*Litocranius walleri*	LightCover	WAT	18.41
NMNH164033	*Litocranius walleri*	LightCover	WAT	18.99
NMNH259457	*Litocranius walleri*	LightCover	WAT	19.43
AMNH187824	*Madoqua kirkii*	HeavyCover	WAT	8.67
AMNH82076	*Madoqua kirkii*	HeavyCover	WAT	9.43
NMNH538104	*Madoqua kirkii*	HeavyCover	WAT	9.97
NMNH538106	*Madoqua kirkii*	HeavyCover	WAT	9.54
NMNH541419	*Madoqua kirkii*	HeavyCover	WAT	9.43
AMNH82051	*Nanger granti*	Open	WAT	22.65
AMNH82056	*Nanger granti*	Open	WAT	21.91
AMNH82057	*Nanger granti*	Open	WAT	22.1
AMNH85152	*Nanger granti*	Open	WAT	20.39
AMNH80111	*Nanger soemmerringii*	Open	WAT	18.77
NMNH582229	*Nanger soemmerringii*	Open	WAT	21.44
AMNH53180	*Neotragus batesi*	Forest	WAT	8.47
AMNH53181	*Neotragus batesi*	Forest	WAT	8.34
AMNH53946	*Neotragus batesi*	Forest	WAT	8.22
AMNH88426	*Neotragus moschatus*	Forest	WAT	8.33
AMNH88427	*Neotragus moschatus*	Forest	WAT	9.52
NMNH367449	*Neotragus moschatus*	Forest	WAT	10.19
AMNH233033	*Oryx gazella*	Open	WAT	29.37
AMNH82043	*Oryx gazella*	Open	WAT	34.22
AMNH82044	*Oryx gazella*	Open	WAT	29.77
AMNH87211	*Oryx gazella*	Open	WAT	31.55
AMNH216387	*Ourebia ourebi*	LightCover	WAT	15.85
AMNH53304	*Ourebia ourebi*	LightCover	WAT	14.47
AMNH53328	*Ourebia ourebi*	LightCover	WAT	13.93
AMNH269894	*Philantomba monticola*	Forest	WAT	9.68
AMNH52726	*Philantomba monticola*	Forest	WAT	9.52
AMNH52753	*Philantomba monticola*	Forest	WAT	9.09
AMNH52758	*Philantomba monticola*	Forest	WAT	9.75
AMNH216389	*Raphicerus campestris*	LightCover	WAT	12.94

AMNH233047	*Raphicerus campestris*	LightCover	WAT	12.45
AMNH34728	*Raphicerus campestris*	LightCover	WAT	12.97
AMNH80538	*Raphicerus campestris*	LightCover	WAT	13.46
AMNH35493	*Redunca arundinum*	LightCover	WAT	23.95
AMNH80506	*Redunca arundinum*	LightCover	WAT	22.03
NMNH367428	*Redunca arundinum*	LightCover	WAT	22.57
NMNH367452	*Redunca arundinum*	LightCover	WAT	21.09
NMNH469909	*Redunca arundinum*	LightCover	WAT	18.25
AMNH27803	*Redunca fulvorufula*	LightCover	WAT	20.08
AMNH82063	*Redunca fulvorufula*	LightCover	WAT	18.63
AMNH82066	*Redunca fulvorufula*	LightCover	WAT	18.58
AMNH82067	*Redunca fulvorufula*	LightCover	WAT	18.37
AMNH53294	*Redunca redunca*	LightCover	WAT	20.98
AMNH53296	*Redunca redunca*	LightCover	WAT	20.97
AMNH90234	*Rupicapra rupicapra*	NA	WAT	19.89
AMNH90235	*Rupicapra rupicapra*	NA	WAT	20.83
AMNH90236	*Rupicapra rupicapra*	NA	WAT	20.77
AMNH17276	*Sigmoceros lichtensteinii*	Open	WAT	32.59
AMNH216382	*Sigmoceros lichtensteinii*	Open	WAT	33.68
AMNH216383	*Sigmoceros lichtensteinii*	Open	WAT	32.99
AMNH53088	*Sylvicapra grimmia*	LightCover	WAT	14.07
AMNH53092	*Sylvicapra grimmia*	LightCover	WAT	14.47
AMNH80562	*Sylvicapra grimmia*	LightCover	WAT	14.94
AMNH80563	*Sylvicapra grimmia*	LightCover	WAT	14.94
AMNH53583	*Syncerus caffer*	LightCover	WAT	36.43
AMNH82005	*Syncerus caffer*	LightCover	WAT	45.27
AMNH82006	*Syncerus caffer*	LightCover	WAT	45.87
AMNH82009	*Syncerus caffer*	LightCover	WAT	51.31
AMNH53519	*Taurotragus derbianus*	HeavyCover	WAT	52.8
AMNH53521	*Taurotragus derbianus*	HeavyCover	WAT	48.52
AMNH53522	*Taurotragus derbianus*	HeavyCover	WAT	48.82
AMNH53523	*Taurotragus derbianus*	HeavyCover	WAT	49.46
AMNH27811	*Taurotragus oryx*	LightCover	WAT	49.04
AMNH34722	*Taurotragus oryx*	LightCover	WAT	44.55
AMNH54386	*Tragelaphus angasii*	HeavyCover	WAT	25.3
AMNH54387	*Tragelaphus angasii*	HeavyCover	WAT	28.7
AMNH54390	*Tragelaphus angasii*	HeavyCover	WAT	26.77
AMNH81002	*Tragelaphus buxtoni*	Forest	WAT	38.36

AMNH81003	*Tragelaphus buxtoni*	Forest	WAT	35.07
AMNH81004	*Tragelaphus buxtoni*	Forest	WAT	40.13
AMNH81014	*Tragelaphus buxtoni*	Forest	WAT	33.44
AMNH81033	*Tragelaphus buxtoni*	Forest	WAT	29.87
AMNH53271	*Tragelaphus eurycerus*	Forest	WAT	37.4
AMNH53279	*Tragelaphus eurycerus*	Forest	WAT	38.55
AMNH53280	*Tragelaphus eurycerus*	Forest	WAT	40.64
AMNH36416	*Tragelaphus imberbis*	HeavyCover	WAT	26.86
AMNH36417	*Tragelaphus imberbis*	HeavyCover	WAT	24.82
AMNH82019	*Tragelaphus imberbis*	HeavyCover	WAT	28.85
AMNH82023	*Tragelaphus imberbis*	HeavyCover	WAT	24.72
AMNH187806	*Tragelaphus scriptus*	Forest	WAT	17.61
AMNH216371	*Tragelaphus scriptus*	Forest	WAT	20.09
AMNH88425	*Tragelaphus scriptus*	Forest	WAT	22.56
AMNH53209	*Tragelaphus spekii*	HeavyCover	WAT	31.82
AMNH53212	*Tragelaphus spekii*	HeavyCover	WAT	30.09
AMNH53213	*Tragelaphus spekii*	HeavyCover	WAT	24.57
AMNH53216	*Tragelaphus spekii*	HeavyCover	WAT	25.28
AMNH233027	*Tragelaphus strepsiceros*	HeavyCover	WAT	38.36
AMNH70328	*Tragelaphus strepsiceros*	HeavyCover	WAT	34.91
AMNH70328a	*Tragelaphus strepsiceros*	HeavyCover	WAT	29.67

Appendix D

Raw measurements for the American Omo bovid astragali measured in Chapter 5. Measurement definitions can be found in Table 3.1. All measurements are in millimeters.

individual	Unit	B	DistRad	DMTD	LML	MIN	MML	PMTD	ProxRad	WAF	WAT
F255 - 11	H-3	18.10	12.50	3.06	46.62	38.80	46.32	5.36	16.00	27.18	29.30
F255 - 12	H-3	19.08	10.50	3.73	40.78	31.88	39.53	5.56	10.09	23.64	23.50
F302 - 5	F-1	11.75	6.24	1.25	28.18	22.30	25.57	4.62	7.79	16.70	16.16
L-56 - 12	E-3	22.25	10.71	1.71	49.91	39.61	45.56	8.30	13.00	30.13	32.89
L-56 - 38	E-3	19.89	10.31	1.91	47.43	37.56	42.60	8.05	12.76	27.91	28.66
L-56 - 61	E-3	20.90	10.50	2.34	51.82	39.58	46.00	9.76	14.73	28.20	30.45
L-56 - 62	E-3	12.14	6.76	1.59	29.16	22.90	27.23	4.64	8.42	17.27	17.60
L-56 - 86	E-3	22.32	11.82	2.39	52.39	41.91	48.09	8.16	14.00	32.22	33.53
L1 - 15	B-11	21.08	12.50	2.41	54.19	42.22	49.98	9.77	16.75	32.35	32.18
L1 - 160	B-11	21.78	10.85	2.42	49.86	40.10	46.38	7.23	14.24	30.36	30.16
L1 - 297	B-11	21.61	10.50	1.88	48.80	38.49	45.68	8.29	13.75	29.83	32.07
L1 - 298	B-11	16.53	9.71	1.60	41.39	33.84	38.45	6.00	12.88	23.30	25.67
L1 - 299	B-11	17.20	8.64	2.69	39.13	31.23	36.13	5.27	10.43	20.81	20.75
L1 - 301	B-11	12.18	7.42	0.97	30.65	17.56	28.75	5.31	9.36	20.02	17.56
L1 - 485	B-11	12.69	7.33	1.07	31.02	24.90	28.37	5.04	8.41	18.92	17.85

L112 - 16	G-7	18.29	11.00	2.78	44.39	34.91	42.21	6.58	13.74	27.43	28.64
L114 - 23	E-4	21.87	10.77	1.93	49.31	39.46	46.41	7.83	14.12	29.95	30.14
L114 - 24	E-4	22.42	11.50	2.24	50.14	39.89	47.03	7.84	13.22	28.80	29.92
L12 - 2	D-2	23.36	10.37	2.80	48.37	38.70	45.69	7.04	12.28	29.55	30.82
L122 - 27	D-3	32.69	13.00	3.19	68.52	53.64	63.90	11.42	17.20	41.52	38.03
L122 - 28	D-3	25.73	9.72	2.60	48.41	38.85	46.25	7.00	11.00	27.92	29.76
L128 - 12	E-4	24.15	9.77	2.88	48.13	37.35	45.19	7.87	11.50	26.41	27.78
L143 - 17	C-9	16.89	8.73	2.04	39.62	31.92	35.44	5.53	10.12	23.48	23.91
L143 - 7	C-9	13.62	7.32	0.99	30.28	24.48	28.19	4.84	7.33	18.89	16.82
L144 - 14	C-9	21.89	13.85	3.00	50.45	41.39	50.16	5.96	14.66	31.13	33.00
L144 - 15	C-9	15.77	5.32	0.72	27.26	22.48	26.14	4.01	5.28	15.55	15.55
L146 - 22	E-1	22.95	11.16	2.49	47.07	40.21	47.30	4.58	13.20	28.43	31.94
L147 - 13	E-4	22.74	10.29	2.11	48.87	39.00	45.09	7.75	12.59	28.36	29.31
L147 - 30	E-4			1.02	51.17	41.97	46.94	8.12		30.55	31.01
L16 - 13	G-4	25.10	13.65	2.80	57.58	46.97	55.16	7.98	16.59	35.93	37.72
L16 - 174	G-4	19.95	10.39	2.16	45.91	37.87	42.91	5.93	12.71	25.94	25.62
L161 - 16	D-3	24.41	10.14	2.26	50.77	40.34	47.45	8.08	13.50	28.26	31.60

L169 - 2	D-4	23.58	15.55	3.62	67.65	50.84	60.07	13.22	21.95	41.66	43.76
L183 - 27	C-5	22.45	11.50	1.74	49.40	43.05	49.20	4.42	15.50	30.36	31.84
L19 - 5	D-4	21.42	11.00	1.97	50.63	40.79	47.46	7.69	15.50	28.65	29.83
L193 - 7	C-8	24.95	11.20	2.10	52.84	43.59	51.24	7.05	15.00	30.24	31.05
L2 - 107	B-10	21.75	11.31	3.24	50.00	38.62	47.02	8.09	14.27	30.80	31.79
L2 - 45b	B-10	19.45	11.73	2.04	49.25	39.33	44.85	8.10	13.76	28.38	29.89
L2 - 45c	B-10		9.26	2.07	37.35	30.82		4.44		21.51	23.29
L2 - 63	B-10	23.90	13.00	3.28	56.53	45.83	53.13	7.50	16.50	34.07	35.01
L20 - 6	F-	29.52	17.00	3.55	69.62	56.22	67.21	9.81	21.00	41.81	45.65
L20 - 7	F-	23.10	13.37	3.23	54.49	43.64	52.80	7.51	16.50	32.76	35.90
L20 - 8	F-	21.98	11.00	2.38	49.58	40.05	45.57	7.56	13.00	30.69	31.19
L200 - 1	C-7	18.78	9.00	2.78	40.35	31.31	37.17	6.45	9.76	25.22	24.52
L21 - 29	D-1	20.37	10.50	2.07	45.32	38.46	44.37	4.59	14.00	28.10	28.77
L21 - 30	D-1	21.75	17.50	3.67	62.71	49.39	58.90	9.58	19.50	38.55	39.43
L21 - 57	D-1	21.37	11.50	2.26	50.43	40.42	47.07	7.68	14.50	29.12	32.43
L215 - 11	F-1	20.73	10.71	2.42	48.90	38.84	45.78	7.39	14.50	29.82	30.23
L215 - 12	F-1	19.65	11.00	2.07	48.57	39.03	45.67	7.44	15.26	29.74	31.75

L218 - 3	C-9	26.43	19.00	2.82	73.74	59.13	67.55	11.76	22.50	49.00	49.54
L227 - 1	D-2	29.97	15.50	3.73	67.81	53.66	64.67	10.61	19.50	42.14	41.81
L23 - 41	C-6	21.25	11.68	2.67	52.24	41.96	48.85	7.62	16.25	31.33	32.26
L23 - 56	C-6	20.46	11.71	2.51	46.37	39.95	46.61	4.20	15.11	30.34	32.25
L230 - 1	D-4	16.95	9.13	1.47	38.07	31.61	36.05	5.43	10.20	25.21	24.22
L235 - 5	E-3	18.40	15.50	1.72	57.55	46.33	52.96	9.08	19.00	32.34	36.67
L238 - 19	F-3	20.23	8.50	1.94	42.91	33.90	39.74	7.03	11.16	24.20	25.24
L239 - 2	F-1	12.23	7.25	1.45	31.03	24.40	28.87	5.29	9.37	18.35	17.56
L243 - 1	F-0	18.43	13.00	2.29	53.10	42.44	49.99	8.29	15.50	32.18	33.68
L25 - 138	G-13	12.74	6.88	1.60	29.30	23.13	27.16	5.22	7.71	18.41	17.27
L25 - 56	G-13	19.22	15.39	2.58	54.81	43.64	50.88	8.46	16.38	32.38	34.04
L258 - 1	F-2	21.50	15.24	1.71	59.32	49.79	56.68	7.91	19.50	37.91	35.97
L26 - 123	E-2	21.72	10.00	2.38	53.19	41.33	48.43	9.27	16.76	31.82	33.00
L26 - 22	E-2	20.31	12.12	2.52	49.23	38.86	45.27	7.84	13.50	28.98	30.04
L26 - 6	E-2	21.44	13.00	1.90	51.47	31.32	48.32	6.39	14.00	31.32	33.49
L26 - 81	E-2	32.28	19.79	5.29		60.32	74.43		22.50	44.72	44.45
L27 - 25	C-5	20.72	10.88	2.21	51.42	40.90	47.21	7.88	16.71	31.06	32.39

L27 - 27a	C-5	11.07	6.00	1.27	27.70	22.17	24.99	4.27	7.92	17.38	15.74
L27 - 27b	C-5			2.40	26.72	20.72	24.19	7.03		16.26	15.79
L28 - 11a	F-1	23.64	11.82	1.83	51.18	42.40	47.51	7.09	12.26	28.84	29.00
L28 - 11b	F-1	11.44	4.43	1.08	21.55	17.62	20.32	2.89	4.43	13.14	12.52
L28 - 11x	F-1	10.21	4.89	1.55	20.62	16.46	19.63	2.64	4.46	12.10	12.80
L28 - 12	F-1	19.82	9.12	1.33	41.42	35.29	40.19	4.77	11.63	23.12	24.61
L28 - 13x	F-1	12.10	7.00	1.54	29.86	23.13	27.01	5.22	8.00	17.69	17.00
L28 - 142	F-1	22.43	12.72	2.74	47.62	39.04	46.42	5.95	11.50	29.63	29.86
L28 - 24	F-1	22.07	12.47	2.50	52.91	42.37	49.49	8.12	15.50	23.40	33.39
L28 - 39	F-1	19.98	12.77	3.58	49.97	37.74	48.03	9.76	15.38	31.87	30.45
L28 - 48	F-1	25.74	13.12	3.18	51.04	43.34	51.98	5.95	13.25	32.20	32.40
L28 - 6	F-1	20.54	13.61	2.79	51.49	40.24	47.20	8.43	13.08	29.60	29.36
L28 - 7	F-1	21.64	9.71	2.83	46.35	37.01	43.79	6.54	12.50	26.64	28.52
L28 - 9	F-1	12.34	7.21	1.51	31.27	23.97	28.33	5.78	8.83	19.43	18.04
L285 - 1	C-4	24.86	12.50	2.05	57.77	48.38	54.78	7.34	17.85	33.79	37.91
L289 - 1	C-4	14.45	7.43	1.73	31.74	25.05	29.59	5.04	8.11	18.51	18.31
L31 - 8	F-0	24.82	18.00	2.68	66.40	54.00	62.72	9.95	20.32	43.12	43.52

L32 - 140	C-6	24.52	16.00	3.85	66.21	49.79	58.98	12.29	19.14	43.21	44.45
L32 - 27	C-6	24.66	12.50	3.83	55.14	43.82	53.45	7.35	16.50	31.95	34.89
L32 - 28	C-6	21.81	12.73	2.88	52.11	42.01	49.97	7.38	15.72	31.17	33.95
L32 - 33	C-6	22.13	11.22	1.94	51.54	42.31	48.04	7.45	15.37	30.37	32.69
L32 - 74	C-6	18.58	10.50	1.48	43.47	37.04	43.10	5.01	14.33	25.72	26.41
L327 - 25	C-6	13.21	7.36	1.05	31.92	25.66	29.44	5.24	8.90	19.60	18.61
L327 - 7	C-6	28.66	15.31	2.85	66.60	53.90	62.55	9.94	19.00	43.87	45.90
L327 - 8	C-6	26.02	14.00	2.29	60.60	48.60	57.67	9.55	18.00	37.65	38.56
L338 - 11	E-3	10.55	7.74	1.58	28.04	21.71	26.46	4.79	8.29	16.84	16.66
L349 - 2	C-7	23.64	14.36	2.51	58.75	49.00	55.24	7.33	17.28	34.82	38.06
L35 - 37	G-5	31.44	16.00	3.71	68.65	54.66	66.07	10.10	18.86	42.19	43.45
L35 - 39a	G-5	18.67	10.00	1.71	46.98	36.98	41.84	8.38	13.39	29.58	29.60
L35 - 39b	G-5	20.68	11.73	2.37	49.29	39.18	45.54	7.86	13.13	28.02	30.57
L35 - 50	G-5	18.88	11.50	2.20	48.58	37.74	44.31	8.65	14.38	30.37	31.55
L35 - 53	G-5	22.02	11.71	2.66	46.85	37.60	45.81	6.68	12.00	29.07	29.99
L37 - 11	C-8	13.03	7.75	1.91	33.12	24.78	30.27	6.15	9.71	21.13	18.64
L377 - 1	B-8	24.49	9.26	2.47	48.54	38.24	45.58	7.74	12.26	25.88	27.91

L378 - 2	B-8	22.71	11.40	1.21	53.90	44.62	49.88	8.51	16.13	33.50	34.52
L39 - 10	F-1	12.44	8.64	1.81	32.89	25.07	30.61	6.06	9.61	20.37	18.89
L39 - 11	F-1	14.82	7.00	1.45	30.60	24.86	29.64	4.38	7.91	19.61	18.82
L39 - 9	F-1	26.64	15.62	4.91	65.33	50.64	62.87	9.86	18.50	37.16	35.64
L398 - 105	F-0	23.01	11.96	2.20	51.02	42.78	50.33	8.98	15.74	33.59	33.97
L398 - 450	F-0	33.25	17.00	3.73	69.00	56.60	68.67	8.47	18.65	42.64	45.93
L4 - 39a	E-3	12.49	8.16	1.42	32.71	24.68	29.33	6.59	8.73	19.59	18.64
L4 - 39b	E-3	14.58	7.50	1.53	32.76	25.67	30.68	5.57	8.78	19.99	19.69
L4 - 39c	E-3	13.84	6.50	0.71	32.23	27.09	29.50	4.60	9.25	19.28	18.73
L4 - 39d	E-3	13.03	7.88	2.48	32.83	24.51	29.11	5.80	8.50	18.88	19.54
L41 - 11	F-1	16.82	10.23	2.25	39.39	31.55	38.33	5.63	11.26	23.57	24.02
L41 - 12	F-1	23.80	6.50	1.08	40.01	35.51	39.47	3.38	9.24	23.62	22.31
L41 - 13	F-1	15.32	13.24	2.03	47.13	38.66	44.94	6.55	16.91	28.71	30.16
L42 - 43	C-5	12.66	7.25	1.25	31.23	25.00	28.80	5.09	9.35	19.48	17.75
L432 - 8	G-7	11.01	7.60	1.28	31.07	24.62	27.87	4.98	9.50	18.43	17.82
L433 - 4	G-7	23.68	12.00	2.28	54.39	43.74	51.47	8.27	16.17	32.02	35.19
L44 - 34a	G-6	21.47	11.00	2.71	51.31	40.07	47.27	8.53	15.30	30.22	31.41

L44 - 34b	G-6	20.74	12.00	3.00	48.06	37.86	45.49	7.20	12.86	30.36	30.45
L45 - 17	C-5	12.82	6.37	0.12	30.01	25.21	27.41	4.50	8.50	18.94	16.44
L455 - 3	D-1	20.76	12.12	2.03	49.77	40.28	47.02	7.46	14.50	29.68	30.35
L465 - 97	F-1	11.45	6.62	1.45	26.29	20.29	24.38	4.46	6.34	14.62	15.26
L467 - 28	F-1	28.35	15.85	3.17	67.06	53.31	62.75	10.59	19.14	40.38	41.33
L467 - 29	F-1	16.54	13.71	3.83	50.14	38.39	46.44	8.05	16.11	31.32	31.77
L47 - 104	C-8	14.50	6.00	1.29	29.49	24.09	28.22	4.71	7.84	16.85	16.65
L47 - 24	C-8	26.26	16.50	4.16	66.57	52.35	62.60	10.05	20.17	38.96	41.47
L47 - 4	C-8	21.28	13.19	2.80	50.39	44.49	53.98	7.06	16.27	30.95	32.77
L47 - 93	C-8	23.49	13.50	2.20	55.26	45.18	51.32	8.11	14.50	32.59	34.24
L474 - 2	G-1	20.36	11.50	2.64	46.60	35.99	44.64	8.10	12.79	29.91	29.35
L477 - 10	G-1	24.87	11.00	2.19	53.83	43.13	50.81	8.53	15.12	31.83	32.07
L477 - 9	G-1	21.45	11.20	2.20	29.23	40.23	46.52	7.10	14.00	28.94	30.70
L480 - 9	G-3	21.50	10.13	1.80	47.65	39.32	44.53	6.52	12.74	16.78	28.46
L485 - 3	G-4	11.33	7.43	0.91	29.24	23.32	26.72	5.02	8.24	17.76	17.23
L489 - 7	G-4	21.50	13.70	3.19	55.37	43.92	52.11	8.50	17.00	34.51	36.92
L503 - 10	G-3	21.13	11.29	2.60	49.29	39.46	46.21	7.08	14.00	28.48	29.14

L504 - 19	G-4	21.35	9.37	1.40	41.18	35.32	41.20	4.60	10.81	28.12	28.22
L504 - 9	G-4	20.59	10.50	2.47	13.80	38.94	43.95	5.43	13.00	26.44	28.32
L51 - 14	C-9	25.88	11.50	3.06	54.71	44.39	50.57	7.48	14.00	31.63	33.24
L51 - 15	C-9	22.23	15.84	2.82	56.46	44.17	50.67	9.70	12.50	33.48	35.64
L51 - 24	C-9	14.43	7.21	0.72	31.17	25.84	29.22	5.52	7.91	18.34	17.70
L51 - 32	C-9	13.24	7.23	0.66	27.72	23.19	26.34	4.01	7.00	16.92	16.28
L51 - 33	C-9	13.22	5.44	1.92	26.76	19.89	25.50	4.90	6.81	16.85	16.35
L510 - 2	G-9	13.15	7.88	1.37	32.50	24.96	29.98	6.15	8.93	19.76	19.21
L511 - 2	G-7	25.43	12.00	2.55	58.11	45.43	51.93	10.06	14.50	34.01	35.19
L52 - 102	F-3	22.32	9.50	2.76	48.32	38.22	44.55	7.35	13.13	27.00	29.29
L52 - 127	F-3	19.90	10.34	2.01	47.10	38.60	43.72	6.50	14.00	27.15	28.08
L52 - 22	F-3	19.36	11.50	2.41	49.70	39.46	46.01	7.96	15.34	29.78	30.25
L52 - 23	F-3	23.18	11.67	2.93	53.38	42.08	49.30	8.32	14.77	30.69	33.29
L52 - 24	F-3	18.89	9.61	2.09	44.72	35.70	40.67	7.09	12.31	27.81	26.75
L52 - 25	F-3	11.35	6.88	1.67	26.07	20.85	26.05	3.68	8.00	17.65	16.32
L52 - 79	F-3	22.10	9.43	2.60	47.47	38.74	45.00	6.12	13.86	26.36	28.79
L523 - 22	G-9	25.48	11.17	2.57	47.24	37.60	45.30	7.05	11.50	28.02	29.08

L524 - 2	G-9	22.16	10.35	2.92	46.30	37.33	44.12	6.00	11.77	27.20	28.25
L539 - 15	G-11	20.01	9.14	1.77	45.21	36.92	42.12	6.36	13.50	26.41	27.61
L539 - 20	G-11	22.86	9.18	2.54	46.01	38.44	43.17	5.32	11.23	28.12	29.03
L554 - 1	D-3	21.31	9.59	1.91	48.54	39.12	44.04	7.54	13.00	28.08	27.89
L56 - 2	C-6	19.67	10.88	2.28	45.60	37.50	43.97	6.89	13.79	28.29	28.62
L585 - 4	C-8	24.64	11.68	2.47	53.35	42.74	49.58	8.47	13.50	32.81	35.06
L59 - 5	C-8	22.83	12.34	2.39	52.47	43.30	50.44	6.85	15.50	33.81	34.02
L596 - 11	G-13	22.48	9.00	3.24	46.74	38.35	43.72	5.13	12.78	25.19	26.56
L607 - 15	G-5	21.17	10.50	0.24	48.37	39.88	45.24	8.13	14.01	29.77	30.17
L61 - 2	G-4	11.93	7.36	1.13	28.48	23.13	26.33	4.23	7.25	16.51	16.62
L615 - 12	G-8	29.57	14.00	3.43	61.76	50.03	58.93	8.52	15.65	38.44	41.65
L615 - 13	G-8	23.04	11.74	2.26	53.49	43.36	50.28	7.86	15.88	31.13	33.52
L615 - 14	G-8	23.25	13.78	3.04	55.86	44.77	53.19	8.17	17.00	35.15	38.18
L622 - 19	G-12	32.62	18.50	4.39	77.48	61.95	73.28	11.16	22.50	46.14	46.63
L624 - 25	G-12	26.62	12.37	3.24	55.78	43.53	52.78	9.10	14.31	34.28	35.63
L626 - 102	G-12	12.73	8.22	1.26	33.59	26.94	31.03	5.54	10.50	18.60	18.62
L626 - 103	G-12	13.67	7.59	1.92	32.03	24.48	29.60	5.69	8.61	20.67	19.77

L627 - 208b	G-12	13.51	8.20	1.44	31.03	24.54	29.37	5.14	8.20	17.87	15.53
L627 - 256	G-12	19.78	11.62	2.63	47.14	37.60	44.87	6.92	13.50	27.91	29.54
L627 - 258	G-12	27.90	22.50	4.42	77.41	62.57	73.22	11.10	22.70	47.86	48.73
L627 - 393	G-12	21.18	11.41	2.25	48.82	40.40	46.76	6.63	14.50	29.54	31.52
L627 - 394	G-12	21.40	12.00	1.76	50.07	41.49	47.98	7.18	15.00	31.47	32.81
L627 - 395	G-12	21.79	11.23	3.00	43.86	38.35	43.86	2.55	11.50	27.23	29.51
L627 - 441	G-12	21.73	11.97	2.19	51.50	41.76	48.90	7.59	15.73	30.49	32.80
L627 - 76	G-12	22.64	9.16	2.83	45.02	36.93	41.85	5.48	10.00	25.59	26.11
L627 - 77	G-12	18.14	10.81	1.67	44.14	35.93	41.23	6.61	12.71	26.78	27.72
L627 - 78	G-12	11.69	6.72	1.74	29.97	22.46	26.46	5.77	8.11	18.20	17.25
L628 - 35	G-3	21.35	12.00	1.83	53.25	43.43	49.86	7.95	16.73	33.14	34.30
L628 - 36	G-3	23.14	11.58	1.74	52.75	42.03	46.70	9.14	13.00	31.86	32.70
L628 - 37	G-3	20.50	12.34	2.49	53.53	41.09	48.14	9.99	15.65	30.65	31.78
L63 - 3	D-3	20.12	12.29	2.27	49.16	39.55	46.48	7.47	13.89	31.60	31.40
L669 - 3	G-9	22.34	11.73	2.21	51.44	42.52	48.28	6.77	14.50	30.01	32.34
L67 - 10	G-8	23.23	11.00	2.78	52.19	42.37	49.11	7.08	15.31	28.92	31.85
L67 - 101	G-8	22.43	12.84	2.31	55.15	45.51	52.70	7.24	17.84	33.68	35.96

L67 - 103	G-8	21.19	12.00	2.58	51.29	39.82	47.07	8.69	14.00	29.90	30.87
L67 - 104	G-8	22.10	10.11	2.67	47.14	38.01	44.80	6.62	13.00	26.65	27.95
L67 - 12	G-8	22.89	8.64	2.23	45.90	37.31	42.95	6.34	11.78	25.85	27.25
L67 - 14	G-8	23.44	9.79	2.42	48.13	39.14	45.20	6.40	12.41	27.14	28.28
L67 - 15	G-8	27.04	10.36	2.36	58.21	46.56	52.63	9.70	15.77	33.41	36.33
L67 - 17	G-8	12.87	7.11	2.31	30.79	23.02	28.87	5.53	8.88	18.68	18.70
L684 - 8	G-6	22.12	12.41	2.93	55.99	43.39	50.65	9.68	16.36	33.19	34.89
L69 - 8	C-8	29.22	14.68	3.89	63.02	51.17	60.66	8.03	17.09	37.26	39.44
L69 - 9	C-8	24.40	15.76	4.56	66.58	50.57	60.39	11.30	20.50	41.18	42.22
L7 - 135	G-5	21.31	10.84	2.74	48.41	38.01	45.16	7.67	13.21	28.74	29.93
L7 - 304	G-5	20.64	14.85	3.06	56.07	42.94	51.52	10.21	16.27	35.91	37.11
L7 - 305	G-5	21.42	10.30	2.15	46.96	37.51	43.92	7.33	12.61	29.29	29.67
L7 - 84	G-5	20.80	10.66	2.07	48.47	38.72	44.25	7.66	13.00	29.71	29.77
L7 - 88	G-5	26.97	13.82	3.89	62.64	49.02	58.46	9.68	18.29	40.26	41.22
L701 - 7	G-8	24.01	11.86	3.85	52.83	40.52	50.25	8.80	14.50	28.98	32.65
L72 - 57	G-12	13.39	8.21	1.67	33.76	26.01	30.95	6.12	9.43	19.54	19.65
L729 - 2	B-10	11.82	8.08	1.34	30.91	24.97	28.89	4.73	9.05	19.56	17.90

L73 - 16	G-12	19.38	10.76	2.05	46.46	38.35	44.05	6.12	14.14	26.08	29.46
L73 - 17	G-12	22.04	10.67	1.46	49.63	40.15	45.14	7.91	12.60	29.25	30.26
L73 - 18	G-12	12.14	7.43	0.99	31.22	24.77	28.59	5.41	9.00	18.63	17.81
L73 - 45	G-12	24.47	13.78	3.29	58.96	46.91	55.56	8.97	17.64	35.36	39.50
L73 - 46	G-12	25.70	11.50	2.77	50.82	40.60	48.55	7.42	11.61	28.90	31.01
L76 - 13	D-4	15.73	8.29	1.75	39.02	31.07	35.37	6.16	11.72	24.35	24.42
L78 - 32	C-8	25.66	15.69	3.47	64.10	52.15	59.95	8.64	18.86	39.52	43.50
L78 - 79	C-8	22.24	14.77	2.08	60.02	48.08	55.30	9.76	18.67	37.04	38.31
L79 - 5c	F-0	10.94	6.78	1.22	26.84	21.39	25.32	4.29	7.59	15.68	14.63
L80 - 68	G-4	21.64	10.27	2.32	48.11	38.98	44.53	6.92	13.00	25.65	27.39
L824 - 1	D-1	23.27	8.81	2.33	44.63	35.39	42.87	6.86	11.41	26.80	25.49
L847 - 1	D-1	23.71	10.26	2.59	49.42	38.81	46.63	7.97	13.08	28.29	29.55
L847 - 2	D-1	11.78	5.97	1.47	25.15	21.68	24.73	2.11	6.90	16.92	15.53
L867 - 8	F-2	26.24	15.19	2.73	63.42	50.34	60.07	10.33	19.00	41.67	42.26
L868 - 3	D-2	18.68	12.34	2.71	49.65	39.81	46.44	7.15	16.00	29.63	31.03
L878 - 1c	F-2	32.57	16.12	3.00	68.70	54.99	64.48	10.34	16.50	38.28	41.25
L88 - 9	E-4	20.45	8.50	1.67	43.42	35.07	40.06	7.01	11.50	24.94	25.94

L885 - 14	C-4	12.96	7.28	1.31	30.26	24.02	28.72	4.96	8.79	17.67	17.87
L885 - 15	C-4	13.30	7.25	1.28	30.70	24.01	29.06	5.49	8.56	19.52	18.23
L886 - 9	C-8	19.61	11.71	2.73	52.33	40.21	47.35	9.38	16.20	30.48	31.73
L892 - 16	G-4	20.11	8.88	2.16	44.07	35.01	40.34	6.97	11.50	27.48	27.15
L9 - 130	D-5	18.09	11.63	2.39	49.99	38.45	45.10	9.17	15.50	29.00	30.10
L9 - 8	D-5	28.59	16.12	3.43	68.81	54.24	64.22	11.11	20.00	45.63	44.50
L99 - 5	?-	16.47	7.50	1.71	36.88	29.01	33.68	6.09	9.75	20.67	19.62
P994 - 48	J-6	17.29	9.88	1.83	42.70	34.28	39.80	6.53	12.68	24.27	25.10
P994 - 49	J-6	21.81	11.46	2.32	49.13	39.52	47.00	7.26	14.21	27.25	31.28
P994 - 50	J-6	21.48	11.80	2.05	49.50	39.93	45.84	7.57	12.70	27.67	29.12
P994 - 54	J-6	18.63	12.64	2.75	48.46	36.95	45.43	8.97	14.15	31.32	30.76
P994 - 98	J-6	22.29	12.00	2.17	51.50	41.82	47.97	7.44	13.78	31.66	32.47
P995 - 16	K-1	18.77	11.15	1.38	47.86	38.15	43.81	8.77	14.50	30.54	30.38
P999 - 1	L-8	19.55		2.81	45.35	36.22	43.84	6.19		27.16	28.76

Appendix E

Habitat predictions and habitat scores for each astragalus in the American Omo collection.

Member	Unit	Individual	Habitat Score	Prediction
B	B-10	L2 - 63	1.918	HeavyCover
B	B-10	L2 - 107	1.941	HeavyCover
B	B-10	L729 - 2	3.967	Open
B	B-10	L2 - 45b	2.836	HeavyCover
B	B-11	L1 - 298	1.762	Forest
B	B-11	L1 - 160	1.505	Forest
B	B-11	L1 - 297	1.463	Forest
B	B-11	L1 - 301	3.989	Open
B	B-11	L1 - 299	1.539	Forest
B	B-11	L1 - 485	3.007	LightCover
B	B-11	L1 - 15	2.446	HeavyCover
C	C-04	L289 - 1	2.755	LightCover
C	C-04	L885 - 15	2.926	LightCover
C	C-04	L885 - 14	2.795	Open
C	C-04	L285 - 1	1.164	Forest
C	C-05	L27 - 27a	2.023	HeavyCover
C	C-05	L42 - 43	2.879	Open
C	C-05	L45 - 17	1.646	Forest

C	C-05	L27 - 25	1.138	Forest
C	C-05	L183 - 27	1.305	Forest
C	C-06	L327 - 8	1.92	HeavyCover
C	C-06	L23 - 56	2.491	HeavyCover
C	C-06	L327 - 7	2.278	HeavyCover
C	C-06	L32 - 140	3.524	Open
C	C-06	L32 - 27	1.281	Forest
C	C-06	L23 - 41	1.451	Forest
C	C-06	L32 - 33	1.283	Forest
C	C-06	L327 - 25	2.592	LightCover
C	C-06	L32 - 74	1.625	Forest
C	C-06	L32 - 28	2.59	HeavyCover
C	C-06	L56 - 2	2.222	HeavyCover
C	C-08	L585 - 4	2.173	HeavyCover
C	C-08	L47 - 24	3.604	Open
C	C-08	L47 - 4	3.113	Open
C	C-08	L47 - 93	2.894	LightCover
C	C-08	L59 - 5	2.229	HeavyCover
C	C-08	L193 - 7	1.102	Forest
C	C-08	L47 - 104	1.084	Forest
C	C-08	L78 - 79	3.696	Open
C	C-08	L886 - 9	1.852	HeavyCover
C	C-08	L78 - 32	2.778	HeavyCover
C	C-08	L37 - 11	3.605	Open

C	C-08	L69 - 8	2.089	HeavyCover
C	C-08	L69 - 9	3.427	Open
C	C-09	L144 - 15	2.032	LightCover
C	C-09	L144 - 14	3.887	Open
C	C-09	L143 - 7	3.019	LightCover
C	C-09	L51 - 24	2.638	LightCover
C	C-09	L51 - 15	3.658	Open
C	C-09	L51 - 32	3.195	LightCover
C	C-09	L51 - 14	1.426	Forest
C	C-09	L143 - 17	2.303	HeavyCover
C	C-09	L218 - 3	3.931	Open
C	C-09	L51 - 33	1.445	Forest
D	D-01	L847 - 1	1.174	Forest
D	D-01	L847 - 2	2.765	LightCover
D	D-01	L21 - 29	1.422	Forest
D	D-01	L21 - 30	3.999	Open
D	D-01	L21 - 57	1.697	HeavyCover
D	D-01	L455 - 3	3.018	Open
D	D-01	L824 - 1	1.074	Forest
D	D-02	L227 - 1	1.997	HeavyCover
D	D-02	L868 - 3	3.787	Open
D	D-02	L12 - 2	1.793	Forest
D	D-03	L161 - 16	1.072	Forest
D	D-03	L122 - 28	1.372	Forest

D	D-03	L554 - 1	1.196	Forest
D	D-03	L122 - 27	1.151	Forest
D	D-03	L63 - 3	3.371	Open
D	D-04	L230 - 1	2.885	LightCover
D	D-04	L76 - 13	1.472	Forest
D	D-04	L19 - 5	1.158	Forest
D	D-04	L169 - 2	3.024	Open
E	E-02	L26 - 22	3.332	Open
E	E-02	L26 - 6	3.889	Open
E	E-02	L26 - 123	1.03	Forest
E	E-03	L235 - 5	3.997	Open
E	E-03	L-56 - 61	1.196	Forest
E	E-03	L-56 - 12	1.837	HeavyCover
E	E-03	L-56 - 86	2.319	HeavyCover
E	E-03	L-56 - 38	1.906	HeavyCover
E	E-03	L-56 - 62	2.242	HeavyCover
E	E-03	L4 - 39c	1.173	Forest
E	E-03	L4 - 39b	2.496	LightCover
E	E-03	L338 - 11	3.997	Open
E	E-03	L4 - 39a	3.852	Open
E	E-03	L4 - 39d	3.299	LightCover
E	E-04	L114 - 23	1.451	Forest
E	E-04	L88 - 9	1.088	Forest
E	E-04	L147 - 13	1.477	Forest

E	E-04	L114 - 24	2.214	HeavyCover
E	E-04	L128 - 12	1.242	Forest
F	F-00	L398 - 105	1.76	Forest
F	F-00	L243 - 1	3.461	Open
F	F-00	L31 - 8	3.982	Open
F	F-00	L79 - 5c	3.879	Open
F	F-00	L398 - 450	2.67	LightCover
F	F-01	L28 - 11x	2.951	LightCover
F	F-01	L215 - 12	1.562	Forest
F	F-01	L28 - 11a	2.687	LightCover
F	F-01	L239 - 2	2.977	Open
F	F-01	L39 - 11	2.656	LightCover
F	F-01	L41 - 11	3.767	Open
F	F-01	L28 - 48	2.97	LightCover
F	F-01	L28 - 6	3.884	Open
F	F-01	L39 - 10	3.987	Open
F	F-01	L28 - 39	3.948	Open
F	F-01	L28 - 9	3.05	LightCover
F	F-01	F302 - 5	2.023	HeavyCover
F	F-01	L28 - 11b	2.745	LightCover
F	F-01	L28 - 24	1.21	Forest
F	F-01	L41 - 13	4	Open
F	F-01	L28 - 12	1.158	Forest
F	F-01	L39 - 9	3.261	Open

F	F-01	L28 - 7	1.215	Forest
F	F-01	L28 - 142	3.112	LightCover
F	F-01	L28 - 13x	3.058	LightCover
F	F-01	L465 - 97	3.226	LightCover
F	F-01	L467 - 29	3.999	Open
F	F-01	L467 - 28	2.529	HeavyCover
F	F-01	L215 - 11	1.459	Forest
F	F-01	L41 - 12	1.003	Forest
F	F-02	L867 - 8	2.761	LightCover
F	F-02	L878 - 1c	2.672	LightCover
F	F-02	L258 - 1	3.968	Open
F	F-03	L52 - 25	3.878	Open
F	F-03	L52 - 102	1.065	Forest
F	F-03	L52 - 79	1.023	Forest
F	F-03	L52 - 127	1.317	Forest
F	F-03	L238 - 19	1.114	Forest
F	F-03	L52 - 23	1.533	Forest
F	F-03	L52 - 24	1.893	HeavyCover
F	F-03	L52 - 22	2.254	HeavyCover
G	G-01	L477 - 9	3.773	Open
G	G-01	L477 - 10	1.112	Forest
G	G-01	L474 - 2	3.163	LightCover
G	G-03	L628 - 37	2.6	HeavyCover
G	G-03	L628 - 35	1.613	HeavyCover

G	G-03	L628 - 36	2.511	LightCover
G	G-03	L480 - 9	1.013	Forest
G	G-03	L503 - 10	1.87	HeavyCover
G	G-04	L485 - 3	3.881	Open
G	G-04	L489 - 7	3.425	Open
G	G-04	L504 - 9	3.999	Open
G	G-04	L892 - 16	1.441	Forest
G	G-04	L16 - 174	1.777	HeavyCover
G	G-04	L504 - 19	2.402	LightCover
G	G-04	L16 - 13	2.288	HeavyCover
G	G-04	L80 - 68	1.218	Forest
G	G-04	L61 - 2	3.552	Open
G	G-05	L35 - 50	2.914	Open
G	G-05	L35 - 39b	2.566	LightCover
G	G-05	L7 - 84	2.129	HeavyCover
G	G-05	L7 - 305	1.951	HeavyCover
G	G-05	L35 - 39a	1.837	HeavyCover
G	G-05	L35 - 53	2.967	LightCover
G	G-05	L7 - 135	1.914	HeavyCover
G	G-05	L7 - 304	3.964	Open
G	G-05	L35 - 37	2.31	LightCover
G	G-05	L607 - 15	1.438	Forest
G	G-05	L7 - 88	1.74	HeavyCover
G	G-06	L44 - 34a	1.28	Forest

G	G-06	L44 - 34b	3.172	LightCover
G	G-06	L684 - 8	1.812	HeavyCover
G	G-07	L112 - 16	3.461	Open
G	G-07	L433 - 4	1.305	Forest
G	G-07	L432 - 8	3.928	Open
G	G-07	L511 - 2	1.81	HeavyCover
G	G-08	L615 - 13	1.291	Forest
G	G-08	L615 - 14	2.896	Open
G	G-08	L67 - 104	1.183	Forest
G	G-08	L67 - 12	1.033	Forest
G	G-08	L67 - 14	1.138	Forest
G	G-08	L67 - 17	2.476	HeavyCover
G	G-08	L67 - 10	1.092	Forest
G	G-08	L701 - 7	1.423	Forest
G	G-08	L67 - 103	2.639	LightCover
G	G-08	L67 - 15	1.019	Forest
G	G-08	L67 - 101	1.593	Forest
G	G-08	L615 - 12	2.395	LightCover
G	G-09	L523 - 22	2.765	LightCover
G	G-09	L510 - 2	3.432	Open
G	G-09	L524 - 2	2.066	HeavyCover
G	G-09	L669 - 3	1.759	HeavyCover
G	G-12	L622 - 19	2.671	HeavyCover
G	G-12	L72 - 57	3.578	Open

G	G-12	L73 - 16	1.477	Forest
G	G-12	L624 - 25	2.208	LightCover
G	G-12	L73 - 18	3.407	Open
G	G-12	L627 - 395	2.86	LightCover
G	G-12	L627 - 441	1.634	Forest
G	G-12	L73 - 17	1.971	HeavyCover
G	G-12	L627 - 77	3.084	Open
G	G-12	L627 - 78	2.788	LightCover
G	G-12	L626 - 102	3.822	Open
G	G-12	L627 - 76	1.833	Forest
G	G-12	L626 - 103	3.004	LightCover
G	G-12	L627 - 208b	3.942	Open
G	G-12	L627 - 256	3.088	Open
G	G-12	L627 - 258	3.998	Open
G	G-12	L627 - 393	1.785	HeavyCover
G	G-12	L627 - 394	2.29	HeavyCover
G	G-12	L73 - 45	1.893	HeavyCover
G	G-12	L73 - 46	2.63	LightCover
G	G-13	L25 - 56	3.998	Open
G	G-13	L25 - 138	2.921	LightCover
G	G-13	L596 - 11	1.019	Forest
J	J-06	P994 - 48	1.962	HeavyCover
J	J-06	P994 - 54	3.943	Open
J	J-06	P994 - 98	2.551	LightCover

J	J-06	P994 - 49	1.503	Forest
J	J-06	P994 - 50	2.683	LightCover

Appendix F

Mesowear scores for American Omo Bovids by submember, by tribe, and by tooth class.

Unit	Tribe	ToothClass	High%	Sharp%	Blunt%	Round%	Low%
B-03	Bovini	upper	100.00	0.00	0.00	100.00	0.00
B-09	Reduncini	lower	100.00	0.00	0.00	100.00	0.00
B-10	Aepycerotini	upper	100.00	100.00	0.00	0.00	0.00
B-10	Tragelaphini	upper	100.00	0.00	0.00	100.00	0.00
B-11	Aepycerotini	upper	100.00	75.00	0.00	25.00	0.00
B-11	Bovini	upper	100.00	0.00	0.00	100.00	0.00
B-11	Reduncini	lower	100.00	50.00	0.00	50.00	0.00
B-11	Reduncini	upper	100.00	100.00	0.00	0.00	0.00
B-11	Tragelaphini	upper	100.00	0.00	0.00	100.00	0.00
B-12	Tragelaphini	lower	100.00	0.00	0.00	100.00	0.00
C-02	Aepycerotini	lower	100.00	100.00	0.00	0.00	0.00
C-03	Tragelaphini	lower	100.00	0.00	0.00	100.00	0.00
C-04	Aepycerotini	lower	100.00	0.00	0.00	100.00	0.00
C-04	Bovini	upper	100.00	0.00	0.00	100.00	0.00
C-04	Reduncini	upper	100.00	0.00	0.00	100.00	0.00
C-04	Tragelaphini	lower	100.00	0.00	0.00	100.00	0.00
C-05	Aepycerotini	upper	75.00	66.67	0.00	33.33	25.00
C-05	Bovini	lower	100.00	0.00	0.00	100.00	0.00

C-05	Bovini	upper	0.00	0.00	0.00	100.00	100.00
C-05	Reduncini	lower	100.00	0.00	0.00	100.00	0.00
C-05	Tragelaphini	lower	100.00	0.00	0.00	100.00	0.00
C-05	Tragelaphini	upper	100.00	0.00	0.00	100.00	0.00
C-06	Aepycerotini	lower	100.00	50.00	0.00	50.00	0.00
C-06	Bovini	upper	83.33	0.00	0.00	91.67	25.00
C-06	Reduncini	lower	100.00	0.00	0.00	100.00	0.00
C-06	Reduncini	upper	100.00	0.00	0.00	100.00	0.00
C-06	Tragelaphini	lower	100.00	0.00	0.00	100.00	0.00
C-06	Tragelaphini	upper	100.00	50.00	0.00	50.00	0.00
C-07	Aepycerotini	lower	100.00	0.00	0.00	100.00	0.00
C-07	Bovini	lower	100.00	0.00	0.00	100.00	0.00
C-07	Bovini	upper	100.00	0.00	0.00	100.00	0.00
C-07	Reduncini	upper	100.00	100.00	0.00	0.00	0.00
C-07	Tragelaphini	lower	100.00	0.00	0.00	100.00	0.00
C-07	Tragelaphini	upper	100.00	100.00	0.00	0.00	0.00
C-08		lower	100.00	100.00	0.00	0.00	0.00
C-08	Aepycerotini	lower	100.00	0.00	0.00	100.00	0.00
C-08	Bovini	lower	66.67	0.00	0.00	100.00	33.33
C-08	Bovini	upper	100.00	0.00	0.00	100.00	0.00
C-08	Reduncini	lower	0.00	0.00	0.00	100.00	100.00
C-08	Reduncini	upper	100.00	50.00	0.00	50.00	0.00
C-08	Tragelaphini	lower	100.00	16.67	0.00	83.33	0.00
C-08	Tragelaphini	upper	100.00	100.00	0.00	0.00	0.00

C-09	Aepycerotini	lower	100.00	0.00	0.00	100.00	0.00
C-09	Aepycerotini	upper	100.00	100.00	0.00	0.00	0.00
C-09	Bovini	lower	100.00	0.00	0.00	100.00	0.00
C-09	Bovini	upper	0.00	0.00	0.00	100.00	100.00
C-09	Tragelaphini	lower	100.00	0.00	0.00	100.00	0.00
C-09	Tragelaphini	upper	100.00	0.00	0.00	100.00	0.00
C-NA	Reduncini	upper	100.00	0.00	0.00	100.00	0.00
D-01	Aepycerotini	lower	100.00	100.00	0.00	0.00	0.00
D-01	Bovini	lower	0.00	0.00	0.00	0.00	100.00
D-01	Reduncini	upper	100.00	33.33	0.00	66.67	0.00
D-02	Aepycerotini	lower	0.00	0.00	0.00	100.00	100.00
D-02	Aepycerotini	upper	100.00	25.00	0.00	75.00	0.00
D-03	Aepycerotini	upper	50.00	0.00	0.00	100.00	50.00
D-03	Bovini	upper	100.00	0.00	0.00	0.00	0.00
D-03	Tragelaphini	lower	100.00	0.00	0.00	100.00	0.00
D-03	Tragelaphini	upper	100.00	100.00	0.00	0.00	0.00
D-04	Aepycerotini	lower	100.00	100.00	0.00	0.00	0.00
D-04	Aepycerotini	upper	100.00	0.00	0.00	100.00	0.00
D-04	Bovini	lower	0.00	0.00	100.00	0.00	100.00
D-04	Reduncini	upper	100.00	100.00	0.00	0.00	0.00
D-04	Tragelaphini	upper	100.00	0.00	0.00	100.00	0.00
D-05	Aepycerotini	lower	0.00	0.00	0.00	100.00	100.00
D-05	Aepycerotini	upper	75.00	75.00	25.00	0.00	25.00
D-05	Alcelaphini	lower	0.00	0.00	0.00	100.00	100.00

D-05	Reduncini	lower	66.67	66.67	33.33	0.00	33.33
D-05	Reduncini	upper	66.67	0.00	0.00	100.00	33.33
D-05	Tragelaphini	lower	80.00	0.00	0.00	100.00	20.00
D-05	Tragelaphini	upper	100.00	0.00	0.00	0.00	0.00
E-01	Aepycerotini	lower	100.00	0.00	0.00	100.00	0.00
E-01	Aepycerotini	upper	100.00	0.00	0.00	0.00	0.00
E-01	Bovini	lower	50.00	0.00	100.00	0.00	50.00
E-01	Reduncini	lower	100.00	100.00	0.00	0.00	0.00
E-01	Reduncini	upper	100.00	0.00	0.00	0.00	0.00
E-01	Tragelaphini	lower	100.00	0.00	0.00	100.00	0.00
E-02	Aepycerotini	lower	100.00	0.00	0.00	100.00	0.00
E-02	Reduncini	lower	100.00	0.00	0.00	100.00	0.00
E-03	Aepycerotini	lower	50.00	0.00	0.00	100.00	50.00
E-03	Aepycerotini	upper	75.00	37.50	0.00	62.50	25.00
E-03	Bovini	lower	100.00	0.00	0.00	100.00	0.00
E-03	Bovini	upper	0.00	0.00	0.00	100.00	100.00
E-03	Reduncini	upper	100.00	50.00	0.00	50.00	0.00
E-03	Tragelaphini	lower	100.00	11.11	0.00	88.89	0.00
E-03	Tragelaphini	upper	100.00	0.00	0.00	100.00	0.00
E-04	Aepycerotini	lower	50.00	0.00	0.00	100.00	50.00
E-04	Aepycerotini	upper	50.00	0.00	0.00	100.00	50.00
E-04	Bovini	lower	100.00	0.00	0.00	100.00	0.00
E-04	Bovini	upper	100.00	100.00	0.00	0.00	0.00
E-04	Reduncini	lower	100.00	33.33	0.00	66.67	0.00

E-04	Reduncini	upper	100.00	0.00	0.00	100.00	0.00
E-04	Tragelaphini	lower	100.00	16.67	0.00	83.33	0.00
E-04	Tragelaphini	upper	100.00	100.00	0.00	0.00	0.00
F-00		upper	100.00	0.00	0.00	100.00	0.00
F-00	Aepycerotini	lower	50.00	0.00	0.00	100.00	50.00
F-00	Bovini	lower	100.00	0.00	0.00	100.00	0.00
F-00	Reduncini	lower	50.00	0.00	0.00	100.00	50.00
F-00	Reduncini	upper	100.00	0.00	0.00	100.00	0.00
F-01		upper	100.00	0.00	0.00	100.00	0.00
F-01	Aepycerotini	lower	50.00	0.00	0.00	100.00	50.00
F-01	Aepycerotini	upper	66.67	12.50	0.00	87.50	33.33
F-01	Bovini	lower	100.00	0.00	0.00	100.00	0.00
F-01	Reduncini	lower	0.00	0.00	0.00	100.00	100.00
F-01	Reduncini	upper	100.00	0.00	0.00	0.00	0.00
F-01	Tragelaphini	lower	100.00	0.00	0.00	100.00	0.00
F-01	Tragelaphini	upper	100.00	0.00	0.00	0.00	0.00
F-03	Aepycerotini	lower	0.00	0.00	0.00	0.00	100.00
F-03	Aepycerotini	upper	60.00	60.00	0.00	40.00	40.00
F-03	Reduncini	lower	100.00	0.00	0.00	100.00	0.00
F-03	Reduncini	upper	100.00	20.00	0.00	80.00	0.00
F-03	Tragelaphini	upper	100.00	0.00	0.00	100.00	0.00
F-04	Aepycerotini	upper	100.00	100.00	0.00	0.00	0.00
F-04	Bovini	upper	100.00	0.00	0.00	100.00	0.00
F-04	Reduncini	upper	0.00	0.00	0.00	0.00	100.00

F-NA	Reduncini	lower	100.00	0.00	0.00	100.00	0.00
G-01	Aepycerotini	lower	0.00	0.00	0.00	100.00	100.00
G-01	Bovini	lower	100.00	0.00	0.00	100.00	0.00
G-01	Bovini	upper	0.00	0.00	0.00	100.00	100.00
G-02	Reduncini	upper	100.00	0.00	0.00	0.00	0.00
G-03	Aepycerotini	lower	75.00	0.00	0.00	100.00	25.00
G-03	Aepycerotini	upper	100.00	50.00	0.00	50.00	0.00
G-03	Bovini	lower	100.00	0.00	0.00	100.00	0.00
G-03	Bovini	upper	100.00	0.00	0.00	100.00	0.00
G-03	Reduncini	lower	100.00	0.00	0.00	100.00	0.00
G-03	Reduncini	upper	100.00	0.00	0.00	100.00	0.00
G-03	Tragelaphini	lower	100.00	0.00	0.00	100.00	0.00
G-03	Tragelaphini	upper	100.00	0.00	0.00	100.00	0.00
G-04	Aepycerotini	lower	50.00	0.00	0.00	100.00	50.00
G-04	Aepycerotini	upper	100.00	100.00	0.00	0.00	0.00
G-04	Alcelaphini	upper	0.00	0.00	0.00	0.00	100.00
G-04	Bovini	lower	100.00	0.00	0.00	100.00	0.00
G-04	Reduncini	lower	100.00	25.00	0.00	75.00	0.00
G-04	Reduncini	upper	125.00	50.00	0.00	25.00	0.00
G-04	Tragelaphini	lower	100.00	0.00	0.00	100.00	0.00
G-04	Tragelaphini	upper	100.00	33.33	0.00	66.67	0.00
G-05	Aepycerotini	lower	33.33	33.33	0.00	66.67	66.67
G-05	Aepycerotini	upper	55.56	28.57	0.00	71.43	44.44
G-05	Alcelaphini	upper	100.00	0.00	0.00	100.00	0.00

G-05	Bovini	lower	100.00	0.00	0.00	100.00	0.00
G-05	Bovini	upper	100.00	0.00	0.00	100.00	0.00
G-05	Reduncini	lower	81.82	9.09	0.00	90.91	18.18
G-05	Reduncini	upper	102.78	33.33	0.00	63.89	0.00
G-05	Tragelaphini	lower	100.00	42.86	0.00	57.14	0.00
G-05	Tragelaphini	upper	100.00	42.86	0.00	57.14	0.00
G-06	Aepycerotini	upper	33.33	0.00	0.00	100.00	66.67
G-06	Reduncini	lower	0.00	0.00	0.00	100.00	100.00
G-06	Reduncini	upper	100.00	0.00	0.00	100.00	0.00
G-06	Tragelaphini	lower	100.00	0.00	0.00	100.00	0.00
G-07	Reduncini	lower	100.00	0.00	0.00	100.00	0.00
G-07	Reduncini	upper	66.67	0.00	0.00	100.00	33.33
G-07	Tragelaphini	lower	100.00	0.00	0.00	100.00	0.00
G-07	Tragelaphini	upper	100.00	100.00	0.00	0.00	0.00
G-08	Aepycerotini	lower	50.00	25.00	0.00	75.00	50.00
G-08	Aepycerotini	upper	50.00	0.00	0.00	100.00	50.00
G-08	Bovini	lower	100.00	0.00	0.00	100.00	0.00
G-08	Reduncini	lower	100.00	25.00	0.00	75.00	0.00
G-08	Reduncini	upper	100.00	60.00	0.00	40.00	0.00
G-08	Tragelaphini	lower	100.00	25.00	0.00	75.00	0.00
G-08	Tragelaphini	upper	100.00	33.33	0.00	66.67	0.00
G-09	Aepycerotini	upper	100.00	0.00	0.00	100.00	0.00
G-09	Bovini	lower	100.00	0.00	0.00	100.00	0.00
G-09	Reduncini	upper	75.00	25.00	0.00	75.00	25.00

G-10	Aepycerotini	upper	25.00	25.00	0.00	75.00	75.00
G-10	Reduncini	lower	100.00	0.00	0.00	100.00	0.00
G-10	Tragelaphini	lower	100.00	0.00	0.00	100.00	0.00
G-11	Aepycerotini	lower	66.67	0.00	0.00	100.00	33.33
G-11	Aepycerotini	upper	100.00	100.00	0.00	0.00	0.00
G-11	Reduncini	lower	100.00	20.00	0.00	80.00	0.00
G-11	Reduncini	upper	100.00	50.00	0.00	50.00	0.00
G-11	Tragelaphini	lower	100.00	0.00	0.00	100.00	0.00
G-12	Aepycerotini	lower	94.74	10.53	0.00	89.47	5.26
G-12	Aepycerotini	upper	77.27	52.38	0.00	47.62	22.73
G-12	Alcelaphini	upper	0.00	0.00	0.00	0.00	100.00
G-12	Bovini	lower	100.00	0.00	0.00	100.00	0.00
G-12	Bovini	upper	100.00	0.00	0.00	0.00	0.00
G-12	Reduncini	lower	100.00	15.38	0.00	84.62	0.00
G-12	Reduncini	upper	100.00	25.00	0.00	75.00	0.00
G-12	Tragelaphini	lower	100.00	25.00	0.00	75.00	0.00
G-12	Tragelaphini	upper	100.00	55.56	0.00	44.44	0.00
G-13	Aepycerotini	lower	50.00	0.00	0.00	100.00	50.00
G-13	Aepycerotini	upper	57.14	40.00	0.00	60.00	42.86
G-13	Alcelaphini	upper	100.00	0.00	0.00	100.00	0.00
G-13	Bovini	lower	100.00	0.00	0.00	100.00	0.00
G-13	Reduncini	lower	66.67	0.00	33.33	66.67	33.33
G-13	Reduncini	upper	83.33	0.00	0.00	100.00	16.67
G-13	Tragelaphini	lower	100.00	66.67	0.00	33.33	0.00

G-16	Aepycerotini	upper	100.00	0.00	0.00	100.00	0.00
G-16	Reduncini	upper	100.00	0.00	0.00	100.00	0.00
G-19	Tragelaphini	upper	100.00	0.00	0.00	0.00	0.00
G-27	Reduncini	upper	100.00	0.00	0.00	100.00	0.00
H-03	Reduncini	lower	100.00	0.00	0.00	100.00	0.00
H-03	Reduncini	upper	75.00	42.86	0.00	57.14	25.00
J-06	Aepycerotini	upper	66.67	66.67	0.00	33.33	33.33
J-06	Reduncini	upper	100.00	0.00	0.00	0.00	0.00
K-NA	Reduncini	lower	100.00	0.00	0.00	100.00	0.00
L-05	Reduncini	lower	100.00	0.00	0.00	100.00	0.00

References

Alemseged Z, Bobe R, and Geraads D. 2007. Comparability of fossil data and its significance for the interpretation of hominin environments. In: Bobe R, Alemseged Z, Behrensmeyer AK, editors. Hominin environments in the East African Pliocene: An assessment of the faunal evidence. Dordrecht: Springer. p 159–181.

Alemseged Z. 2003. An integrated approach to taphonomy and faunal change in the Shungura Formation (Ethiopia) and its implication for hominid evolution. Journal of Human Evolution 44:451–478.

Alexander RM, and Bennett MB. 1987. Some principles of ligament function, with examples from the tarsal joints of the sheep (*Ovis aries*). Journal of Zoology 211:487–504.

Babyak MA. 2004. What You See May Not Be What You Get: A Brief, Nontechnical Introduction to Overfitting in Regression-Type Models. Psychosom Med 66:411–421.

Barr W, and Scott R. 2014. Phylogenetic comparative methods complement discriminant function analysis in ecomorphology. American Journal of Physical Anthropology. 153:663 – 674.

Behrensmeyer AK, Damuth JD, DiMichele WA, Potts R, Sues HD, and Wing SL eds. 1992. Terrestrial Ecosystems Through Time: Evolutionary Paleoecology of Terrestrial Plants and Animals. University of Chicago Press.

Behrensmeyer AK, Todd NE, Potts R, and McBrinn GE. 1997. Late Pliocene Faunal Turnover in the Turkana Basin, Kenya and Ethiopia. Science 278:1589–1594.

Behrensmeyer AK. 1975a. The taphonomy and paleoecology of Plio-Pleistocene vertebrate assemblages east of Lake Rudolf, Kenya. Bulletin of The Museum of Comparative Zoology 146:473–578.

Behrensmeyer AK. 1975b. Taphonomy and paleoecology in the hominid fossil record. Yearbook of Physical Anthropology 19:36–50.

Benjamini Y, and Hochberg Y. 1995. Controlling the false discovery rate: a practical and powerful approach to multiple testing. Journal of the Royal Statistical Society. Series B (Methodological):289–300.

Bibi F, Souron A, Bocherens H, Uno K, and Boisserie J-R. 2013. Ecological change in the lower Omo Valley around 2.8 Ma. Biol. Lett. 9:20120890.

Bibi F. 2011. *Tragelaphus nakuae*: evolutionary change, biochronology, and turnover in the African Plio-Pleistocene. Zoological Journal of the Linnean Society 162:699–711.

Biewener AA. 1983. Allometry of quadrupedal locomotion: the scaling of duty factor, bone curvature and limb orientation to body size. Journal of Experimental Biology 105:147–171.

Bishop LC, Plummer TW, Hertel F, and Kovarovic K. 2011. Paleoenvironments of Laetoli, Tanzania as determined by antelope habitat preferences. In: Paleontology and geology of Laetoli: Human evolution in context. Springer. p 355–366.

Blomberg SP, Garland JR. T, and Ives AR. 2003. Testing For Phylogenetic Signal In Comparative Data: Behavioral Traits Are More Labile. Evolution 57:717–745.

Blondel C, Merceron G, Andossa L, Taisso MH, Vignaud P, and Brunet M. 2010. Dental mesowear analysis of the late Miocene Bovidae from Toros-Menalla (Chad) and early hominid habitats in Central Africa. Palaeogeography, Palaeoclimatology, Palaeoecology 292:184–191.

Bobe R, Behrensmeyer A, and Chapmam R. 2002. Faunal change, environmental variability and late Pliocene hominin evolution. Journal of Human Evolution 42:475–497.

Bobe R, and Behrensmeyer AK. 2004. The expansion of grassland ecosystems in Africa in relation to mammalian evolution and the origin of the genus *Homo*. Palaeogeography, Palaeoclimatology, Palaeoecology 207:399–420.

Bobe R, and Eck GG. 2001. Responses of African bovids to Pliocene climatic change. Paleobiology 27:1–47.

Bobe R. 2006. The evolution of arid ecosystems in eastern Africa. Journal of Arid Environments 66:564–584.

Boisserie J-R, Delagnes A, Beyene Y, and Schuster M. 2010. Reconstructing the African background to human expansions in Eurasia: New research in the Shungura Formation, Ethiopia. Quaternary International 223–224:426–428.

Boisserie J-R, Guy F, Delagnes A, Hlukso LJ, Bibi F, Beyene Y, and Guillemot C. 2008. New palaeoanthropological research in the Plio-Pleistocene Omo Group, Lower

Omo Valley, SNNPR (Southern Nations, Nationalities and People Regions), Ethiopia. Comptes Rendus Palevol 7:429–439.

Bonnefille R, and Dechamps R. 1983. Data on fossil flora. In: de Heinzelin J, editor. The Omo Group: archives of the International Omo Research Expedition. Tervuren, Belgium: Musee Royale de L'Afrique Centrale Annale, serie in 8. p 191–207.

Boyer DM. 2008. Relief index of second mandibular molars is a correlate of diet among prosimian primates and other euarchontan mammals. Journal of Human Evolution 55:1118–1137.

Brain CK. 1980. The Hunters or the Hunted?: An Introduction to African Cave Taphonomy. Chicago: University of Chicago Press.

Brown F, and Feibel C. 1985. "Robust" Hominids and Plio-Pleistocene Paleogeography of the Turkana Basin, Kenya and Ethiopia. In: Grine F, editor. Evolutionary History of the "Robust" Australopithecines. Aldine de Gruyter. p 325–341.

Bunn JM, Boyer DM, Lipman Y, St Clair EM, Jernvall J, and Daubechies I. 2011. Comparing Dirichlet Normal Surface Energy of Tooth Crowns, a New Technique of Molar Shape Quantification for Dietary Inference, With Previous Methods in Isolation and in Combination. Am. J. Phys. Anthropol. 145:247–261.

Cerling TE, Levin NE, Quade J, Wynn JG, Fox DL, Kingston JD, Klein RG, and Brown FH. 2010. Comment on the Paleoenvironment of Ardipithecus ramidus. Science 328:1105–d.

Coombs WP. 1978. Theoretical Aspects of Cursorial Adaptations in Dinosaurs. The Quarterly Review of Biology 53:393–418.

Curran S. 2009. Hominin Paleoecology and Cervid Ecomorphology. Unpublished PhD Thesis. University of Minnesota.

Dagosto M, Marivaux L, Gebo DL, Beard KC, Chaimanee Y, Jaeger J-J, Marandat B, Soe AN, and Kyaw AA. 2010. The phylogenetic affinities of the Pondaung tali. American Journal of Physical Anthropology 143:223–234.

Damuth J, and Janis CM. 2011. On the relationship between hypsodonty and feeding ecology in ungulate mammals, and its utility in palaeoecology. Biological Reviews 86:733–758.

Dechant Boaz D. 1994. Taphonomy and the fluvial environment: examples from Pliocene deposits of the Shungura Formation, Omo Basin, Ethiopia. In: Corruccini RS,

Ciochon RL, editors. Integrative Paths to the Past. New Jersty: Prentice Hall. p 377–414.

DeGusta D, and Vrba E. 2003. A method for inferring paleohabitats from the functional morphology of bovid astragali. Journal of Archaeological Science 30:1009–1022.

DeGusta D, and Vrba E. 2005. Methods for inferring paleohabitats from the functional morphology of bovid phalanges. Journal of Archaeological Science 32:1099–1113.

deMenocal PB. 1995. Plio-Pleistocene African Climate. Scíence 270:53–59.

deMenocal PB. 2004. African climate change and faunal evolution during the Pliocene-Pleistocene. Earth and Planetary Science Letters 220:3–24.

Estes RD. 1992. The Behavior Guide to African Mammals: Including Hoofed Mammals, Carnivores, Primates. University of California Press.

Feibel CS, Brown FH, and McDougall I. 1989. Stratigraphic context of fossil hominids from the Omo group deposits: Northern Turkana Basin, Kenya and Ethiopia. American Journal of Physical Anthropology 78:595–622.

Felsenstein J. 1985. Phylogenies and the Comparative Method. The American Naturalist 125:1–15.

Fernandez MH, and Vrba ES. 2006. Plio-Pleistocene climatic change in the Turkana Basin (East Africa): Evidence from large mammal faunas. Journal Of Human Evolution 50:595–626.

Fortelius M, and Solounias N. 2000. Functional characterization of ungulate molars using the abrasion-attrition wear gradient: a new method for reconstructing paleodiets. American Museum Novitates:1–36.

Fortelius M. 1981. Functional aspects of occlusal cheek-tooth morphology in hypsodont, non-ruminant ungulates. In: International Symposium on Concept and Method in Paleontology. Contributed Papers. . p 153–162.

Fortelius M. 1985. Ungulate cheek teeth: developmental, functional, and evolutionary interrelations. Acta Zoologica Fennica 180:1–76.

Freckleton RP, Harvey PH, and Pagel M. 2002. Phylogenetic Analysis and Comparative Data: A Test and Review of Evidence. Am Nat 160:712–726.

Gagnon M, and Chew AE. 2000. Dietary preferences in extant African Bovidae. Journal of Mammalogy 81:490–511.

Gambaryan PP. 1974. How animals run: anatomical adaptations. New York: Wiley.

Gani MR, and Gani ND. 2011. River-margin habitat of *Ardipithecus ramidus* at Aramis, Ethiopia 4.4 million years ago. Nature Communications 2:602.

Garland T, and Carter PA. 1994. Evolutionary physiology. Annual Review of Physiology 56:579–621.

Garland T, Dickerman AW, Janis CM, and Jones JA. 1993. Phylogenetic Analysis of Covariance by Computer Simulation. Systematic Biology 42:265 –292.

Garland T. 1992. Rate Tests for Phenotypic Evolution Using Phylogenetically Independent Contrasts. The American Naturalist 140:509–519.

Gebo DL, and Schwartz GT. 2006. Foot bones from Omo: Implications for hominid evolution. American Journal of Physical Anthropology 129:499–511.

Gentry AW. 1970. The Bovidae (Mammalia) of the Fort Ternam Fossil Fauna. In: Maglio VJ, Cooke HBS, editors. Fossil Vertebrates of Africa. Vol. 2. London: Academic Press. p 243–323.

Gentry AW. 1985. The Bovidae of the Omo Group deposits, Ethiopia (french and american collections). In: Coppens Y, Howell FC (eds). Les Faunes Plio-Pleistocenes de la basse vallee de l'Omo (Ethiopie); I: Perissodactyles-Artiodactyles (Bovidae). Paris: CNRS. p 119–191.

Geraads D, and Coppens Y. 1995. Evolution des faunes de mammifères dans le Plio-Pléistocène de la basse vallée de l'Omo (Ethiopie): apports de l'analyse factorielle. Comptes Rendus De L Academie Des Sciences Serie II 320:625–637.

Gradstein FM. 2012. The Geologic Time Scale. Amsterdam; Boston: Elsevier.

Greenacre MJ, and Vrba ES. 1984. Graphical display and interpretation of antelope census data in African wildlife areas, using correspondence analysis. Ecology 65:984–997.

Hamrick MW. 1996. Articular size and curvature as determinants of carpal joint mobility and stability in strepsirhine primates. Journal of Morphology 230:113–127.

Hartenberg RS, and Denavit J. 1964. Kinematic synthesis of linkages. MacGraw-Hill, New York.

Harvey PH, and Pagel MD. 1991. The Comparative Method in Evolutionary Biology. Oxford ; New York: Oxford University Press.

De Heinzelin J, and Haesaerts P. 1983. The Shungura Formation. In: de Heinzlen J, editor. The Omo Group: archives of the International Omo Research Expedition. Tervuren, Belgium: Musee Royale de L'Afrique Centrale Annale, serie in 8. p 25–147.

Hernández Fernández M, and Vrba ES. 2005. A complete estimate of the phylogenetic relationships in Ruminantia: a dated species-level supertree of the extant ruminants. Biol Rev Camb Philos Soc 80:269–302.

Hildebrand M, and Goslow G. 2001. Analysis of Vertebrate Structure. 5th ed. Wiley.

Hildebrand M. 1987. The mechanics of horse legs. American Scientist 75:594–601.

Hofmann RR, and Stewart DRM. 1972. Grazer or browser: a classification based on the stomach-structure and feeding habits of East African ruminants. Mammalia 36:226–240.

Hussain ST, Sondaar PY, Shah SMI, Thewissen JGM, Cousin EFHM, and Spoor CF. 1983. Fossil mammal bones of Pakistan, a field atlas. Part I: the artiodactyl astragalus. Memoirs of Geological Survey of Pakistan 14.

Jacobs FB. 1921. Cam Design and Manufacture. D. Van Nostrand Company.

Janis CM, and Fortelius M. 1988. On the means whereby mammals achieve increased functional durability of their dentitions, with special reference to limiting factors. Biological Reviews of the Cambridge Philosophical Society 63:197.

Janis CM. 1988. An estimation of tooth volume and hypsodonty indices in ungulate mammals, and the correlation of these factors with dietary preference. In: Russell DE, Santoro JP, Sigogneau-Russell D, editors. Teeth revisited: Proceedings of the VII International Symposium on Dental Morphology. Vol. 43.

Jarman PJ. 1974. The Social Organisation of Antelope in Relation to Their Ecology. Behaviour 48:215–267.

Johanson DC, and White TD. 1979. A systematic assessment of early African hominids. Science 203:321–330.

Jones KE, Bielby J, Cardillo M, Fritz SA, O'Dell J, Orme CDL, Safi K, Sechrest W, Boakes EH, Carbone C, et al. 2009. PanTHERIA: a species-level database of life history, ecology, and geography of extant and recently extinct mammals. Ecology 90:2648.

Jones KE, and Purvis A. 1997. An optimum body size for mammals? Comparative evidence from bats. Functional Ecology 11:751–756.

Jungers W. 1991. Scaling of postcranial joint size in hominoid primates. Human Evolution 6:391–399.

Jungers WL, Falsetti AB, and Wall CE. 1995. Shape, relative size, and size-adjustments in morphometrics. Yearbook of Physical Anthropology 38:137–161.

Kaiser TM, and Fortelius M. 2003. Differential mesowear in occluding upper and lower molars: Opening mesowear analysis for lower molars and premolars in hypsodont horses. Journal of Morphology 258:67–83.

Kaiser TM. 2011. Feeding Ecology and Niche Partitioning of the Laetoli Ungulate Faunas. In: Harrison T, editor. Paleontology and Geology of Laetoli: Human Evolution in Context. Vertebrate Paleobiology and Paleoanthropology. Springer Netherlands. p 329–354. Available from: http://link.springer.com/chapter/10.1007/978-90-481-9956-3_16

Kamilar JM, and Cooper N. 2013. Phylogenetic signal in primate behaviour, ecology and life history. Phil. Trans. R. Soc. B 368: 20120341.

Kappelman J, Plummer T, Bishop L, Duncan A, and Appleton S. 1997. Bovids as indicators of Plio-Pleistocene paleoenvironments in East Africa. Journal of Human Evolution 32:229–256.

Kappelman J. 1984. Plio-Pleistocene environments of Bed I and Lower Bed II, Olduvai Gorge, Tanzania. Palaeogeography, Palaeoclimatology, Palaeoecology 48:171–196.

Kappelman J. 1988. Morphology and locomotor adaptations of the bovid femur in relation to habitat. Journal of Morphology 198:119–130.

Kappelman J. 1991. The paleoenvironment of *Kenyapithecus* at Fort Ternan. Journal of Human Evolution 20:95–129.

Kimbel WH, Johanson DC, and Rak Y. 1997. Systematic assessment of a maxilla of *Homo* from Hadar, Ethiopia. American Journal of Physical Anthropology 103:235–262.

Kimbel WH, Walter RC, Johanson DC, Reed KE, Aronson JL, Assefa Z, Marean CW, Eck GG, Bobe R, Hovers E, et al. 1996. Late Pliocene *Homo* and Oldowan Tools from the Hadar Formation (Kada Hadar Member), Ethiopia. Journal of Human Evolution 31:549–561.

Kimbel WH. 1995. Hominid Speciation and Pliocene Climatic Change. In: Paleoclimate and Evolution with Emphasis on Human Origins. Yale University Press, New Haven. p 425–437.

Kingdon J. 1974. East African Mammals. University of Chicago Press.

Kingston JD, and Harrison T. 2007. Isotopic dietary reconstructions of Pliocene herbivores at Laetoli: Implications for early hominin paleoecology. Palaeogeography Palaeoclimatology Palaeoecology 243:272–306.

Kingston JD. 2007. Shifting adaptive landscapes: Progress and challenges in reconstructing early hominid environments. American Journal of Physical Anthropology 134:20–58.

Klein RG, Franciscus RG, and Steele TE. 2010. Morphometric identification of bovid metapodials to genus and implications for taxon-free habitat reconstruction. Journal of Archaeological Science 37:389–401.

Kohler M. 1993. Skeleton and Habitat of Recent and Fossil Ruminants. Munchner Geowissenschaftliche Abdhandlungen 25:1–88.

Kovarovic K, Aiello LC, Cardini A, and Lockwood CA. 2011. Discriminant function analyses in archaeology: are classification rates too good to be true? Journal of Archaeological Science 38:3006–3018.

Kovarovic K, and Andrews P. 2007. Bovid postcranial ecomorphological survey of the Laetoli paleoenvironment. Journal of Human Evolution 52:663–680.

Levin NE, Brown FH, Behrensmeyer AK, Bobe R, and Cerling TE. 2011. Paleosol carbonates from the Omo Group: Isotopic records of local and regional environmental change in East Africa. Palaeogeography, Palaeoclimatology, Palaeoecology 307:75–89.

Losos JB, Leal M, Glor RE, de Queiroz K, Hertz PE, Schettino LR, Lara AC, Jackman TR, and Larson A. 2003. Niche lability in the evolution of a Caribbean lizard community. Nature 424:542–545.

Losos JB. 2008. Phylogenetic niche conservatism, phylogenetic signal and the relationship between phylogenetic relatedness and ecological similarity among species. Ecology Letters 11:995–1003.

Louchart A, Wesselman H, Blumenschine RJ, Hlusko LJ, Njau JK, Black MT, Asnake M, and White TD. 2009. Taphonomic, Avian, and Small-Vertebrate Indicators of *Ardipithecus ramidus* Habitat. Science 326:66–664.

Louys J, Ditchfield P, Meloro C, Elton S, and Bishop LC. 2012. Stable isotopes provide independent support for the use of mesowear variables for inferring diets in African antelopes. Proc. R. Soc. B 279:4441–4446.

Lucas PW. 1979. The dental-dietary adaptations of mammals. Neues Jahrbuch für Geologie und Paläontologie, Monatshefte 8:486–512.

Mahler DL, Revell LJ, Glor RE, and Losos JB. 2010. Ecological Opportunity And The Rate Of Morphological Evolution In The Diversification Of Greater Antillean Anoles. Evolution 64:2731–2745.

Manly BFJ. 2004. Multivariate Statistical Methods: A Primer, Third Edition. 3rd ed. Chapman and Hall.

Martin L. 1985. Significance of enamel thickness in hominoid evolution. Nature 314:260–263.

Martins EP, and Garland T. 1991. Phylogenetic analyses of the correlated evolution of continuous characters: a simulation study. Evolution:534–557.

Merceron G, Blondel C, Viriot L, Koufos GD, and de Bonis L. 2007a. Dental microwear analysis of bovids from the Vallesian (late Miocene) of Axios Valley in Greece: reconstruction of the habitat of *Ouranopithecus macedoniensis* (Primates, Hominoidea). Geodiversitas 29:421–433.

Merceron G, Schulz E, Kordos L, and Kaiser TM. 2007b. Paleoenvironment of Dryopithecus brancoi at Rudabánya, Hungary: evidence from dental meso- and micro-wear analyses of large vegetarian mammals. Journal of Human Evolution 53:331–349.

Motani R, and Schmitz L. 2011. Phylogenetic Versus Functional Signals in the Evolution of Form–function Relationships in Terrestrial Vision. Evolution 65:2245–2257.

Muller M. 1996. A Novel Classification of Planar Four-Bar Linkages and its Application to the Mechanical Analysis of Animal Systems. Philosophical Transactions: Biological Sciences 351:689–720.

Mundry R, and Sommer C. 2007. Discriminant function analysis with nonindependent data: consequences and an alternative. Animal Behaviour 74:965–976.

Münkemüller T, Lavergne S, Bzeznik B, Dray S, Jombart T, Schiffers K, and Thuiller W. 2012. How to measure and test phylogenetic signal. Methods in Ecology and Evolution 3:743–756.

Nowak RM. 1999. Walker's Mammals of the World. 6th ed. The Johns Hopkins University Press.

Nunn CL, and Barton RA. 2001. Comparative methods for studying primate adaptation and allometry. Evolutionary Anthropology: Issues, News, and Reviews 10:81–98.

Nunn CL. 1995. A simulation test of Smith's "degrees of freedom" correction for comparative studies. American Journal of Physical Anthropology 98:355–367.

Oksanen J, Blanchet FG, Kindt R, Legendre P, Minchin PR, O'Hara RB, Simpson GL, Solymos P, Stevens MHH, and Wagner H. 2012. vegan: Community Ecology Package. Available from: http://CRAN.R-project.org/package=vegan

Orme D, Freckleton R, Thomas G, Petzoldt T, Fritz S, and Isaac N. 2011. caper: Comparative Analyses of Phylogenetics and Evolution in R. Available from: http://CRAN.R-project.org/package=caper

Ousley S, Jantz R, and Freid D. 2009. Understanding race and human variation: Why forensic anthropologists are good at identifying race. American Journal of Physical Anthropology 139:68–76.

Pagel M. 1994. Detecting Correlated Evolution on Phylogenies: A General Method for the Comparative Analysis of Discrete Characters. Proceedings of the Royal Society of London B 255:37–45.

Du Plessis WP. 1999. Linear regression relationships between NDVI, vegetation and rainfall in Etosha National Park, Namibia. Journal of Arid Environments 42:235–260.

Plummer TW, Bishop LC, and Hertel F. 2008. Habitat preference of extant African bovids based on astragalus morphology: operationalizing ecomorphology for palaeoenvironmental reconstruction. Journal of Archaeological Science 35:3016–3027.

Plummer TW, and Bishop LC. 1994. Hominid paleoecology at Olduvai Gorge, Tanzania as indicated by antelope remains. Journal of Human Evolution 27:47–75.

Potts R. 1996. Evolution and Climate Variability. Science 273:922–923.

Potts R. 1998a. Variability Selection in hominid evolution. Evolutionary Anthropology 7:81–96.

Potts R. 1998b. Environmental hypotheses of hominin evolution. American Journal of Physical Anthropology 107:93–136.

Quinn GGP, and Keough MJ. 2002. Experimental Design and Data Analysis for Biologists. Cambridge University Press.

R Development Core Team. 2011. R: A language and environment for statistical computing. Vienna, Austria: R Foundation for Statistical Computing.

Rak Y, Ginzburg A, and Geffen E. 2002. Does Homo neanderthalensis play a role in modern human ancestry? The mandibular evidence. American journal of physical anthropology 119:199–204.

Reed D, Barr W, Kappelman J, McPherron, and Urban T. 2013. PaleoCore: Data Integration for Paleoanthropology. Abstract at Paleoanthropology Society Annual Meeting, Honololu, HI.

Reed D. 2003. Micromammal paleoecology: past and present relationships between African small mammals and their habitats.

Reed KE. 1997. Early hominid evolution and ecological change through the African Plio-Pleistocene. Journal of Human Evolution 32:289–322.

Reed KE. 2008. Paleoecological patterns at the Hadar hominin site, Afar Regional State, Ethiopia. Journal of Human Evolution 54:743–768.

Revell LJ, and Reynolds RG. 2012. A New Bayesian Method For Fitting Evolutionary Models To Comparative Data With Intraspecific Variation. Evolution 66:2697–2707.

Revell LJ. 2008. On the analysis of evolutionary change along single branches in a phylogeny. Am. Nat. 172:140–147.

Revell LJ. 2009. Size-correction and principal components for interspecific comparative studies. Evolution 63:3258–3268.

Revell LJ. 2010. Phylogenetic signal and linear regression on species data. Methods in Ecology and Evolution 1:319–329.

Revell LJ. 2012. phytools: an R package for phylogenetic comparative biology (and other things). Methods in Ecology and Evolution 3:217–223.

Rice WR. 1989. Analyzing Tables of Statistical Tests. Evolution 43:223–225.

Rivals F, Mihlbachler MC, and Solounias N. 2007. Effect of ontogenetic-age distribution in fossil and modern samples on the interpretation of ungulate paleodiets using the mesowear method. Journal of Vertebrate Paleontology 27:763–767.

Rohlf FJ. 2006. A Comment on Phylogenetic Correction. Evolution 60:1509–1515.

Ruff C. 1988. Hindlimb articular surface allometry in Hominoidea and *Macaca*, with comparisons to diaphyseal scaling. Journal of Human Evolution 17:687–714.

Safont S, Malgosa A, and Subira ME. 2000. Sex assessment on the basis of long bone circumference. Am. J. Phys. Anthropol. 113:317–328.

Schaeffer B. 1947. Notes on the origin and function of the artiodactyl tarsus. American Museum Novitates 1356:1–24.

Schaeffer B. 1948. The Origin of a Mammalian Ordinal Character. Evolution 2:164–175.

Schmitz L, and Motani R. 2011. Nocturnality in Dinosaurs Inferred from Scleral Ring and Orbit Morphology. Science 332:705–708.

Schrenk F, Bromage TG, Betzler CG, Ring U, and Juwayeyi YM. 1993. Oldest *Homo* and Pliocene biogeography of the Malawi Rift. Nature 365:833–836.

Schwartz GT. 2000. Taxonomic and functional aspects of the patterning of enamel thickness distribution in extant large-bodied hominoids. Am. J. Phys. Anthropol. 111:221–244.

Scott K. 1979. Adaptation and Allometry in Bovid Postcranial Proportions.

Scott K. 1985. Allometric trends and locomotor adaptations in the Bovidae. Bulletin of the American Museum of Natural History 179:197–288.

Scott R, and Barr W. In Press. Ecomorphology and phylogenetic risk: implications for habitat reconstruction using fossil bovids. Journal of Human Evolution.

Scott R. 2004. The Comparative Paleoecology of Late Miocene Eurasian Hominoids. PhD Dissertation. The University of Texas at Austin. Austin, TX.

Scott RS, Kappelman J, and Kelley J. 1999. The paleoenvironment of *Sivapithecus parvada*. Journal of Human Evolution 36:245–274.

Scott RS, and Maga M. 2005. Paleoecology of the Akkaşdag ı hipparions (Mammalia, Equidae), late Miocene of Turkey. Geodiversitas [Internet] 27. Available from: http://www.albany.edu/~ag856732/PRG/Scott%20and%20Maga%202005.pdf

Shackleton NJ, Backman J, Zimmerman H, Kent DV, Hall MA, Roberts DG, Schnitker D, Baldauf JG, Desprairies A, Homrighausen R, et al. 1984. Oxygen isotope calibration of the onset of ice-rafting and history of glaciation in the North Atlantic region. Nature 307:620–623.

Shipman P, and Harris J. 1988. Habitat Preference and Paleoecology of Australopithecus boisei in Eastern Africa. In: Grine F, editor. Evolutionary History of the "Robust" Australopithecines. New York: Aldine. p 343–381.

Skinner JD, and Chimimba CT. 2006. The Mammals of the Southern African Sub-region. 3rd ed. Cambridge University Press.

Smith RJ. 1994. Degrees of freedom in interspecific allometry: An adjustment for the effects of phylogenetic constraint. American Journal of Physical Anthropology 93:95–107.

Sokal RR, and Rohlf FJ. 2001. Biometry. Freeman New York.

Solounias N, Fortelius M, and Freeman P. 1994. Molar wear rates in ruminants: a new approach. In: Annales Zoologici Fennici. Vol. 31. p 219–227.

Souron A, Balasse M, and Boisserie J-R. 2012. Intra-tooth isotopic profiles of canines from extant Hippopotamus amphibius and late Pliocene hippopotamids (Shungura Formation, Ethiopia): Insights into the seasonality of diet and climate. Palaeogeography, Palaeoclimatology, Palaeoecology 342-343:97–110.

Spencer LM. 1995. Morphological correlates of dietary resource partitioning in the African Bovidae. Journal of Mammalogy 76:448–471.

Strait DS, Grine FE, and Moniz MA. 1997. A reappraisal of early hominid phylogeny,. Journal of Human Evolution 32:17–82.

Suwa G, White TD, and Howell FC. 1996. Mandibular postcanine dentition from the Shungura Formation, Ethiopia: Crown morphology, taxonomic allocations, and Plio-Pleistocene hominid evolution. American Journal of Physical Anthropology 101:247–282.

Van Valen L. 1960. A Functional Index of Hypsodonty. Evolution 14:531–532.

Venables WN, and Ripley BD. 2002. Modern Applied Statistics with S. Fourth. New York: Springer. Available from: http://www.stats.ox.ac.uk/pub/MASS4

Vrba ES, Denton GH, and Prentice ML. 1989. Climatic Influences on Early Hominid Behavior. Ossa 14:127–156.

Vrba ES. 1980. The significance of bovid remains as indicators of environment and predation patterns. In: Behrensmeyer AK, Hill A, editors. Fossils in the Making: Vertebrate Taphonomy and Paleoecology. Chicago University Press, Chicago. p 247–272.

Vrba ES. 1985. Ecological and adaptive changes associated with early hominid evolution. In: Delson E, editor. Ancestors: the hard evidence. New York: Alan R. Liss. p 63–71.

Vrba ES. 1987. Ecology in relation to speciation rates: some case histories of Miocene-Recent mammal clades. Evol Ecol 1:283–300.

Vrba ES. 1988. Late Pliocene climatic events and hominid evolution. In: Grine FE, editor. Evolutionary History of the "Robust" Australopithecines. New York: Aldine. p 405–426.

Vrba ES. 1992. Mammals as a Key to Evolutionary Theory. Journal of Mammalogy 73:1–28.

Vrba ES. 1995. On the connections between paleoclimate and evolution. In: Vrba ES, Denton GH, Partridge TC, Burckle LH, editors. Paleoclimate and Evolution with Emphasis on Human Origins. New Haven: Yale University Press. p 24–45.

Walker PL. 2005. Greater sciatic notch morphology: Sex, age, and population differences. American Journal of Physical Anthropology. 127:385–391.

Wang F. 1990. Fuzzy supervised classification of remote sensing images. IEEE Transactions on Geoscience and Remote Sensing 28:194–201.

Weinand DC. 2007. A study of parametric versus non-parametric methods for predicting paleohabitat from Southeast Asian Bovid astragali. Journal of Archaeological Science 34:1774–1783.

Wesselman HB. 1984. The Omo micromammals: Systematics and Paleoecology of Early Man Sites from Ethiopia. Karger.

Wesselman HB. 1995. Of mice and almost-men: regional paleoecology and human evolution in the Turkana Basin. In: Vrba ES, Denton GH, Partridge TC, Burckle LH, editors. Paleoclimate and evolution, with emphasis on human origins. Yale University Press. p 356–368.

White T. 1995. African omnivores: global climatic change and Plio-Pleistocene hominids and suids. In: Vrba ES, Denton GH, Partridge TC, Burckle LH, editors. Paleoclimate and Evolution with Emphasis on Human Origins. New Haven: Yale University Press. p 369–384.

White TD, Ambrose SH, Suwa G, Su DF, DeGusta D, Bernor RL, Boisserie J-R, Brunet M, Delson E, Frost S, et al. 2009a. Macrovertebrate Paleontology and the Pliocene Habitat of *Ardipithecus ramidus*. Science 326:67–93.

White TD, Asfaw B, Beyene Y, Haile-Selassie Y, Lovejoy CO, Suwa G, and WoldeGabriel G. 2009b. *Ardipithecus ramidus* and the Paleobiology of Early Hominids. Science 326:64–86.

Wickham H. 2009. ggplot2: Elegant Graphics for Data Analysis. 2nd Printing. Springer.

Wiens JJ, and Graham CH. 2005. Niche Conservatism: Integrating Evolution, Ecology, and Conservation Biology. Annual Review of Ecology, Evolution, and Systematics 36:519–539.

Vita

William Andrew Barr completed his B.S in 2005 at Tulane University with a double major in Anthropology and French. He completed his M.A. in 2008 at the University of Texas at Austin in Anthropology, and his PhD in 2014.

Permanent email address: wabarr@gmail.com

This dissertation was typed by the author.